CHROMATIC, ADAPTIVE, AND GENERAL PROPERTIES OF CAT

RETINAL GANGLION AND LATERAL GENICULATE CELLS:

A MID-MESOPIC STUDY

by

B. AHMED

Dissertation presented to the University of
Keele for the degree of Doctor of Philosophy

December, 1978

Research Department of
Communication and Neuroscience,
University of Keele.

.... To my parents ....

ABSTRACT

Data were collected at the retinal ganglion (RGC) and lateral geniculate cell (LGC) levels in lightly anaesthetised cats at a mid-mesopic background adapting luminance. Investigation of the rod- and cone-mediated properties of cells was accomplished by differentially influencing the rod and cone mechanisms with narrow-band light at short (452 nm) and long (578 nm) wavelengths respectively.

For RGCs, area ratios of rod-mediated to cone-mediated receptive field centres (RFCs) ranged from 0.6:1 to 2.9:1, with 66% of cells having larger rod than cone centres. RFCs were elliptical, the magnitude of ellipticity being similar for rod and cone centres and in agreement with values given by Hammond (1974). Almost 60% of maps had their major axis orientated within ±20° of horizontal, confirming the results of Hammond (1974). In addition, 69% exhibited non-concentric rod and cone centre maps and 24% displayed two spatially separate regions of maximal sensitivity, possibly one for cones and the other for rods. The adaptive state, assessed by the technique of Hammond and James (1971) and based upon that of Barlow and Levick (1968), was found to vary over a 0.6 log. units range. However, in contrast to the results and predictions of Enroth-Cugell and Shapley (1973b) its value was not correlated with the visual field location of the receptive field or with RFC area. Moreover, the mean value of the adaptive state did not differ between brisk sustained and transient cells, despite their dissimilar RFC sizes.

For LGCs, the rod- to cone-centre area ratios ranged from equality to 1.4:1, with 35% having larger rod than cone centres. 68% of maps had horizontally oriented major axes. The calculated mean ellipticity ratios

were similar for rod and cone centres, and comparable to the retinal data.

ACKNOWLEDGEMENTS

C O N T E N T S

G L O S S A R Y

IRR	intra-retinal recording
RGC	retinal ganglion cell
ROT	right optic tract
OTF	optic tract fibre
LGN	dorsal lateral geniculate nucleus
LGC	lateral geniculate cell

Classification of unit (after Cleland *et al.*, 1971, 1974a,b).

S	brisk sustained unit
S^s	sluggish sustained unit
T	brisk transient unit
+	on-centre unit
-	off-centre unit

Each unit is identified according to the following scheme.

IRR.16.05

ROT.25.12

LGN.32.09

The pre-fixed letters IRR, ROT, or LGN denote whether the recording was from a retinal ganglion cell, from an optic tract fibre, or from a geniculate cell, respectively. The digits denote the experimental (e.g. 16, 25, and 32) and the unit (e.g. 05, 12, and 09) identification numbers.

Additional abbreviations used.

I/P	intra-peritoneal
I/V	intra-venous
H-C coordinates	Horsley-Clarke coordinates

EEG	electro-encephalography
PSTH	peri-stimulus time histogram
AC	area centralis
OD	optic disk
r (or r_{xy})	correlation coefficient for the linear regression between parameters x and y.
RS	Relative sensitivity - defined as the ratio between the measured 578nm-yellow and 452nm-blue threshold sensitivities.
maintained (or resting) discharge/ activity	Refers to the mean spike rate of retinal ganglion or lateral geniculate cells at a fixed background adapting level in the absence of specific visual stimulation.

Chapter 1   I N T R O D U C T I O N

1.1 Cat retinal ganglion cell classification

Physiological and morphological classification schemes for retinal ganglion cells (RGCs) are reviewed in the following sections.

1.1.1 Physiological classification of RGCs

On the basis of the discharge patterns elicited by a small diameter flashing light spot, Kuffler (1953) defined the general functional organisation of the retinal ganglion cell's (RGC) receptive field. Under this scheme, the RGCs could be classified into two types - "on-" and "off-centre". On-centre units gave a discharge over the central region of the receptive field (the receptive field centre) at light "on" and a discharge over an annular region surrounding the centre (receptive field surround) at light "off". Off-centre units gave the opposite discharge configuration, i.e. discharge from the receptive field centre (RFC) at light "off" and discharge from the receptive field surround at light "on".

Enroth-Cugell & Robson (1966), by studying the spatial summation properties within the receptive field of RGCs to sinusoidally modulated gratings (i.e. the intensity perpendicular to the grating pattern varies sinusoidally about a mean level), found that the magnitude of response to the grating was dependent upon the position of the stationary pattern (the phase angle of the grating) with respect to the RFC. For some cells (X-cells), the presentation and withdrawal of this pattern, at a particular phase angle of the grating, caused no change in their maintained activity. In other cells (Y-cells), the maintained activity was altered

for all phase angles of the stationary sinusoidal grating pattern.
These properties were independent of the on- and off-centre dichotomy.
Accordingly, Enroth-Cugell & Robson suggested that spatial summation
over the receptive field of X-cells was approximately linear, whereas
for Y-cells summation was non-linear. These authors also noted that:

(i) the RFC size of X-cells was smaller than that of Y-cells,
and

(ii) the maintained activity of Y-cells was greatly increased
when grating patterns drifted across the receptive field.

Cleland, Dubin and Levick (1971) confirmed the findings of Enroth-
Cugell and Robson and, on the basis of a series of tests - standing
contrast, square-wave grating resolution, size and speed of contrasting
targets, the presence or absence of the periphery effect (McIlwain,
1964, 1966), and axonal conduction velocity - elucidated further
differences between X- and Y-cells. These authors, however, adopted a
different terminology and classified the units as sustained (X-cells)
and transient (Y-cells). Furthermore, the suggested correlation between
sustained units and X-cells, and between transient units and Y-cells was
only inferred from similarities between their properties. Sustained
units differed from transient units by having an elevated spike discharge
above the prestimulus level throughout the presentation of the standing
contrast, and for a given eccentricity of their receptive field from the
area centralis by:

(i) a weaker or absent periphery effect,

(ii) slower axonal conduction velocities,

(iii) smaller RFC sizes, and

(iv) higher spatial resolving frequencies of square-wave gratings.
Cleland, Dubin and Levick extended this sustained/transient terminology

to include cells in the dorsal lateral geniculate nucleus (LGN), but pointed out that at this level the differences were not as clear cut as for RGCs.

Saito, Shimahara and Fukada (1970), Fukada (1971), and Fukada & Saito (1971) were the first to propose a type I (phasic) and type II (tonic) dichotomy based upon RGC responses to standing contrast, intermittent photic stimulation (flicker) and conduction velocity. For type II units, the mean spike activity was independent of variations in flicker frequency but for type I units, the discharge rate increased, reached a peak value for flicker frequencies between 10 to 20Hz, and then decreased. On the basis of such data, Fukada & Saito (1971) suggest that type I units are suitable for processing temporal information while type II are suitable for processing spatial information.

By the use of selective visual stimuli, many other investigators have similarly classified RGCs into two basic categories. For example, Enroth-Cugell & Pinto (1972) referred to cells as "surround revealing" (sustained) or "surround concealing" (transient) on the basis of whether an annulus presented in the receptive field periphery, with a centrally located steady adapting spot, gave pure surround responses or not. Similarly, Winters, Pollack and Hickey (1972), Winters, Hickey and Pollack (1973), Winters, Hickey and Skaer (1973), and Hickey, Winters and Pollack (1973) distinguished two classes of on-centre RGCs (Group I and Group II) on the basis of surround responses to annuli with or without a central spot. Group I cells always gave mixed responses (i.e. on and off) to annuli flashed in the receptive field surround, whereas group II cells gave only off-responses. They suggest that for group I cells (transient) the centre and surround mechanisms are spatially coextensive in the receptive field, whereas for group II cells (sustained) the centre

mechanism only partially overlaps the surround mechanism in the receptive field (Hickey, Winters and Pollack, 1973). Hamasaki, Campbell and Zengel (1972), Hamasaki, Zengel and Campbell (1973), and Hamasaki, Campbell, Zengel and Hazelton (1973) classified on-centre RGCs into types I and II according to response patterns elicited by a moving light bar across the receptive field. Type I units gave excitation as a light bar entered the RFC and inhibition as it left the RFC, whereas type II units gave inhibition both before and after the target reached the RFC.

The relationships between the differing classification schemes are summarized in Table 1.1.
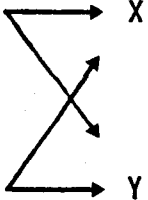
The classification schemes, so far, have been solely based on cat RGCs with concentric centre-surround receptive fields (Kuffler, 1953). However, a number of reports in the literature showing departures from such an organisation (Rodieck, 1967; Stone & Fabian, 1966; Spinelli, 1966, 1967) and the presence of a trichotomy in axonal conduction velocities, led Stone and Hoffmann (1972) to propose a 3-group classification of RGCs. These authors adopted the X- and Y-cell scheme of Enroth-Cugell and Robson (1966), but extended this to include the third class which they termed W-cells. This term was chosen since the alphabetical series W, X, Y followed the axonal conduction velocities of the three groups, i.e. W-cells < X-cells < Y-cells.

Stone and Fukuda (1974a) and Fukuda and Stone (1974) have further elucidated the properties of W-cells and suggest that they may constitute 40% [Rowe and Stone (1976) propose up to 60%[1]] of the entire RGC

---

[1]Rowe and Stone's proposal is based on the findings that:
  (i)   almost 70% of RGCs in the visual streak (central retina) have cell
        body diameters less than 14 μm and these are assumed to be W-cells
        (section 1.1.2; Boycott & Wässle, 1974); and
  (ii) in the non-streak (i.e. peripheral) retina W-cells comprise 19.1%
        of the physiological sample, whereas in the streak they form 47.6%
        of the sample.

Table 1.1   A summary of cat retinal ganglion cell (RGC) groupings. Arrows denote that each class includes on- and off-centre units.

Authority	Kuffler (1953)	Enroth-Cugell & Robson (1966)		Cleland *et al.* (1971)	Fukada (1971)	Enroth-Cugell & Pinto (1972)	Hickey *et al.* (1973)	Hamasaki *et al.* (1973)
RGC Classes	on-centre, off-surround	⟶	X	sustained	Type II	surround-revealing	Group II	Type II
	off-centre, on-surround	⟶	Y	transient	Type I	surround-concealing	Group I	Type I

population. This percentage, however, includes RGCs with tonic (18%), phasic (6%), and on-off (12%) responses. The remaining 4% is composed of units with "specialised" receptive fields, e.g. on-off direction-selective, suppressed-by-contrast, and on-centre direction-selective units.

Cleland and Levick (1974a,b) have modified and extended their original sustained/transient classification scheme (Cleland, Dubin and Levick, 1971; Cleland and Levick, 1972; Cleland, Levick and Sanderson, 1973). They now propose two broad categories - the concentric and the non-concentric - for classification of RGCs. The concentric scheme includes all RGCs with the Kuffler type of concentric centre-surround receptive field. Hence, although the original sustained/transient classes are included in the concentric scheme, each class is sub-divided into brisk and sluggish. The brisk sustained and transient (on- or off-centre) units are equated with the X- and Y-classes, respectively. The sluggish units (sustained and transient, on- or off-centre) form an entirely new group, and are characterised by:

(i)   low maintained discharge rates (<10 spikes s^{-1}),

(ii)   slowest axonal conduction velocities,

(iii) absence of the periphery effect, and

(iv)   possession (except for on-centre sluggish sustained units) of an extra region in addition to the centre and antagonistic surround - termed the silent inhibitory surround.

The non-concentric category includes all the rarely encountered type of units with "specialised" receptive field organisation. From their total RGC sample (n = 960), Cleland and Levick (1974b) distinguished five specialised classes: uniformity detectors, local edge detectors, direction-selective units, edge inhibitory off-centre units, and colour-coded units.

Table 1.3 summarises the relationship between the W, X, Y and the Concentric/Non-concentric terminologies.

1.1.2 Morphological classification of RGCs

Based on measurements of the dendritic spreads and cell body sizes, Brown and Major (1966) suggested a bimodal classification for peripheral RGCs. They distinguished groups with:

(i)   small cell body sizes (range 11-25μm) and dendritic spreads ranging between 70 and 200μm in diameter, and

(ii) large cell body sizes (range 17-36μm) and dendritic spreads between 400 and 700μm.

Leicester and Stone (1967) classified peripheral RGCs, according to morphology of the dendritic arborizations, into four groups:

(i)   deep multidentrite cells,

(ii) loose single dendrite cells,

(iii) dense single dendrite cells, and

(iv) shallow multidendrite cells.

They were unable to characterise central RGCs because of difficulties in staining the small diameter dendrites either with methylene blue or silver stain. In contra-indication to the results of Brown and Major, Leicester and Stone found the dendritic spreads of all four groups overlapped, and Honrubia & Elliott (1970) showed a systematic increase in cell size and in dendritic fields of RGCs with eccentricity from the area centralis. The latter authors also showed the existence in the cat retina of a giant type of RGC with dendritic fields ranging from 70 to 700μm in diameter.

Shkolnik-Yarros (1971) distinguished RGCs according to:

(i)   size of dendritic spreads (4 types: 60-80μm, 180-260μm, 300-400μm,

and 400-850μm),

(ii) cell body sizes (5 types: miniature, small, medium, large and
gigantic), and

(iii) character of dendritic ramification (7 types: bushy densely
branched, bushy sparsely branched, large horizontal broad
range, small horizontal broad range, unilateral horizontal
broad range, central, and diffuse).

Boycott and Wässle (1974) compared dendritic spreads, cell body
sizes, axon diameters, and dendritic branching patterns of RGCs at
equivalent retinal locations. Based on these parameters, these authors
suggested 3 basic morphological types of RGCs: alpha, beta, and gamma.
At a given retinal location:

(i) The alpha cells have large cell bodies, a well defined "thick"
axon, and sparsely branched dendrites but with a large dendritic
spread;

(ii) the beta cells have smaller cell bodies, are densely branched
but with fine dendrites, and the smallest dendritic spreads; and

(iii) the gamma cells are characterised by the smallest cell bodies,
large but sparsely branched dendritic fields, and "thin" axons.

Another morphological type of RGC - the delta cells - has also been
described by Boycott and Wässle; the delta cells' mean cell body size was
larger than that of gamma cells and the pattern of dendritic ramification
was similar to the alpha cells. Furthermore, at a given retinal location,
the delta cells when compared with:

(i) alpha cells had the smaller dendritic spans and cell body sizes,
and the thinner dendrites and axons; and

(ii) beta cells had a similar range of cell body sizes but larger
dendritic spans.

However, because of the small number of cells (n = 11) with these characteristics, Boycott and Wässle preferred not to define another distinct morphological class, but instead classified the delta cells as a sub-category of the gamma cells.

The distributions of various morphological characteristics, and the relationship of these between the 3 morphological classes are shown in Figs. 1.1, 1.2, 1.3, and 1.4. Boycott and Wässle have suggested that the alpha, beta, and gamma morphological classes may be correlated with the physiological classes Y, X, and W, respectively. The evidence for such a correlation is considered in the next section (1.1.3).

Table 1.2 tentatively links the various morphological schemes in terms of the alpha-, beta-, and gamma-cell classes.

Shkolnik-Yarros (1971) noted that the topography of dendritic spreads (i.e. depth of location of the processes) was variable, their location being at different levels of the inner plexiform layer. Recently, in the cat (Nelson, Famiglietti and Kolb, 1978) and the carp (Famiglietti, Kaneko and Tachibana, 1977), and based on physiological (intracellular recording) and morphological parameters (through dye injection of cell), the on- and off-centre RGC dichotomy has been shown to be correlated with the different levels of stratification of the dendritic processes in the inner plexiform layer.

1.1.3 Physiological/morphological correlations

The suggestion by Boycott and Wässle - viz: the morphological types (alpha, beta, gamma) are correlated with the physiological types (Y, X, W) - was accepted by Stone and Fukuda (1974a) and Cleland and Levick (1974a,b). Cleland and Levick, however, suggested a correlation between alpha cells and brisk transient units, between beta cells and sustained

Fig. 1.1

Cell body diameters for RGCs of the three morphological types expressed as a function of their dendritic field diameters. Alpha, beta, and gamma cells are represented by the filled circles, crosses, and open circles, respectively. The open triangles represent the special category of gamma cells called delta cells.

(From Boycott and Wässle, 1974).

Fig. 1.2

Cell body diameter of alpha, beta, and gamma cells as a function of distance from the area centralis. Symbol convention as in Fig. 1.1.

(From Boycott and Wässle, 1974).
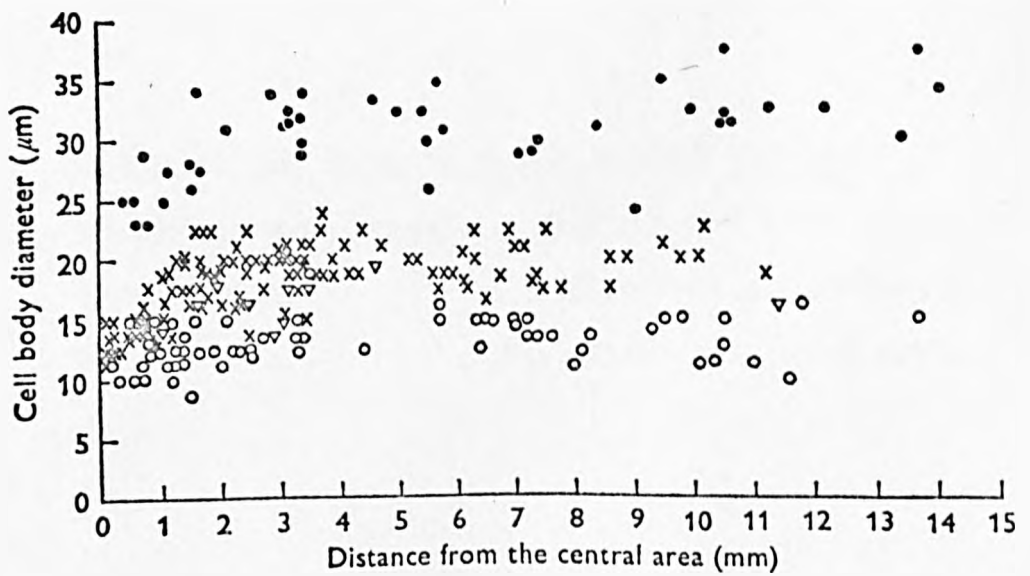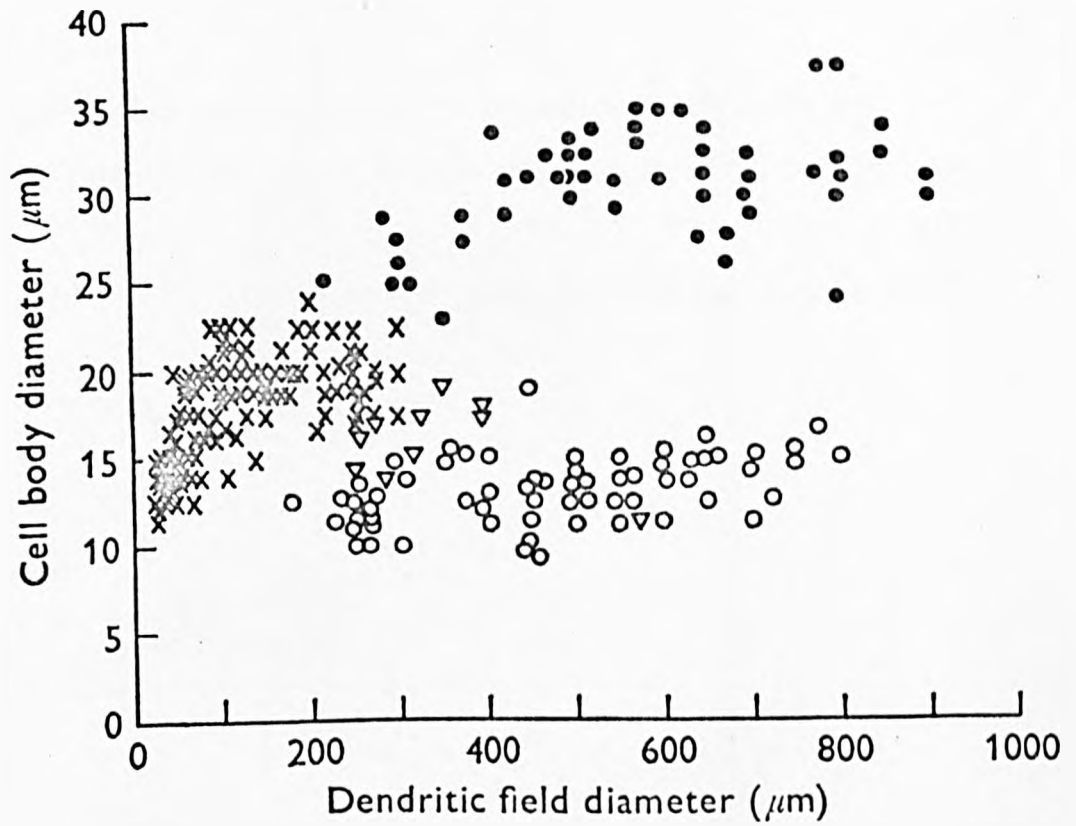
Fig. 1.3

   Dendritic field diameters of alpha and beta cells as a
function of distance from the central area. Conventions as in
Fig. 1.1.
(From Boycott and Wässle, 1974).

Fig. 1.4

   Dendritic field diameters of gamma (and its subcategory
delta) cells as a function of distance from the central area.
Conventions as in Fig. 1.1.
(From Boycott and Wässle, 1974).
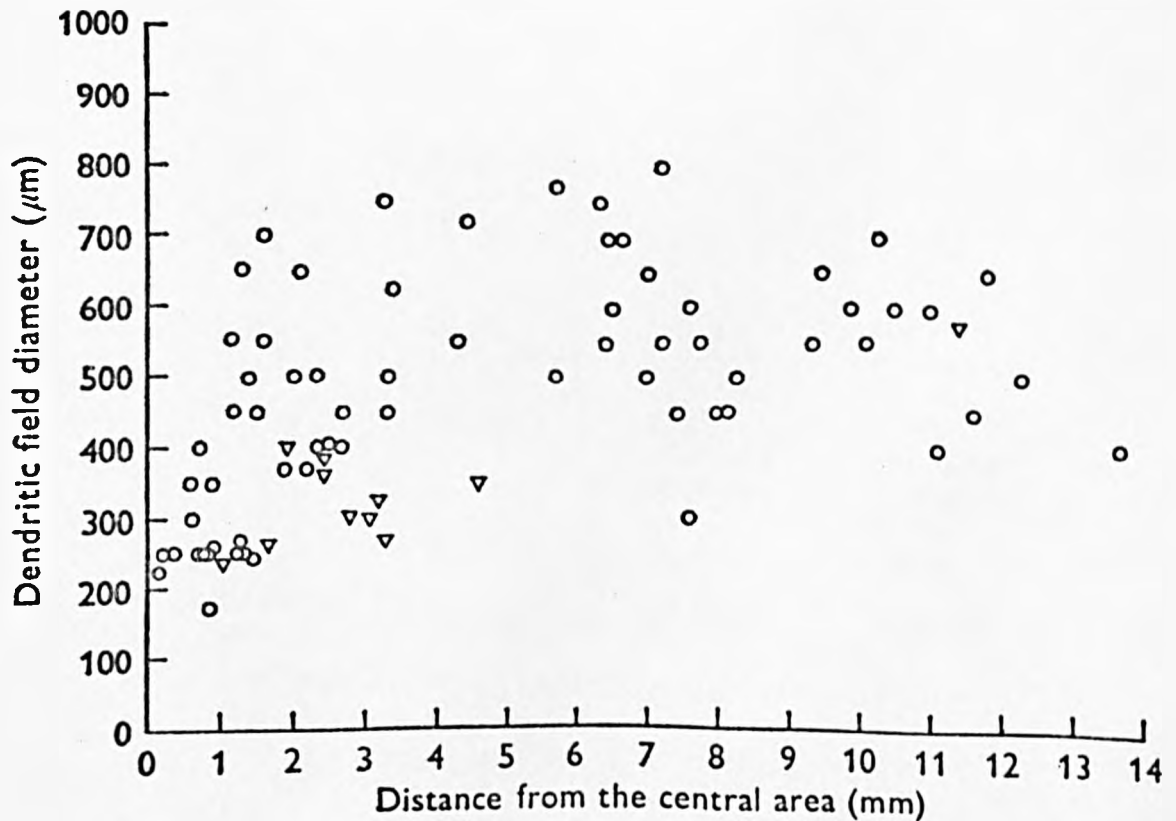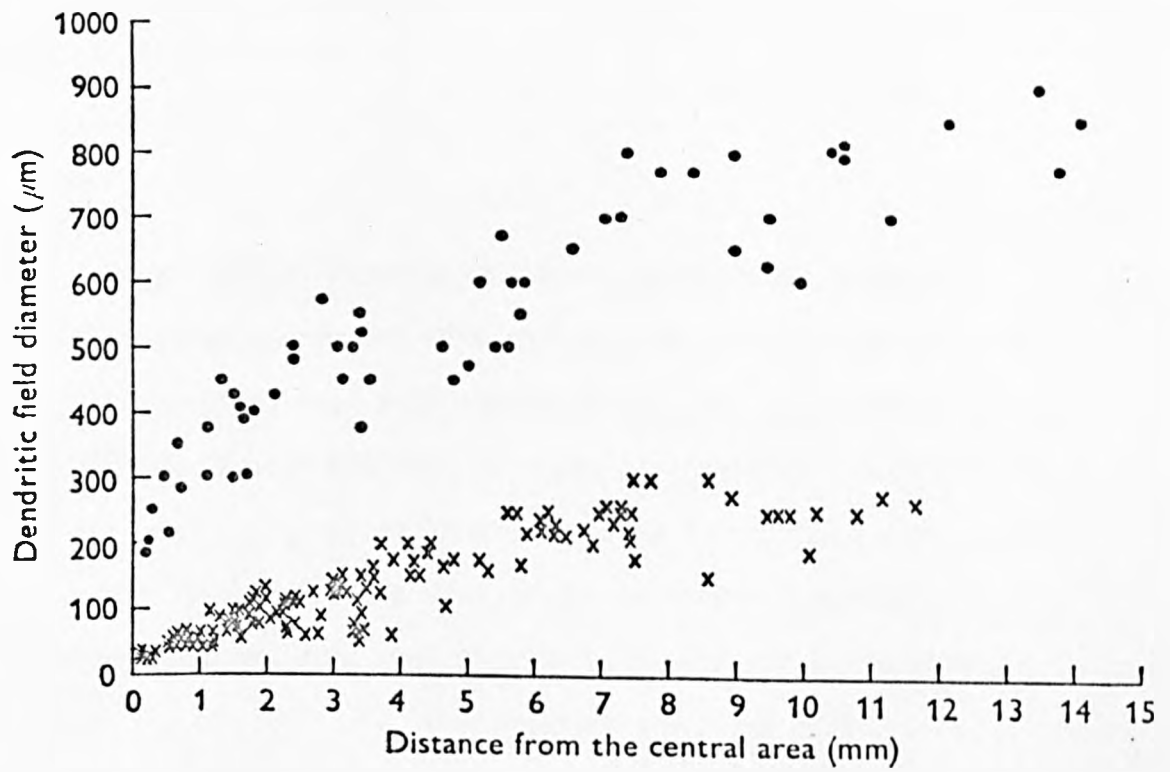
Table 1.2

      Tentative relationship between the morphological types described by various investigators with the alpha, beta, and gamma terminology. The relationships have been based on morphological descriptions: range of cell body sizes, dendritic spans, and character of dendritic ramifications.

* - a suggested correlation may be with the sub-type of the gamma cells (delta) based on cell body size and description of dendritic branching pattern.

Table 1.2

Authority	Dimensions	Morphological cell classes			
		alpha	beta	gamma	others
Boycott & Wässle (1974)	Dendritic span (μm)	180-1000	20-300	180-800	-
	cell body size (μm)	23-38	11-24	8-18	-
	Axon diam.	thick	medium	thin	-
Brown & Major (1966)	Type	large cells	small cells	-	-
	Dendritic span (μm)	400-700	70-200	-	-
	cell body size (μm)	17-36	11-25	-	-
Leicester & Stone (1967)	Type	Deep multi-dendrite cells	Dense single dendrite cells; shallow multi-dendrite cells	Anomalous cells	Loose single dendrite cells*
	Dendritic span (μm)	70-710	30-165	500-700	18-135
	cell body size (μm)	15-35	12-21	small	11-21
Honrubia & Elliott (1970)	Type	Giant cells	-	-	-
	Dendritic span (μm)	70-700	-	-	-
Shkolnik-Yarros (1971)	Type	large horizontal broad range	bushy densely branched; bushy sparsely branched	small horizontal broad range; unilateral horizontal broad range	central; diffuse
	Dendritic span (μm)	260-700	60-190	120-750	-
	cell body size (μm)	18-70	12-27	7-25	-

units, and between gamma cells and sluggish and non-concentric units.
Such correlations were based on similarities between:

    (i) dendritic spread versus RFC size, and

    (ii) axon and/or cell body size versus conduction velocity.

Also, for the gamma type, the heterogeneity in morphological features was
correlated with the heterogeneity in the W-cells' (or sluggish and non-
concentric types') physiological properties.

    Independently, Fukuda and Stone (1975) and Cleland, Levick and
Wässle (1975) have attempted to provide direct evidence for the above
correlations.

    By classifying RGCs, dye-marking their location, and subsequently
identifying and measuring their cell body sizes, Fukuda and Stone
successfully showed the correspondence: Y-cells with the largest cell
body sizes, W-cells with the smallest, and X-cells with the intermediate
sizes. However, although supporting the previously suggested correlation,
their data were based on only 2 Y-cells, 5 X-cells, and 5 W-cells.

    Cleland, Levick and Wässle demonstrated the rather precise
correspondence between the receptive field centre location of brisk
transient units and the distribution of alpha cells over a selected
section of the retina. Although exact coincidence was not obtained, the
data showed a good correspondence.

    In summary, evidence of a correlation through direct indentification
is strong only between alpha cells and brisk transient units (Y-cells).

1.1.4 <u>Present status in RGC classification</u>

    Basically still two schemes, based on:

    (i) Cleland and Levick's (1974a,b) concentric/non-concentric

        division and the extension of this to include the cells in the

lateral geniculate nucleus (Cleland, Levick, Morstyn and
Wagner, 1976); and

(ii) Stone and Fukuda's (1974a) W, X, Y division.

Table 1.3 shows the relationship between these schemes. It should be noted,
however, that exact correspondence between X- and Y-cells, and brisk
sustained and brisk transient units, respectively, has not been demonstrated.
In fact, in contra-indication, Hochstein & Shapley (1976a) have shown
that the response time course obtained with standing contrast is not by
itself a reliable index for correspondence between X-cells and brisk
sustained units, and between Y-cells and brisk transient units.

The projection, whether ipsilateral or contralateral, of RGCs located
in the temporal retina has been shown to differ between the different RGC
classes (Stone & Fukuda, 1974b; Kirk, Levick, Cleland and Wässle, 1976;
Kirk, Levick and Cleland, 1976). Stone and Fukuda found that, with
respect to the area centralis:

(i) X-cells located in the nasal retina projected contralaterally,

     and those located in the temporal retina projected

     ipsilaterally, i.e. the naso-temporal division was sharpest

     in this class;

(ii) in addition to Y-cells in nasal retina, about 5% of the Y-cells

      located in the temporal retina also projected contralaterally;

      and

(iii) in addition to W-cells in nasal retina, about 60% of the W-cells

       located in the temporal retina also projected contralaterally.

Similarly, the studies by Kirk, Levick, Cleland and Wässle, and Kirk
Levick and Cleland have shown the following sequence of increasingly
imprecise segregation of crossed and uncrossed representations of the
temporal retina for:

(i) brisk sustained units;

(ii) brisk transient and sluggish sustained units; and

(iii) sluggish transient and non-concentric units.

Accordingly, Rowe and Stone (1977) have used this evidence to extend the

Table 1.3

       The relationship between the two physiological
classification schemes and the morphological types. The
percentage values for each class are derived from total number
of recorded units. Rowe and Stone's values are also derived
from the distribution of cell body sizes in the central and
peripheral retina.

Table 1.3

PHYSIOLOGICAL CLASSIFICATION SCHEMES			MORPHOLOGICAL CORRELATES
Cleland & Levick (1974a,b)	Stone & Fukuda (1974a)	Rowe & Stone (1976)	Boycott & Wässle (1974)
CONCENTRIC CATEGORY			
brisk sustained (55%)	X ⎤ (60%)	40%	beta
brisk transient (25%)	Y ⎦	<10%	alpha
sluggish sustained (5%)			
sluggish transient (3%)			
NON-CONCENTRIC CATEGORY	phasic (6%)		
local edge detectors (5%)	tonic (18%)		
direction selective (1%)	W — on-off (12%)	>50%	gamma
colour coded (<1%)	on-off direction selective		
uniformity detectors (<1%)	suppressed-by-contrast — (4%)		
edge inhibitory off-centre (<1%)	on-centre direction selective		
unclassified (<1%)			

W-cell category into two sub-groups: W_1 (principally uncrossed) and W_2 (principally crossed). A summary of this extension is given in table 1.4 (reproduced from Rowe and Stone's table III, page 205).

1.2 <u>Cat colour vision</u>

Behavioural and physiological investigations into cat colour vision are reviewed.

1.2.1 <u>Behavioural evidence for cat colour perception</u>

Based on a study lasting 28 months, DeVoss and Ganson (1915) concluded that cats were colour blind. However, these authors emphasized that the term "colour-blindness" was used -

> "not because colour-vision should be denied of an animal as a result of a single investigation, no matter how carefully it may have been conducted, but because the results of our experiments certainly make the term "colour-blindness" a less presumptuous one than "colour-vision" when applied to these animals."

Evidence supporting DeVoss and Ganson has been provided by Gregg, Jamison, Wilkie and Radinsky (1929), Meyer, Miles and Ratoosh (1954), Gunter (1954b), and Ducker (1957). However, more recent behavioural studies have shown that the cat has some ability to discriminate between certain colours (Clayton, 1961; Bonaventure, 1964; Mello and Peterson, 1964; Sechzer and Brown, 1964; Meyer and Anderson, 1965; Clayton and Kamback, 1966; Daw and Pearlman, 1970; LaMotte and Brown, 1970; Brown, Shiveley, LaMotte and Sechzer, 1973; Loop and Bruce, 1978). This ability, however, seems to be limited to distinguishing spectral extremes, i.e. red from yellow, green or blue and blue from yellow or green (Clayton, 1961; Sechzer and Brown, 1964; Clayton and Kamback, 1966; Daw and Pearlman, 1970; Brown, Shiveley, LaMotte and Sechzer, 1973; Loop and Bruce, 1978),

Table 1.4

Suggested subgrouping of W-cells.

(From Rowe and Stone, 1977).

Table 1.4

Subgroups suggested	Response to standing contrast	Axonal velocity (extraretinal)	Soma size	Projection from temporal retina	Receptive field organizations recognised	Relative numbers and retinal distribution
W_1	mostly tonic	relatively fast mean 11.7 m/sec	relatively large	principally uncrossed	Off-centre, On-surround; On-centre, Off-surround; suppressed-by-contrast; colour-coded	approximately 50% of W-cell group; relatively more common outside visual streak
W_2	phasic	relatively slow mean 6.6 m/sec	relatively small	principally crossed	Off-centre, On-surround; On-centre, Off-surround; On-Off-centre, inhibitory or On- or Off-surround; On-Off-centre; direction selective; On-centre, direction-selective	approximately 50% of W-cell group; relatively more common in visual streak

but not the middle range of the spectrum, i.e. 570nm to 520nm (Clayton and Kamback, 1966; Brown, Shiveley, LaMotte and Sechzer, 1973). Furthermore, cats, whether successful or not in distinguishing between pairs of colours, have always found the brightness discrimination task easy (Gunter, 1954b; Meyer, Miles and Ratoosh, 1954; Sechzer and Brown, 1964; Loop and Bruce, 1978).

1.2.2 Physiological evidence for cat colour vision

Granit (1943, 1945), recording from optic nerve fibres of the cat, measured threshold sensitivities for a range of wavelengths. The spectral sensitivity curves gave:

(i)   a single peak near 500nm for the dark adapted retina; and

(ii) three peaks, near 460nm, 530nm and 600nm, for the light adapted retina using selective adaptation with red, green, and blue lights.

Gunter (1952, 1954a) also determined the spectral sensitivity of the cat under conditions of dark- and light-adaptation, but using a behavioural paradigm. Cats were trained to choose the dimmer of two light stimuli, irrespective of colour, and in this way he determined the relative spectral energy at which cats subjectively equated brightness between various coloured stimuli and a white test stimulus of constant intensity. For the dark adapted condition, the data gave a single peak near 500nm; whereas in the light adapted condition two peaks were obtained, near 470nm and 555nm.

Weale (1953) showed that in the living cat's eye the ratio between the rate of pigment recovery and light absorption depended upon the wavelength of light. Therefore, he concluded that the cat has more than one photosensitive pigment, and suggested that one of these pigments has a

spectral absorption peak near 500nm.

Determinations of the spectral response curves from optic tract and optic radiation fibres (Suzuki, Taira and Motokawa, 1960) revealed:

(i)   a scotopic spectral sensitivity peak at 500nm, and

(ii) at higher levels of illumination, two spectral sensitivity elevations extending over 420-480nm and 520-600nm.

Barlow, Fitzhugh and Kuffler (1957a) and Dodt and Elenius (1960), recording the threshold sensitivities of optic tract fibres, showed:

(i)   a distinct cone-rod break during the time-course of dark adaptation, and

(ii) that the cone and rod photopigments had separate spectral sensitivities.

Evidence from the above investigations (Granit, 1943, 1945; Gunter, 1952, 1954a; Suzuki, Taira and Motokawa, 1960), although showing a single scotopic spectral sensitivity peak near 500nm, are at variance both in the number and in the peak spectral sensitivity values for the light adapted situation, i.e. the cone processes. Furthermore, in the light adapted cat retina, the presence of peaks in the spectral sensitivity curves does not necessarily imply distinct cone processes. As pointed out by Daw and Pearlman (1969), the presence of such peaks can be explained by a single cone process interacting with rods, as well as by several cone processes, since none of these investigators determined the range over which both rods and cones are active (mesopic range) or attempted to eliminate the rods by using high background intensities.

Daw and Pearlman (1969) and Andrews and Hammond (1970a,b) determined the spectral sensitivities of optic tract fibres under scotopic and high mesopic background adapting luminances. Their data confirmed results from previous investigations by showing cat rods to have a maximal

sensitivity value near 500nm (500nm according to Daw and Pearlman; 507nm according to Andrews and Hammond). However, they obtained evidence only for a single cone process with maximal spectral sensitivity at 556nm. These investigators, therefore, suggested that the ability of cats to behaviourally discriminate between colours may be based on rod-cone interaction in the mesopic range of adapting luminances. Such interactions leading to sensations of colour have been shown to occur in psychophysical experiments on man (McCann and Benton, 1969; McCann, 1972).

However, evidence for the presence of another cone process with peak spectral sensitivity near 450nm was obtained by Pearlman and Daw (1970) and Daw and Pearlman (1970). These investigators recorded four colour coded cells (out of a sample of 434 cells) in lamina B (C laminae - after Guillery, 1970) of the cat's dorsal lateral geniculate nucleus. All four units were on-centre for blue light and off-centre for green or red light (single opponent cells). However, two were double opponent (reviewed by Daw, 1973) since stimulation of the receptive field surround with blue and green lights, respectively, caused inhibition and excitation. The presence of opponent cells in the C laminae has been confirmed by Wilson and Stone (1975) and Cleland, Morstyn, Wagner and Levick, (1975).

Colour coded RGCs with excitatory input from blue-sensitive cones and inhibitory input from medium-wavelength cones have been described by Cleland and Levick (1974b) and Rowe and Stone (1976). Cleland and Levick obtained 6 colour coded cells (sample size = 960) which gave on-centre responses to blue light and off-centre to green and red light. For these cells, the area-threshold curves for blue and green lights differed in size. Hence, these authors suggest that, besides colour opponency, their receptive fields may have a colour based spatial organisation. Rowe and Stone (1976) describe two colour coded cells

(sample size = 696) with tonic on-responses to a blue spot and tonic off-responses to white, red or green spots.

Rabin, Mehaffey and Berson (1976) have shown the presence of a blue-sensitive mechanism, with maximal sensitivity near 460nm, in the cone electro-retinogram of the cat eye. They used a bright yellow (7 log. td; wavelength transmission > 470nm) adapting stimulus, and then measured the spectral sensitivity (i.e. at each wavelength the log. relative quantum flux required to elicit a criterion response in the cone electro-retinogram) of the eye to 40Hz stimuli. Rabin, Mehaffey and Berson suggest, from the small size of the blue cone electro-retinogram, that the number of blue cone photoreceptors may be small.

Based on optic tract fibre and lateral geniculate cell recordings, Saunders (1977) suggests the existence of a cone process with a 600nm spectral sensitivity peak. His data were based on spectral response curves (i.e. the measured response (in spike rate) produced by a sinusoidally varying (at 2Hz) stimulus of narrow-band (half-width = 10nm) light collected over the spectral range 400nm to 690nm in approximately 20nm steps) obtained in the dark adapted situation, as well as when the retina was selectively adapted to red, green and blue lights. Five units (sample size approximately 100) displayed a well defined spectral response peak at 600nm, but only in the dark adapted retina. Saunders relates the poor performance of cats in behavioural experiments on colour discrimination to an inadequately developed colour opponent mechanism.

However, Hammond (1978a) points out that Saunders' (1977) results may be explained in terms of rod-cone interaction allowing spatial *plus* spectral opponency, since the rod-mediated RFC of a RGC can be larger than the cone-mediated RFC (Andrews and Hammond, 1970b; Chapter 4, section 4.3.3).

In a recent report, Ringo, Wolbarsht, Wagner, Crocker and Amthor (1977) have shown evidence for the presence of a cone process with peak spectral sensitivity at 500nm in an off-centre W-cell. The spectral sensitivity curves, obtained in the dark- and light-adapted retina, both showed peaks at 500nm. Added to this was the evidence that the two dark adaptation curves, obtained from threshold sensitivity measurements with 500nm and 620nm narrow-band lights during the time course of dark adaptation, showed a distinct cone-rod break but no change in spectral sensitivity. Ringo *et al.*, therefore, concluded that the W-cell was coupled to a 500nm-cone and a 500nm-rod system.

In summary, the available information suggests that the cat has overwhelmingly a 500nm-rod and a 556-nm cone system and, in addition, a weak contribution from a cone process with spectral sensitivity peak near 450nm. Recent reports indicate the presence of rare cone processes with peaks at 500nm and 600nm. Accordingly, the cat may be considered to have photopic trichromatic (Ringo *et al.*, 1977) or even tetrachromatic (Saunders, 1977) vision. However, from a behavioural standpoint the contribution, as far as colour discrimination is concerned, of the 500nm and 600nm cone processes must be negligible.

1.3 Objectives of the present study

This study was designed specifically to:

(i) resolve the discrepancy between the results of Andrews and Hammond (1970b) and Enroth-Cugell, Hertz and Lennie (1977b) regarding rod and cone centre sizes of RGCs;

(ii) test whether ellipticity in the shape of the RFC (Hammond, 1974) could be explained by circular, but non-concentric, rod and cone centres (H.B. Barlow, personal communication);

(iii)   examine whether the adaptive state of RGCs was related to their RFC areas (Enroth-Cugell and Shapley, 1973b); and

(iv)   compare and contrast the lateral geniculate cell results with the retinal data.

Besides these specific aims, the general properties of retinal ganglion and lateral geniculate cells and their responses to different stimulating parameters were also investigated. These results have been:

(i)   considered in terms of the sustained/transient terminology, and

(ii)   compared with other reports in the literature.

Chapter 2   GENERAL METHODS

2.1 Animal preparation

An adequate level of surgical anaesthesia was maintained in adult

cats (mean weight = 2.8kg, range 1.8 to 3.6kg), by using either

pentobarbitone (Nembutal, Abbott) or halothane (Fluothane, ICI).

Pentobarbitone was given by an intraperitoneal (I/P) injection, initially

on the basis of 35mg.kg^{-1} of body weight, further doses during the

surgical procedure averaging 4mg.kg.hr^{-1}. Halothane, 2-3% in oxygen, was

administered with a Fluotec Mk 3 (Cyprane).

Surgery involved tracheotomy, bilateral cervical sympathectomy

(Rodieck, Pettigrew, Bishop, and Nikara, 1967), and cannulation of the

left and right cephalic veins, for intravenous (I/V) infusion, and the

left carotid artery, for blood pressure (BP) monitoring. Some cats were

intubated with an appropriately sized Magill, cuffed endotracheal tube

(Franklins; internal diameters from 2.5mm to 4.5mm in steps of 0.5mm),

butterfly cannulae (23G/25G) were introduced into the left and right

cephalic veins, and the ECG was differentially recorded across skin

electrodes attached to the left latero-medial thorax. The cat was placed

in a modified Narishige stereotaxic frame, and the head was initially

held by means of ear and eye bars (defining a horizontal stereotaxic

plane) in Horsley-Clarke (H-C) coordinates. Cauterisation along the mid-

line of the scalp and the reflexion of the underlying temporalis muscles

were carried out. Two self-tapping stainless steel screws were inserted

respectively over the left visual and auditory cortices for the

differential recording of the surface-cortical EEG. A craniotomy (5mm

diameter), centred on appropriate H-C coordinates (see later) using

Snider and Niemer's (1961) stereotaxic atlas, was performed.

A head-holder was then screwed to the skull which held the head firmly in the stereotaxic position on removal of the eye and ear bars with no obstruction of the visual field. All wound margins were infiltrated with a local anaesthetic (Xylocaine spray, Astra).

A rectal thermistor monitored the body temperature and a homoeothermic blanket control (type 8185, C.F. Palmer) maintained it at 38.5°C. The end-tidal CO_2, monitored breath-by-breath by an infra red medical gas analyser (Beckman LB-2), was maintained between 3.8% and 4.0% by adjusting the stroke volume of an artificial respirator (C.F. Palmer, fixed rate of 28 strokes min.$^{-1}$).

During the recording stages a lightly anaesthetised preparation was used. Hence, before paralysis, depending upon whether surgery had been performed under pentobarbitone or halothane, the following procedure was adopted:

(i)   The pentobarbitone-anaesthetised cats were administered lower I/P doses averaging 2.5mg.kg^{-1}.hr^{-1}. Any further barbiturate requirement was given I/V.

(ii)   Halothane was gradually replaced by a nitrous oxide/oxygen mixture ($N_2O:O_2$ 70%:30%). This $N_2O:O_2$ mixture was supplemented by small I/V doses of pentobarbitone averaging 0.4-1mg.kg^{-1}.hr^{-1} (Russell, 1973; Richards & Webb, 1975; Hammond, 1978b,c).

In both of these anaesthetic regimes and before paralysis adequacy of anaesthesia was continuously checked through monitoring of the EEG, BP or heart rate, % end-tidal CO_2, and muscle tone.

The cats were paralysed by an initial I/V administration of 20mg.kg^{-1} of gallamine triethiodide (Flaxedil, May & Baker). Subsequently, a continuous infusion at 20mg.hr^{-1}, in a 5% dextrose solution, was given to maintain eye-immobilisation.

2.2 Optics

The eyes were washed with warm 0.9% NaCl solution. Atropine Sulphate (1% W/V, B.P.C) and phenylephrine hydrochloride (10% W/V, B.P.C) eye drops were then applied, respectively to dilate the pupils and withdraw the nictitating membranes and eye-lids. The corneae were protected from drying by a pair of two-curve neutral contact lenses (Hamblin). The lenses were selected from three pairs (base/peripheral curve - 8.0/8.5mm, 8.5/9.0mm, and 9.0/9.5mm; all with base/peripheral diameter 8.0/12.0mm) according to the relation:

$$Y = 7.28 + 0.34X$$

derived by Andrews and Hammond (1970a) relating the corneal radius of curvature (Y mm) and body weight (X kg), and based on the data of Vakkur, Bishop and Kozak (1963) and Vakkur and Bishop (1963).

Slit retinoscopy (Keeler) was carried out to focus the eyes at a distance of 57in. Corrective lenses, range -3.0 to +4.5 dioptres in steps of 0.25 dioptres, were available. The projections of each area centralis and optic disk were marked on a tangent screen using the back-projection method of Fernald & Chase (1971). Artificial pupils (5mm diameter) were aligned centrally in front of the corneae whilst the area centralis was ophthalmoscopically viewed through the aperture.

Regular checks were made on the quality of the optic media, corneal transparency, retraction of the nictitating membrane, dilation of the pupils, and position of the area centralis. Opacity due to corneal clouding was successfully dealt with by topical application of 3% NaCl solution (H. Ikeda, personal communication) and subsequent washing of the cornea with warm 0.9% NaCl solution.

2.3 Recording equipment

The spike activity was initially passed through a Bak pre-amplifier with unity gain and negative capacitance neutralisation. Subsequently, it was amplified (A101 Isleworth preamplifier, gain 100, band-pass 0.2-5kHz), displayed (RM565 dual-beam (upper beam vertical plug-in unit type 2A63 differential amplifier, and lower beam vertical plug-in type 3A74 four-trace amplifier) oscilloscope, Tektronix), and for off-line analysis recorded (in earlier experiments on a T 3000, Thermionic products (Electronics) Ltd. 4 channel-4 speed FM recorder/reproducer, at a tape speed of $3\frac{3}{4}$i.p.s, band-width 0-1250Hz; and in later ones on a CR 3000, Bell and Howell, 4 channel-2 speed FM/AM recorder/reproducer, tape speed $1\frac{7}{8}$i.p.s, and FM/AM band-width 0-625Hz/0.1-6kHz respectively). The conversion of the raw spike data into 1μs pulses was carried out by a window-discriminator. These pulses (discriminated spikes) were displayed as:

(i) Spike rate on a linearized oscillograph pen-recorder (400 MD/2, Washington).

(ii) Dot display (where each dot represents a single discriminated spike) on a single beam storage oscilloscope (Tektronix).

(iii) Peri-stimulus time histograms (PSTHs) by a Biomac 1000 data retrieval computer (Data lab.). Usually, 16 presentations were averaged using a bin-width of 10ms.

(iv) Individual counts by electronic counters (TC11A 15MHz timer counters, Advance Instruments) suitably gated for duration.

The raw noise and any spike activity picked up by the electrodes, or the discriminated spikes, were acoustically monitored through a loud-speaker.

Permanent records of the data, on- or off-line, were obtained as:

(i) PSTHs, either drawn by an X-Y plotter (PL 100, JJ Instruments

'XY' plotter) and/or photographed (Nihon Koden PC2A 35mm
continuous recording camera); and

(ii) Dot displays, photographed using the Shackman Polaroid
camera (Super 7 MKII with supplementary lens).

The EEG (amplified by a Devices 3160, gain 1000, bandwidth 0.8-
50Hz; and additional amplification by Ancom 15-1 broadband operational
amplifier), and either blood pressure (Bell and Howell 4-422 physiological
pressure transducer) or heart rate were continuously monitored on a
Devices M2, 2-channel, heat-sensitive pen-recorder. The breath-by-breath
end-tidal CO_2, measured by a Beckman LB-2 infrared medical gas analyzer,
was continuously monitored on the Washington 400 MD/2 pen-recorder, and
maintained between 3.8-4.0% by adjusting the pump stroke volume.

2.4 Visual stimulation equipment

Two modified Rank-Aldis slide projectors (Tutor 2; fitted with Atlas
A1/223, 24V, 250W tungsten-halogen quartz projection lamp) front-projected
onto a matt white, translucent, tangent screen (44° horizontally by 33°
vertically) placed 57 in. in front of the nodal points of the eyes. Both
projectors were pivoted to give sufficient horizontal and vertical motion
for manual positioning of the appropriate stimuli. One projector was
exclusively used to project a graduated cross-wire image onto the screen.
This image, formed of deep red light (Kodak, Wratten 29; 1% transmission
at λ = 610nm and 80% at λ > 640nm) whose intensity was kept sub-threshold
for the cat but suprathreshold for human observers, greatly aided the
exact localisation of the receptive field. The other projector was
fitted with:

(i) a pendulum mechanical shutter driven by a Ling Altec V47
vibration generator (rise and fall times for 8°, 4°, 2°, 1°,
and 0.5°, respectively, being 20ms, 12ms, 8ms, 5ms and 4ms);

(ii) two front silvered mirrors driven by Ling Altec V47
      vibration generators pivoted to permit electronic adjustment
      of stimulus position in horizontal and vertical planes;

(iii) a slide holder with a fine manual control (microscope, X-Y
      stage micrometer; Prior) to give a 4° by 4° displacement of
      the image of the slide;

(iv) a manual and 22-8411 Ealing electronic shutter (Ilex Optical
      Co.) with an aperture of 63.5mm diameter and an opening and
      closing time (for full aperture) of ~10ms;

(v)   a photodiode (R.S. Components) for monitoring stimulus
      duration; and

(vi) a filter holder designed with 3 compartments, one for a
      narrow-band interference filter (Balzer's B40) and 2 for
      neutral density filters (Kodak Wratten, glass mounted) - see
      later.

The following range of slides was available for projecting:

(i)   light spots (diameters 0.25°, 0.5°, 0.75°, 1.0°, 1.5°, and
      2° to 10.0° in steps of 1.0°);

(ii) concentric annuli (outer/inner diameter: $n/n-1$, where n had
      values from 1.5° to 10° in steps of 0.5°);

(iii) square wave gratings (spatial frequencies ¼, ½, 1, 2, 3 and
      4 cycles.deg^{-1}); and

(iv) light bars (length 4° or 8°, and width 0.25° to 1° in 0.25°
      steps).

The intensity and chromaticity of the projected stimuli could be
altered, respectively, by neutral density (Kodak, Wratten; nominally 0.1
to 4.0 log. units in steps of 0.1 log. units) and narrow-band interference
(Balzers Filtraflex B-40; 400 to 700nm in 25nm steps with half-widths 6

or 7nm and appropriately 40% transmission) filters.

The front-projection system provided for increments in contrast above the adapting level; decrements were achieved by hand held wands. These consisted of:

(i)   black discs (diameters 0.5° to 4° in 0.5° steps);

(ii) black bars (1° by 6° and 2° by 6°) and squares (10° by 10°); and

(iii) square wave gratings (spatial frequencies $\frac{1}{4}$, $\frac{1}{2}$, 1, 2 and 4 cycles.deg^{-1})

2.5 Calibration of filters

The spectral sensitivity of a high gain photomultiplier (RCA 6217) was first calibrated against a Hilger-Schwartz vacuum thermopile. This calibrated photomultiplier was placed in the stereotaxic frame and pointed at the tangent screen placed 57in. distant. The Rank-Aldis tutor 2 projector, used as the light source, front-projected an 8° diameter light spot onto the screen. The optical densities were then measured using neutral density filters of nominal values ranging from 0.1 to 1.0 (in 0.1 log. units steps) and 2.0 log. units for:

(i) white light; and

(ii) narrow-band blue and yellow light produced, respectively, by interposing Balzers interference filters with transmission maxima at 452nm and 578nm, and half-widths 7nm and 6nm.

The results are given in tabulated form (Table 2.1). The transmission characteristics for these two interference filters were checked with a Beckman DK-2 automatic recording spectrophotometer (Andrews and Hammond, 1970a), and recently rechecked on a Unicam S.P. 800 spectrophotometer (Fig. 2.1). For the blue and yellow filters the relative quantal

Table 2.1

Optical density values (log. units) obtained from the manufacturer's (Kodak, Wratten) specifications (Nominal values) and those calculated using the calibrated photomultiplier for white light, and narrow-band blue (452nm) and yellow (578nm) lights. The relative quantal difference (N_Y/N_B) denotes the increased quantal transmittance (by 0.29 log. units) of the 578 nm to the 452nm filters.

Table 2.1

Nominal	White	452 nm	578 nm
0.1	0.08	0.08	0.08
0.2	0.21	0.22	0.20
0.3	0.32	0.34	0.31
0.4	0.43	0.46	0.41
0.5	0.44	0.46	0.42
0.6	0.64	0.67	0.62
0.7	0.73	0.77	0.72
0.8	0.86	0.91	0.83
0.9	0.98	1.03	0.97
1.0	1.06	1.12	1.04
1.1	1.14	1.20	1.12
1.2	1.27	1.34	1.24
1.3	1.38	1.46	1.35
1.4	1.49	1.58	1.45
1.5	1.50	1.58	1.46
1.6	1.70	1.79	1.66
1.7	1.79	1.89	1.76
1.8	1.92	2.03	1.87
1.9	2.04	2.15	2.01
2.0	2.07	2.18	2.05

Relative Quantal Difference (N_Y/N_B): 0.29

Fig. 2.1

The transmittance of the narrow-band 452nm and 578nm filters were obtained on a Unicam S.P. 800 Spectrophotometer. As the figure shows there were no secondary peaks within the visual region of the spectrum. The half-band widths for the 452nm and 578nm filters were, respectively 7nm and 6nm.
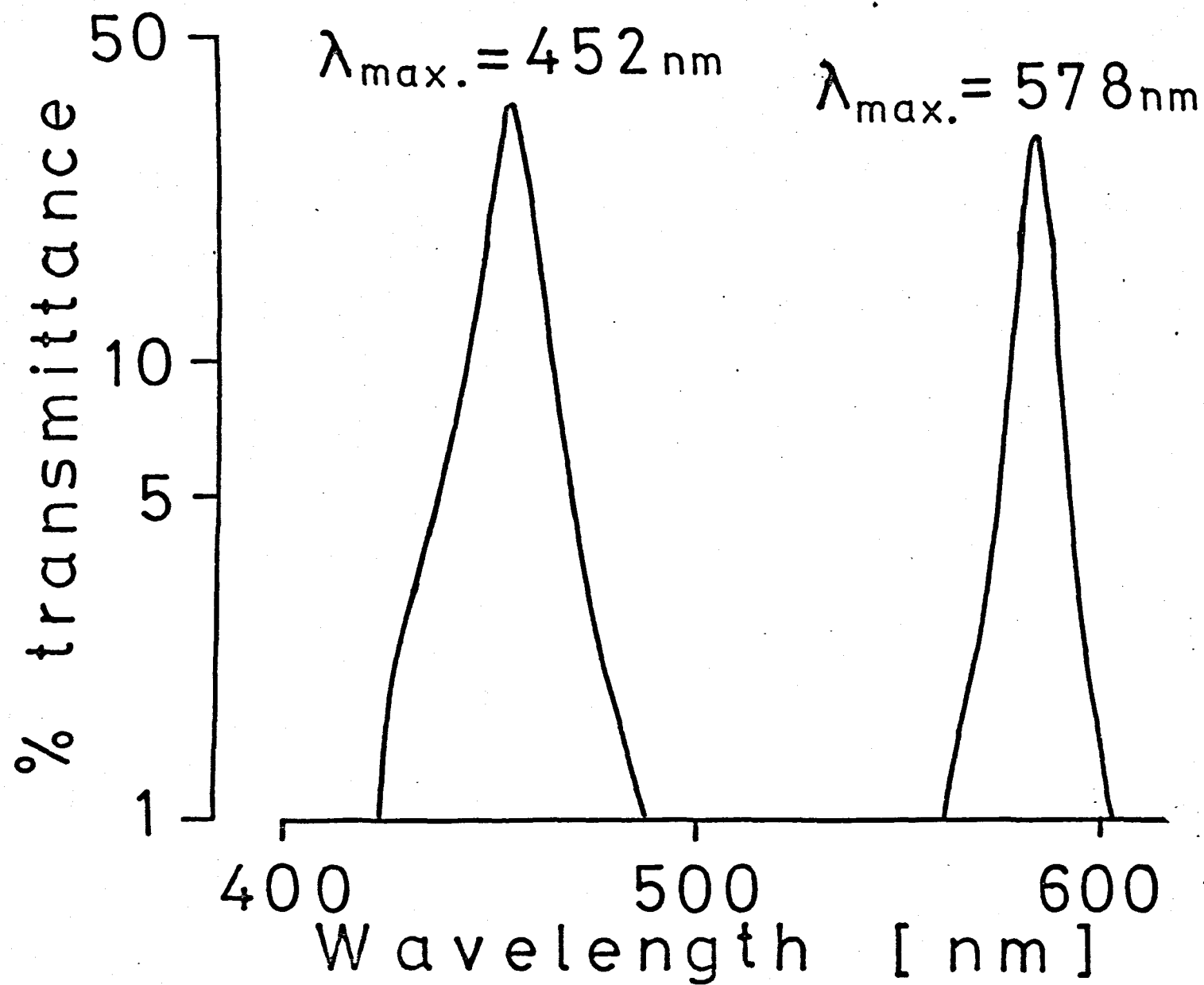
transmission difference was also measured[1].

All these measurements were carried out in a darkened room (background intensity approx. -2.0 log. cd.m^{-2}).

A range of background adapting luminances were obtained by illuminating a matt white, translucent, tangent screen, placed 57in. infront of the cat, by banks of tungsten filament light bulbs. The luminance values of this range, as measured by an S.E.I. photometer, were -0.91, -0.54, -0.24, 0.18, 0.53, 0.87, 1.24, 1.56, and 2.0 log cd.m^{-2}.

2.6 Fibre and cell recordings

Optic tract fibre (OTF) recordings were achieved using high impedance (DC impedance 6-15MΩ, measured in 2.7MKCl solution - the impedance approximately doubling in neural tissue) glass micro-pipettes filled with

---

[1]The total energy (E) measured by the photomultiplier is given by the relationship:

$$E = h \sum_{i=a}^{i=b} n_x v_i \qquad \cdots\cdots\cdots\cdots\cdots\cdots \quad (1)$$

where h is Planck's constant, n_x is the number of photons detected at the frequency v_i, and a and b define the limits of the frequencies transmitted by the source.

By assuming that the transmission of frequencies by these filters was "narrow". Equation (1) can be simplified to

$$E \propto n.h/\lambda \qquad \cdots\cdots\cdots\cdots\cdots\cdots \quad (2)$$

since $v \propto 1/\lambda$, where λ is the wavelength of light.

The total energy readings given by the photomultiplier, E_B and E_Y, for the blue and yellow filters respectively were measured. The relative quantal transmission difference was obtained by rearrangement of equation (2) to give the following relationship:

$$\frac{n_Y}{n_B} = \frac{E_Y \cdot \lambda_Y}{E_B \cdot \lambda_B} \qquad \cdots\cdots\cdots\cdots\cdots \quad (3)$$

where λ_B and λ_Y are the transmission maxima for the blue and yellow filters respectively. The value of the relative quantal difference (n_Y/n_B) measured in this way was +0.29 log. units.

2.7M KCl solution. The electrodes were introduced through a craniotomy
with the dura reflected, zeroed on the cortical surface, and then
vertically moved down under coarse control with a micro-manipulator
(Narishige) to a depth of 18mm (craniotomy centred at H-C coordinates
A=10 and RL=7.0) or 11mm (A=6.0 and RL=10.5). The application of warm
(40°C) 2% agar solution, around the electrode, cooled to form a plug
effectively sealed the craniotomy. This improved the stability of
recordings by limiting the effects of any pulsations. The searching for
optic fibres was accomplished by fine vertical movements of the electrode
using a hydraulic microdrive (backlash < 2μm over a length of 10mm).

Extracellular recordings, from the lateral geniculate nucleus and
intra-retinally from retinal ganglion cells, were carried out using low
impedance (DC impedance 1-3MΩ when measured in the filling solution)
glass micro-pipettes. They were filled with either 4M NaCl solution or
2% pontamine sky blue in 0.9% NaCl solution. Additionally, for intra-
retinal recordings, tungsten-in-glass electrodes constructed by the method
of Merril & Ainsworth (1972) were used.

For geniculate recordings, a craniotomy was centred at A=6.0 and
RL=9.5, and the electrode advanced vertically to a depth of 10mm before
searching for units with fine movements under the control of the hydraulic
microdrive. Details of intra-retinal recordings are given in section 2.7.

2.7 Intra-retinal recordings

2.7.1 Eye preparation

Before surgery, the nitrous oxide/oxygen mixture was replaced by
2-3% halothane-in-oxygen and end-tidal CO_2 was kept between 3.8-4.0%.
Paralysis was not antagonised.

The surgery involved cauterisation of the skin obliquely across from the mid-saggital suture to the eye-lids, and then its reflexion to clear the orbital area. The wound margins were then infiltrated with a local anaesthetic (Xylocaine spray, Astra). Great care had to be taken during the cauterising procedure in order that the corneal surface was not damaged by heat. The tissue (orbital fascia) overlying the scleral surface, the conjunctiva, and the nictitating membrane were removed. To allow the attachment of a brass eye-holder, the size of the exposed scleral surface was increased by snipping off some of the orbital bone. The eye-holder was then attached to the scleral surface using cyano-acrylate tissue adhesive (I.S.-12, Loctite Ltd.). A small puncture, with the hot tip of the cautery unit, was made in the scleral surface through the central bore of the eye-holder without damaging the choroidal surface (Ikeda and Pringle, 1971; H. Ikeda, personal communication). The animal was taken back to the nitrous oxide/oxygen mixture and given 6mg of pentobarbitone intravenously.

2.7.2 Intra-retinal microdrive

The intra-retinal microdrive is a modified version of that described by Ikeda and Pringle (1971). Figures 2.2 and 2.3 show the basic design of this instrument.

To hold the eye rigidly in one position, the brass eye-unit (a) of this instrument consisted on one side of a curved brass section for attachment to the scleral surface by the cyano-acrylate adhesive, whilst the other side was firmly held in the stereotaxic frame. The curved brass section formed centrally a ball joint base for the micro-pipette advancer assembly (h). The weight of the whole instrument was taken up by the guide rail section (j) which was attached to a magnetic "snake"

Fig. 2.2

Intra-retinal microdrive showing separate micro-pipette advancer assembly (h) and brass eye unit (a).

b - stainless steel tube with a ball base which forms a ball joint with the curved section of the eye unit (a).

c - stainless steel micro-pipette guide tube.

d - shaft of the micro-pipette advancer assembly (h).

e - 1mm socket making electrical contact with the electrode.

f - 2ml glass syringe attached to a hydraulic microdrive (not shown).

g - syringe plunger fitted with a perspex piston which has a central bore and a screw-based clamp (for the electrode).

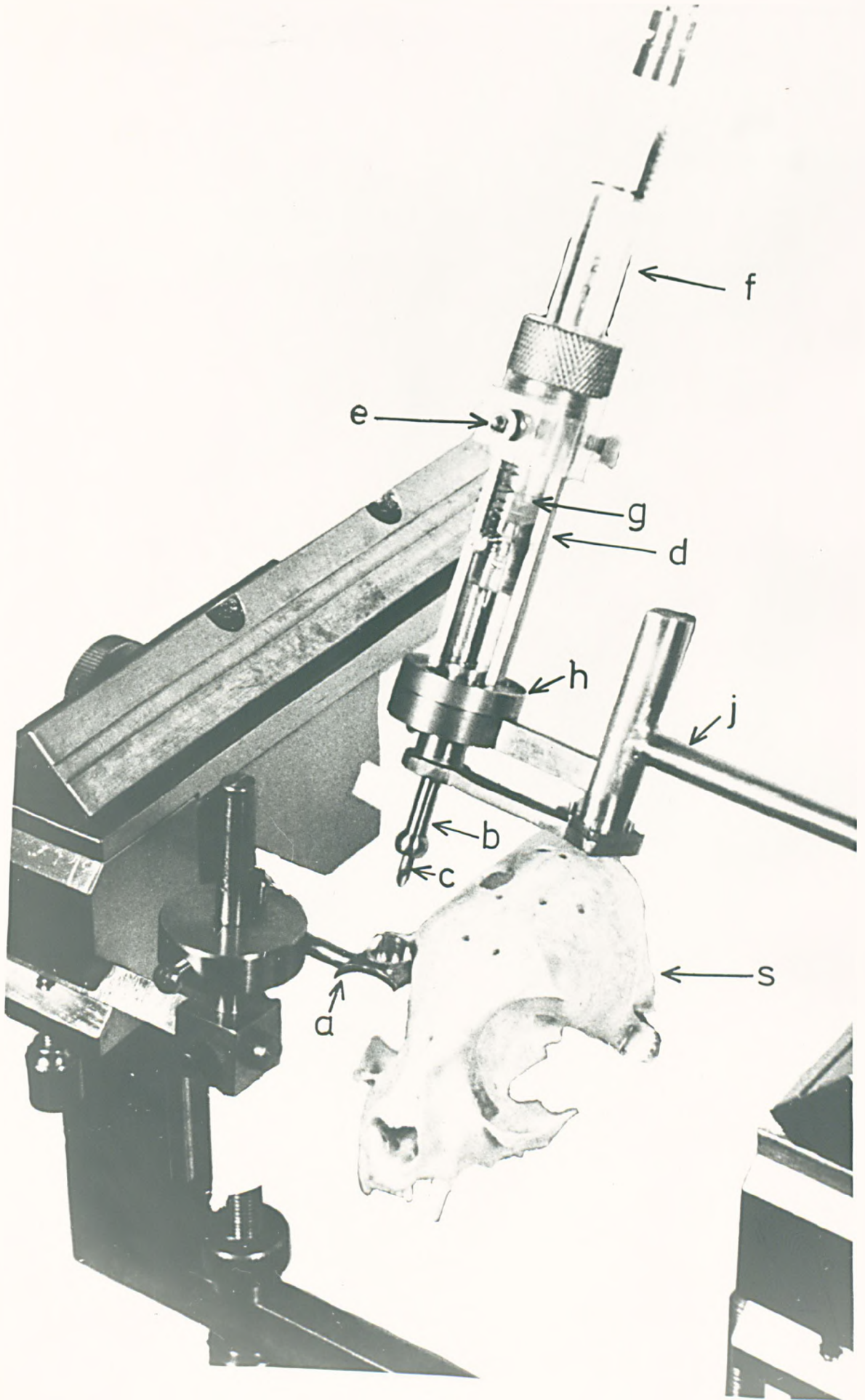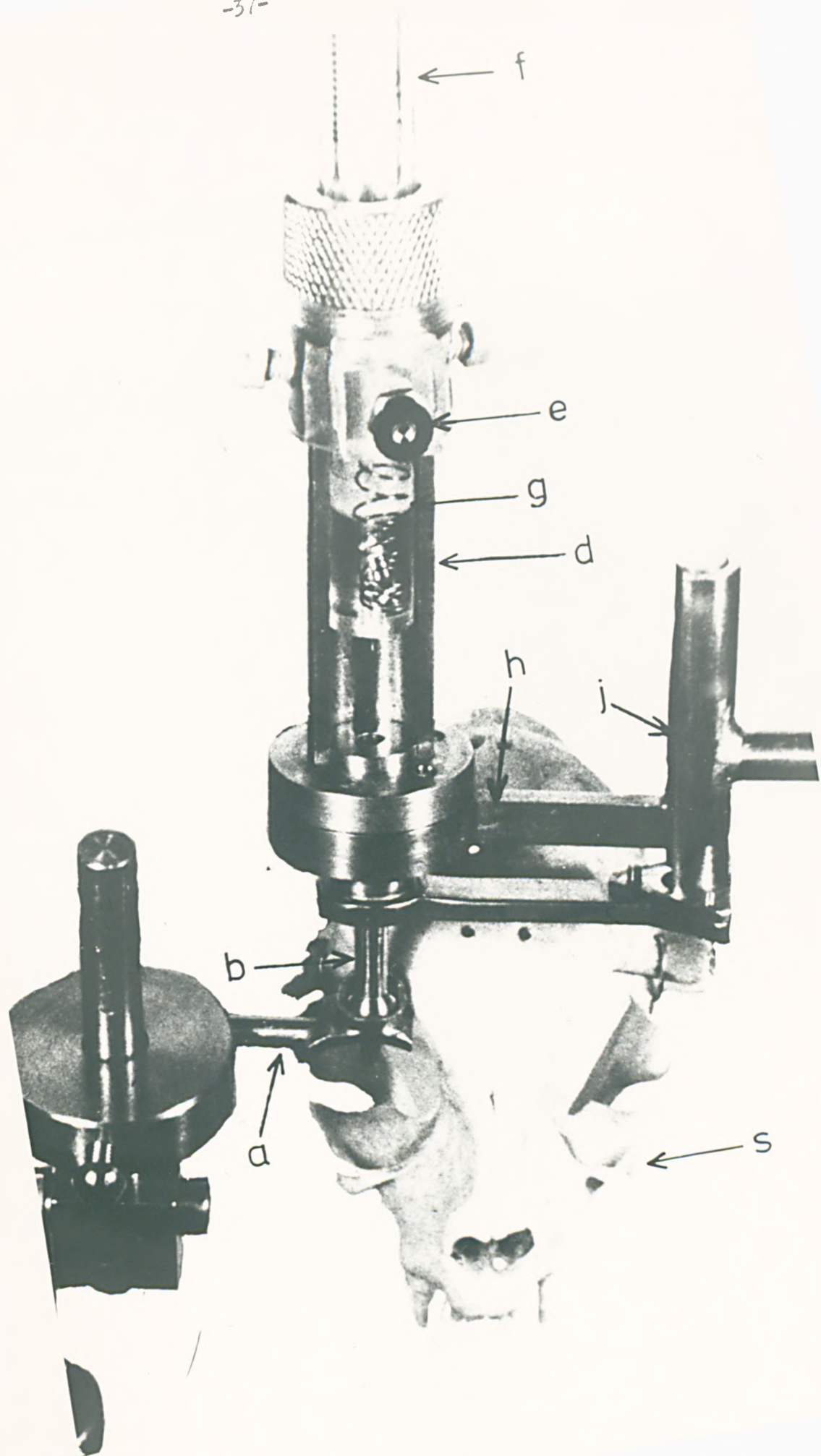j - guide-rail unit.

s - cat skull.

Fig. 2.3

      Intra-retinal microdrive showing the micropipette advancer assembly forming the ball joint with the eye unit. Symbol convention as in Fig. 2.2.

supporting stand (not shown).

2.7.3 Retinal ganglion cell recording

A syringe needle, with its internal bore designed to accommodate either a glass micro-pipette (outer diameter = 1.5mm) or a tungsten-in-glass electrode (outer diameter = 0.13mm), punctured the choroidal surface and entered the vitreous to a depth of 5mm. The electrode was then moved into the vitreous to a depth of 10mm from the scleral surface. The shaft of the electrode was viewed ophthalmoscopically through the pupil, and slowly moved down until the tip was near the vitreal surface of the retina. By back-projecting this region onto the tangent screen, the approximate location of the receptive field was obtained.

Although fine vertical movement was achieved by the hydraulic microdrive, small lateral positional changes of the electrode were accomplished by adjustment of a collar on the magnetic "snake" supporting stand (Polar Hydraulics Ltd.). This procedure gave a circular region on the retina where recording of different cells was made possible. Any major re-location of the electrode required the angle of the electrode holder to be changed.

The advantages of retinal over fibre recordings were:

(i)   stable cell recording for very much longer than was possible with fibres; and

(ii) cell recordings from any particular retinal location.

The disadvantages related to the loss of vitreous from the puncture. This resulted in:

(i)   progressive closing of the pupil which could not be overcome by atropine sulphate administration;

(ii) progressively increasing refractive error; and

(iii) a limit of six to ten hours of recording time following

the introduction of the electrode into the vitreous.

Besides these problems, both retinoscopy and pupil size had to be checked

regularly. As a result, only a few intra-retinal experiments were

carried out and always after OTF recordings from the same animal. This

procedure served both to increase the total retinal unit recordings, and

as an indicator of the condition of the retina by comparing it to fibre

activity and sensitivity.

Chapter 3   GENERAL PROPERTIES OF RETINAL GANGLION

AND LATERAL GENICULATE CELLS

3.1 Introduction

Cleland, Dubin and Levick (1971), Cleland and Levick (1974a,b),
and Cleland, Levick, Morstyn and Wagner (1976) have suggested a
classification scheme for RGCs and LGCs based upon:

(i)   the spatial organization of the receptive field, and

(ii) the responses elicited by a series of tests (some tests are
described in section 3.2.1).

This scheme subdivides the receptive fields into the concentric and non-
concentric categories. Units in the concentric category (concentric
units) have the centre-surround type of receptive field organization
described originally by Kuffler (1953), and comprise on- or off-centre
brisk and sluggish cells in the sustained and transient classes (Cleland
and Levick, 1974a). The non-concentric category incorporates all other
units, i.e. edge detectors, uniformity detectors, colour coded units, etc.
(Cleland and Levick, 1974b). This classification scheme is here adopted
in preference to the WXY scheme (Enroth-Cugell and Robson, 1966; Stone and
Hoffmann, 1972; Stone and Fukuda, 1974; Rowe and Stone, 1977) because of
the simplicity of the tests and the rapidity with which units could be
classified.

All recorded units were classified according to their:

(i)   responses to standing contrast, periphery effect, and square-wave
gratings,

(ii) maintained discharge rates,

(iii) RFC sizes, and

(iv) spatial organization of the receptive fields.

This chapter specifically compares and contrasts these properties:

(i)   between the different classes of units, and

(ii) with other reports in the literature.

3.2 Procedure

Except as detailed below, procedure was as described in the preceding chapter.

3.2.1 Classification tests

After pinpointing the receptive field location on the tangent screen, the unit was classified according to the scheme of Cleland and Levick (1974a,b) using some of the tests described by Cleland, Dubin and Levick (1971) and Cleland and Levick (1974a): viz. standing contrast, periphery effect, discharge rate, and moving square-wave grating.

Standing contrast test. A light spot (usually $\frac{1}{2}°$ or $1°$ in diameter) approximately 1 log. unit above centre threshold was projected onto, or a black disk ($1°$ or $2°$ in diameter) was unmasked at, the most sensitive region of the RFC for approximately 30 s. The spike rate before, during, and after presentation was recorded on a linearised Washington MD2 pen-recorder. This test alone was always adequate to distinguish between on- and off-centre units, and usually sufficient to decide between sustained and transient units. A distinguishing feature for sluggish sustained units (as reported by Cleland *et al*, 1974a) was the reduction and sometimes absence of a clear, initial transient burst of spike activity before the maintained component of the discharge.

Periphery effect. Movement of a black card ($10°$ by $10°$) remote from the receptive field of the unit caused a modulation of the spontaneous discharge (McIlwain, 1964, 1966; Levick, Oyster, and Davis, 1965). This effect was always strong in brisk transient and weak or absent in brisk and sluggish

sustained, and sluggish transient units (Cleland, Dubin and Levick, 1971; Cleland and Levick, 1974a; Ikeda and Wright, 1972a; Barlow, Derrington, Harris and Lennie, 1977).

Discharge rate. The spike rate was recorded at the mid-mesopic adapting level of +0.53 log. cd.m^{-2}. Cleland and Levick (1974a) point out that sluggish units can be distinguished from brisk by their lower discharge rate.

Square-wave grating. Gratings of various spatial frequencies ($\frac{1}{4}$, $\frac{1}{2}$, 1, 2 and 4 cycles deg.$^{-1}$) were moved across the receptive field in order to determine each unit's highest resolving frequency (the highest spatial frequency for which a modulated discharge was apparent to sequential light and dark bars crossing the receptive field). In some units, the response to the passage across the receptive field of a grating with spatial frequency higher than the unit could resolve was recorded.

3.2.2 RFC areas

RFC mapping and area determinations are detailed in Chapter 4. Briefly, the threshold (section 4.2.2) for a small-diameter, flashing light spot (presented for 400ms every 1.6 s) placed in the most sensitive region of the RFC was determined. The RFC was then defined by iso-sensitivity points around the most sensitive region (section 4.2.3) using a spot intensity 1 log. unit above centre threshold. RFC area was then calculated (section 4.3.5).

3.3 Results and Discussion

3.3.1 Retinal study

Out of a total of 610 units, 564 possessed concentric receptive

fields - 370 brisk sustained (on-: off-centre, 240:130), 17 sluggish sustained (on-: off-centre, 10:7), and 177 brisk transient (on-: off-centre, 116:61). Of the remaining 46, 6 possessed non-concentric receptive fields (see section 3.3.6) and the rest (n = 40) were not classified (see section 3.3.7).

3.3.2 Standing contrast test.

The spike activity of RGCs was recorded before, during, and after the presentation of a circular contrasting target (black disk for off-centre and light spot for on-centre units) within the RFC. The majority of units could be clearly distinguished as brisk sustained or transient by this test. Fig. 3.1 shows the firing rate for such units. The effects of intensity differences, size and position of the light spot in the RFC, on the response profile were considered specifically for on-centre units.

For brisk sustained units, both the initial transient and the sustained components of the response could be altered in strength by increasing spot intensity or size, although the general response profile was not greatly influenced between 1.0 and 2.0 log. units above centre-threshold (Ikeda and Wright, 1972a).

The effect of imperfect centring of the light spot within the RFC had little influence on the sustained component but profoundly affected the initial transient component of the discharge to the extent that the latter could be abolished or much reduced in strength. For brisk transient units the effect of intensity, size, and position of the light spot changed the strength of the initial transient burst of spike activity but had little, if any, effect on the response during the remaining duration of presentation.

Response profiles of all cells, obtained from the region of maximal

Fig. 3.1

Response to standing contrast for brisk sustained and transient, on- and off-centre, units.

For on-centre units a light spot ($\frac{1}{2}°$ in diameter and at approximately 1.0 log. units above centre threshold) was presented for approximately 30s. The duration of presentation is shown by the upward deflection of the continuous line below each response profile.
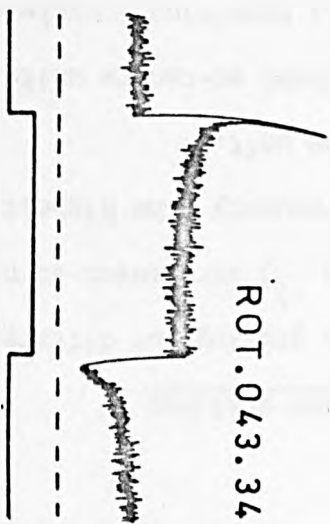
For off-centre units a black disk ($1°$ in diameter) was unmasked, and the duration of presentation is shown by the downward deflection.

The dashed line represents the zero level of discharge rate. The time constant of the rate meter was 80ms.
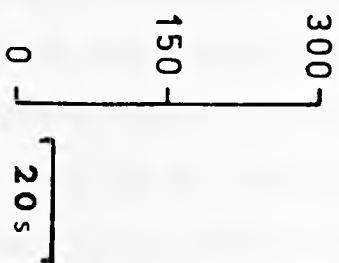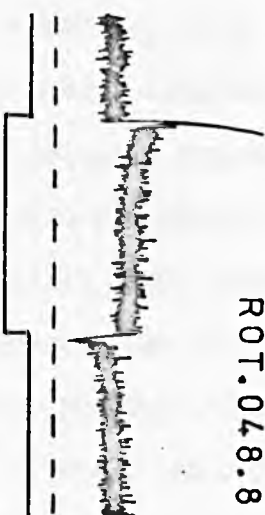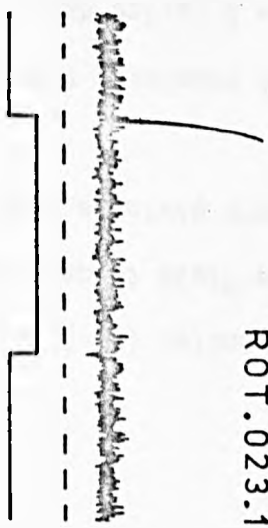
Brisk Transient

Brisk Sustained

On-centre

ROT.023.1

ROT.043.34

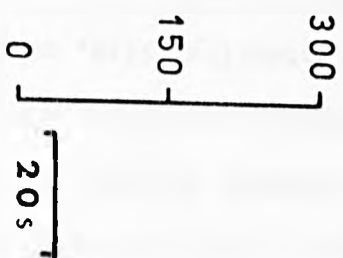Spikes s^{-1}

Spikes s^{-1}

0 150 300

0 150 300

20s

20s

Off-centre

ROT.045.1

ROT.048.8

sensitivity within the RFC, using an intensity of 1.0 log. unit above centre-threshold, exhibited a continuum from brisk sustained to brisk transient. Fig. 3.2 shows examples of this gradual change in the response profiles. This change, although not related to eccentricity of the unit from the area centralis, was correlated with the strength of the periphery effect (McIlwain, 1964, 1966; Levick, Oyster and Davis, 1965). A remote stimulus caused no perceptible change in the maintained activity of units with the type of response profiles shown at the top of Fig. 3.2 (e.g. ROT. 43.33.S+), a weak periphery effect for units with intermediate response profiles (e.g. ROT. 38.21.S+), and a strong effect for those with response profiles as shown at the bottom of Fig. 3.2 (e.g. ROT. 40.25.T+).

Sluggish sustained units (on-: off-centre, 10:7) were distinguished from the brisk units on the basis of their response profiles. They showed little or no initial transient to presentation of the contrasting target. This difference was not related to intensity, size, or mislocation of the stimuli in the RFC. In addition, sluggish units displayed only very weak or imperceptible periphery effects. These findings are in agreement with those of Cleland and Levick (1974a).

3.3.3 Square-wave gratings

Square-wave gratings of different spatial frequencies ($\frac{1}{4}$, $\frac{1}{2}$, 1, 2 and 4 cycles deg.$^{-1}$) were moved across the receptive field to determine the resolving frequency (the highest spatial frequency giving a modulated response) for the unit.

Brisk sustained on-centre units had the highest resolving frequencies, with the majority resolving 1 cycle deg.$^{-1}$ and a few 2 cycles deg.$^{-1}$. Brisk transient and sluggish sustained, on- and off-centre, and brisk sustained off-centre units had a maximum resolution of 1 cycle deg.$^{-1}$

Fig. 3.2

Response to standing contrast for brisk sustained (S) and transient (T) on-centre (+) units. The eccentricity (Ecc.) from the area centralis is given in degrees for each unit.

Data have been selected to show the progressive decline of the sustained component of the response, i.e. the continuous change from sustained to transient response profiles. Conventions are as in Fig. 3.1.
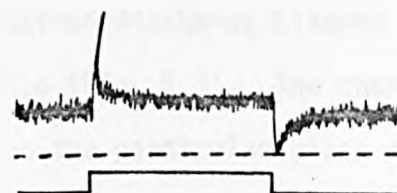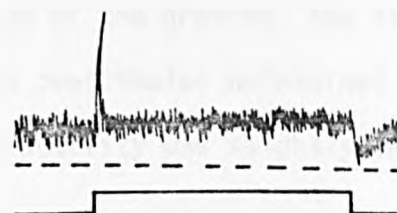
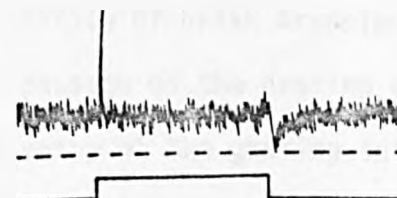ROT.43.33.S+
Ecc. = 21°

ROT.47.9.S+
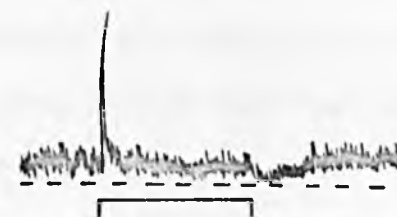Ecc. = 25·9°
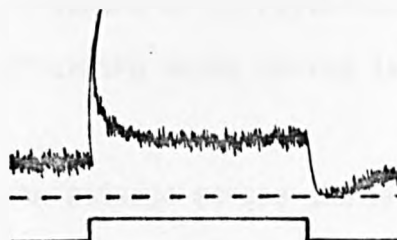
ROT.43.31.S+
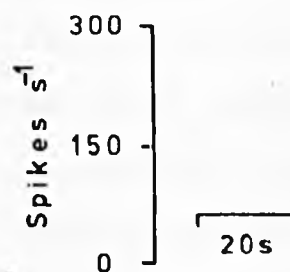Ecc. = 17·2°

ROT.38.21.S+
Ecc. = 23·1°

ROT.41.37.T+
Ecc. = 18·3°

ROT.41.14.T+
Ecc. = 20·2°

ROT.40.25.T+
Ecc. = 15·6°

Spikes s^{-1}

300

150

0

20s

although the majority of units could only resolve the $\frac{1}{2}$ cycle deg.$^{-1}$ grating. In general, the present findings support previous results (Cleland *et al* 1971, 1974a) in showing that transient units have a lower spatial resolving power than sustained units. The discrepancy between the on- and off-centre brisk sustained data is probably correlated with the off-centre units having larger RFCs (see section 3.3.5).

The response to the passage across the RFC of a square-wave grating of spatial frequency higher than the unit could resolve was also recorded. In all units the maintained discharge altered as the grating entered and left the receptive field (Fig. 3.3). The change in the maintained activity was related to the particular class of unit. The brisk sustained on-centre units gave a complex response profile (as shown for ROT. 50.03.S+) and, during the passage of the grating, the discharge rate remained fairly constant but below the prestimulus maintained level. For brisk sustained off-centre units, the activity was slightly increased during grating motion.

The maintained activity of brisk transient on-centre units was strongly attenuated during the passage of the grating compared with brisk sustained on-centre units. The entry of the grating into the receptive field caused a sharp fall in activity whilst its removal restored the prestimulus level. The brisk transient off-centre units differed from the brisk transient on-centre units in that their maintained activity was elevated during the passage of the grating.

These results conflict with those of Cleland *et al.* (1971, 1973, 1974a), who found that, when the spatial frequency of a moving grating was not resolved, brisk sustained units showed no change in activity, whereas brisk transient units gave an unmodulated increase in mean discharge.

Fig. 3.3

Passage of a square-wave grating across the receptive field.
The figure shows the effect on the maintained activity of brisk
sustained (S) and transient (T), on- (+) and off-centre (-),
units to a square-wave grating of spatial frequency (S.F. in
cycles deg.$^{-1}$) higher than the units could resolve. The upward
deflection of the continuous line denotes movement of the grating
in one direction and the downward deflection movement in the
opposite direction. Conventions as in Fig. 3.1 and 3.2.

ROT.50.03.S+
Ecc. = 5·7°
S.F. = 4
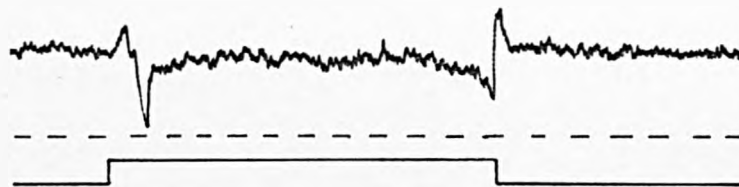
ROT.50.19.S-
Ecc. =10·5°
S.F. = 2

ROT.50.11.T+
Ecc. = 13·2°
S.F. = 1

ROT.50.21.T-
Ecc. = 14·9°
S.F. = 1

200 spikes s^{-1}

5 s

3.3.4 <u>Maintained discharge rate</u>
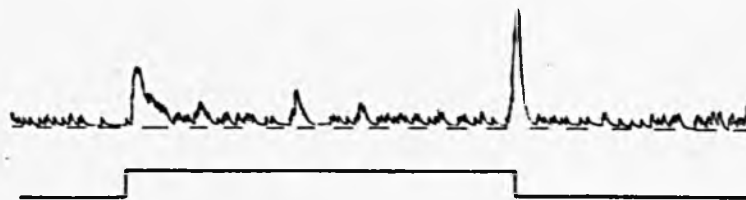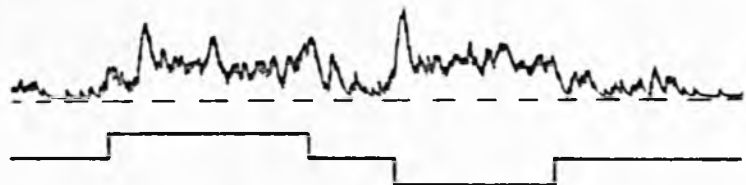
The steady maintained discharge, at a fixed background adapting level of +0.53 log. cd.m^{-2}, was measured for the brisk transient and sustained, and sluggish sustained classes. The mean values of the maintained discharge were calculated separately for on- and off-centre units in each class and for the two anaesthetic preparations used - nitrous oxide/oxygen (supplemented by I/V pentobarbitone), and pentobarbitone respectively. The results are shown in Table 3.1.

(i) In the brisk sustained and transient classes, on-centre units have a significantly[1] higher maintained firing rate than off-centre units.

[1]Under nitrous oxide/oxygen anaesthesia:

(i) brisk sustained on-centre units (n=75) have a mean discharge rate of 63.1±2.2 spikes s^{-1} and off-centre units (n=60) a mean rate of 43.8±1.8 spikes s^{-1}. The calculated t value, using the two sample student t-test, was 6.55, and from tables $t_{0.05, 133}$ = 1.66. Therefore the difference is significant at the 5% level.

(ii) brisk transient on-centre units (n=53) have a mean discharge rate of 45.0±3.7 spikes s^{-1} and off-centre units (n=18) have a mean rate of 21.6±5.2 spikes s^{-1}. The calculated t value was 3.38 and from tables $t_{0.05, 69}$ = 1.67. Hence, the difference is significant at the 5% level.

Under pentobarbitone anaesthesia:

(i) On- and off-centre brisk sustained units have significantly different mean discharge rates, respectively of 40.6±2.8 and 24.4±3.2 spikes s^{-1}, since the calculated t value was 3.34 and, from tables, $t_{0.05, 59}$ = 1.67.

(ii) On- and off-centre brisk transient units have mean discharge rates, respectively of 18.9±4.1 and 9.0±2.9 spikes s^{-1}. The calculated t value was 2.83 and from tables $t_{0.05, 19}$ = 1.73. Hence, the difference was significant at the 5% level.

Table 3.1

The mean maintained activity at the +0.53 log. cd.m^{-2} background adapting level is shown under two anaesthetic regimes - $N_2O:O_2$ (supplemented by pentobarbitone), and pentobarbitone. The mean firing rates for brisk sustained (S) and transient (T), and sluggish sustained (S^S), on- (+) and off-centre (-), units are shown separately. The ± value denotes 1 S.E.M.

Table 3.1

ANAESTHETIC REGIME	CLASS	S+	S-	T+	T-	S^S+	S^S-
$N_2O{:}O_2$	No. of UNITS	75	60	53	18	10	7
	MEAN DISCHARGE RATE	63.1	43.8	45.0	21.6	31.0	29.2
	(Spikes s^{-1})	±2.2	±1.8	±3.7	±5.2	±4.6	±9.3
PENTOBARBITONE	No. of UNITS	43	18	16	5	-	-
	MEAN DISCHARGE RATE	40.6	24.4	18.9	9.0	-	-
	(Spikes s^{-1})	±2.8	±3.2	±4.1	±2.9	-	-

(ii) Brisk on- and off-centre sustained units have a significantly[1] higher firing rate than the brisk on- and off-centre transient units respectively.

(iii) Sluggish on- and off-centre sustained units have similar maintained firing rates[2].

(iv) Comparison between the two anaesthetic regimes shows that the maintained activity is reduced markedly in the pentobarbitone preparation. This decrease in maintained discharge may possibly be related to the state of arousal of the animal. Certainly, the EEG activity in the pentobarbitone preparation has a distinctly different pattern (large amplitude, slow-wave activity alternating periodically with small amplitude, fast-wave activity) from the nitrous oxide:oxygen preparation (large amplitude, slow-wave activity superimposed on small amplitude, fast-wave activity). In the latter preparation, supplementation with small I/V doses of pentobarbitone was required to maintain anaesthesia.

Stone and Fukuda (1974a), using nitrous oxide/oxygen, give the mean maintained firing rates for:

(i) on- and off-centre X (sustained) units as 49 and 39 spikes s^{-1}, and

---

[1] In the nitrous oxide/oxygen preparation:

(i) for on-centre sustained and transient units, the calculated t value was 4.71 and from tables $t_{0.05, 126} = 1.66$; and

(ii) for off-centre sustained and transient units, the t value was 5.46 and from tables $t_{0.05, 76} = 1.67$.

In the pentobarbitone preparation:

(i) for on-centre sustained and transient units, the t value was 4.29 and from tables $t_{0.05, 57} = 1.67$; and

(ii) for off-centre sustained and transient units, the t value was 2.73 and from tables $t_{0.05, 21} = 1.72$.

Hence, in all cases, the difference in discharge rates was statistically significant at the 5% level.

[2] On-centre sluggish sustained units have a mean discharge rate of 31.0+ 4.6 (n=10) and off-centre units have a mean rate of 29.2+9.3 (n=7). The calculated t value was 0.21 and from tables the $t_{0.05, 15} = 1.75$. Therefore, the difference is non-significant at the 5% level.

(ii) on- and off-centre Y (transient) units as 33 and 17 spikes
 s^{-1}, respectively.

The general trends in the firing rates, from Stone and Fukuda's data,
are similar but reduced in magnitude compared with the present study.

Recently, Pollack and Winters (1978) have looked at the maintained
activity of X and Y RGCs at six different adapting levels in lightly-
anaesthetised cats.[1] Their results show that, apart from low background
adapting levels (-1.71 and -2.71 log. cd.m^{-2}), X units have a higher
maintained firing rate than Y units. Unfortunately, these authors:

(i) combined their data for on- and off-centre units, and

(ii) used adapting levels of 0.28 and 1.28 log. cd.m^{-2}.

Hence, in order to compare their results with those in Table 3.1, the
mean maintained activity for X and Y units at these two adapting levels
was calculated as 48.3 (n=19) and 24.7 (n=18) spikes s^{-1} respectively.
From the data in Table 3.1, the mean activity for sustained and
transient units is 53.5±2.1 (n=135) and 33.3±4.5 (n=71) respectively,
in good agreement with Pollack and Winters (but see footnote 4).

Cleland, Levick and Sanderson (1973), using nitrous oxide/oxygen
anaesthesia, found that at 1.0 log. cd.m^{-2} adapting level the mean
discharge rates of on- and off-centre:

(i) brisk sustained units were 33.3 (n=19) and 15.0 (n=17)

---

[1]Pollack and Winters (1978) refer to Winters, Hickey and Pollack (1973)
for the anaesthetic regime. Winters, Hickey and Pollack used a
pentobarbitone preparation with the anaesthetic given intravenously.
In the present study, pentobarbitone was given by intra-peritoneal
injection with intravenous supplementation. A comparison between
Pollack and Winters' values and those derived from the pentobarbitone
data of Table 3.1 (S± = 35.8; T± = 16.5) shows that the maintained
activity was higher for the two classes in their data.

spikes s^{-1} respectively, and

(ii) brisk transient units were 17.7 (n=9) and 4.4 (n=18) spikes s^{-1}, respectively.

The trend is similar to Table 3.1 although rates are lower overall.

Cleland and Levick (1974a) note that sluggish sustained units tend to have maintained activities of less than 10 spikes s^{-1}, rates again lower than for the limited data for on- and off-centre sluggish units in Table 3.1.

3.3.5 RFC areas

The RFCs were mapped using the iso-sensitivity technique (Chapter 4, section 4.2.3) and the areas calculated (Chapter 4, section 4.3.5). Out of the total sample (n=610), 90 units were successfully mapped - 62 brisk sustained (on-: off-centre, 40:22) and 28 brisk transient (on-: off-centre, 21:7). The RFC areas of these units are plotted against their eccentricity from the area centralis in Fig. 3.4.

In support of previous studies (Wiesel, 1960; Ikeda and Wright, 1972b), the data show a systematic increase in RFC area with eccentricity. Furthermore, sustained units have smaller RFC sizes than transient units for a given eccentricity from the area centralis (Ikeda & Wright, 1972a; Cleland et al., 1973, 1974a; Stone & Fukuda, 1974a; Hammond, 1974).

As Fig. 3.4 A shows, the off-centre brisk sustained units have much larger centre areas (dashed line) than on-centre brisk sustained units (continuous line). These results corroborate the general trend obtained by Hammond (1974), but the magnitude of the differences in this study is much larger.

Fig. 3.4

Scatter of RFC areas with eccentricity from the area centralis.

A - sustained units. The linear regression lines for on-
    (S+) and off-centre (S-) data are shown by the
   continuous and dashed lines, respectively.

B - transient units. The linear regression line is for
    both on- (T+) and off-centre (T-) data.

One transient off-centre unit (shown by ⊗) resembled both:

(i) a sluggish type - possessed low maintained discharge
    (≈ 10 spikes s^{-1}) and small RFC area (0.4 deg.^{2}) - and

(ii) a brisk type - possessed strong periphery effect and
    brisk response to the contrast test.

In this figure, the best fit regression lines have been
drawn for the data. For the off-centre brisk sustained data,
because of the limited sample size the dashed line (Fig. 3.4 A)
erroneously crosses the continuous line (for on-centre brisk
sustained data) and the abscissa. The author does not wish to imply
from this that off-centre brisk sustained units:

(i) are absent from the area centralis, or

(ii) have smaller RFCs compared with on-centre brisk sustained
    units in the vicinity of the area centralis.
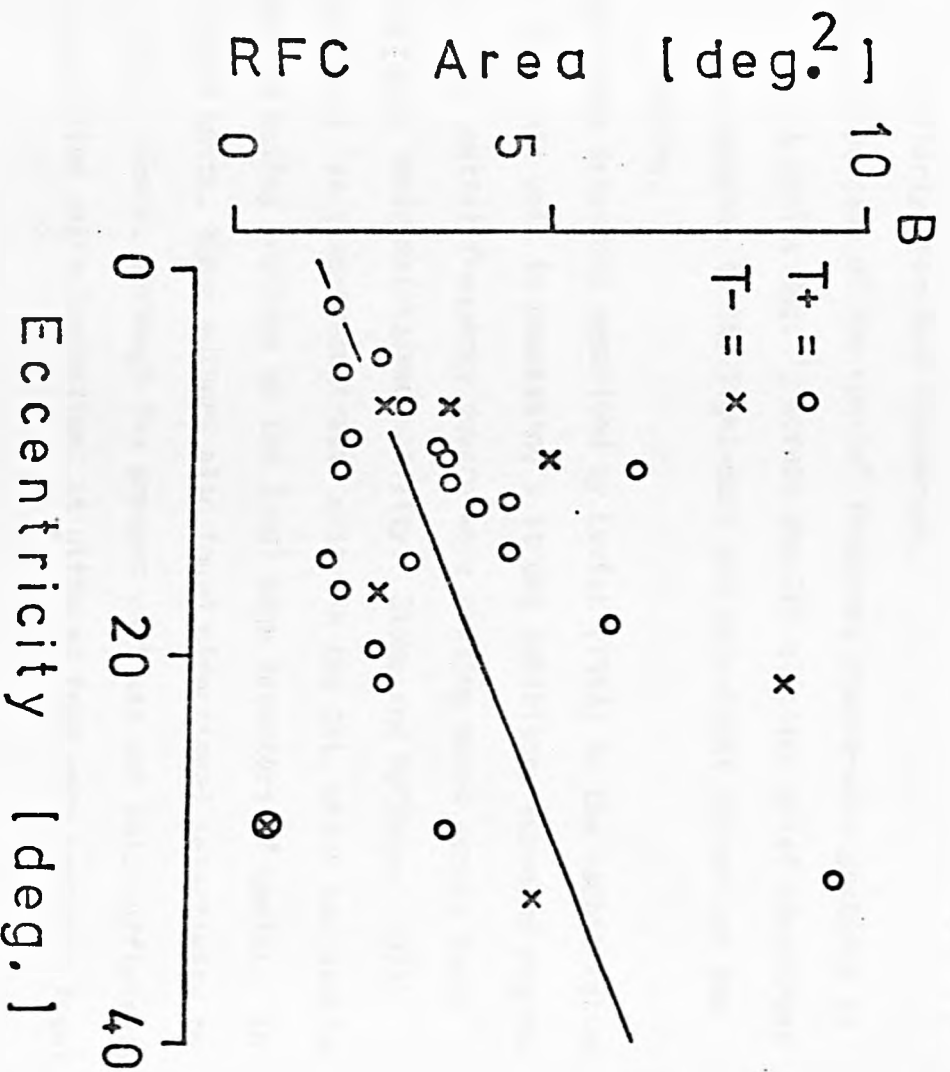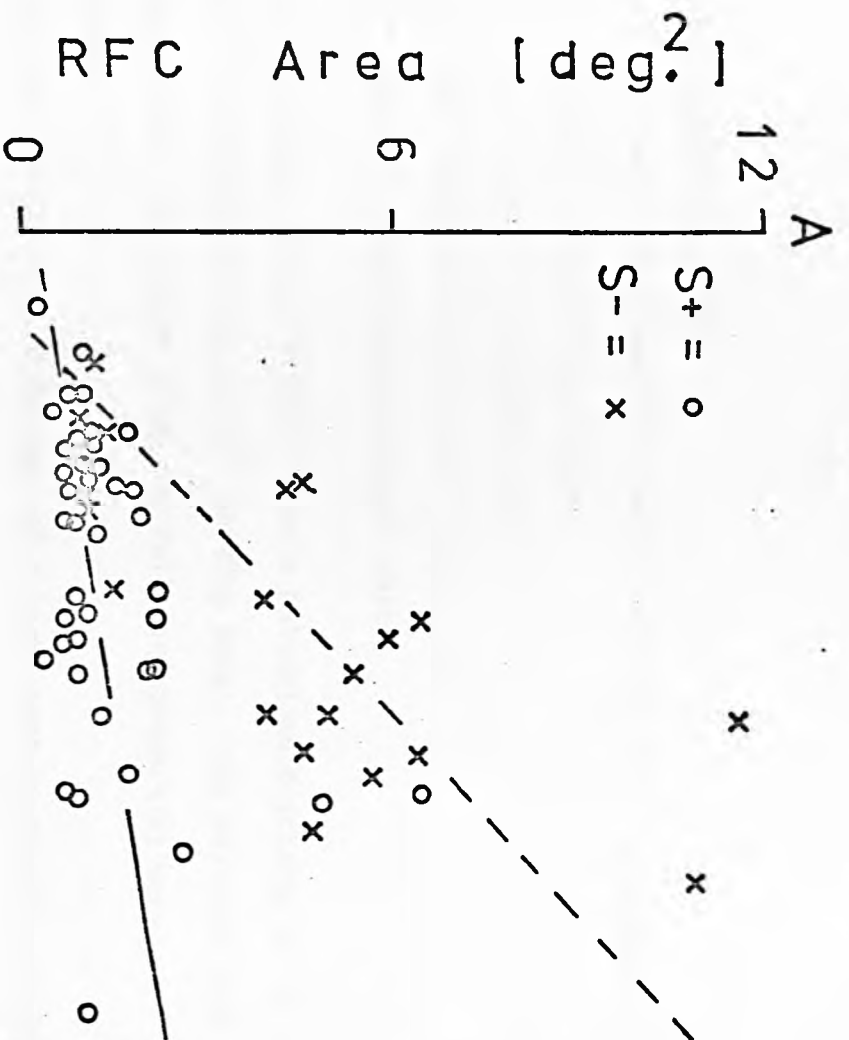
3.3.6 Non-concentric units

Six units with non-concentric fields were classified according to their responses to contrasting targets:

(i)   an "excited-by-contrast" unit,

(ii) two "suppressed-by-contrast" units, and

(iii) three "vertical-edge-detector" units.

Excited-by-contrast unit. This unit had a maintained discharge of 20 spikes s^{-1} at the +0.53 log. cd.m^{-2} adapting level. The unit was held for a very short time during which the following properties were established.

(i)   Presentation and withdrawal of a light spot in the RFC elicited transient discharges at onset and offset.

(ii) Presentation and removal of a black disk in the RFC, elicited similarly transient discharges.

(iii) The passage of low spatial frequency square-wave gratings ($\frac{1}{4}$ and $\frac{1}{2}$ cycles deg.$^{-1}$) across the RFC elicited brief discharges in response to the light-dark and dark-light borders of the grating.

The local edge detectors described by Levick (1967) in the rabbit retina differ from this unit in possessing a strong inhibitory surround region. Hence, a low spatial frequency square-wave grating moved across their RFCs depressed their maintained activity. Stone and Hoffmann (1972) have described "excited-by-contrast" units in the cat, which had similar responses to moving gratings as the local edge detectors of Levick. In two of these units, these authors also found directional selectivity to moving spots. Hence, although the present unit was not held sufficiently long for detailed characterisation, it differed from both Levick's local

edge detectors and Stone and Hoffmann's excited-by-contrast units.

Suppressed-by-contrast units. These units had high maintained discharge rates of approximately 60 spikes s^{-1}. The presentation of a contrasting target (black disk or light spot) caused a long latency depression in the maintained discharge which then rose to a level below the original pre-stimulus level. On removal of the target, the activity was again transiently depressed before returning to the pre-stimulus level. Fig. 3.5 shows these changes in activity for a $\frac{3}{4}$° and 2° light spot, and a 2° black disk.

Rodieck's (1967) and Stone and Hoffmann's (1972) suppressed-by-contrast units differ from those described here, since the activity of their units remained depressed throughout stimulation, returning to the pre-stimulus level at extinction. Cleland and Levick (1974b) describe "uniformity detectors", which exhibit transient suppression of activity, lasting some 200ms, to the presentation and subsequent removal of contrasting targets. Hence, the present suppressed-by-contrast units seem to have properties intermediate between the types described by Rodieck (1967) and Stone and Hoffmann (1972), and by Cleland and Levick (1974b).

Vertical-edge-detector units. These units had low maintained activity of approximately 20 spikes s^{-1}. Their receptive fields were strongly elongated in shape, with an excitatory "on" region (some 2° wide and 20° long) bounded on all sides by a silent inhibitory (suppressive) surround. The receptive fields of all three units were located inferiorly in the visual field, along the zero vertical meridian, extending from a few degrees below the projection of the area centralis. The following responses were elicited from these units.

Fig. 3.5

Responses of a suppressed-by-contrast unit to standing contrast. The presumed RFC size of the unit is shown by the dashed circle. The open and filled circles lying within the dashed circles represent dimensions of the light spot and black disk, respectively. The duration of stimulus presentation is shown by an upward (for light spot) or downward (for black disk) deflection of the continuous line below the response profiles.

A and B show the effect on the unit's maintained activity of the presentation and subsequent removal of a $\frac{3}{4}°$ and 2° diameter light spot, respectively. C shows the effect for a 2° diameter black disk.

Dashed line denotes zero level of spike activity.

A

60 Spikes s^{-1}

10 s

B

60 Spikes s^{-1}

10 s

C

60 Spikes s^{-1}

10 s

-56-
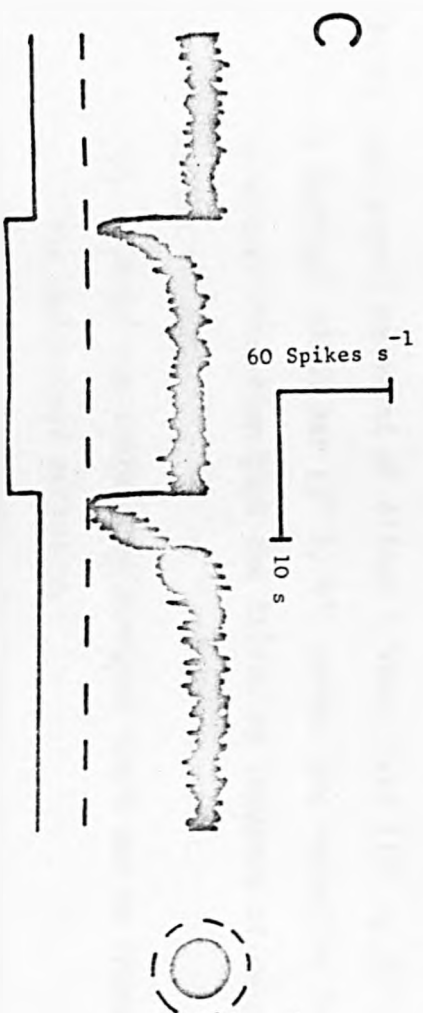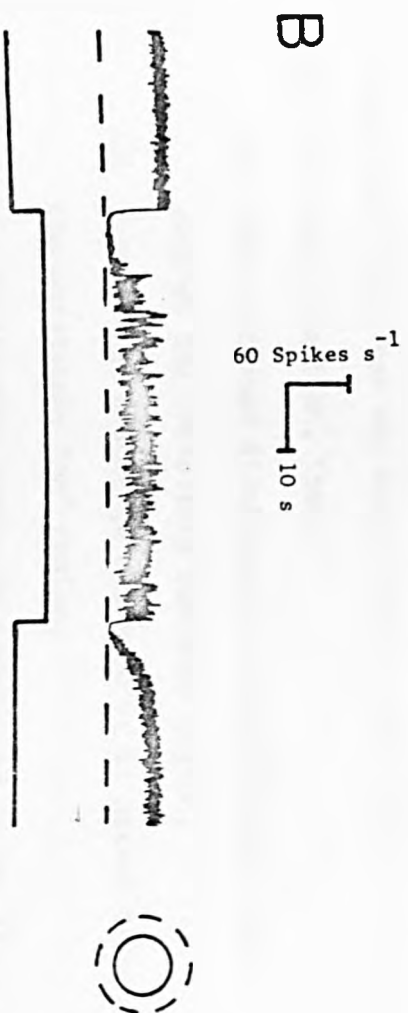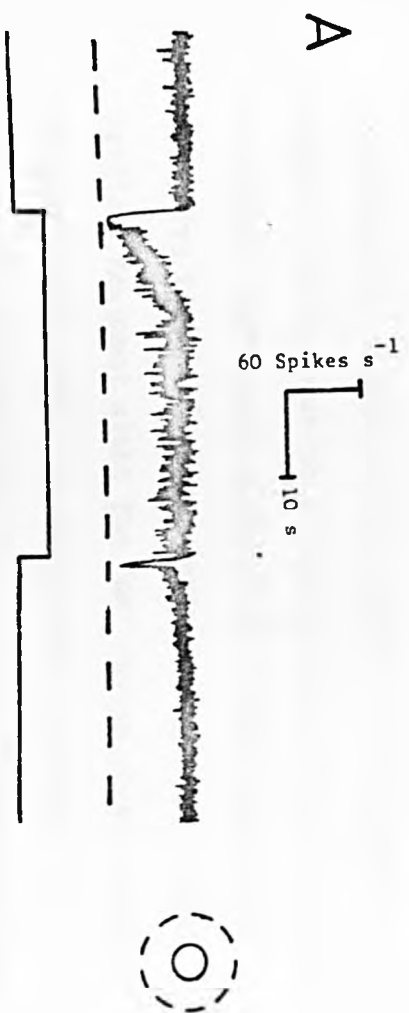
(i) A flashing light spot (1° in diameter) elicited transient discharges at stimulus onset within the elongated "on" region, and suppression of maintained activity from the surround. Horizontal movement of a light spot across the receptive field evoked a transient discharge, whilst vertical movement along the "on" region gave a sustained discharge well above the maintained activity.

(ii) A vertical, flashing light bar (½° by 4°) gave the same results as the light spot, but the magnitude of effects was greater.

If a vertical light bar was moved horizontally across the receptive field in either direction, then:

   (a) the maintained discharge was suppressed as the bar entered the inhibitory surround region,

   (b) a transient discharge occurred as it passed through the excitatory "on" region,

   (c) the firing rate was again suppressed as the light bar entered the second inhibitory surround, and

   (d) the maintained discharge returned to the pre-stimulus level as the bar left the inhibitory region.

(iii) Horizontal movement of either a black card (10° by 10°) or a vertical black bar (½° by 4°) across the receptive field in either direction gave the following sequence of responses. As the target:

   (a) entered the inhibitory surround there was no change in the maintained activity,

   (b) entered the excitatory "on" region, the maintained activity was suppressed, and

(c) left the excitatory "on" region, a transient discharge occurred.

Hammond (1974) has described an "orientation-specific" unit with exactly the same receptive field position, shape, and organization.

3.3.7 Unclassified units

A total of 40 units could not be classified, because they were held only briefly or because the location of their receptive field could not be determined. In the latter case, the maintained firing rate could be altered by either changing the ambient background luminance or by flashing a large diameter light spot on the tangent screen. These units probably had peripheral receptive fields, obscured by the 5mm diameter artificial pupil's annular stop and/or the corrective lens holder. Evidence in support of this assumption was obtained for one unit by removing both the artificial pupil and the lens holder. The RFC was then found to be located in the far periphery, approximately 75° from the projection of the area centralis and 15° above the horizontal meridian in the contralateral visual hemi-field (left eye, nasal retina).

3.4.1 Geniculate study

A total of 105 lateral geniculate cells (LGCs) were recorded mainly from laminae A and A_1. From this sample 94 units could be classified, using the scheme of Cleland et al. (1971), as sustained units (37; on-: off-centre, 28:9) or transient units (57; on-: off-centre, 31:26). Of the remaining 11 units, 9 gave transient on-off responses to a flashing spot in the RFC (these have been denoted in the text by T±), one was direction selective, and the other had adjacent on and off regions surrounded by a silent inhibitory (suppressive) surround.

Representative responses from sustained and transient, on- and off-centre, units to standing contrast are shown in Fig. 3.6. In comparison with the retinal data (Fig. 3.1), these examples show:

(i)   a lower maintained, prestimulus discharge rate;

(ii)   a stronger transient discharge on presentation of the appropriate contrast stimulus;

(iii)   for sustained units, a much reduced sustained component during presentation; and

(iv)   for transient units, on removal of the contrasting stimulus, a brief elevation of discharge above the prestimulus level.

Dubin and Cleland (1977) have described two groups of interneurones - intrageniculate (located in the interlaminar zones of the dorsal lateral geniculate nucleus (LGN) and peri-geniculate interneurones (located above the LGN at its border with the peri-geniculate nucleus). According to these authors, intrageniculate interneurones resemble relay cells (Burke and Sefton, 1966a,b,c) and, in the present study, may erronously have been included in the sustained and transient classes. The peri-geniculate interneurones they describe gave on-off responses and were *generally* driven binocularly.
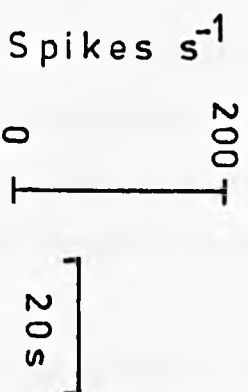
In the present study, although the T± units gave on-off responses to a flashing spot, they were *all* monocularly activated. Stimulation of their RFCs with narrow-band wavelengths over the spectral range 450nm to 600nm (in steps of approximately 25nm) did not reveal any spectral dependency in their response. Since no histological reconstructions of the electrode tracks were made the evidence that these units are peri-geniculate interneurones is purely speculative.

Most of the geniculate units' receptive fields were located close to the area centralis (n = 68, mean eccentricity = 8.7°) and, as expected,

Fig. 3.6

Responses to standing contrast for geniculate sustained and transient, on- and off-centre, units. All units were recorded from *the right lateral geniculate nucleus (LGN). Conventions as in* Fig. 3.1 and 3.2.

Transient

Sustained

On-centre

L G N · 3 9 · 2 · S +
Ecc. = 6·3°

L G N · 3 5 · 1 · T +
Ecc. = 3·1°

Spikes s^{-1}

Spikes s^{-1}

0

0

200

200

20s

20s

L G N · 4 3 · 1 · S −
Ecc. = 3·9°

L G N · 3 6 · 4 · T −
Ecc. = 3·8°
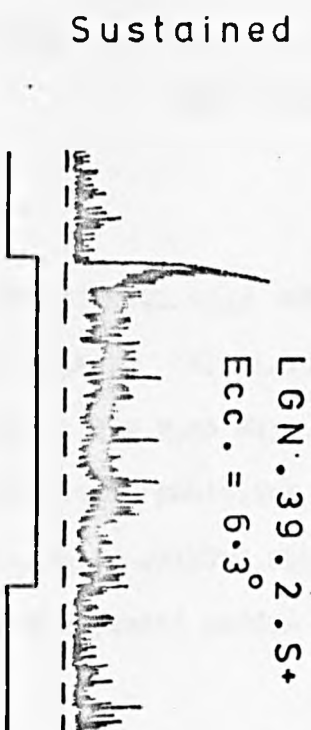
Off-centre
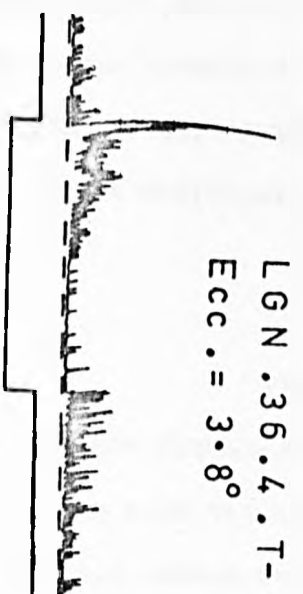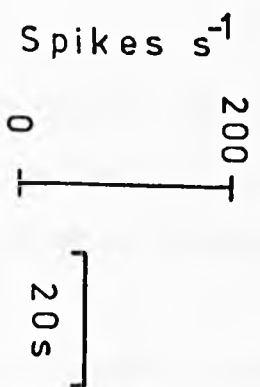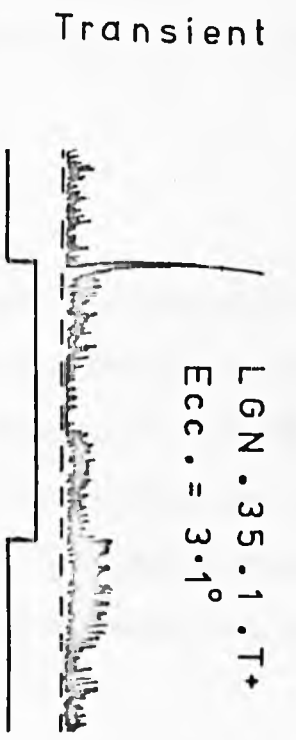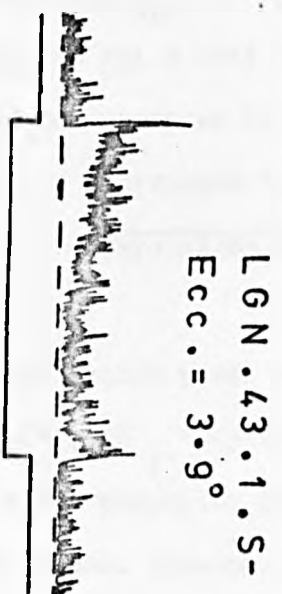
showed high spatial frequency resolution for square-wave gratings. The great majority of both sustained and transient units were capable of resolving the 2 cycles deg.$^{-1}$ grating. A few on-centre sustained units (n = 5) even resolved the 4 cycles deg.$^{-1}$ grating.

3.4.2 Maintained discharge rate

As with RGCs, the maintained activity of geniculate units was evaluated under nitrous oxide/oxygen (supplemented with pentobarbitone) anaesthesia, averaged over a 16s period. This procedure was necessary because, at +0.53 log. cd.m^{-2} background adapting levels, LGCs tended to discharge in high-frequency bursts separated by periods of low-level activity.

The mean maintained activity for the sustained, transient, and on-off transient (T±) units is shown in Table 3.2. The general trend in mean discharge rate is the same as for the retinal results, except that rates are systematically lower.

3.4.3 RFC areas

The RFCs were mapped (section 4.2.3), and their areas calculated (section 4.3.5). The scatter of RFC areas versus eccentricity from the area centralis for sustained, transient, and on-off transient units is shown in Fig. 3.7. The data are limited but RFC area shows little increase with eccentricity. As with RGCs, the two off-centre sustained units had much larger RFCs than sustained on-centre units at comparable eccentricity.

3.4.4 Non-concentric units

Of a total of 105 LGCs, 11 possessed the non-concentric receptive

Table 3.2

Mean discharge rate for geniculate units at a background adapting luminance of +0.53 log. cd.m^{-2}, under nitrous oxide/ oxygen anaesthesia.

The mean maintained activity for sustained (S) and transient (T), on- (+) and off-centre (-), and for on-off transient (T±), units is shown separately, and the ± value denotes 1 S.E.M.

Table 3.2

CLASS	S+	S-	T+	T-	T±
No. of UNITS	25	9	31	26	9
MEAN DISCHARGE RATE (Spikes s^{-1})	12.0 ±1.7	9.1 ±2.0	7.9 ±1.3	5.8 ±1.2	4.2 ±0.3

Fig. 3.7

Scatter of RFC areas with eccentricity from the area centralis for geniculate units.

A - sustained on- (O) and off-centre (Δ) units. The on-centre data show a weak positive correlation between RFC area and eccentricity (correlation coefficient (r) = 0.56).

B - transient on- (O) and off-centre (Δ), and on-off transient (□) units. No correlation exists between RFC area and eccentricity.
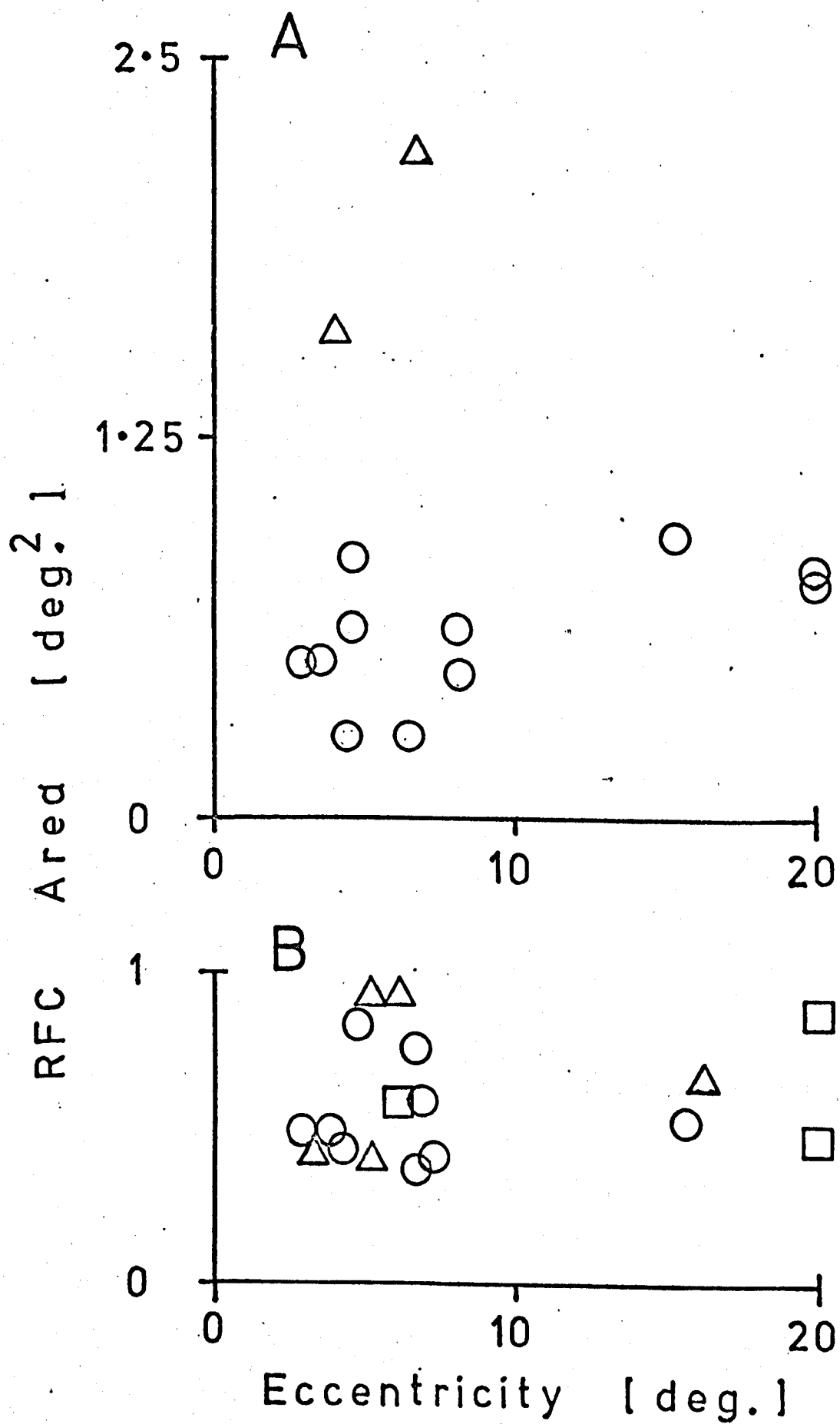
fields. The property of the 9 on-off transient units have been dealt with in the preceding sections.

One direction selective unit was located 6.3° from the area centralis and possessed an excitatory "on" region (2° by 0.8°; with the long axis vertical), surrounded by an inhibitory (suppressive) surround. A vertical light bar ($\frac{1}{2}$° by 2°) moved horizontally, evoked transient discharges as it crossed the unit's receptive field in either direction. The response decreased for oblique orientations and vertical motion of a horizontal bar suppressed the maintained activity.

One geniculate unit, resembling a visual cortical simple/complex cell (Hubel and Wiesel, 1962; Bishop and Henry, 1972; Henry and Bishop, 1972; Bishop, Coombs and Henry, 1973), possessed *on- and off-regions* with an inhibitory surround. The separate on- and off-regions (each 1° by $\frac{3}{4}$° were separated by $\frac{1}{2}$° of on-off overlap. The complex triphasic (positive/ negative/positive) waveform, and the duration of the spike (Bishop, Burke and Davis, 1962a,b,c) excluded the possibility that the unit was a cortico-geniculate fibre.

3.5 Conclusions

The retinal results lead to the following conclusions.

(i) On the basis of the standing contrast test, there is a continuum between RGCs giving sustained and transient response profiles. In agreement with Cleland and Levick (1972), it is not therefore possible to classify units into the brisk sustained or transient classes solely on the basis of this test.

(ii) On-centre brisk sustained units have the highest square-wave resolving frequency. However, in disagreement with Cleland *et al.*

(1971, 1974a), brisk transient units do not give an
unmodulated increase in maintained activity during the
passage across the receptive field of a grating of spatial
frequency higher than the unit can resolve; and, furthermore,
differential responses are obtained from different classes of
units.

(iii) Under pentobarbitone anaesthesia, the maintained activity of
cells is depressed but this effect occurs equally in all
classes of cells such that the overall trend in resting
discharge rate (S+ > S- $\sim$ T+ > T-) is maintained.

(iv) For a given visual field eccentricity, the on-centre brisk
sustained units have the smallest RFC sizes.

Similar trends were obtained for geniculate units in the following
cases:

(i) in the maintained activity levels under nitrous oxide/oxygen
anaesthesia, and

(ii) in the highest resolving frequency for a square-wave grating.
Unlike RGCs, the data for LGCs were inadequate in deciding whether RFC
size increased with eccentricity from the area centralis. However,
Mason (1976) has shown a systematic increase in RFC size of LGCs with
eccentricity.

Chapter 4   CHROMATIC STUDY

4.1 Introduction

The aims of this study were to clarify the discrepancies between the results of Andrews and Hammond (1970b) and Enroth-Cugell, Hertz and Lennie (1977b) regarding the extent of the rod- and cone-mediated inputs to the RFC of RGCs. Furthermore, to test whether the ellipticity in the shapes of the RFC (Hammond, 1974) could be explained by circular but non-concentric rod- and cone-mediated inputs (H.B. Barlow, personal communication) (see section 4.1.2).

4.1.1 Rod and cone centre sizes

In RGCs with both cone and rod inputs, Andrews and Hammond (1970b) distinguished according to the temporal response profile of the cell, an initial high frequency, short latency, transient discharge and a longer latency, lower frequency maintained phase referred to, respectively as the P1 and P2 components. Those cells with only rod input showed exclusively a P2 component. Accordingly, both P1 and P2 were used to examine the spatial extent, respectively, of the cone and rod inputs to the RGCs. The results established that the RFC was substantially larger for rod than cone input with a range from equality to 3:1 in rod:cone input diameter ratios.

Enroth-Cugell, *et al.* (1977b) have measured the centre sizes of the cone and rod inputs to the RGCs at a mesopic background adapting level. These authors obtained area-threshold curves for red and blue-green test flashes which, respectively, stimulated the cone and rod inputs. Their results, however, established that the spatial summation areas for these test lights were similar; and, hence, the cone- and rod-mediated centre sizes the same.

4.1.2 RFC ellipticity

An extensive mapping study, carried out by Hammond (1974) on RGCs, established that a systematic bias towards elliptical symmetry occurred in the shape of the RFCs. Accordingly, Hammond suggested asymmetry in the dendritic arborization of ganglion cells as a likely candidate. However, since cat RGCs have inputs from both rods and cones (Barlow, Fitzhugh, and Kuffler, 1957a,b ; Daw and Pearlman, 1969; Andrews and Hammond, 1970a,b; Hammond and James, 1971; Hammond, 1973; Enroth-Cugell *et al.* 1977a,b), H.B. Barlow (personal communication) suggested that ellipticity could also arise through the non-concentric overlap of circular rod- and cone-mediated inputs to the cell's RFC - Fig. 4.1A represents this diagrammatically.

Another possibility is asymmetry in the strength of antagonism between the centre and surround mechanisms in different parts of the receptive field (Fig. 4.1B). Evidence in favour of this possibility is provided by the receptive field maps, using a constant intensity flashing spot, of Rodieck and Stone (1965b).

4.1.3 Rod and cone sensitivity profiles

The rod-mechanism, in the cat, has maximal sensitivity at 507nm whilst the cone-mechanism has maximal sensitivity at 556nm (Andrews and Hammond, 1970a,b). Using the Dartnall nomogram (Dartnall, 1953), the sensitivity profiles for the rod and cone absorption spectra were derived by Andrews and Hammond (1970a). These are shown in Fig. 4.2, where the left-hand curve is for the rod-mechanism and the right-hand curve for the cone-mechanism.

As the background adapting luminance is varied, the relative position of these curves to each other shift vertically.

Fig. 4.1

    Diagrammatic illustration of two mechanisms which may
generate RFC ellipticity.

    A - circular but non-concentric rod and cone centres

          (left) and the resultant elliptical RFC map (right)

          formed by the envelope (continuous line).

    B - a circular centre bounded by an annular surround.

          The shaded area of the surround represents a somewhat

          weakly antagonistic region compared to the unshaded

          region. The resultant RFC map (right-hand side

          diagram) extends into this region to give rise to the

          ellipticity.

A

Cone Centre

Rod Centre

Resultant RFC
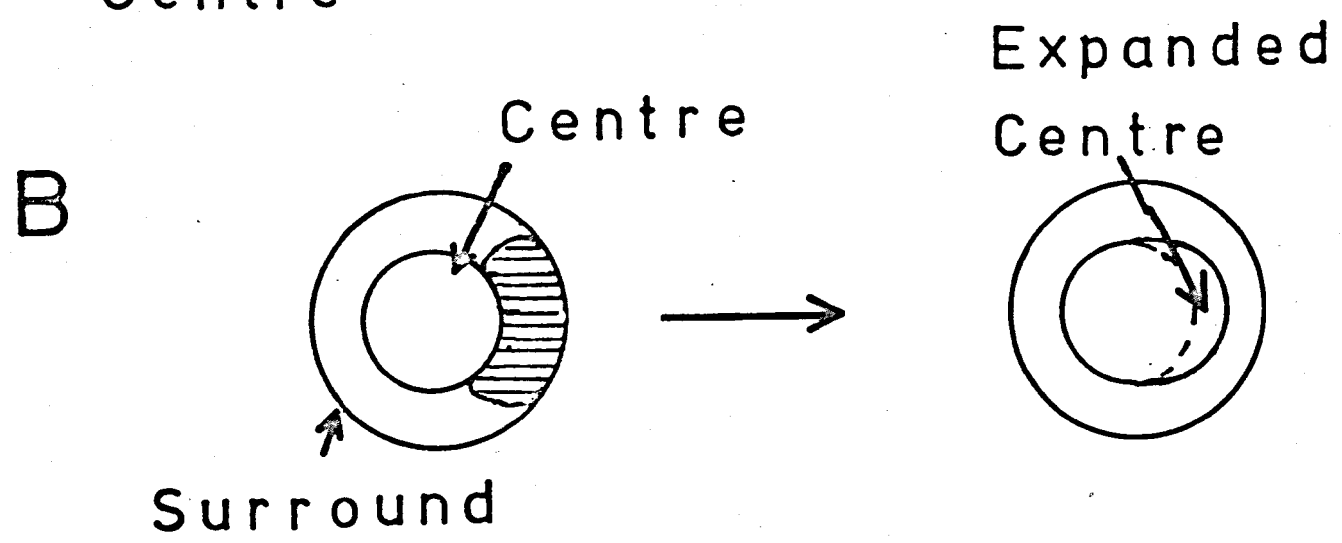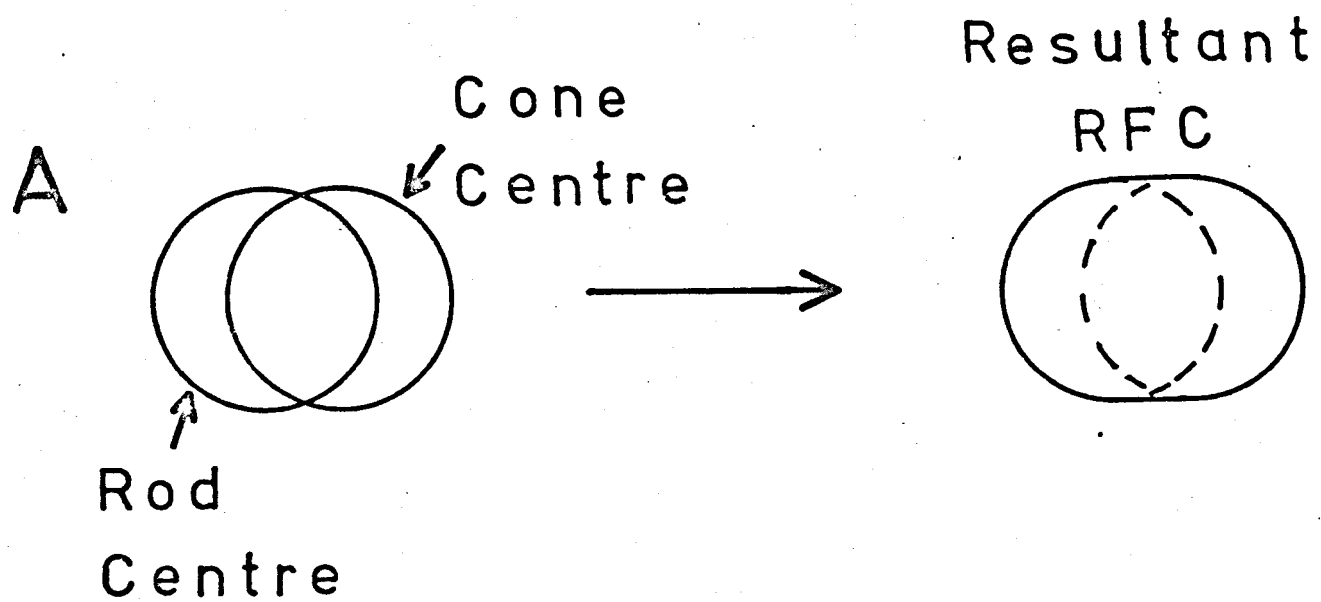
B

Centre

Surround

Expanded Centre

Fig. 4.2

Sensitivity profiles for the rod and cone absorption spectra derived by Andrews and Hammond (1970a), from the Dartnall nomogram (Dartnall, 1953), respectively for visual pigments with maximal sensitivity at 507nm (left-hand profile) and 556nm (right-hand profile).

At the mesopic adapting level of +0.53 log. cd.m^{-2}, the difference in sensitivity to the blue (452nm) and yellow (578nm) lights is 0.11 log. units. Hence, the two sensitivity profiles have been matched in their relative sensitivity position, and Δ denotes this difference.

The relative sensitivity differences between the rod and cone absorption spectra have been derived for blue (452 nm), yellow (578nm), and red (600nm) lights and are, respectively 0.75 (S_B), 0.52 (S_Y), and 0.87 (S_R) log. units.
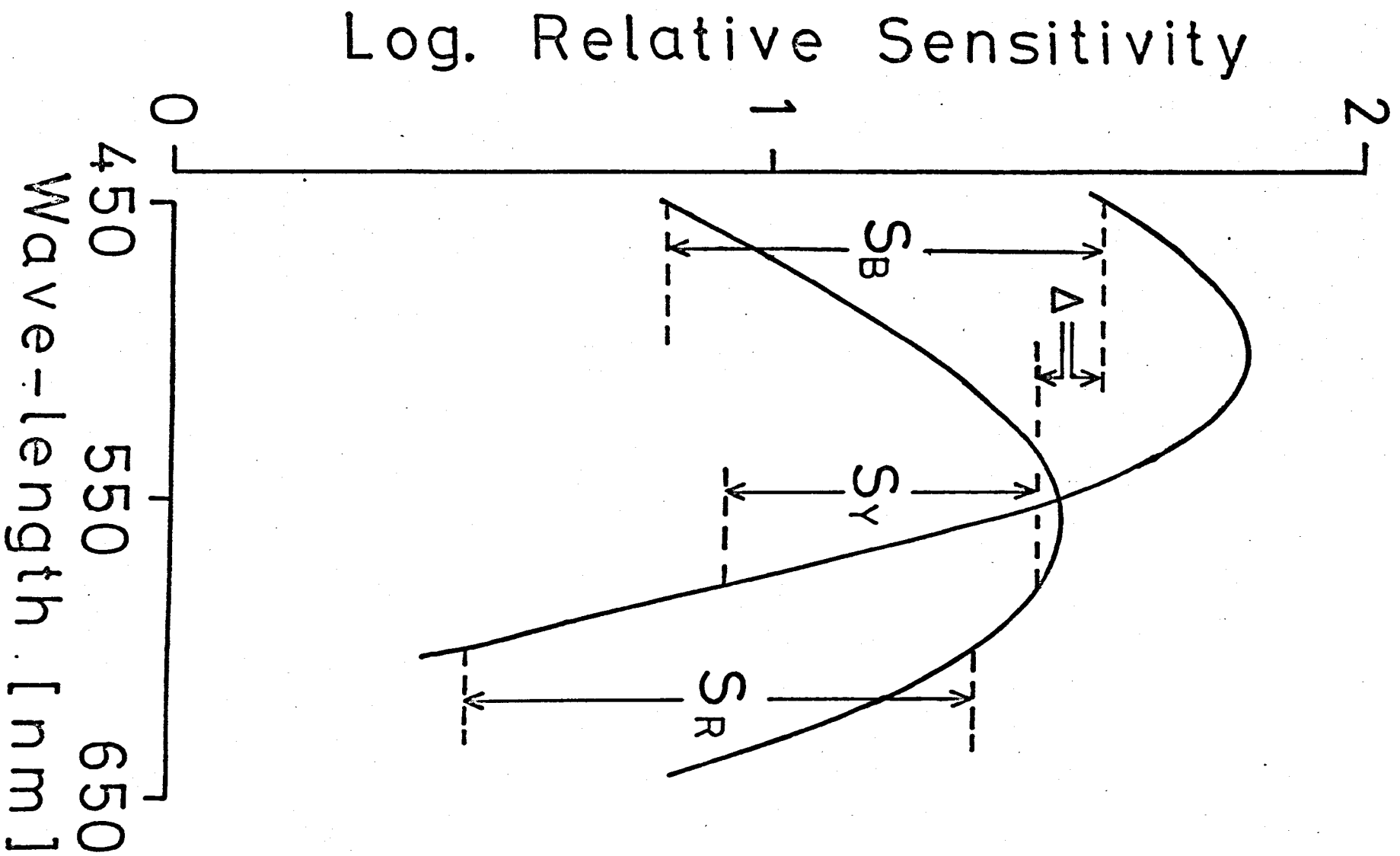
At a mid-mesopic adapting level of +0.53 log. cd.m^{-2} (in conjunction with 5mm diameter artificial pupils), the mean value of the threshold sensitivities of RGCs obtained for two narrow-band lights, one with transmission maximum at 452nm (blue) and the other at 578nm (yellow), differed by 0.11 log. units (Ahmed *et al.* 1977). Hence, the rod and cone sensitivity profiles can be exactly matched in their vertical position by making the relative sensitivity difference between them, at these wavelengths, the same order of magnitude. This has been done in this figure (Fig. 4.2), and Δ represents a difference of 0.11 log. units.

At this adapting luminance, the rod-mechanism is relatively more sensitive to the blue light and the cone-mechanism to the yellow light, the relative sensitivity difference with the blue light (S_B) being 0.75 log. units, with the yellow light (S_Y) 0.52 log. units, and with the red light (S_R) 0.87 log units.

Hence, these wavelengths were used to differentially stimulate the rod- and cone-mediated inputs both to the retinal ganglion and lateral geniculate cells.

4.2 Procedure

General details of the animal preparation, and stimulating and recording equipment are given in Chapter 2. Specific details of methodology are given in the following sections.

4.2.1 RFC mapping techniques

Two methods were available for the measurement of the rod and cone centres of RGCs and LGCs - the area-threshold and the iso-sensitivity mapping techniques.

The area-threshold technique involves the determination of thresholds

for flashing light spots of increasing size, and a graphical plot of threshold versus spot size then gives a measure of the RFC size (Barlow, Fitzhugh and Kuffler, 1957b). However, the accuracy to which RFC size can be determined depends upon the step sizes of both the flashing spot and the neutral density filters, the ellipticity of the RFC, and the position of the most sensitive region in the RFC. Available apparatus gave the following limitations:

(i) for an accuracy of 0.1° in determination of the RFC size, slides with spot sizes ranging from 0.5° to 5.0° (in steps of 0.1°) would have been required;

(ii) the neutral density filters were available only in optical density steps of 0.1 log units;

(iii) for determination of the RFC size on a tangent screen, with the flashing spot front-projected, any major deviation from the normal point of the projected spot would have resulted in the spot becoming elliptical in shape.

Added to these problems were the ellipticity in RFC shape and the location of the maximally sensitive region being near, but not at, the geometric centre of the receptive field (Kuffler, 1953; Rodieck and Stone, 1965b; Fukada, 1971; Hammond, 1974). Hence, the circular spots would only partially cover the RFC before stimulating the surround-mechanism and, therefore, lead to an inaccurate estimate of its size.

Because of these objections, the iso-sensitivity mapping technique was employed (see section 4.2.3). The accuracy of this method depended upon the spot size used - for spot sizes of 0.25°, 0.5°, and 1.0° the accuracy in determination of the iso-sensitivity region was better than 0.05°, 0.1°, and 0.2° respectively. Furthermore, this technique allowed for the detection of asymmetries in RFC shape. However, since the intensity of the stimulating spot was 1 log. unit above centre threshold, this

technique did not exclusively stimulate the rod mechanism with the blue light or the cone mechanism with the yellow light (see section 4.5.2).

4.2.2 Threshold determination

The RFC, whether on- or off-centre, was stimulated (duration 400ms, presented every 1.6s) using an appropriately sized ($\frac{1}{4}°$, $\frac{1}{2}°$, $\frac{3}{4}°$, or 1° diameter) spot centred in the most sensitive region of the field with either white, yellow (578nm), or blue (452nm) lights. The intensity was decreased by interposing neutral density filters in nominal steps of 0.1 log units. Two 400ms gates were set for the period during (gate 1) and following (gate 2) the stimulus, allowing for response latency. The discriminated spikes in gates 1 and 2 were counted, separately, by electronic counters either for each individual stimulus cycle or accumulated over many cycles.

The method of determination of threshold depended upon the level of maintained activity. For units with a fairly constant resting discharge, threshold was determined by comparing:

(i)   total spike counts in gate 1 with gate 2 such that the total counts difference never exceeded two spikes per stimulus cycle, and the total counts in gate 1 exceeded those in gate 2 only 50% of the time;

(ii) total spike counts in gates 1 and 2 over at least 20 stimulus cycles, such that they did not differ by more than 1% of the total count in each gate; and

(iii) for recordings with mainly low resting discharge, audio-visual

collation was also used.

Certain fibres, mainly of the transient category, displayed periodic bursting of their resting discharge (approximately every 3s). For these fibres, threshold was difficult to determine and in addition to the above methods:

(i)   peri-stimulus time histograms were obtained for at least 20 stimulus cycles; and

(ii) the total spike counts in gates 1 and 2 were compared between blank runs and stimulus runs over at least 20 cycles.

In all cases, the optical density at which no change in the activity of the recording could be distinguished, during and following the stimulation, was taken as the threshold and its value noted.

4.2.3   Iso-sensitivity contour maps

Initially, the position of the most sensitive region in the RFC was obtained with a $\frac{1}{2}°$ or 1° white flashing spot, and its location pinpointed on the tangent screen with the red, subthreshold (for the cat) cross-wire image. This test was then repeated for yellow (578nm) and blue (452nm) lights by flashing a suprathreshold $\frac{1}{2}°$ spot, and marked on white paper (12° by 8°) attached to the front of the screen. Separately, for the yellow and blue lights, the threshold at this point (centre threshold) was determined for $\frac{1}{4}°$, $\frac{1}{2}°$, or 1° flashed spots (duration 400ms, presented every 1.6s) (see section 4.2.2) by interposing neutral density filters in steps of 0.1 log units. The size of the spot was chosen to give a centre threshold value at least 1 log unit below the unattenuated source intensity.

Using the yellow light, the appropriately sized flashing spot, at an intensity 1 log unit above centre threshold, was moved continuously away from

the most sensitive region of the RFC until a position was reached when the spike activity of the fibre:

    (a)   did not change during and following the flash, or

    (b)   the total spike counts for the 400ms flash were the same as for the 400ms following the flash.

At this position (the iso-sensitivity point), the centre of the spot was carefully marked, and this routine was repeated until a total of four such positions were obtained around the most sensitive region of the RFC. The procedure was now repeated for the blue light. This mapping technique of interleaving the filters was necessary as a check against contour differences being a result of an eye-movement. In such a case, a shift in the marked positions of the most sensitive region of the RFC and the iso-sensitivity points for both the yellow and blue lights would be seen. Such a procedure was used until sufficient points (8 to 25, depending upon the size of the RFC) were obtained to clearly define the shapes of the RFC for each wavelength. By joining these iso-sensitivity points two contours of iso-sensitivity were obtained defining the centre-surround boundary, respectively, for the rod-mediated (rod centre) and the cone-mediated (cone centre) inputs.

Wherever possible the contours were redetermined at 0.8 and 1.2 log units above centre threshold to confirm that any difference between the rod and cone centres was not due to incorrect threshold determination.

Since, the rod and cone centres were plotted on the tangent screen, the resultant maps underwent a distortion related to their location peripheral from the "normal-points" of the eyes (the point directly in-front of the cat on the tangent screen and 57in. from the cat's eyes with the cartesian coordinates (0,0,57)). These maps were, therefore, corrected using cartesian geometry and tested for accuracy by direct

comparison with redrawn maps using the method of Hammond (1974).

Another method involved projecting a circular light spot onto the tangent screen in horizontal, vertical, and oblique directions at progressively peripheral locations from the normal-point. At each location, the projected light spot was mapped, and the resultant corrected map, then, compared with the size and shape of the light spot obtained at the normal-point for the projector.

Since correction involved an iterative procedure for each iso-sensitivity point, computer programs were devised which calculated:

(i)   the corrected positions for each iso-sensitivity point, the maximal sensitivity point, the area centralis, and the optic disk;

(ii) eccentricity of the maximal sensitivity point from the area centralis, optic disk, and the normal-point; and

(iii) area within the polygon formed by joining the iso-sensitivity points.

Details of the correction procedure are given in Appendix A.

RESULTS

4.3 Retinal study

The results are based on 74 recordings (65 OTFs and 9 RGCs), 51 brisk sustained (on-: off-centre, 39:12) and 23 brisk transient (on-: off-centre, 17:6), which were held sufficiently long to complete the mapping procedure. This small sample-size is related to the difficulty encountered in holding optic tract fibres for a period of at least 40 mins. - required for complete mapping.

The majority of fibres could only be held for 10-20 mins., and only one

fibre (out of some 500 fibre recordings) was held for as long as 110 mins.

4.3.1 RFC categories

By inspection of the size, shape, and relative position of the rod-
and cone-mediated iso-sensitivity contours (the rod and cone centres) for
each unit, it was possible to formulate four RFC categories. These were
denoted by A1, A2, B1 and B2.

4.3.1.1 Category A1

Those units for which the rod and cone centres were concentric and
the same size and shape, were placed in this category. Four typical
examples are given in Fig. 4.3. In this figure, the region of maximal
sensitivity is denoted by the plus (+) sign, and the direction (continuous
line) and distance (bracketed value in degrees) of the right (R) or
left (L) area centralis (AC) and optic disk (OD), as appropriate, are also
shown. The iso-sensitivity points lying around the region of maximal
sensitivity, defining the iso-sensitivity contour, are denoted by the
filled circles (for the rod centre) and triangles (for the cone centre).

Out of the total sample (n=74), for which cone and rod maps were
completed, 15 units, 6 brisk sustained (on-: off-centre, 2:4) and 9 brisk
transient (on-: off-centre, 8:1), were placed in this category.

4.3.1.2 Category A2

The rod and cone centres of units placed in this category were
typically the same size and shape, but were *not* concentric. Fig. 4.4
shows four examples. All such units (n=10), 9 on-centre brisk sustained
and one on-centre brisk transient, had the rod centre displaced with
respect to the cone centre. The reasons for such a displacement will be

Fig. 4.3

The iso-sensitivity points defining the rod- and cone-
mediated RFCs are shown for four representative units from
category A1. The rod centre is denoted by the filled circles and
the cone centre by the filled triangles. The maps have been
corrected for tangent screen distortion. The position of the
point of maximal sensitivity is indicated by the + sign, and the
directions of the right (R) or left (L) area centralis (AC) and
optic disk (OD), as appropriate, are shown by the continuous
lines. The bracketed numerical values represent the separation
(in deg.) of + from AC or OD. All units were mapped using a ½°
diameter spot.
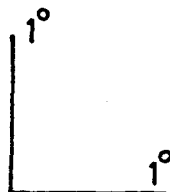
As these examples show, the rod and cone centres are
concentric, and the same size and shape.

LOD
(17°)   LAC
(11·3°)

ROT.40.5.S+
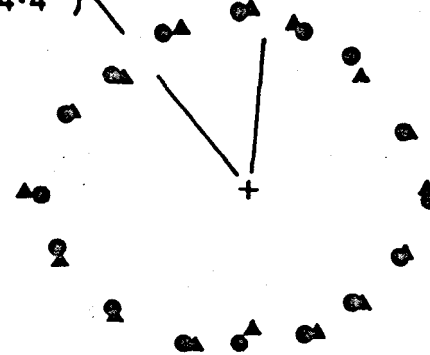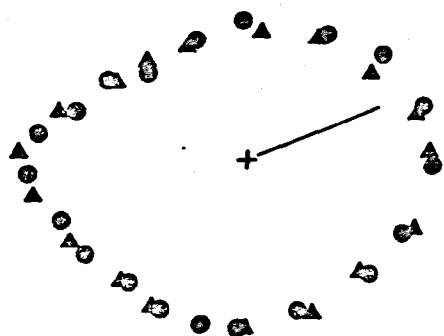
LAC (13°)

LOD
(24·4°)

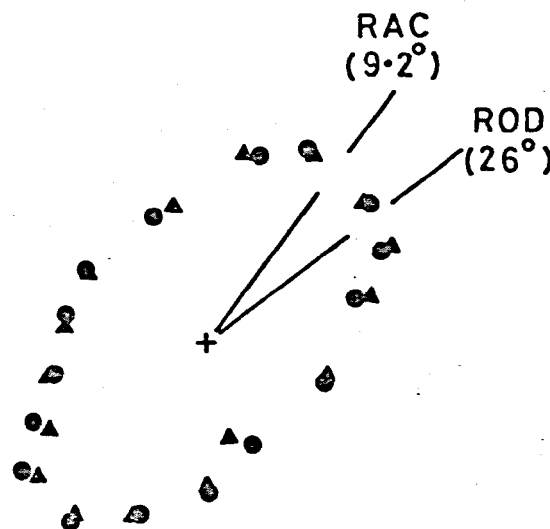ROT.30.6.T+

1°

1°
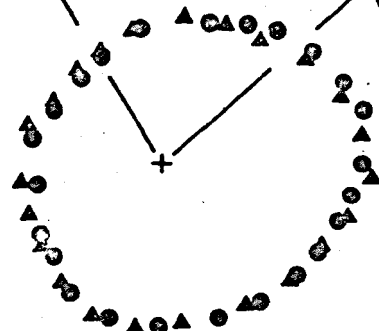
RAC (7·4°)
ROD (22·4°)

ROT.30.5.T-

RAC
(9·2°)   ROD
(26°)

ROT.46.22.T+

Fig. 4.4

    The iso-sensitivity points defining the rod- and cone-mediated RFCs are shown for four units placed in category A2. ROT.25.1.S+ was mapped using a $\frac{1}{2}°$ diameter spot, and the remaining units with a $\frac{1}{4}°$ diameter spot. The symbol conventions are as in Fig. 4.3.

    Units placed in this category exhibit non-concentricity in their rod and cone centres, although these centres are the same size and shape. Hence, by laterally displacing the rod centre with respect to the cone centre the two centres can be superimposed.

ROT.16.1.S+

LOD
(11°)

LAC
(27°)

ROT.26.9.S+

ROD (41°)

RAC (23°)

1°

1°

RAC (21°)

ROD
(35°)

ROT.25.1.S+

ROD
(34°)

RAC
(17°)

ROT.36.4.S+

-78-
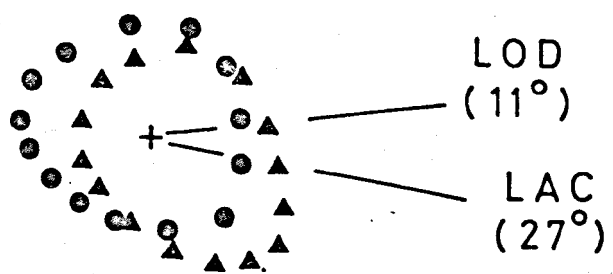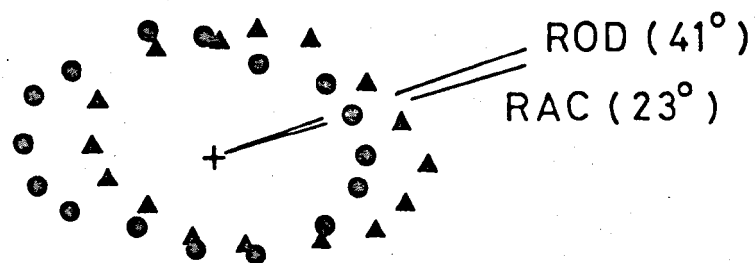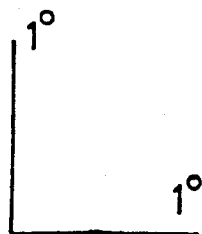
dealt with in later sections.

4.3.1.3 Category Bl

This category comprised units for which the rod and cone centres were concentric and of similar shape, but the size of the rod centre was larger than the cone centre. Hence, the iso-sensitivity points d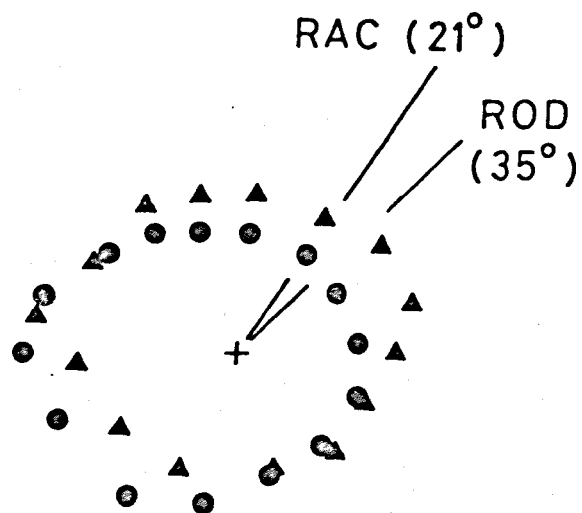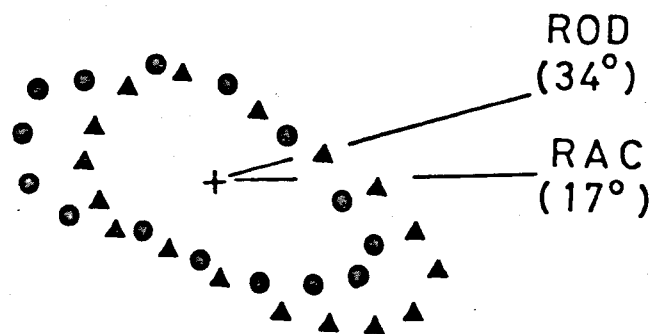efining the rod centre encircled those defining the cone centre. Typical examples are given in Fig. 4.5. Of 8 such units, 5 were brisk sustained (on-: off-centre, 4:1) and 3 brisk transient (on-: off-centre, 2:1).

4.3.1.4 Category B2

In this category the rod and cone centres differed in size and overlapped along part of their contour. However, by consideration of the size and shape of these centres, the units could be further differentiated into 3 sub-categories.

(i) The "asymmetric" units. The size of the rod centre was larger than the cone centre, but by lateral displacement of the rod centre it was *not* possible to concentrically encircle the cone centre. This sub-category formed the majority with a total of 24 units, 19 brisk sustained (on-: off-centre, 15:4) and 5 brisk transient (on-: off-centre, 3:2). Two examples are shown in Fig. 4.6B.

(ii) The "symmetric" units. Again the size of the rod centre was larger than the cone centre. In these units, however, lateral displacement of the rod centre resulted in the concentric encirclement of the cone centre. 15 units were placed in this sub-category, 10 brisk sustained (on-: off-centre, 7:3) and 5

Fig. 4.5

Iso-sensitivity points defining the rod and cone centres for category Bl units. All units were mapped using a $\frac{1}{2}°$ diameter spot. Conventions as in Fig. 4.3.

In this category the larger rod centre (filled circles) concentrically surrounds the smaller cone centre (filled triangles).
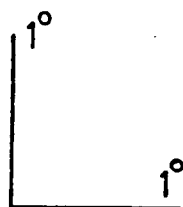
LOD (19°)   LAC (9°)

ROT.10.34.S+

IRR.16.2.T-

ROD (17°)

RAC (7·4°)

1°

1°

LOD (23°)   LAC (15°)

ROT.30.11.T+

LAC (5°)

LOD (15·6°)

ROT.14.7.S+
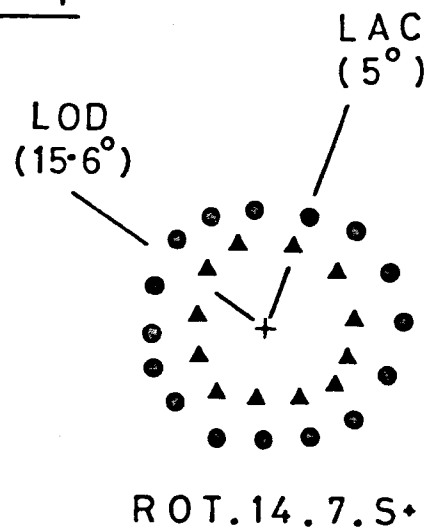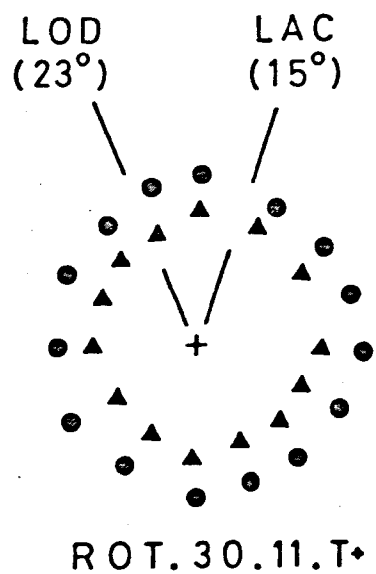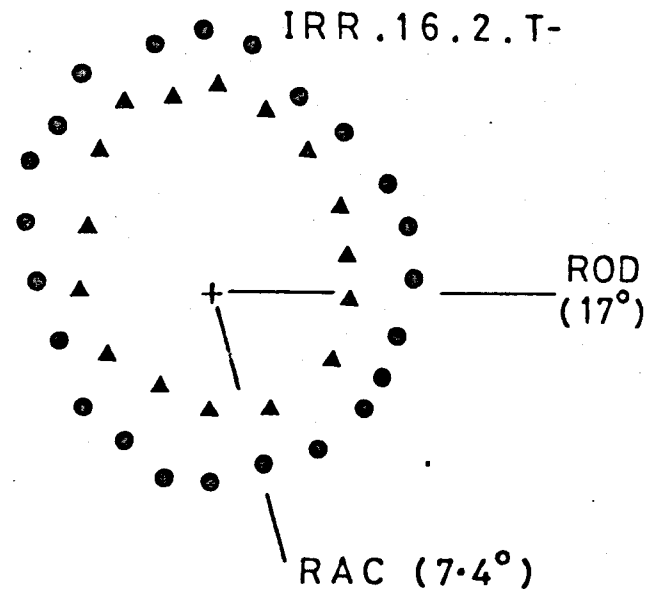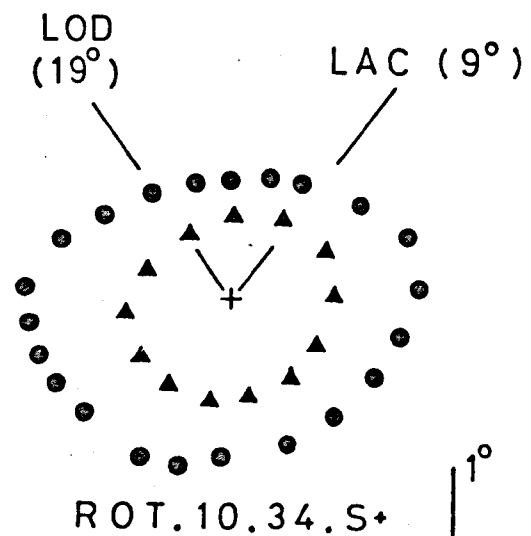
Fig. 4.6

Iso-sensitivity points defining the rod and cone centres
for category B2 units. Units denoted by ROT.19.6.S+, IRR.21.3.S-,
and ROT.35.20.S+ were mapped using a $\frac{1}{4}°$ diameter spot, and the
remainder with a $\frac{1}{2}°$ diameter spot. Conventions as in Fig. 4.3.

A - The larger rod centre surrounds smaller cone centre
and are non-concentric such that along part of the
contour the two centres actually overlap, but differ
only in size. These two units are representative
examples of the "symmetric" sub-category. Hence, if
the rod centre is displaced with respect to the cone
centre, the rod centre will concentrically surround
the smaller cone centre.

B - These two units are representative examples of the
"asymmetric" sub-category. The larger rod centre is
of such a shape that by displacement, with respect to
the cone centre, it will not concentrically surround
the smaller cone centre.

C - These two units are the only ones for which the cone
centres (filled triangles) were larger than their
respective rod centres. They have been placed in the
B2 category because the centres overlapped along a
part of the contour.

A — ROT.10.25.S+ — LOD (19°), LAC (18·3°)

ROT.14.13.S+ — LOD (15·4°), LAC (6·6°)

B — ROT.19.6.S+ — LOD (8·2°), LAC (19·4°)

IRR.21.3.S- — RAC (9°), ROD (27°)

C — ROT.06.13.T+ — LOD (4°), LAC (13°)

ROT.35.20.S+ — RAC (13°), ROD (27°)
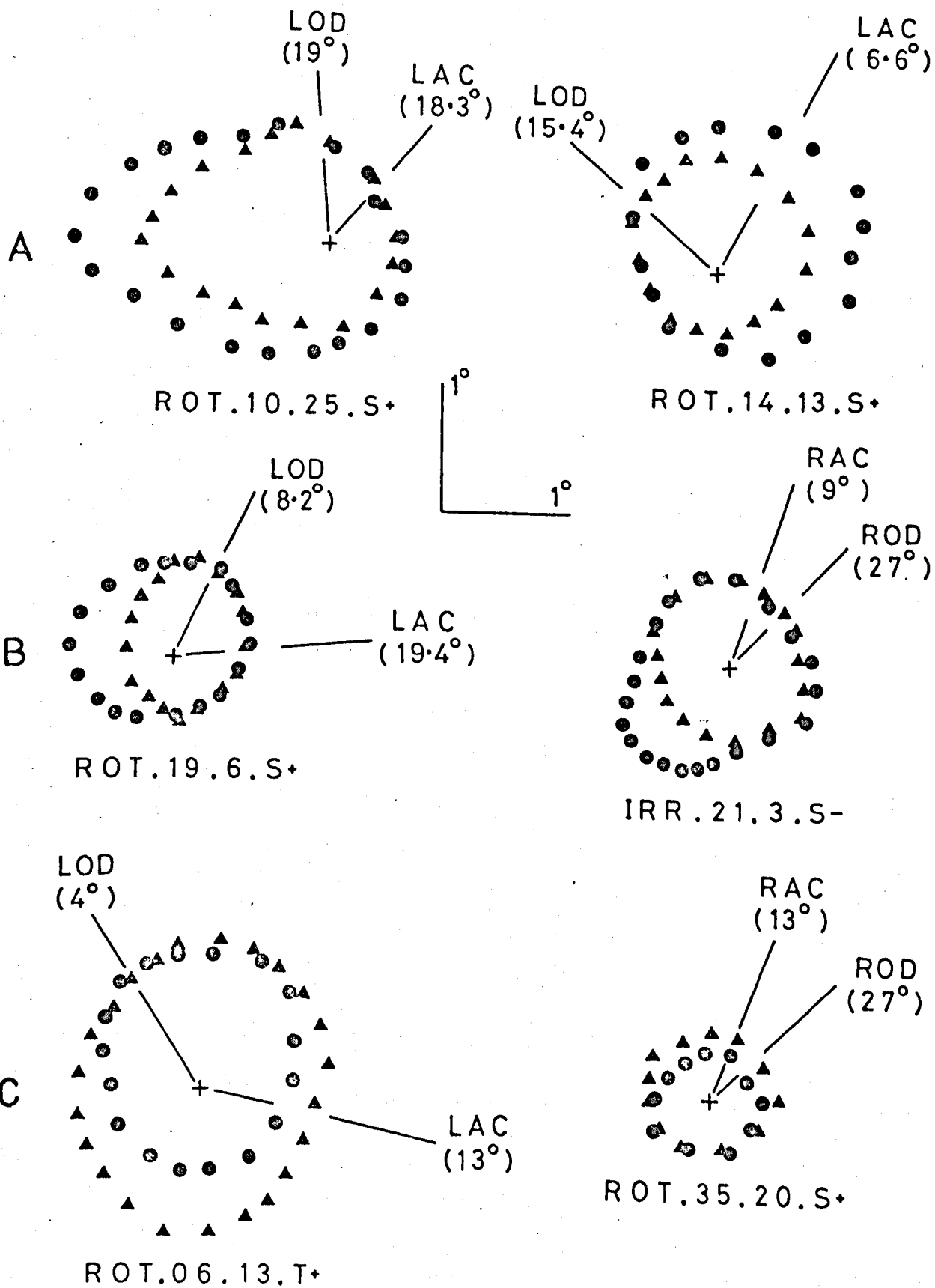
brisk transient (on-: off-centre, 3:2), typical examples are shown in Fig. 4.6A.

(iii) Two units, both on-centre brisk sustained, of the "symmetric" type, but their *cone* centres were larger in size than their rod centres. Both units are shown in Fig. 4.6C.

For each RFC category, the visual field location of the unit's receptive field with respect to the area centralis is shown in Fig. 4.7. Noteworthy is the peripheral distribution of units in category A2 (mean eccentricity = 23.5°) compared with the other categories A1, B1, and B2 with mean eccentricities of 16.9°, 15.0°, and 13.4°, respectively.

A summary of the relationship between these four categories and the sustained and transient classification scheme is given in Table 4.1.

4.3.2 Effect of intensity on RFC size

Since the rod and cone centres were obtained at an intensity 1 log. unit above the measured centre thresholds, any differences in their size may reflect incorrect threshold determinations, the systematic error in threshold determination being 0.1 log. units - the step size between the neutral density filters. Fig. 4.8 shows how the centre size varies with the intensity of 0.5° flashing spot at a constant background adapting luminance. In this on-centre brisk sustained unit, the percentage change in RFC area (see section 4.3.5 for method of determining area) for a presumed error of 0.1 log. units is 9.5%[1]. This, however, represents a

---

[1]Area of RFC at 0.9 log. units above threshold = 5.2 deg.^{2}
Area of RFC at 1.0 log. units above threshold = 5.8 deg.^{2}
Area of RFC at 1.1 log. units above threshold = 6.3 deg.^{2}
Therefore, percentage change in area for an error of 0.1 log. units is given by:

$$(0.55/5.8) \times 100 = 9.5\%$$

Fig. 4.7

Location of RFCs in the left-visual field with respect to the area centralis. Each unit's position has been related to a horizontal axis, by assuming a position angle of 25° between this axis and the line joining the right or left area centralis to its respective optic disk (Bishop, Kozak and Vakkur, 1962).

A - scatter of centres for the RFC categories A1 (open squares) and A2 (closed squares).

B - scatter of centres for the RFC categories B1 (closed triangles) and B2 (open triangles).
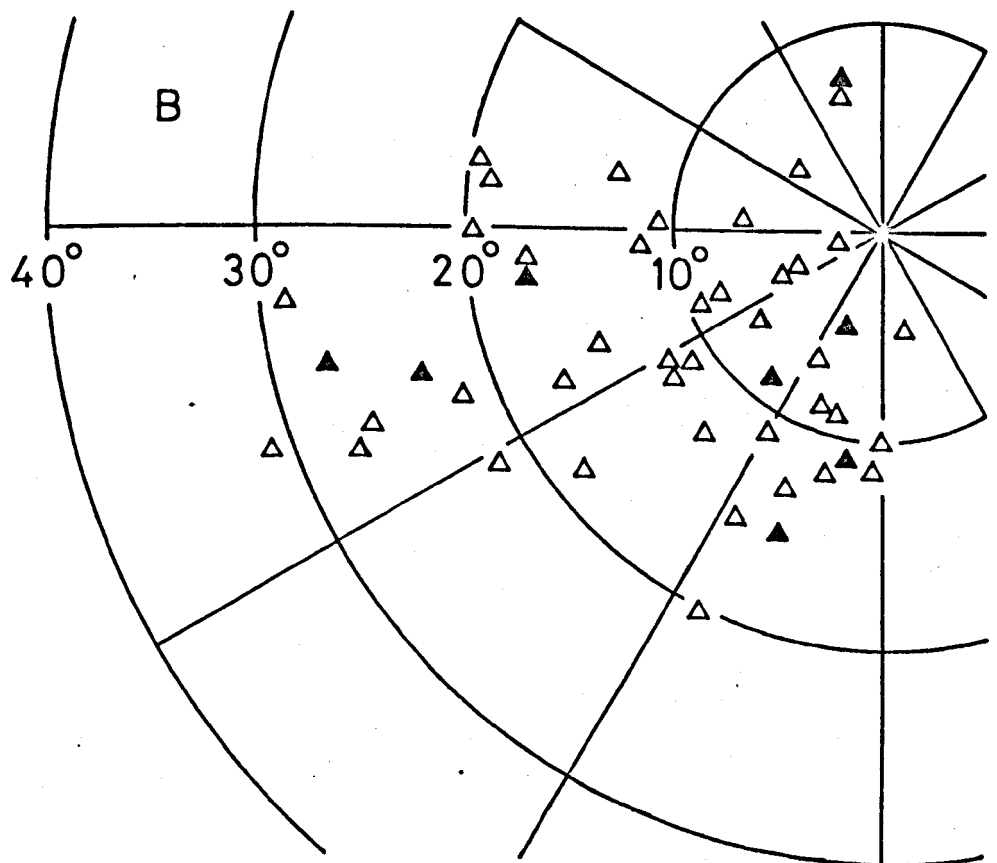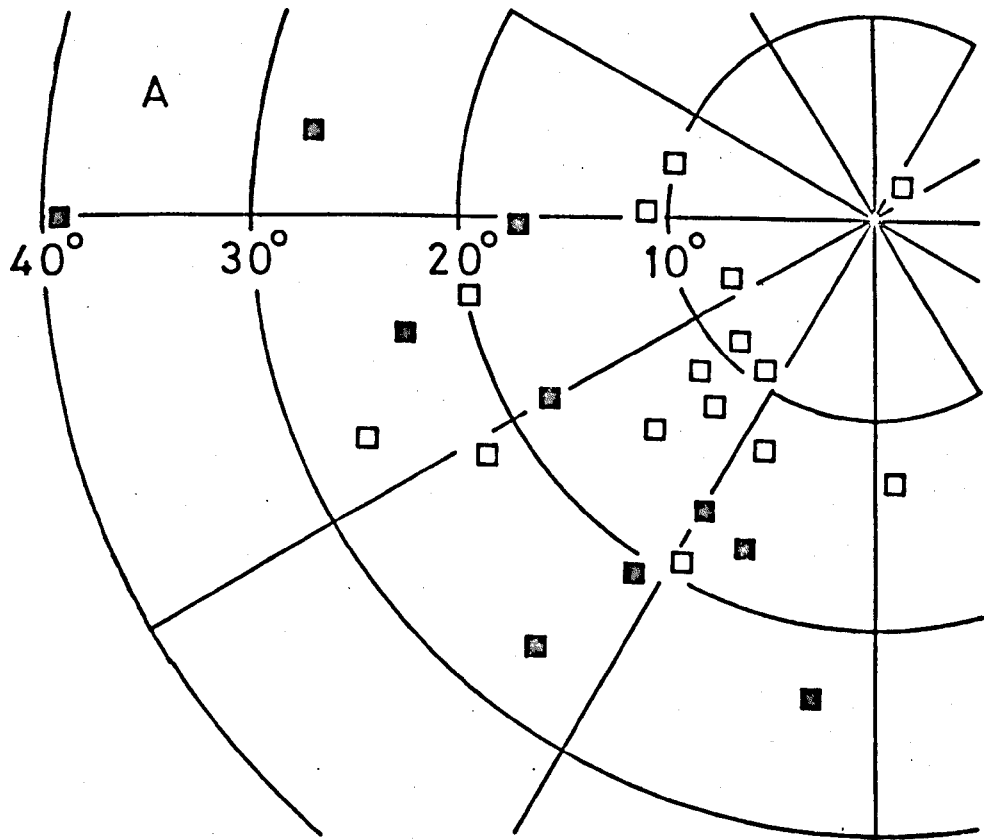
Table 4.1

Distribution of four RFC categories into the sustained (S) and transient (T) classes. On- and off-centre units are represented by + and - signs respectively.

Table 4.1

RFC CATEGORIES

	A1	A2	B1	B2	TOTAL
S+	2	9	4	24	39
S-	4		1	7	12
T+	8	1	2	6	17
T-	1		1	4	6
TOTAL	15	10	8	41	74

Fig. 4.8

Variation of RFC area with the intensity of the mapping spot for a brisk sustained, on-centre unit (Eccentricity = 27.8°). Iso-sensitivity points were obtained around the maximal sensitivity region with a $\frac{1}{2}$° diameter flashing spot at 0.8, 1.0, 1.5, and 2.0 log. units above centre-threshold. Areas were then calculated at each intensity (section 4.3.5).
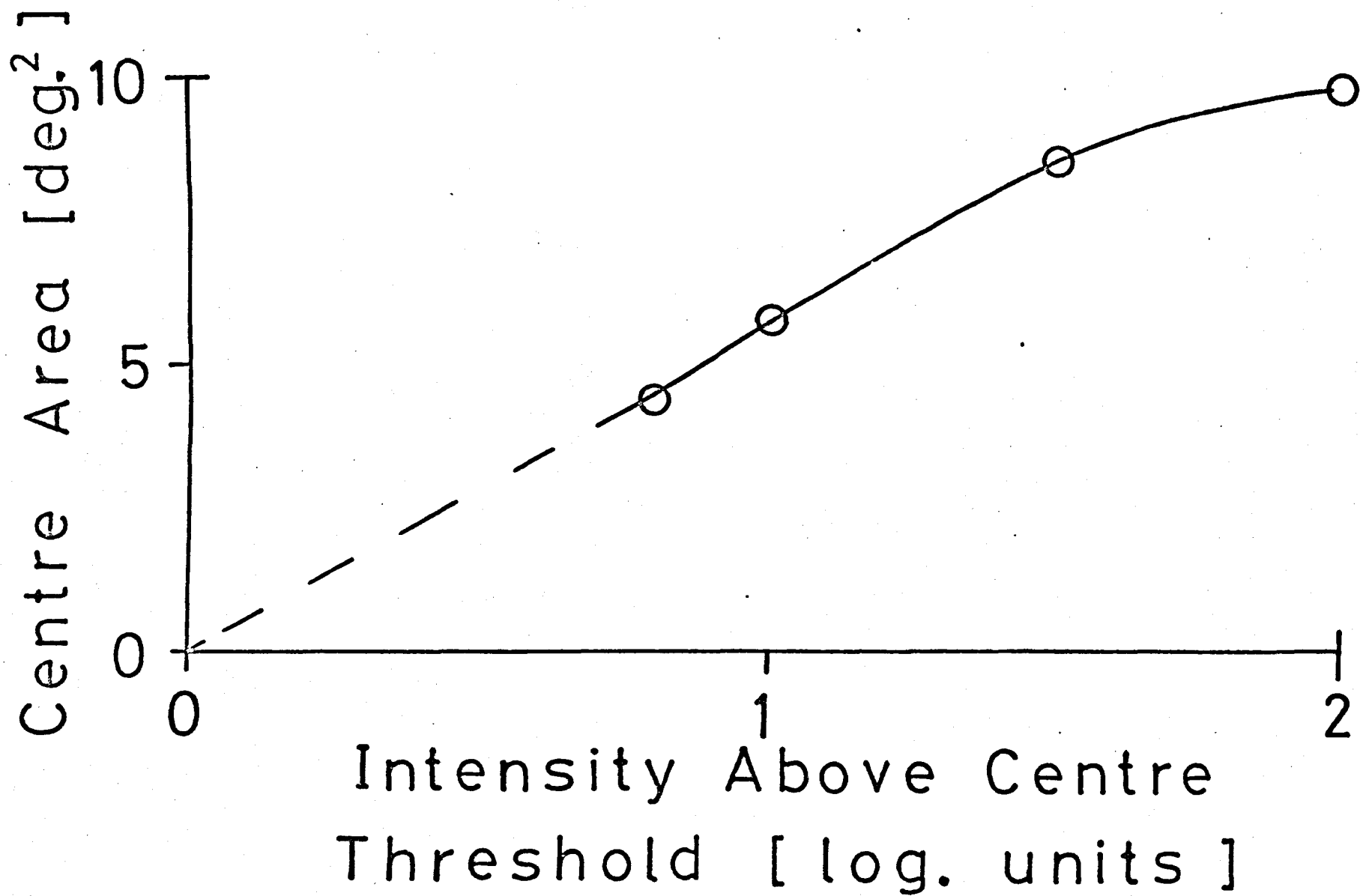
change in the contour, defined by the iso-sensitivity points, of 0.07° [1] which is well within the assumed error of 0.1° (for the 0.5° spot used to plot this unit's RFC). Hence, the systematic error (in threshold determination) does not overtly influence the RFC size.

In stable units, for which the rod and cone centre maps were completed at 1.0 log. units above centre threshold, the centre maps were redetermined at 0.8 and/or 1.2 log. units above their respective centre thresholds. Again, these mappings were designed to test whether the intensity of the spot might cause a significant change between the previously determined rod and cone centres. The effect of intensity on three units from categories A1, B1, and B2 respectively, are shown in Fig. 4.9. These examples, as well as similar data on other units, establish that the size differences in the mapped rod and cone centres are not primarily a result of intensity variation due to incorrect threshold determinations.

4.3.3 Non-concentric rod and cone centres

A total of 51 units, 10 in category A2 and 41 in category B2, exhibited non-concentric rod and cone centres. For these, the displacement (lateral displacement) required to either superimpose the rod and cone centres (for category A2 units) or for the larger centre to concentrically surround the smaller (for category B2 units), and the maximum separation between the centres were determined. These measurements were obtained to

---

[1] Assuming RFC to be a perfect circle:

R_1, Radius at 1 log. unit above threshold = $(5.8/\pi)^{\frac{1}{2}}$ = 1.36°

R_2, Radius at 0.9 log. units above threshold = 1.29°

Therefore, difference in contours $(R_1 - R_2)$ = 0.07°

Fig. 4.9

Variation of rod and cone centre sizes with intensity of the mapping spot for units in categories A1, B1 and B2. The + sign denotes the point of maximal sensitivity.

The left-hand maps are for the rod (open circles) and cone (open triangles) centres at 1.0 log. units above the determined centre-thresholds. The right-hand maps represent for these units in categories:

   (i)   A1 and B1, the cone centres determined at 0.8 (open triangles) and 1.2 (filled triangles) log. units above centre-threshold; and

   (ii) B2, the cone centre (open triangles) determined at 1.2 and the rod centre (open circles) at 1.0 log. units above centre-threshold.

Although, there is variation in the sizes with intensity of the mapping spot, the variation is small. Hence, these RFC categories are not a result of incorrect threshold determination.

A1

ROT. 22.3.T+

B1

ROT. 10.34.S+

B2

ROT. 24.3.S+
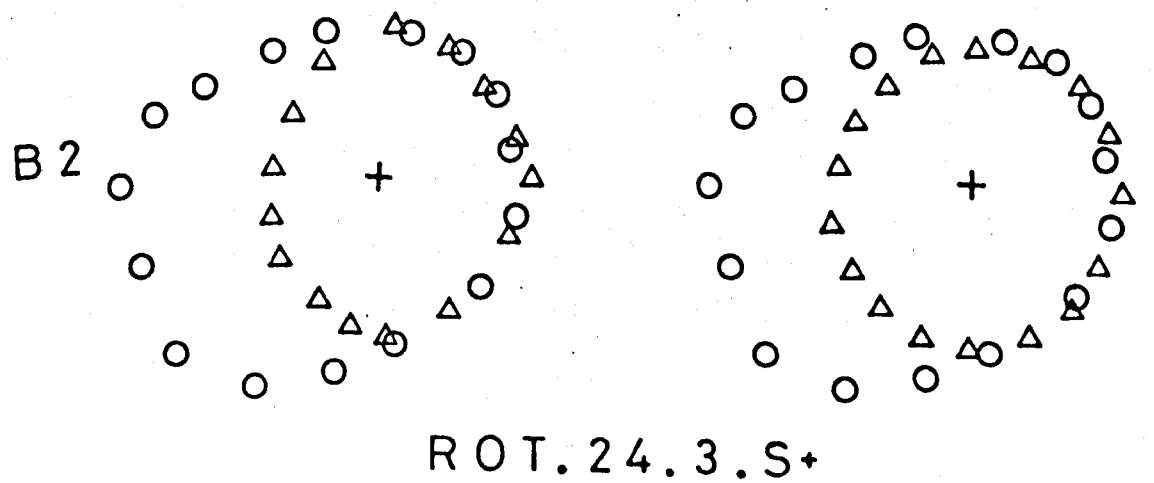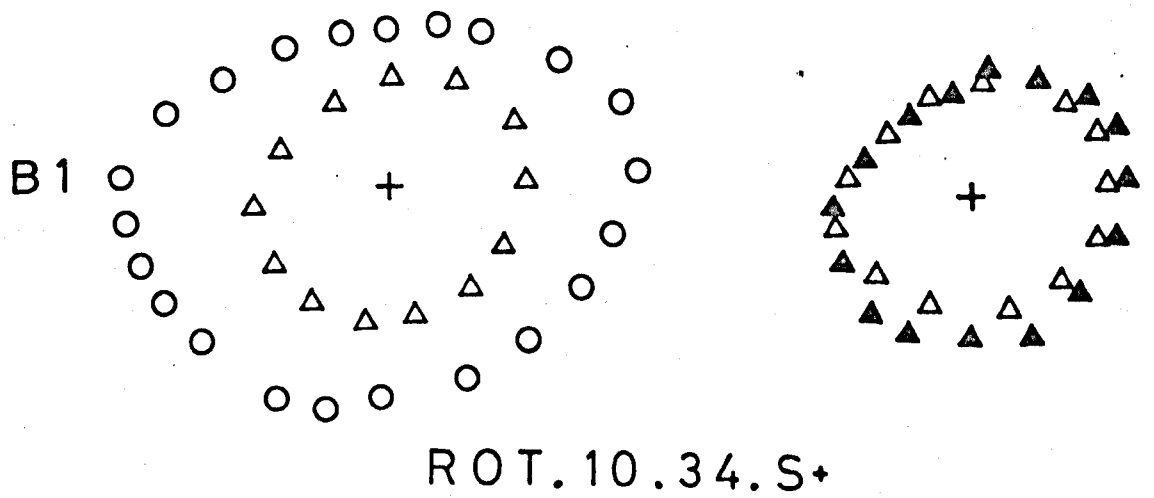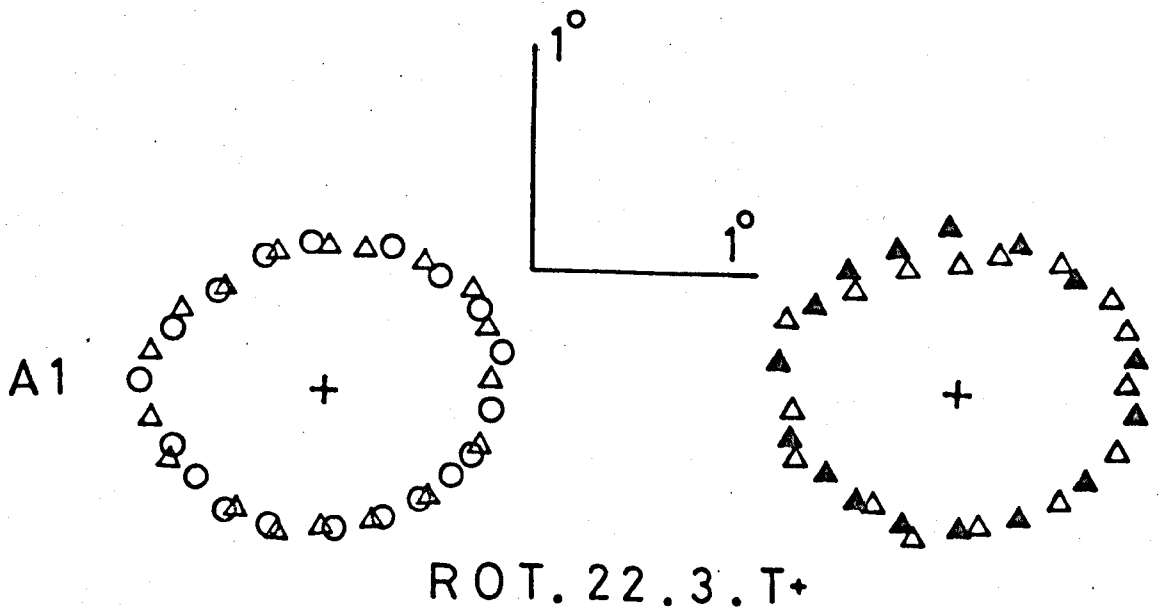
establish if a systematic relationship existed between the magnitude of non-concentricity and the visual field location of the unit. Fig. 4.10 shows in diagrammatic form the derivation of the lateral displacement and the maximum separation.

The scatter of values for the lateral displacement versus eccentricity for category A2, and the symmetric and asymmetric sub-categories of category B2 are shown, respectively, in Fig. 4.11A, B and C. The data for all 51 units have been plotted in Fig. 4.12A and B. Fig. 4.12 A represents the scatter for the lateral displacement and Fig. 4.12B that for the maximum separation. Although there was no systematic increase in the lateral displacement[1] with eccentricity for the individual categories or collectively for the whole data, the mean values of the lateral displacement, between categories A2 and B2, differed significantly[2]. Similar analysis for the maximum separation data gave a poor correlation (r_{xy}=0.01) and, furthermore, failed to show any

---

[1]Linear regression analysis of the data gave the following correlation coefficients (r_{xy}) for:

(i) category A2 (n=10, mean eccentricity = 23.0°, lateral displacement mean = 0.26°) r_{xy} = -0.38.

(ii) category B2, symmetric, (n=17, mean eccentricity = 12.3°, lateral displacement mean = 0.13°) r_{xy} = 0.11,

(iii) category B2, asymmetric, (n=24, mean eccentricity = 14.1°, lateral displacement mean = 0.15°) r_{xy} = 0.14, and

(iv) the total data (n=51, mean eccentricity = 15.3°, lateral displacement mean = 0.17°) r_{xy} = 0.26.

[2]The lateral displacement means for categories A2 (n=10) and B2 (n=41) were, respectively, 0.26° and 0.14°. The calculated t value was 3.58, and from the tables $t_{0.05, 49}$ = 1.68. Therefore, the means are significantly different.

Fig. 4.10

Derivation of maximum separation and lateral displacement.
The left-hand side diagram represents a category A2 unit and the
right-hand side a category B2 unit. The maximum separation
(measured in degrees) between the rod and cone centres has been
denoted by X and/or Y. The lateral displacement is defined as
the displacement of the rod centre required to superimpose (for
category A2) or concentrically surround (for category B2) the
cone centre. Hence, in category A2 this is the mean of X and
Y, i.e. $\frac{1}{2}(X+Y)$. In category B2 this is approximately half the
maximum separation, i.e $\frac{1}{2}X$. The maximum separation value for
category A2 is taken as the greater of X or Y.

Cone
Centre

Rod
Centre

X   Y   X
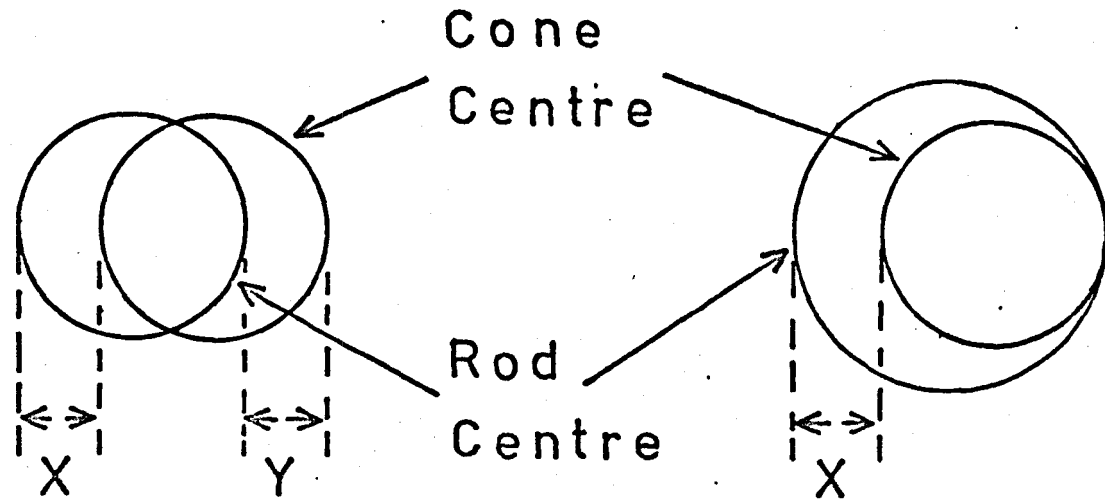
Lateral
Displacement $[X+Y]/2$ $X/2$

Maximum
Separation $[if\ X > Y]$ X
                     X

Fig. 4.11

Distribution of lateral displacement values with
eccentricity from the area centralis, separately for categories
A2 (Fig. 4.11A) and B2 (symmetric subcategory - Fig. 4.11B;
asymmetric subcategory - Fig. 4.11C).

Lateral Displacement [deg.]

Eccentricity [deg.]

A

B

C
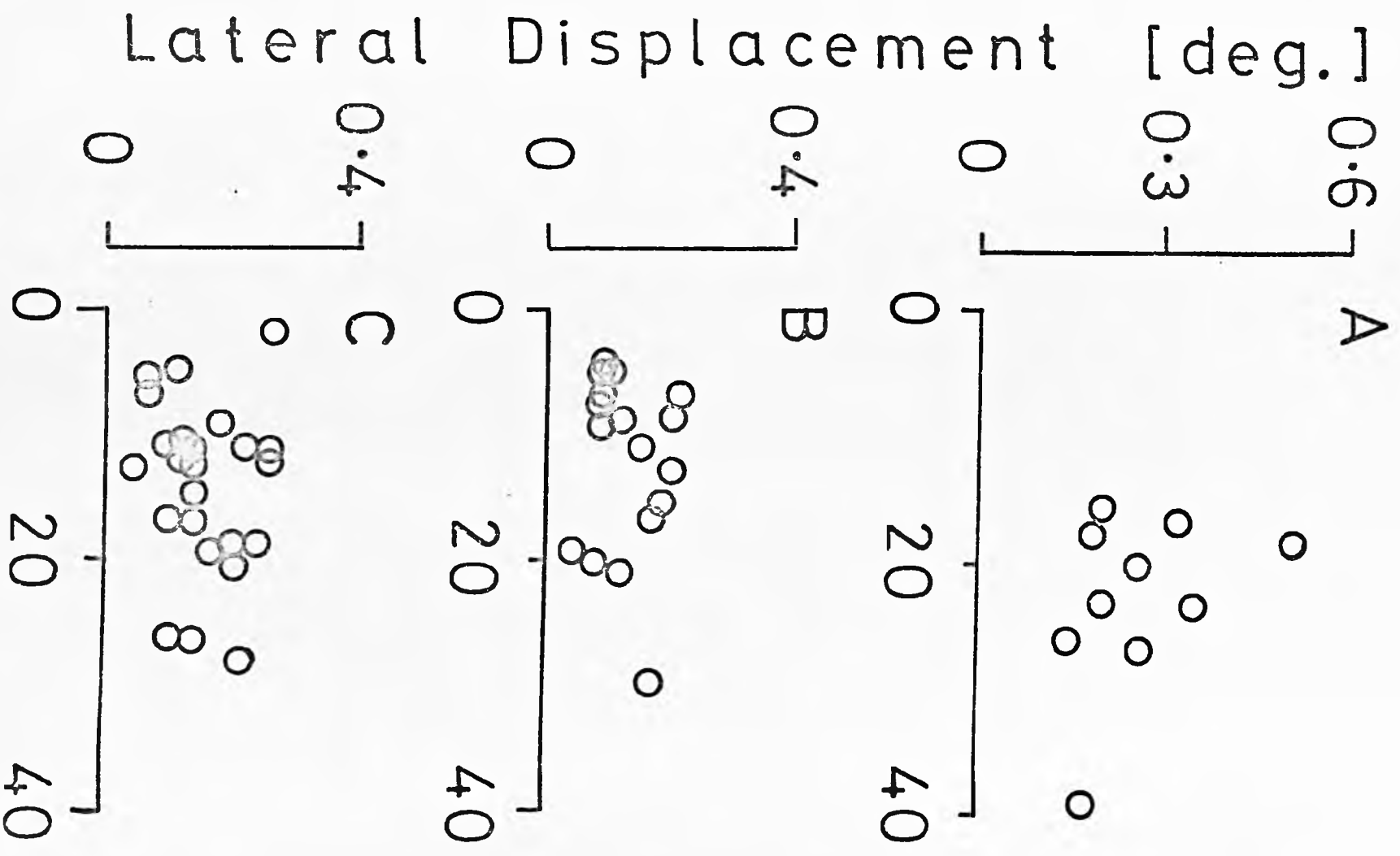
Fig. 4.12

Distribution of the lateral displacement (Fig. 4.12A) and
the maximum separation (Fig. 4.12B) values for the complete data
with eccentricity from the area centralis.

Regression analysis of the scatter in Fig. 4.12A gave the
correlation coefficient value of 0.26, and the best fit line of
slope 0.0029. At this slope, an increase of 0.12° is predicted
in the lateral displacement over the eccentricity range of 40 .
This is a negligible increase when one considers the systematic
error in positioning of the iso-sensitivity points of 0.1° for
the $\frac{1}{2}$° diameter spot.

Similarly, for Fig. 4.12B, the correlation coefficient for
the data was 0.01 and the best fit line had the slope 0.0002,
representing an increase of only 0.08° in the maximum
separation over the eccentricity range of 40°.

Hence, the magnitude of non-concentricity, measured in terms
of both the lateral displacement and the maximum separation, is
independent of the visual field location of the unit's receptive
field with respect to the area centralis.

Eccentricity [deg.]
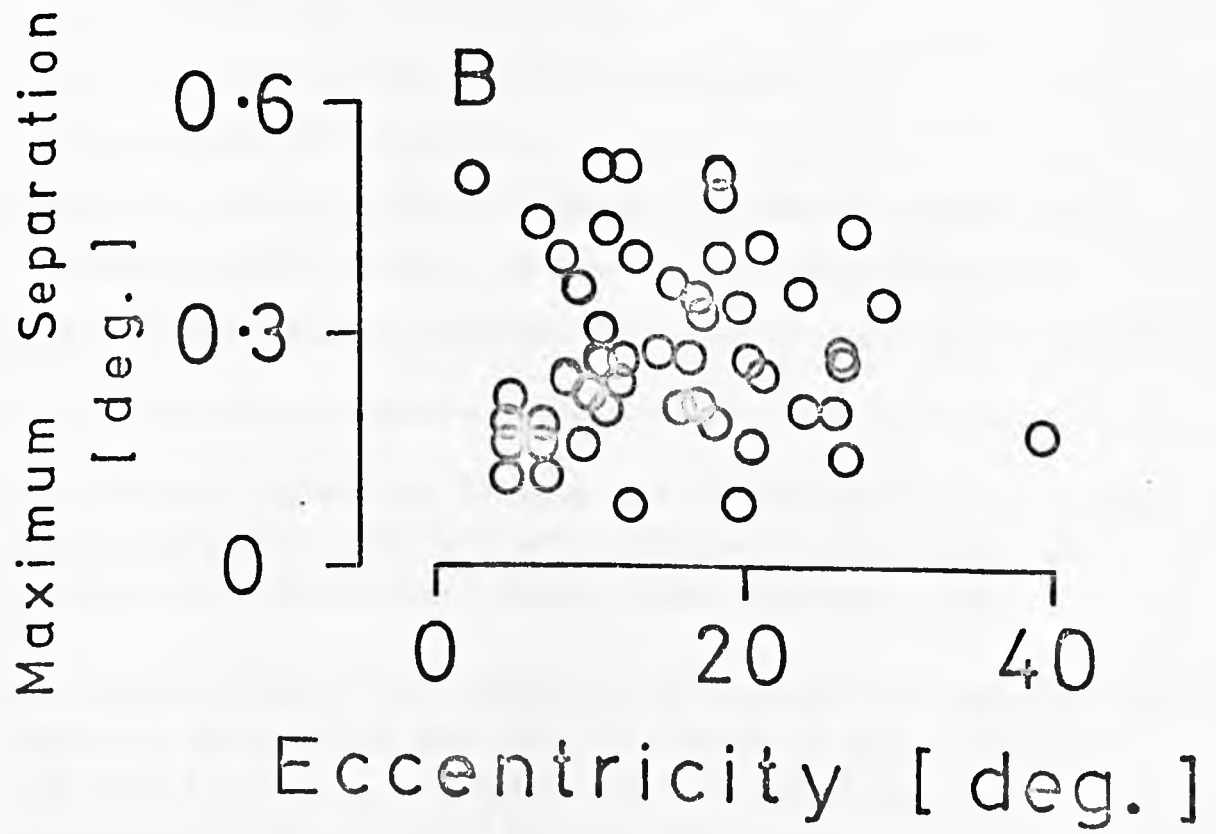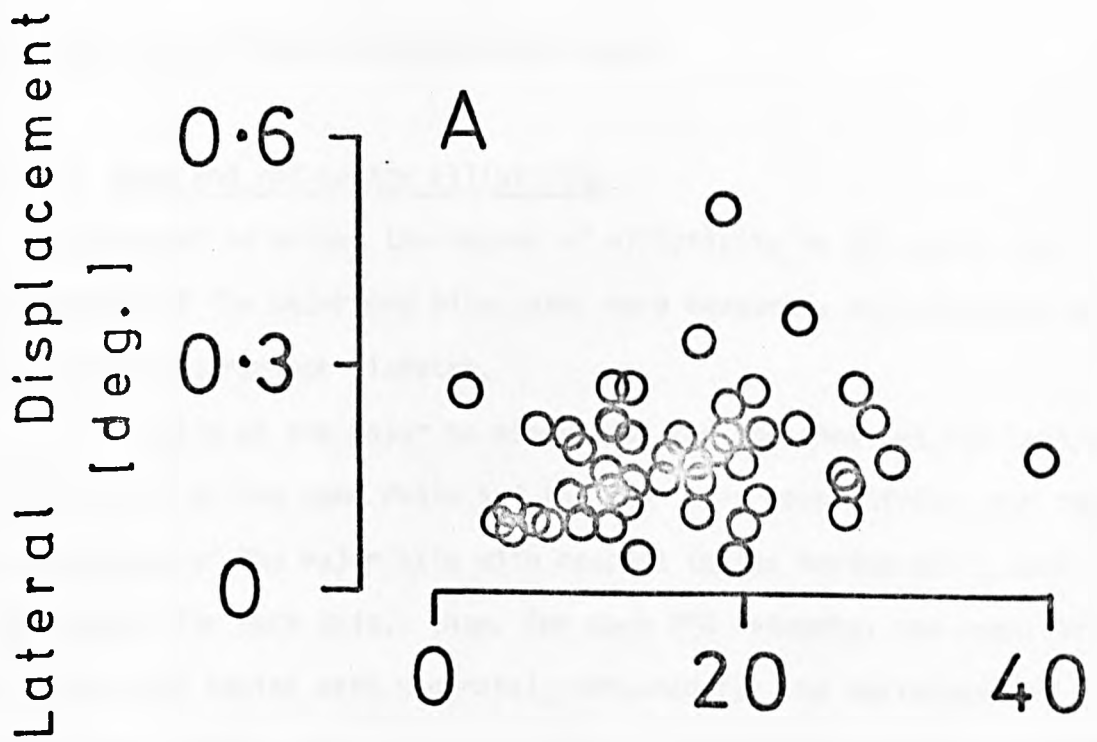
significant differences between the means.

4.3.4 Cone and rod centre ellipticity

In order to assess the degree of ellipticity in RFC maps, the diameters of the major and minor axes were measured, and expressed as the ratio major/minor diameter.

The ratio of the major to minor axes for the cone and rod centres referred to as the cone ratio and the rod ratio respectively, and the orientation of the major axis with respect to the horizontal[1], were determined for each unit. Then, for each RFC category, the means of the rod and cone ratios were separately obtained for the sustained and transient classes, and the total sample. The purpose of these measurements was to establish if any systematic differences occurred between:

(i)   the mean cone and rod ratios;

(ii)   the sustained and transient classes; and

(iii)   the four RFC categories.

Additionally, these results were compared with those of Hammond (1974).

Within each RFC category, the cone and rod ratios exhibited no statistically significant variation[2] for either the sustained or transient

---

[1]The horizontal was defined, for each unit, by assuming the line joining the area centralis to the optic disk subtended an angle of 25°, the position angle, to horizontal (Bishop, Kozak and Vakkur, 1962).

[2]The 2-sample student t-test carried out on the cone (1.39) and rod (1.28) ratios for the sustained units (n=5) in category B1 gave a t value of 0.56 (from tables $t_{0.05, 8}$ = 1.86). Hence, the means were not significantly different at the 5% probability level.

classes (Table 4.2).

In order to compare the extent of ellipticity of the RFCs of sustained and transient units, the combined cone and rod ratios were averaged to give a mean ellipticity ratio[1] for each class. For the sustained units (n=51, mean eccentricity = 15.8°) this ratio was 1.27, and for the transient units (n=23, mean eccentricity = 13.2°) it was 1.36. These ratios show that the RFCs of sustained units are less elliptical than those of transient units, although the difference is non-significant[2] at the 5% probability level. This statistically non-significant value, however, may be due to the slightly more peripheral distribution for the sustained class.

Therefore, sustained units in RFC category B2 were compared with the total sample of transient units, since both samples had a similar retinal distribution with mean eccentricity of 13.4° and 13.2° respectively. The ellipticity ratios for the sustained (n=31) and transient (n=23) units were, respectively 1.19 and 1.36. The difference, in this case, was

---

[1] For sustained units:
    Mean Cone Ratio = sum of individual cone ratios/No. of units
    Mean Rod Ratio = sum of individual rod ratios/No. of units
 and Mean Ellipticity Ratio = (Mean cone ratio + mean rod ratio)/2 = 1.27

Similarly, for transient units,
    Mean Ellipticity Ratio = 1.36

[2] Using the 2-Sample t-test on the mean ellipticity ratios for sustained (n = 51, mean eccentricity = 15.8°) and transient (n = 23, mean eccentricity = 13.2°) units gave a t value of 1.15, whilst $t_{0.05, 72}$ = 1.67. Hence, the mean ellipticity ratios are not statistically different at the 5% significance level.

Table 4.2

Average cone and rod ratios for the sustained and transient
classes obtained separately for each RFC category and for the
total data. The cone and rod ratios represent the mean values
obtained from individual calculations of the ratio of major to
minor axis, for the cone and rod centres respectively. Limits
are ±1 S.E.M.

Table 4.2

RFC CATEGORY		SUSTAINED UNITS	TRANSIENT UNITS	TOTAL SAMPLE
	No. OF UNITS	6	9	15
	MEAN CONE RATIO	1.36 ±0.25	1.36 ±0.07	1.36 ±0.11
A1	MEAN ROD RATIO	1.36 ±0.25	1.36 ±0.07	1.36 ±0.11
	MEAN ECCENTRICITY (DEG.)	16.9 ±2.7	10.8 ±1.7	13.3 ±1.6
	No. OF UNITS	9	1	10
	MEAN CONE RATIO	1.48 ±0.15	1.34	1.46 ±0.14
A2	MEAN ROD RATIO	1.43 ±0.13	1.19	1.41 ±0.12
	MEAN ECCENTRICITY (DEG.)	23.5 ±2.4	18.3	23.0 ±2.2
	No. OF UNITS	5	3	8
	MEAN CONE RATIO	1.39 ±0.17	1.18 ±0.06	1.31 ±0.11
B1	MEAN ROD RATIO	1.28 ±0.11	1.31 ±0.12	1.29 ±0.07
	MEAN ECCENTRICITY (DEG.)	15.0 ±4.3	13.1 ±2.9	14.3 ±2.8
	No. OF UNITS	31	10	41
	MEAN CONE RATIO	1.17 ±0.02	1.45 ±0.17	1.24 ±0.05
B2	MEAN ROD RATIO	1.22 ±0.04	1.39 ±0.14	1.26 ±0.05
	MEAN ECCENTRICITY (DEG.)	13.4 ±1.3	14.9 ±2.9	13.8 ±1.2
	No. OF UNITS	51	23	74
	MEAN CONE RATIO	1.27 ±0.05	1.37 ±0.08	1.30 ±0.04
ALL	MEAN ROD RATIO	1.28 ±0.04	1.36 ±0.07	1.30 ±0.04
	MEAN ECCENTRICITY (DEG.)	15.8 ±1.1	13.2 ±1.5	15.0 ±0.9

statistically significant[1]. Hence, for a given visual field location the RFCs of sustained units are more circular than those of transient units.

Indirectly, the above results also lead to the inference that ellipticity in RFC shape increases as units are located successively away from the area centralis. However, regression analyses, separately, for the rod and cone ratios show no systematic increase with eccentricity (n = 74, correlation coefficient has the values, respectively, of 0.21 and 0.19, (see also Fig. 4.25A and B). For sustained units, mean ellipticity ratios increase in the following sequence of RFC categories - B2, B1, A1 and A2 (Table 4.3), i.e. in the same order as the mean retinal eccentricity value for each category. The same analysis cannot, unfortunately, be applied to the transient units because of the small sample size in categories A2 (n=1) and B1 (n=3). A direct comparison of these parameters between categories A1 (n=9) and B2 (n=10) (Table 4.3), corroborates the above trend. However, it must be emphasized that these results show a statistically non-significant trend but in the right direction.

The orientation of the major axis with respect to the horizontal (see footnote 1 on page 92) was obtained separately for the cone and rod centres. Since the angle subtended by the major axis was measured anti-

[1]Using the 2-Sample t-test on the ellipticity ratios for sustained units in category B2 (n = 31, mean eccentricity = 13.4°) and transient units (n = 23, mean eccentricity = 13.2°) gave a t value of 2.15, whilst $t_{0.05, 52}$ = 1.68. Hence, the ellipticity ratios are significantly different at the 5% probability level.

Table 4.3

Mean ellipticity ratios for each RFC category, given separately for the sustained and transient classes.

Although the total data gave a poor correlation between the extent of ellipticity and the eccentricity from the area centralis, significant differences were found for the ellipticity ratios between the sustained units of RFC categories B2 and A2 which correlate with their different mean eccentricities.

Table 4.3

SUSTAINED CLASS.

RFC CATEGORY	No. OF UNITS	MEAN ECCENTRICITY (DEG.)	MEAN ELLIPTICITY RATIO
B2	31	13.4	1.19
B1	5	15.0	1.33
A1	6	16.9	1.36
A2	9	23.5	1.45

TRANSIENT CLASS.

| A1 | 9 | 10.8 | 1.36 |
| B2 | 10 | 14.9 | 1.42 |

clockwise from horizontal, 0° and 180° represent the horizontal and 90° the vertical orientations. The results are shown in histogram form (Fig. 4.13) with orientation intervals of 10°.

The distribution of the orientations for the cone centres (Fig. 4.13A) and rod centres (Fig. 4.13B) are very similar, as expected from visual inspection of their centre shapes. Only a few units (n=9) showed widely different orientations between the major axes (separation at least 60°) of their rod and cone centres. The percentage of units with the orientation ±20° around the horizontal for the cone centres was 54% and for the rod centres 58%. This bias towards a horizontally oriented major axis confirms the previous findings of Hammond (1974).

4.3.5 Rod and cone centre areas

As discussed previously, four receptive field categories were defined: those for which the rod and cone centre sizes were similar (categories A1 and A2), and those where the sizes differed (categories B1 and B2). Variation of the rod and cone centre sizes in these categories was evaluated by comparing the area within each rod- and cone-mediated iso-sensitivity contour[1].

[1]The area (A), within a polygon of n sides with each corner having the coordinates (X_i, Y_i), is given by the equation:

$$A = \frac{1}{2} \left((X_n \cdot Y_1 - X_1 \cdot Y_n) + \sum_{i=1}^{i=n} (X_i \cdot Y_{i+1} - X_{i+1} \cdot Y_i) \right) \quad \ldots\ldots\ldots\ldots (1)$$

A CAI Alpha based computer, given the coordinates of the iso-sensitivity points defining the contour, calculated equation (1).
Another method frequently employed involved, first, the plotting of the contour on paper and, then, the area determination by a planimeter. The agreement between these two methods, for the same contour, was better than 0.05 deg.[2].

Fig. 4.13

Orientations of the major axes for RGCs' RFCs   with respect
to the horizontal. The horizontal was defined by assuming a
position angle of 25° to horizontal, subtended by the line
joining the area centralis to the optic disk (Bishop, Kozak and
Vakkur, 1962). Orientation was measured anti-clockwise from the
horizontal and the histograms were obtained using orientation
intervals of 10°.

Fig. 4.13A is the data for the cone centres and Fig. 4.13B
for the rod centres. Although, almost all orientations are
represented, there is a systematic bias in favour of horizontal.
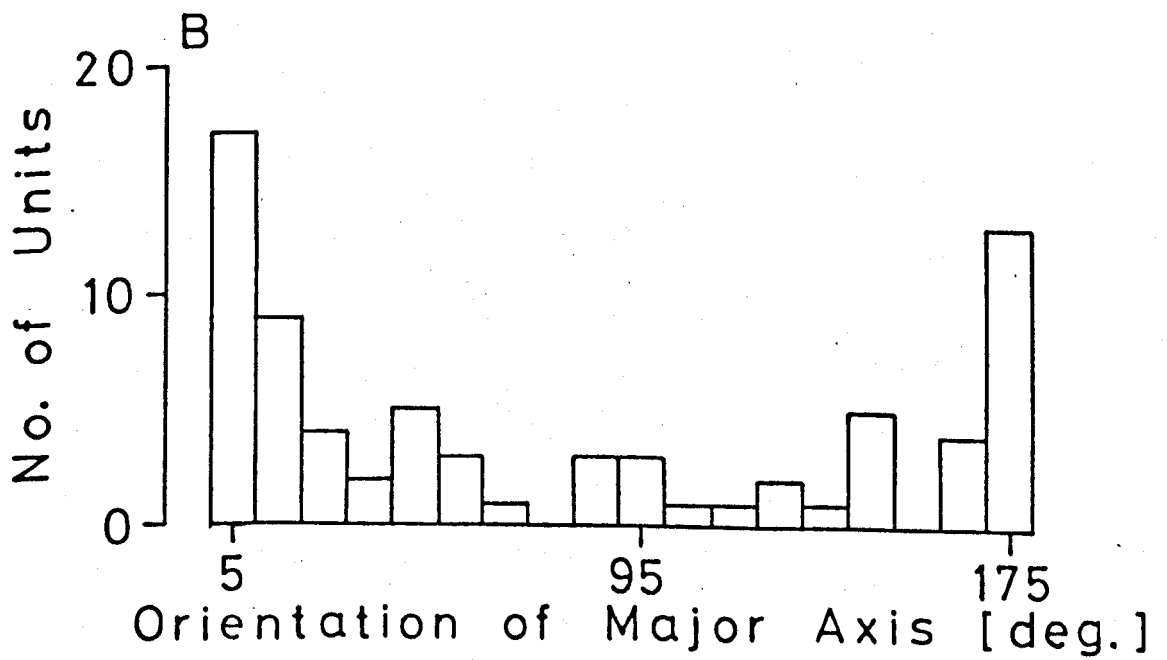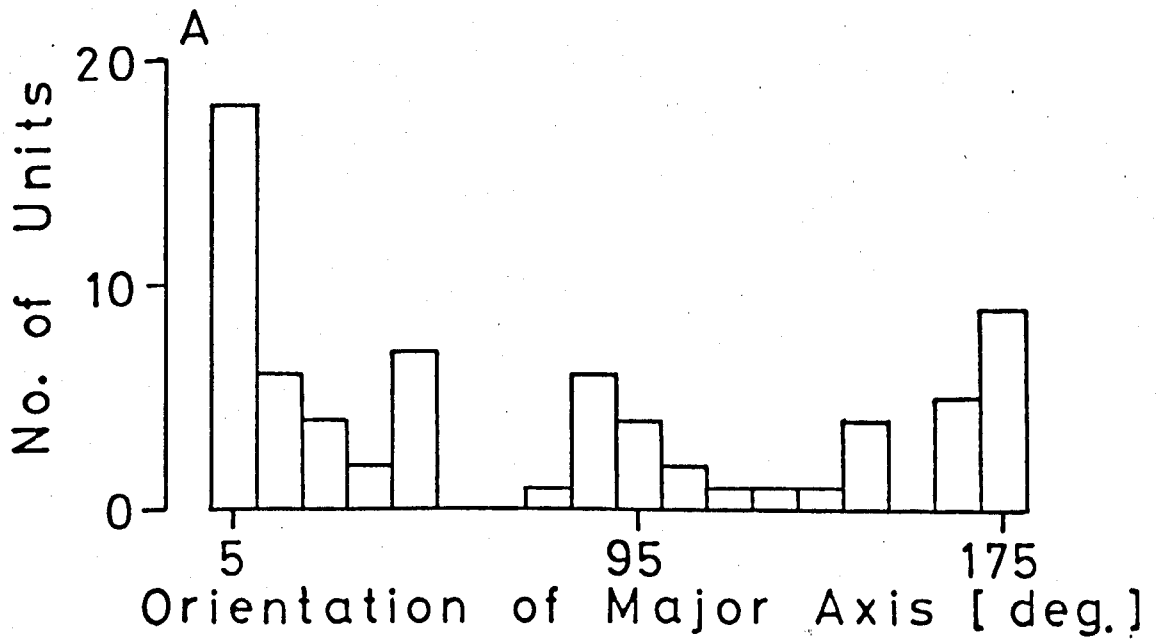
The scatter of rod versus cone centre areas for categories A1 (open triangles) and A2 (open circles) is shown in Fig. 4.14A. The majority of the data points lie on or near the line representing equal rod and cone areas (continuous line), as expected from visual inspection of centre sizes. In these, any slight divergence from the continuous line derives from considering RFCs as straight-sided polygons. However, there are a few cases where a significant divergence from equality is apparent. In these, although visual inspection of the rod and cone centre maps show no obvious difference, the number of iso-sensitivity points defining the respective contour differs, leading to discrepancies in determination of centre area.

The data for categories B1 (open triangles) and B2 (open circles) are shown in Fig. 4.14B. The continuous line again represents equality of area between the cone and rod centres. Points above the line represent those units with larger rod centres and those below with larger cone centres. For units in category B1, the rod:cone area ratios ranged from 1.3:1 to 2.9:1 with a mean value of 1.9:1 (n=8, s.e.m. = ±0.2). The majority of B2 units had appreciably larger rod centres, with rod:cone ratios ranging from 1.2:1 to 2.4:1 with a mean of 1.5:1 (n=39, s.e.m = ±0.1). In a few B2 units, the calculated rod and cone centre areas were very similar, although visual inspection in these cases revealed a small systematic difference between the rod and cone iso-sensitivity points defining the respective centres. Two units had smaller rod than cone centres - rod:cone ratios of 0.8:1 and 0.6:1 respectively.

These results show that the rod:cone area ratios for retinal ganglion cells range from 0.6:1 through equality to a maximum of 2.9:1, heavily weighted in favour of larger rod centres. 65% of the total sample (n=74) had larger rod than cone centres, with a mean value for the rod:cone area

Fig. 4.14

The scatter of rod versus cone centre areas on log.-log.
coordinates. 45° line in each figure represents equality of
area.

    A - category A1 (Δ) and A2 (0) units. As expected from
          visual inspection, the rod and cone centres were
          similar in size. The slight deviations from equality
          can be attributed to the method of calculating the
          areas.

    B - category B1 (Δ) and B2 (0) units. Except in two
          units, rod centre areas were larger than cone centre
          areas.

Area of Rod Centre
[Deg^2]

Area of Cone Centre [deg.^{2}]
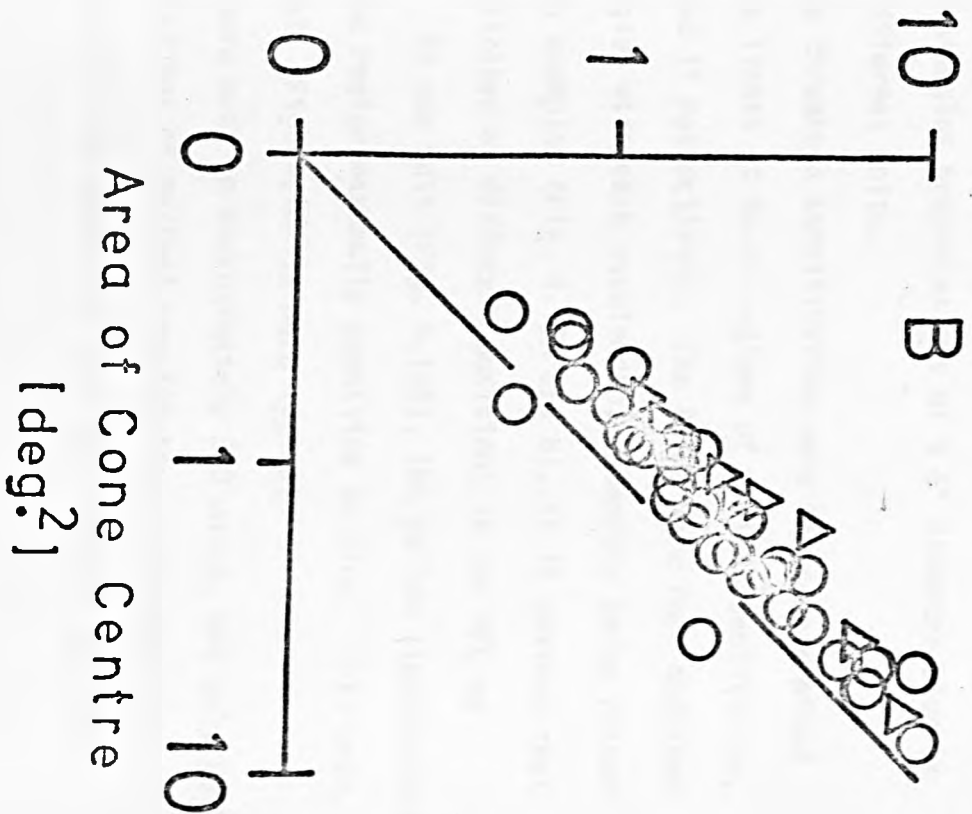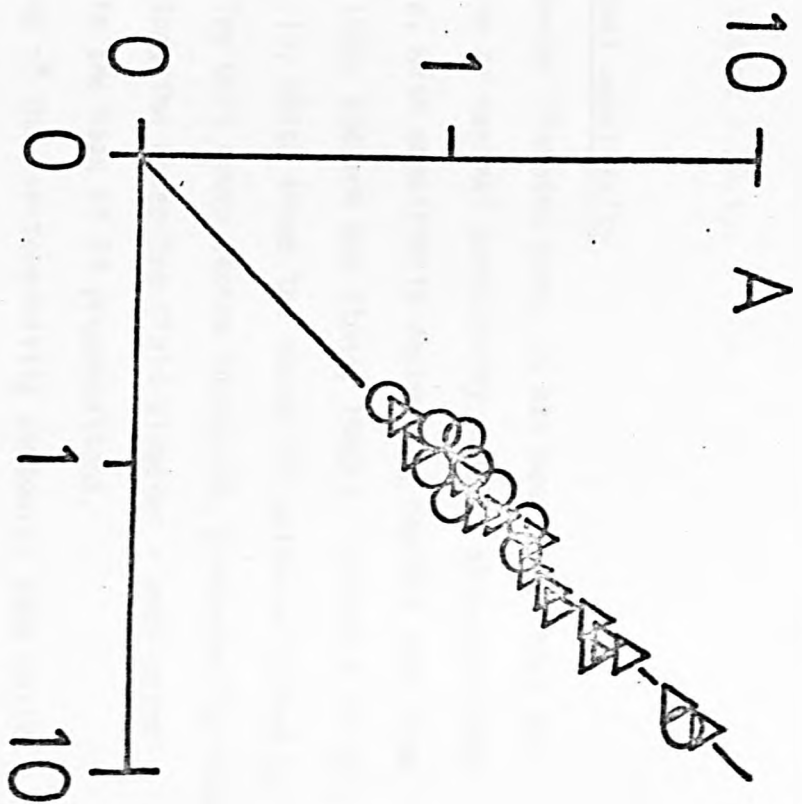
ratio of 1.6:1 (n=48, s.e.m. = ±0.1).

4.3.6 Regions of maximal sensitivity

Using a small-diameter flashing spot, it has been shown that the RFC of RGCs has a region of maximal sensitivity usually situated close to the geometric centre, with sensitivity decreasing rapidly away from this region (Kuffler, 1953; Rodieck and Stone, 1965b). Evidence of this is presented in Fig. 4.15, which shows the number of spikes elicited by a $\frac{1}{2}°$ diameter spot, 1 log unit above centre threshold, presented for 400ms at successive points along the receptive field diameter - each point (open circle) represents the mean of 20 presentations.

During the plotting of the iso-sensitivity contours, some units showed two regions of maximal sensitivity, one for short wavelengths (blue) and the other for long wavelengths (yellow). Fig. 4.16 shows PSTHs obtained with 16 stimulus presentations of a $\frac{1}{2}°$ diameter blue or yellow light for two different units.

In both units, the threshold sensitivities were first determined for the yellow and blue lights at their regions of maximal sensitivity, denoted by regions I and II respectively. The PSTHs were then obtained by stimulating each region with each wavelength, intensity being raised by 1 log unit. In both examples (Fig. 4.16A and B), it is obvious that maximal response was elicited at different positions in the RFC by different wavelengths. In one unit (Fig. 4.16B), the yellow light evoked little response from the region maximally sensitive to blue. This unit, however, was exceptional. Fig. 4.16A is more typical.

Systematic tests were made in approximately 350 units, but only in 18 instances were the locations of maximal sensitivity wavelength-dependent. Fourteen of these were held long enough to plot both the rod and cone

Fig. 4.15

Responses of an on-centre sustained unit along one diameter
of the receptive field passing through the region of maximal
sensitivity. Responses were elicited by a $\frac{1}{2}°$ diameter flashing
spot of white light as 1 log. unit above centre-threshold. Each
point represents the mean number of spikes elicited from 20
consecutive presentations of the stimulus of duration 400ms.
The dashed line represents the unit's maintained discharge.
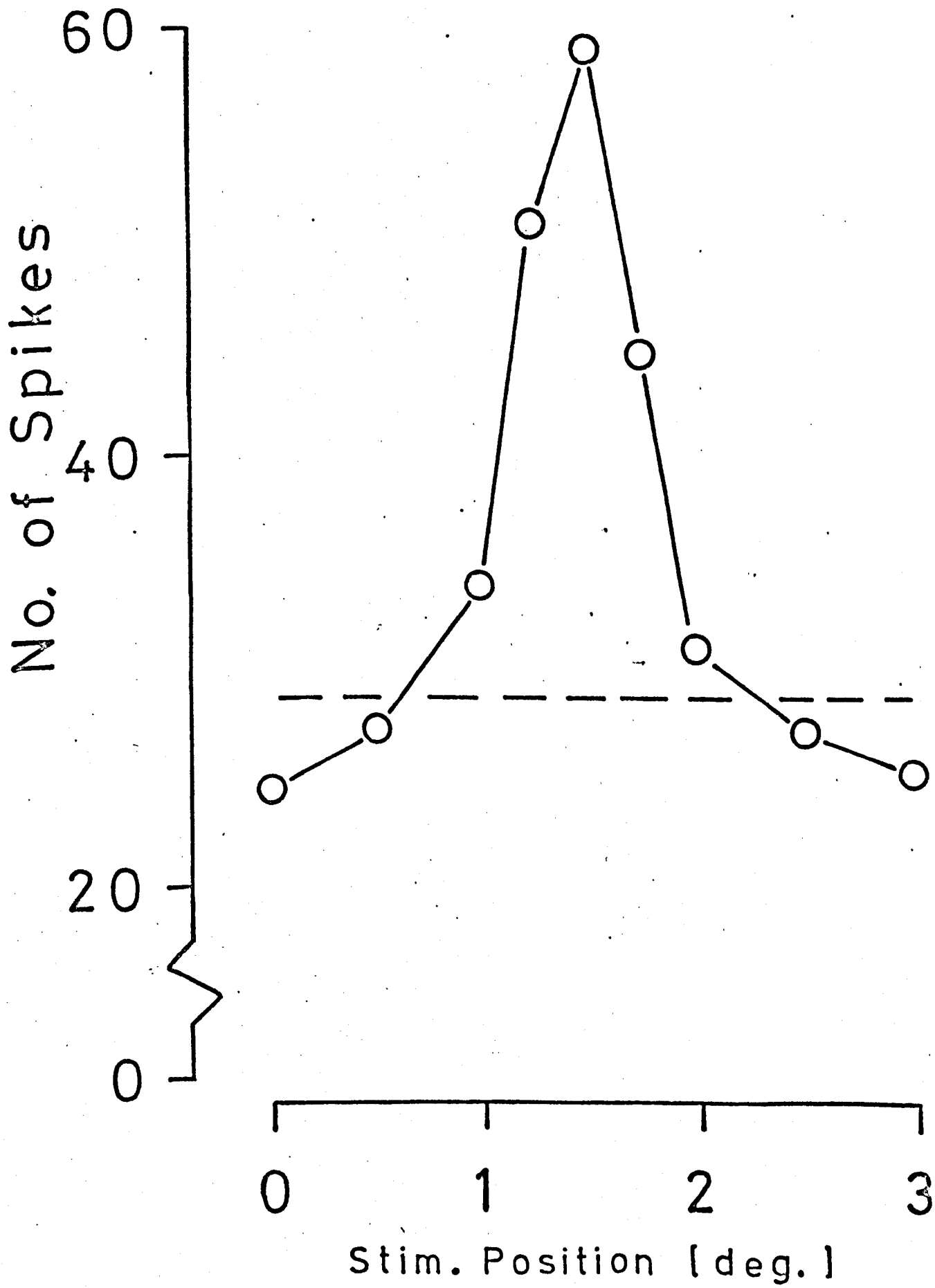
Fig. 4.16

Peri-stimulus time histograms (PSTHs) of responses to 0.5°
spots of blue or yellow light flashed in the receptive field
centre. Two positions (denoted by Regions I and II) were found
such that at one a maximal response could be elicited by the
yellow and at the other by the blue light. Examples of two
units showing this property are given (Figs. 4.16A and B).
Each PSTH was formed with 16 consecutive presentations of the
appropriate light stimulus, duration 400ms (dark bar)
presented every 1.6 s. The bin-width was 10ms.

A - on-centre brisk sustained unit. Eccentricity =
23.4°.

B - on-centre brisk sustained unit. Eccentricity =
27.2°.

ROT.026.09

Maximal   Sensitivity

Region II   Region I   A

400ms

Yellow Light

Blue Light

400ms

Spikes/bin

0   50

ROT.026.01

Maximal   Sensitivity

Region II   Region I   B

400ms

Yellow Light

Blue Light

400ms

Spikes/bin

0   50
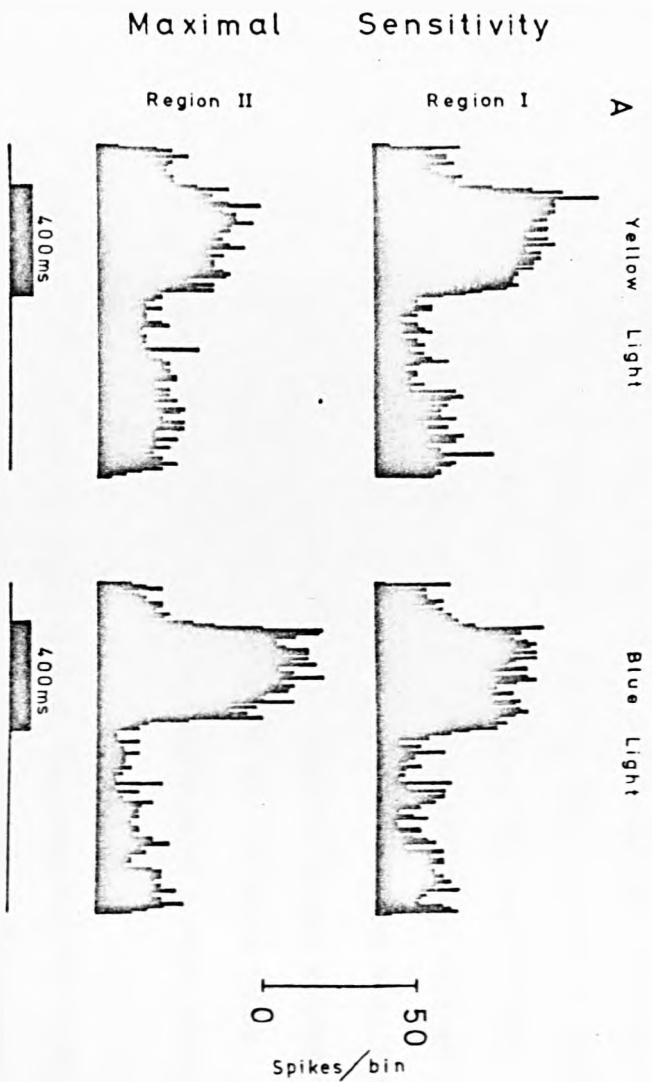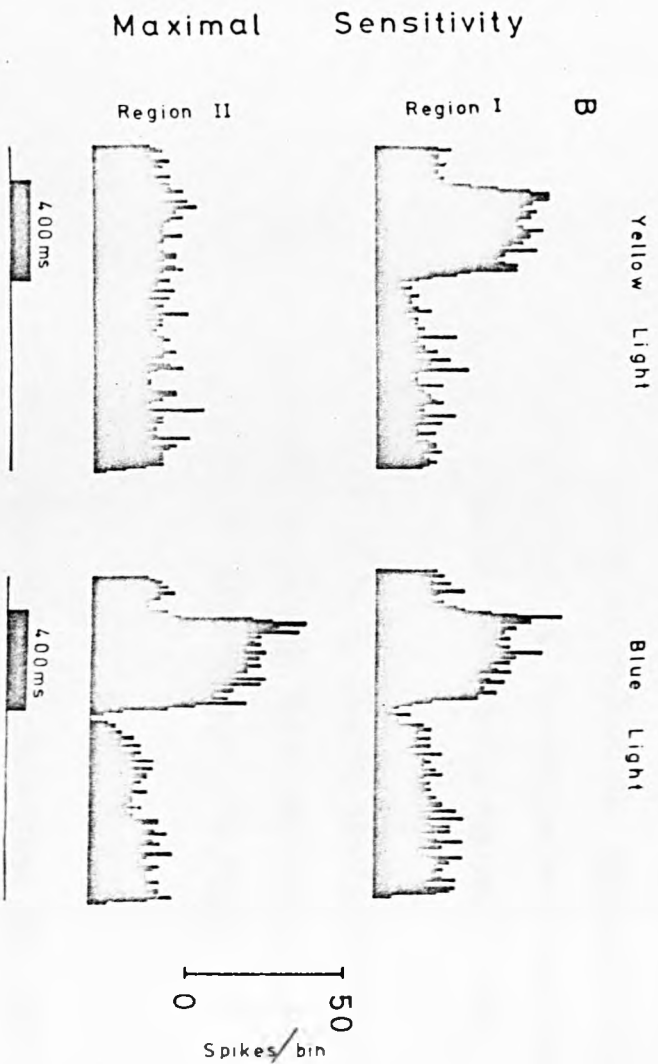
centres. These were, accordingly, placed into the contour categories A2 (n=6) and B2 (n=8). An example, for each of these categories, is given in Fig. 4.17. In both these examples the rod centre (either shifted laterally, Fig. 4.17B, or expanded asymmetrically, Fig. 4.17A) is displaced relative to the cone centre in the same direction as the unit's blue sensitive region. However, the magnitude of the separations between the two regions of maximal sensitivity and the respective rod and cone centre boundaries are not the same for each example. Comparable measurements made on the remaining units are pooled in Fig. 4.18. In both cases (Fig. 4.18A and B), regression analysis of the data gave a poor correlation between these parameters.

The relationship between the separation of the sensitivity regions and eccentricity from the area centralis was also considered. The scatter of these parameters, for the total sample of 18 recordings, is shown in Fig. 4.19. The best fit regression line, determined for the data points and shown in the figure as the dashed line, has a slope of 0.0025. This represents an increase of $0.1°$ in the separation over the eccentricity range of $40°$, which is no greater than the inherent error in estimating the separation. Separation of the two sensitivity regions is thus independent of eccentricity.

For the total sample (n=18) of units showing displaced regions of maximal sensitivity, the separation between these regions ranged from $0.25°$ to $0.44°$ with a mean value of $0.35°$ (S.E.M = $±0.01$).

4.4 Geniculate study

In the preceding retinal study, very few recordings were obtained from units with receptive fields in the central region of the retina near the area centralis. Hence, a geniculate study was undertaken to record

Fig. 4.17

The position of the two sensitivity regions with respect to the rod and cone centres are shown. The direction and position of the area centralis (AC) and optic disk (OD) from the right (R) or left (L) eye are shown, respectively by the line and the bracketed value in degrees.

A - The maximal sensitivity regions for the rod (open circles) and cone (open triangles) centres are denoted, respectively by the closed and open squares for an on-centre brisk sustained category B2 unit.

B - The maximal sensitivity regions are shown for an on-centre brisk sustained category A2 unit. The symbol conventions are as above.

A

RAC (27°)
ROD (44°)

ROT. 38.10

B

LOD (26°)
LAC (39°)

ROT. 30.1

1°

1°
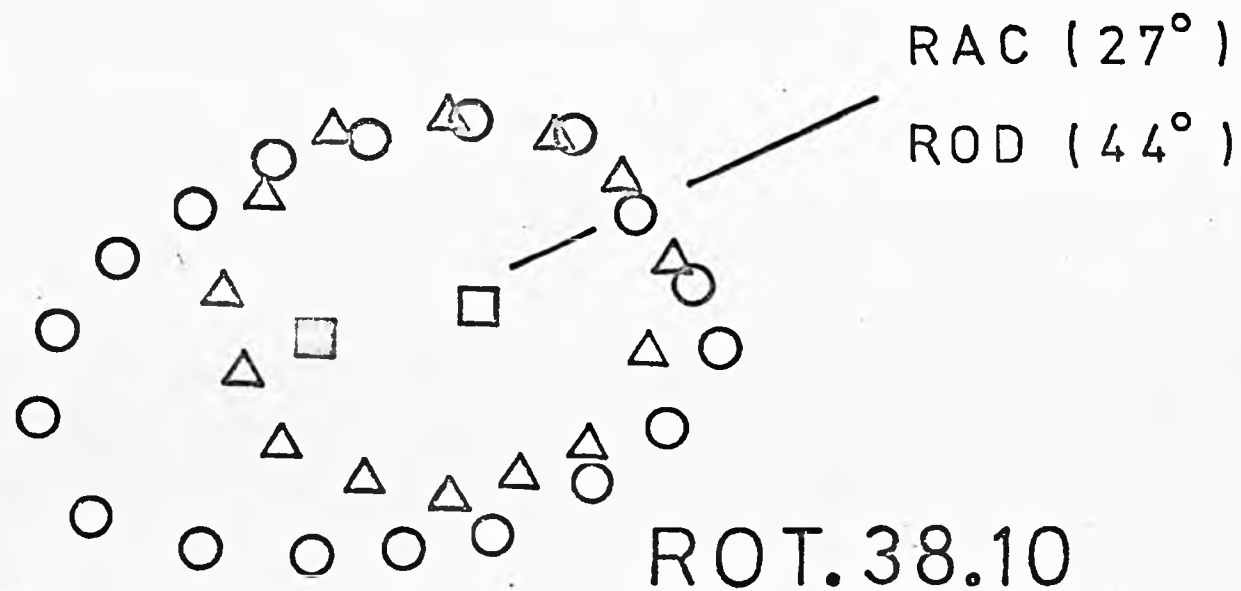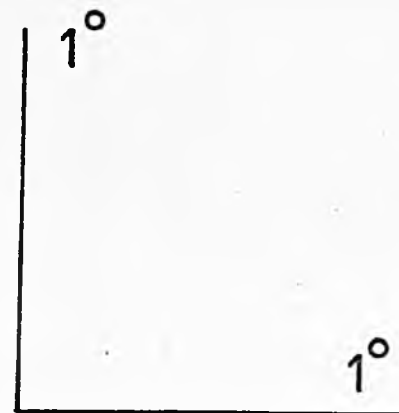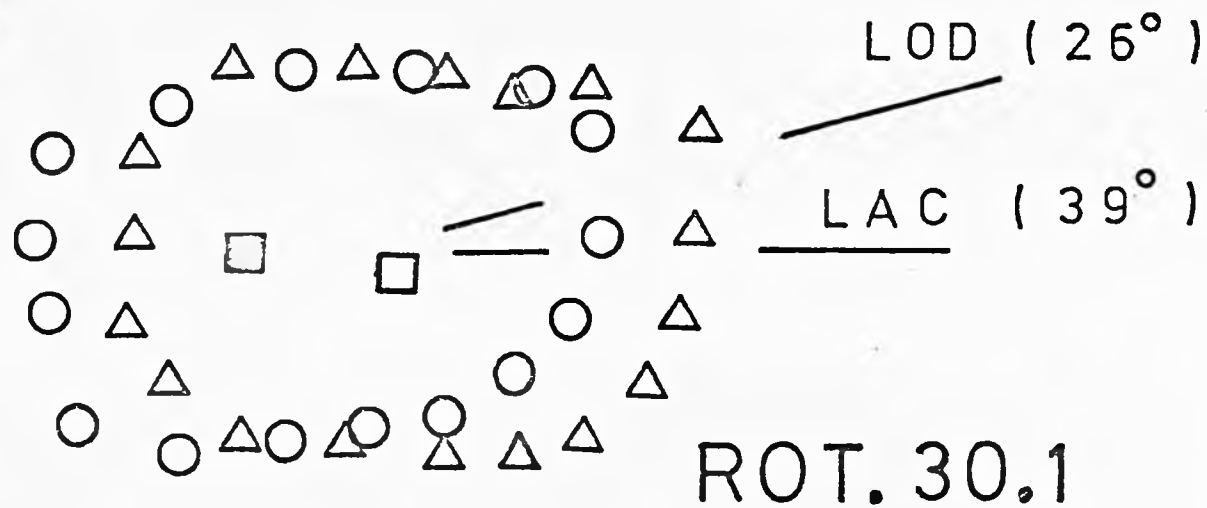
Fig. 4.18

Scatter of the lateral displacement (Fig. 4.18A) and the
maximum separation (Fig. 4.18B) of cone and rod centres versus
the separation between the maximal sensitivity regions. The
continuous line represents the line of equality. Values for
categories A2 and B2 are shown, respectively by the open
triangles and open circles.
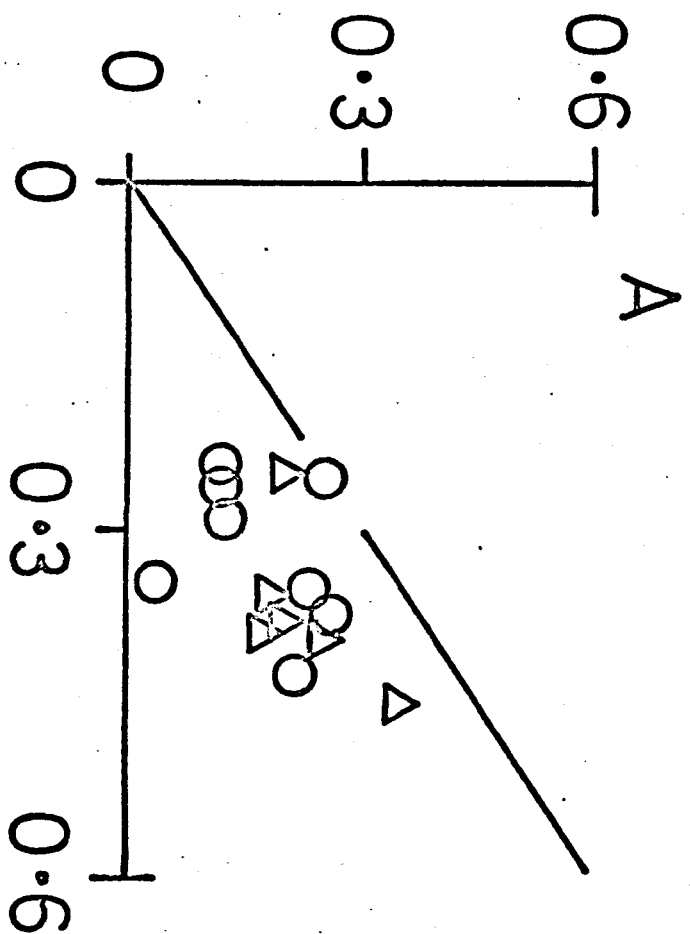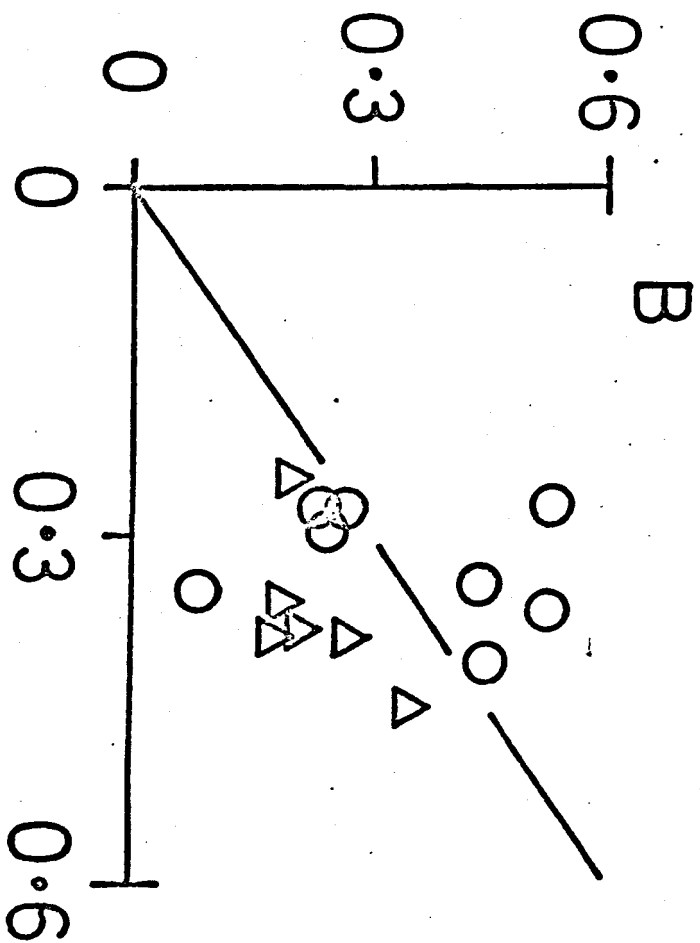
Fig. 4.19

Correlation of separation between the maximal sensitivity regions with eccentricity of the receptive field from the area centralis. The dashed line represents the best fit regression line (correlation coefficient = -0.38) and has a slope of 0.0025. This slope represents an increase of 0.1° in the separation over the eccentricity range of 40°.
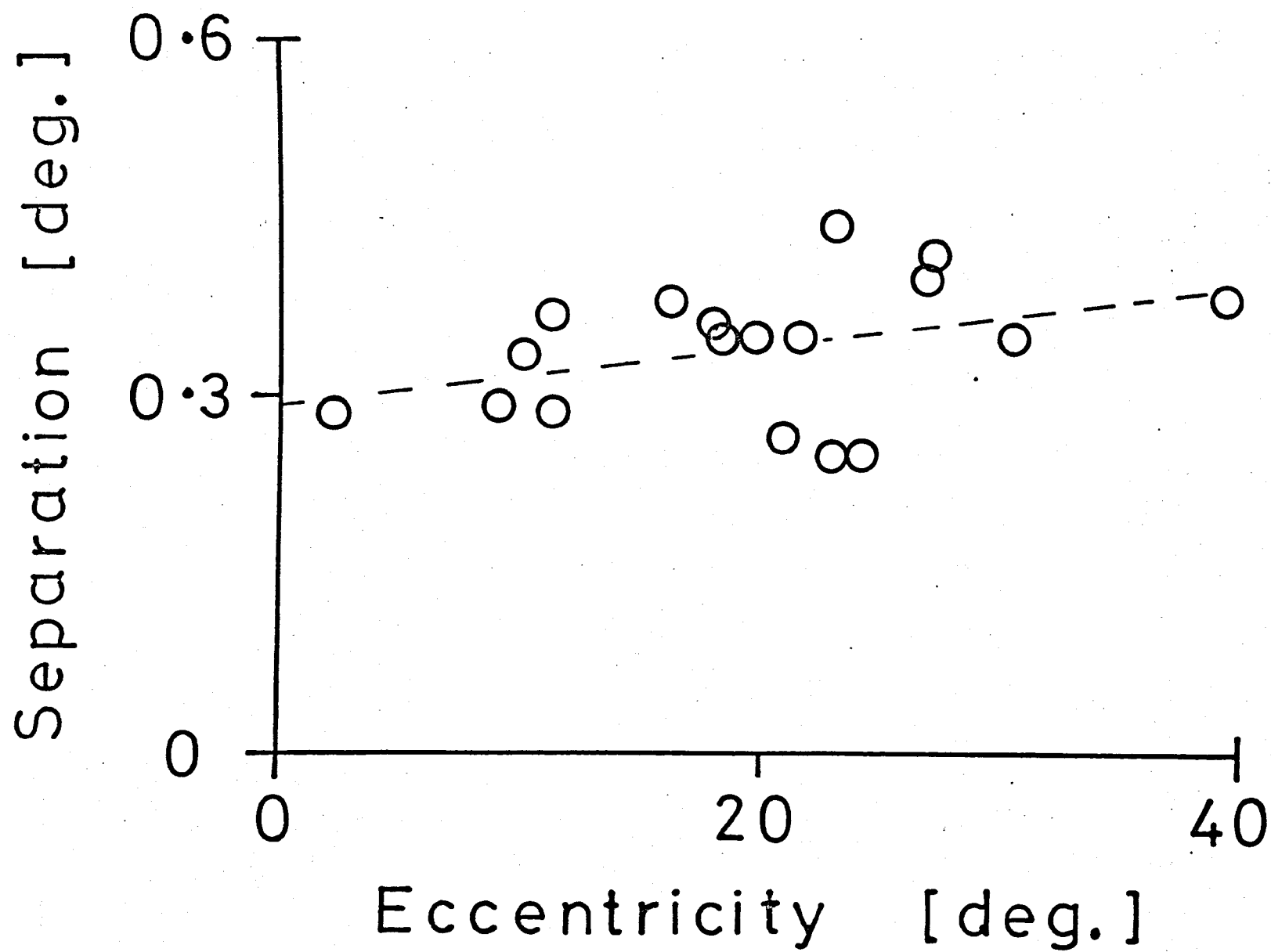
from cells receiving their inputs from this central region.

Rod and cone centre maps were obtained for a total of 31 cells, 14 sustained (on-: off-centre, 11:3) and 17 transient (on-: off-centre, 12:5), with 24 units being centrally (mean eccentricity = 5.4°) and 7 peripherally (mean eccentricity = 15.4°) located.

4.4.1 RFC categories

By comparing the size, shape, and position of the rod and cone centres, all 31 units could be placed into the RFC categories A1 (n=20) and B2 (n=11). In the latter category (B2), 8 units were in the asymmetric and 3 in the symmetric sub-categories, and all possessed rod centres larger in size than the cone centres.

The location of units in the visual field, with respect to the area centralis, and their distribution into the sustained and transient classes for categories A1 and B2 are shown, respectively, in Fig. 4.20 and Table 4.4

4.4.2 Non-concentric rod and cone centres

The lateral displacement and the maximum separation between the rod and cone centres for the 11 units in category B2 were determined. These parameters are separately plotted against eccentricity in Fig. 4.21.

The mean values of the lateral displacement obtained for centrally located (arbitrarily assumed for units with eccentricity < 15°) and peripherally located (eccentricity > 15°) units were analysed using the 2-sample t-test. The two means were just not significantly different[1]

[1]The mean values of the lateral displacement for:
(i) centrally located units (n=6, mean eccentricity = 6.2°) was 0.09°; and
(ii) peripherally located units (n=5, mean eccentricity = 19.5°) was 0.14°. The calculated t value was 1.79, and from the tables $t_{0.05, 9}$= 1.83.

Fig. 4.20

Location of the RFCs in the visual field with respect to the area centralis. Categories A1 (open squares) and B2 (open triangles) are shown separately in Fig. 4.20 A and B. The visual field positions were obtained as described for the retinal data (Fig. 4.7).
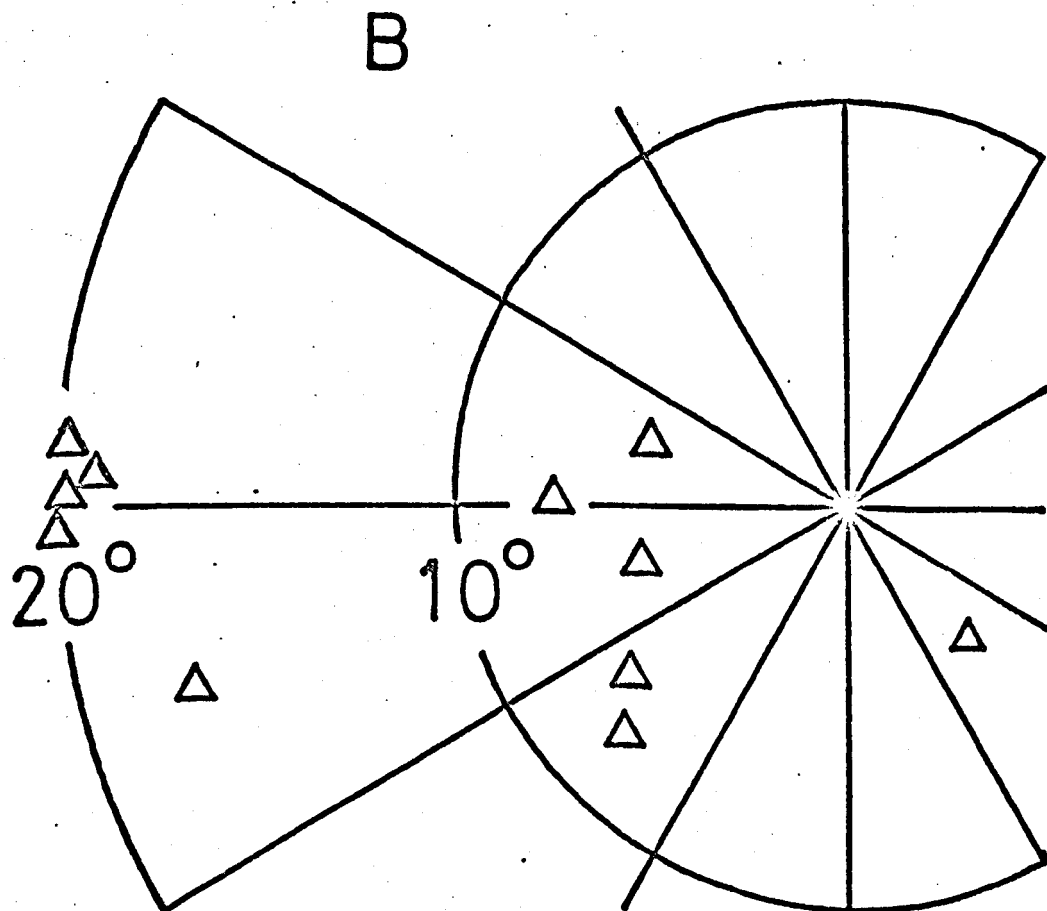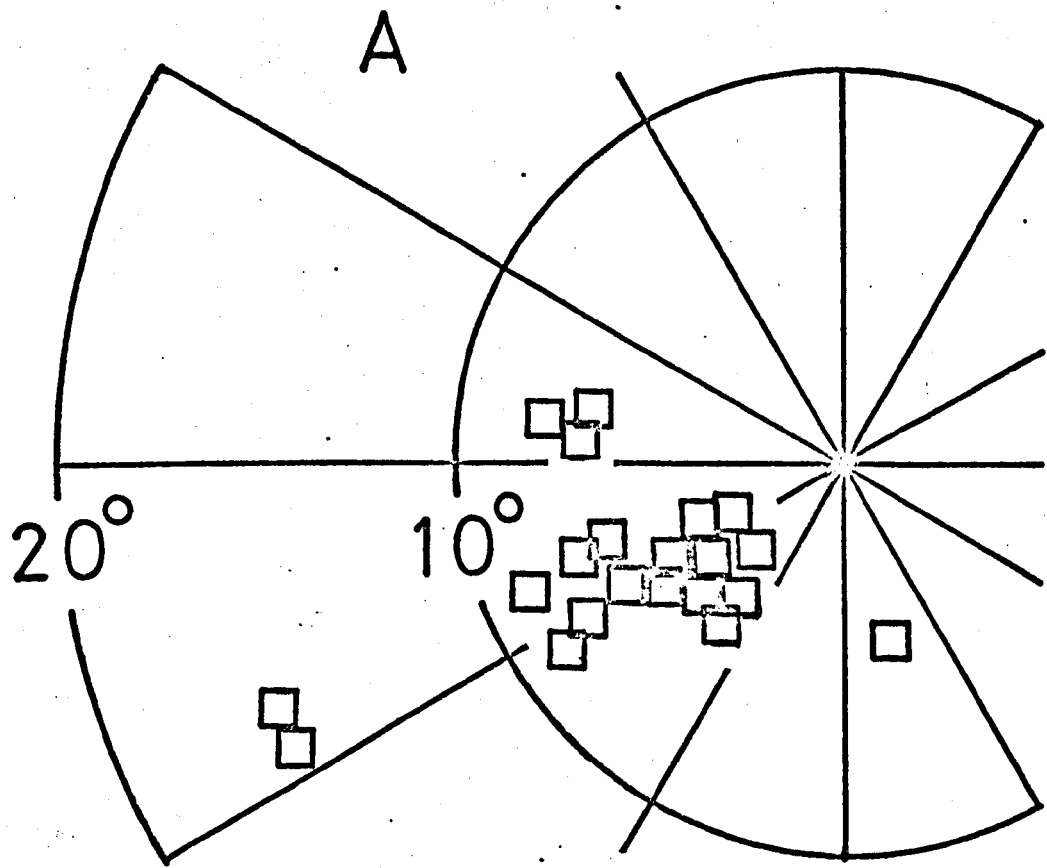
Table 4.4

The distribution of sustained (S) and transient (T), on-
or off-centre (+ or -), lateral geniculate cells (LGCs) into
the RFC categories A1 and B2.

Table 4.4

RFC CATEGORIES

	A1	B2	TOTAL
S+	7	4	11
S-	2	1	3
T+	7	5	12
T-	4	1	5
TOTAL	20	11	31

Fig. 4.21

The scatter of the lateral displacement (Fig. 4.21A) and the maximum separation (Fig. 4.21B) values with receptive field eccentricity from the area centralis.

Maximum Separation [deg.]

Lateral Displacement [deg.]

0 0·2 0·4

0 0·2 0·4

A

B

0 10 20
Eccentricity [deg.]
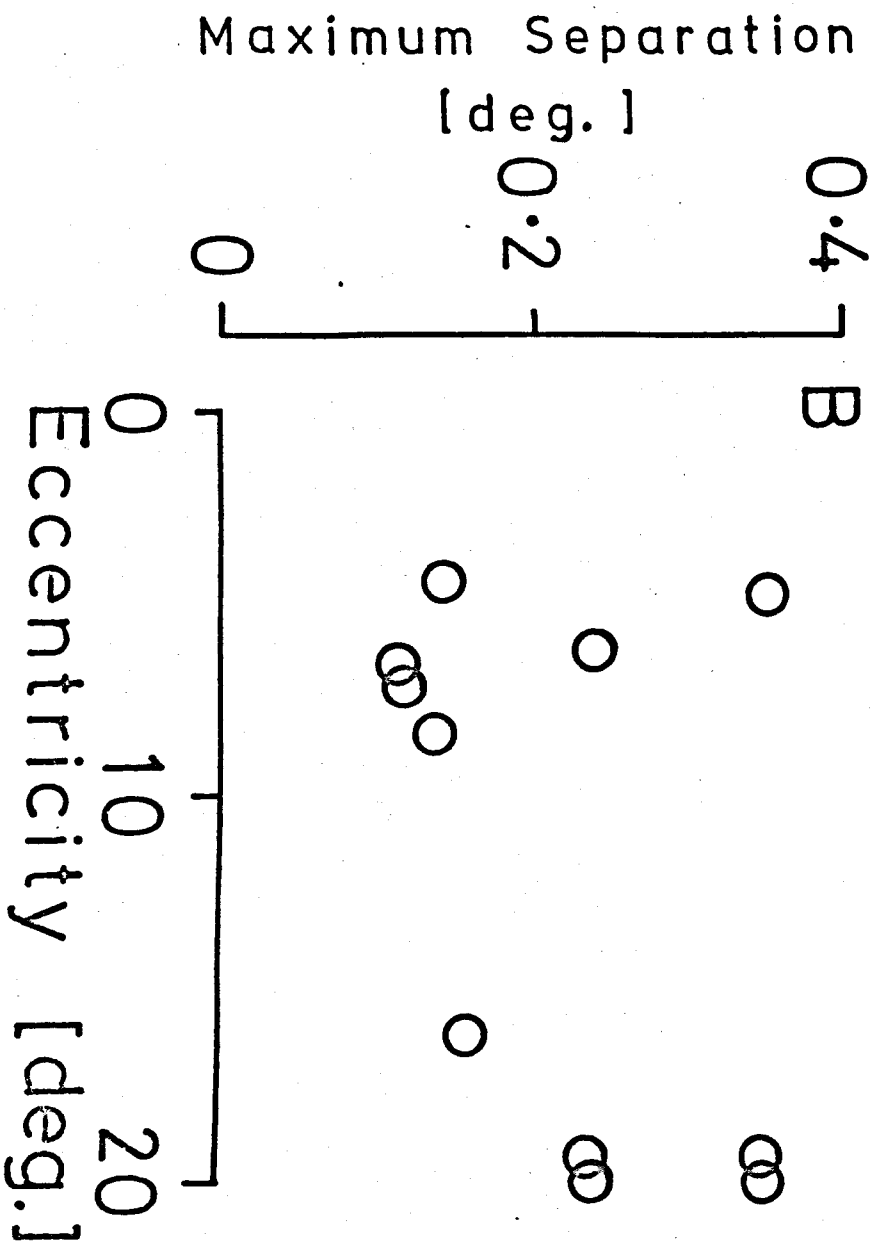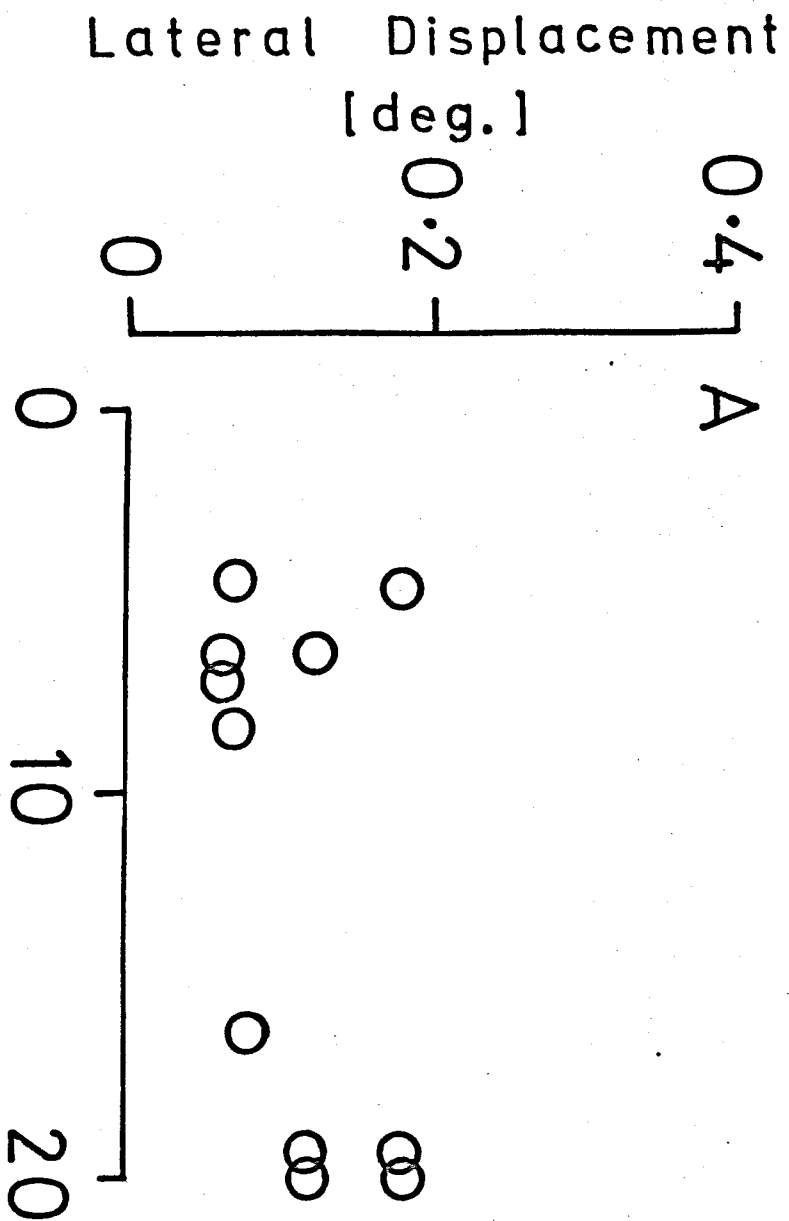
at the 5% probability level. The data for the maximum separation, similarly analysed, also gave a non-significant[1] variation.

Like the retinal data, these results also show no systematic increase in non-concentricity with eccentricity.

4.4.3 Rod and cone centre ellipticity

The rod and cone ratios were determined (section 4.3.4) for each LGC, and the means were then calculated separately for:

   (i)   the sustained and transient units,

  (ii)   categories A1 and B2, and

 (iii)   the total data.

The mean ellipticity ratio ($\frac{1}{2}$(mean rod ratio + mean cone ratio)) was also obtained. The results are shown in Table 4.5.

In agreement with the retinal results, the geniculate data show that:

   (i)   the mean rod and mean cone ratios for the sustained (or the transient) class were not significantly different; and

  (ii)   the extent of ellipticity was not related to the visual field distribution of the receptive fields, the difference in the mean ellipticity ratio, between categories A1 (mean eccentricity = 6.2°, n=20) and B2 (mean eccentricity = 12.3°, n=11), being non-significant[2] ($p < 0.05$). However, there is disagreement,

---

[1]The mean values of the maximum separation for:

   (i)   centrally located units (n=6, mean eccentricity = 6.2°) was 0.19°; and

  (ii)   peripherally located units (n=5, mean eccentricity = 19.5°) was 0.27°.

The calculated t value was 1.48, and from the tables $t_{0.05, 9} = 1.83$.

[2]Category A1 : mean ellipticity ratio = 1.32

  Category B2 : mean ellipticity ratio = 1.36

Table 4.5

Ellipticity parameters for the LGCs, obtained separately for the sustained and transient classes.

Table 4.5

RFC CATEGORY		SUSTAINED UNITS	TRANSIENT UNITS	TOTAL SAMPLE
	No. OF UNITS	9	11	20
	MEAN CONE RATIO	1.33 ±0.05	1.32 ±0.06	1.32 ±0.04
A1	MEAN ROD RATIO	1.33 ±0.05	1.32 ±0.06	1.32 ±0.04
	MEAN ELLIPTICITY RATIO	1.33	1.32	1.32
	MEAN ECCENTRICITY (DEG.)	6.3 ±1.3	6.1 ±1.0	6.2 ±1.3
	No. OF UNITS	5	6	11
	MEAN CONE RATIO	1.22 ±0.08	1.49 ±0.15	1.37 ±0.1
B2	MEAN ROD RATIO	1.36 ±0.13	1.36 ±0.09	1.36 ±0.08
	MEAN ELLIPTICITY RATIO	1.29	1.43	1.36
	MEAN ECCENTRICITY (DEG.)	11.9 ±3.5	12.6 ±3.0	12.3 ±2.1
	No. OF UNITS	14	17	31
	MEAN CONE RATIO	1.29 ±0.05	1.38 ±0.07	1.34 ±0.04
ALL	MEAN ROD RATIO	1.34 ±0.06	1.34 ±0.05	1.34 ±0.04
	MEAN ELLIPTICITY RATIO	1.32	1.36	1.34
	MEAN ECCENTRICITY (DEG.)	8.3 ±1.6	8.4 ±1.4	8.3 ±1.0

between the retinal and geniculate data, concerning the degree of ellipticity of the sustained and transient classes. For the geniculate data, the mean ellipticity ratios for the sustained and transient classes were similar[1] and, hence, the units in these classes were comparable in shape. For the retinal data, there was evidence of sustained units being more circular than transient units (section 4.3.4). Finally, the mean ellipticity ratio for the total LGC sample (n=31, mean ellipticity ratio = 1.34, mean eccentricity = 8.4°) was of the same order of magnitude as that for the RGC sample (n=74, mean ellipticity ratio = 1.30, mean eccentricity = 15.0°) despite the visual field distribution being significantly[2] different.

In the LGC sample, the orientation of the major axis, with respect to the horizontal, was found to be the same for the rod and cone centres. Hence, in the histogram representing orientation of major axis (Fig. 4.22) data for rod and cone centres are combined. The distribution of orientations is similar to the RGC data, with 68% of units having their major axis orientated within ±20° of horizontal. The systematic bias towards horizontally oriented major axes seen at the RGC level is

---

[1]Sustained units:
   mean ellipticity ratio = 1.32 (n = 14, mean eccentricity = 8.3°).

 Transient units:
   mean ellipticity ratio = 1.36 (n = 17, mean eccentricity = 8.4°).

[2]   LGC sample: mean eccentricity = 8.4°
   RGC sample: mean eccentricity = 15.0°
The calculated t value was 4.32, and from tables $t_{0.05, 103} = 1.66$

Fig. 4.22

Orientation of the major axis for RFCs of LGCs. The convention adopted is the same as for the retinal data (Fig. 4.13). The distribution shows a systematic bias towards horizontally orientated major axes.
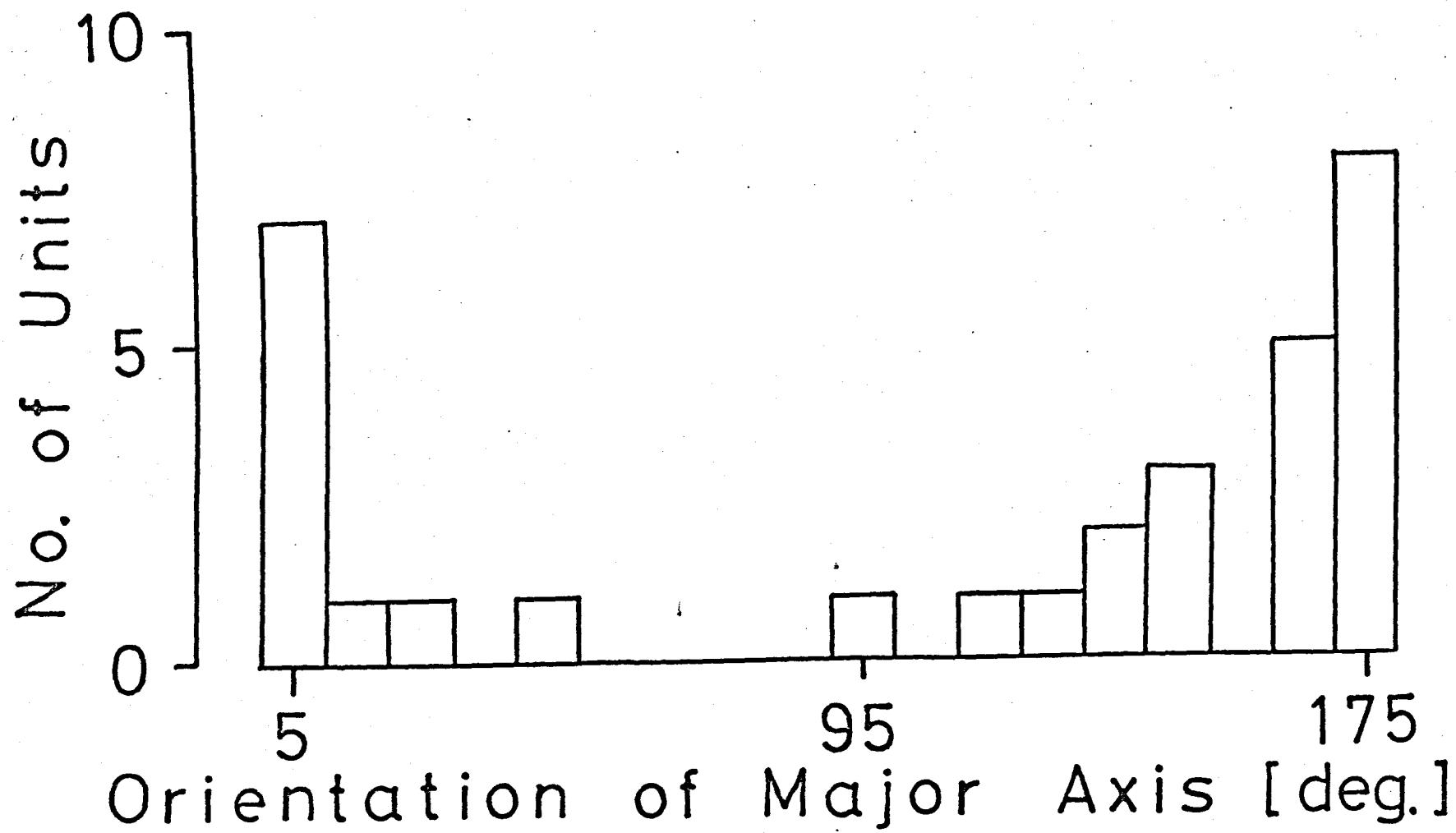
reflected at the level of the LGN.

4.4.4 Rod and cone centre areas

The areas within the rod and cone centres were determined using the same procedure as before, and the relationships between rod and cone centre areas are shown separately for RFC categories A1 (Fig. 4.23 A) and B2 (Fig. 4.23B).

As expected from visual inspection of the size and shape of the rod and cone centre maps, in all the LGC units in category A1 the rod and cone centres were approximately equal in area.

Those in category B2 invariably had larger rod than cone centres although the differences were small (rod to cone area ratios ranging from 1.11:1 to a maximum of 1.42:1, with a mean at 1.27:1; n=11, S.E.M.= ±0.03). This may reflect the fact that RFCs of LGCs were comparatively small (0.28 deg.^{2} to 1.29 deg.^{2}) compared with those of RGCs.

4.5 Discussion

4.5.1 Optical aberrations

The possible influence of optical aberrations on the data, especially regarding RFC ellipticity, non-concentricity of rod and cone centres, and the clustering of major axes about the horizontal, were considered under the following headings:

(i)   incurred (arising from the use of neutral contact lenses and suitable corrective lens spheres) and inherent aberrations (due to the cat's natural optics); and

(ii) chromatic aberration (resulting from the use of selective wavelength stimuli).

Fig. 4.23

Comparison between the area of rod and cone centres. The
continuous line represents equality of area. Values for
categories A1 and B2 have been separately plotted in A and B
respectively.
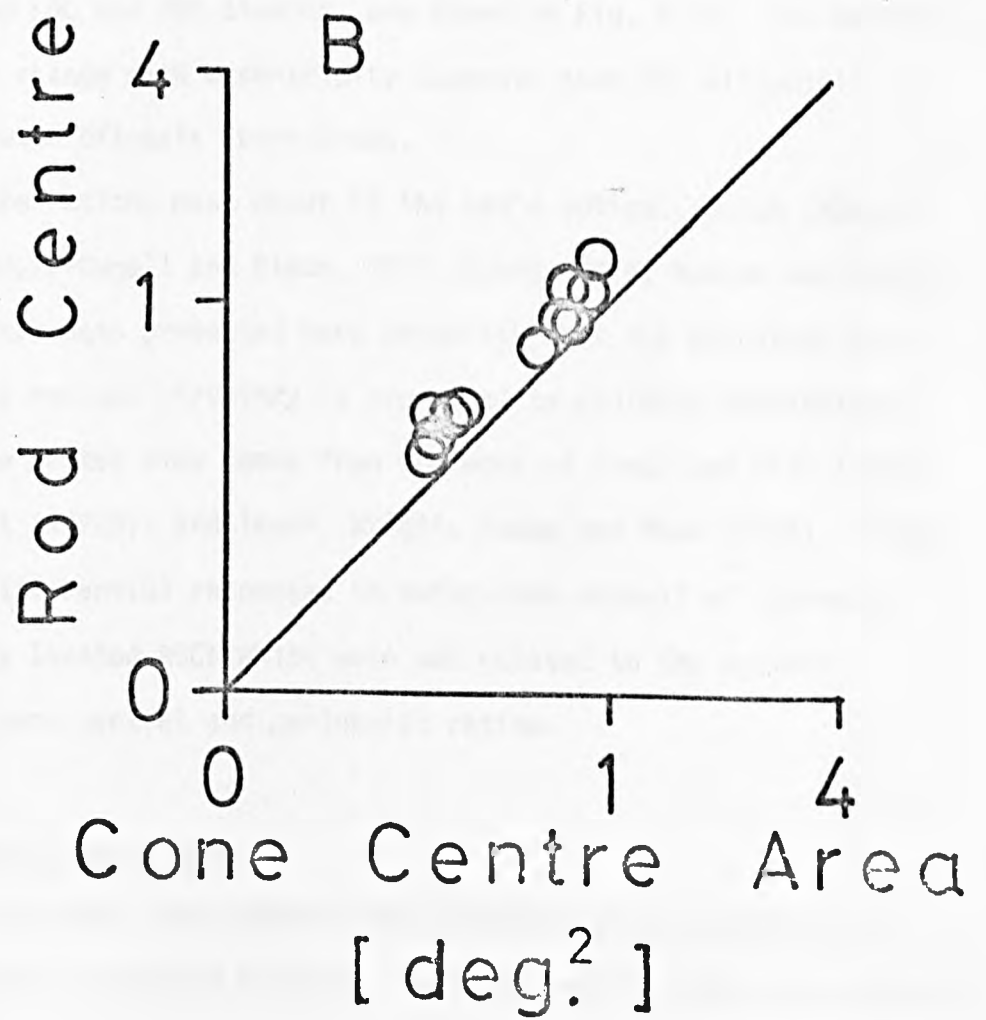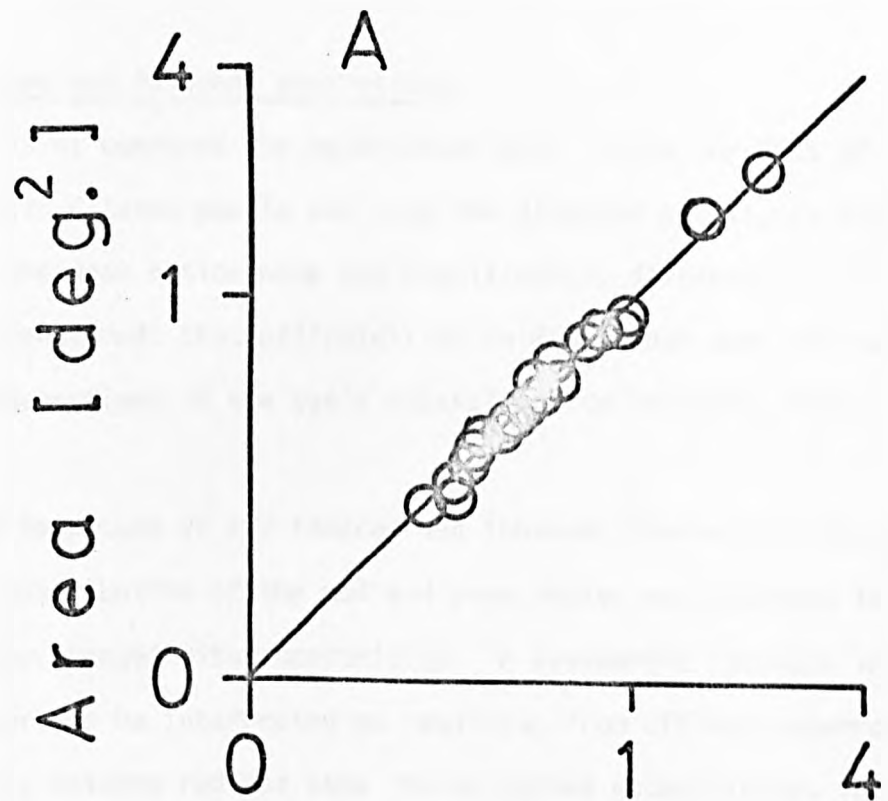
4.5.1.1 Incurred and inherent aberrations

Hammond (1974) compared the major/minor axis ratios for RFCs of RGCs, mapped with dilated pupils and with 3mm diameter artificial pupils. He found that the mean ratios were not significantly different. Therefore, he concluded, that ellipticities in RFC shapes were not due to the inherent aberrations in the cat's natural optics resulting from mydriasis.

Since the magnitude of any induced and inherent aberrations increases off-axis, the distribution of the rod and cone ratios was examined to discern how they changed with eccentricity. A systematic increase in these ratios could perhaps be interpreted as resulting from off-axis aberrations. The relationship between rod and cone ratios versus eccentricity, for the pooled data from LGC and RGC studies, are shown in Fig. 4.24. The absence of a systematic change with eccentricity suggests that RFC ellipticity is not correlated with off-axis aberrations.

Although aberrations must occur in the cat's optical system (Wässle, 1971; Bonds, Enroth-Cugell and Pinto, 1972; Bonds, 1974; Robson and Enroth-Cugell, 1978), the data presented here establish that the magnitude must be small or that retinal circuitry is pre-wired to minimise aberrations. Evidence for the latter view comes from the work of Ikeda and Hill (1971), Ikeda and Wright (1972b), and Ikeda, Wright, Young and Nuza (1973). These authors found differential responses to defocussed stimuli of centrally and peripherally located RGCs which were not related to the optical differences between central and peripheral retina.

4.5.1.2 Chromatic aberration

Since two coloured lights (452nm-blue and 578nm-yellow), with transmission maxima separated by 126nm, were employed to stimulate the rod-

Fig. 4.24

Variation of the cone (Fig. 4.24A) and rod (Fig. 4.24B)
ratios with eccentricity of the RFCs with respect to the area
centralis. The length of bars represents 1 S.E.M. The data
show no systematic change over the eccentricity range used.
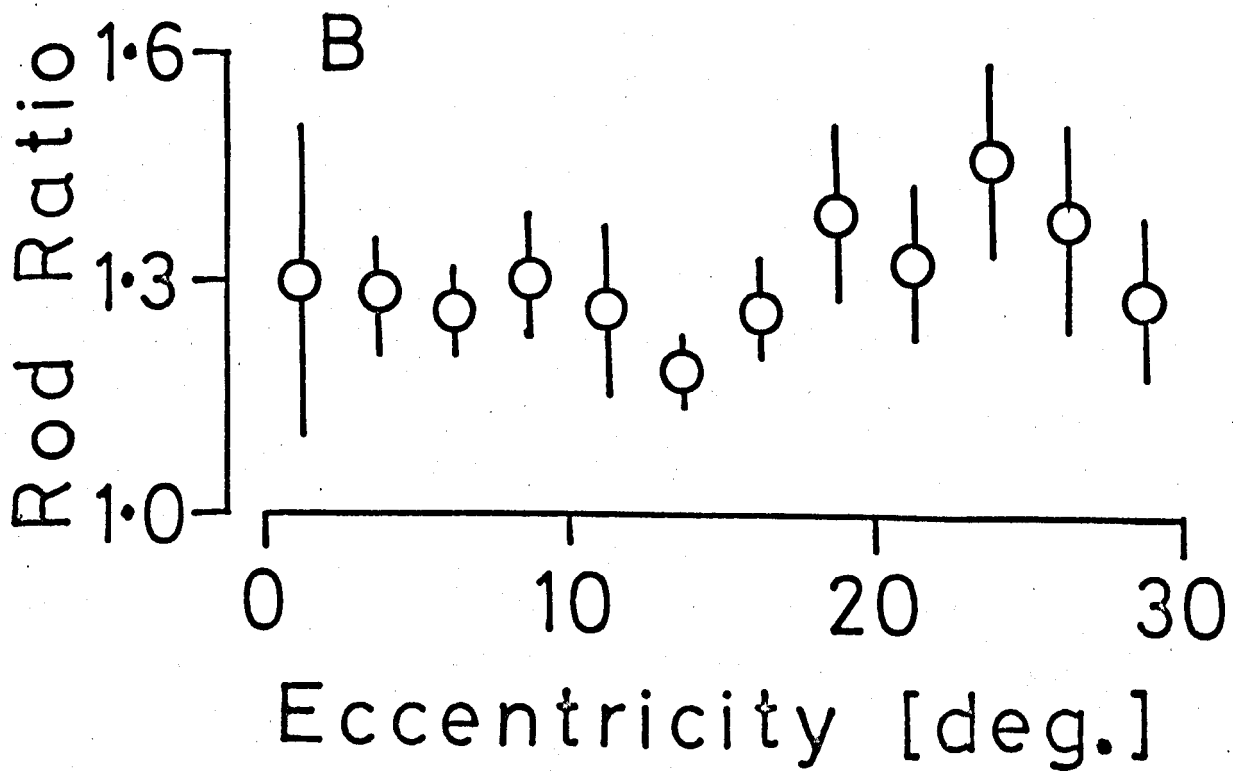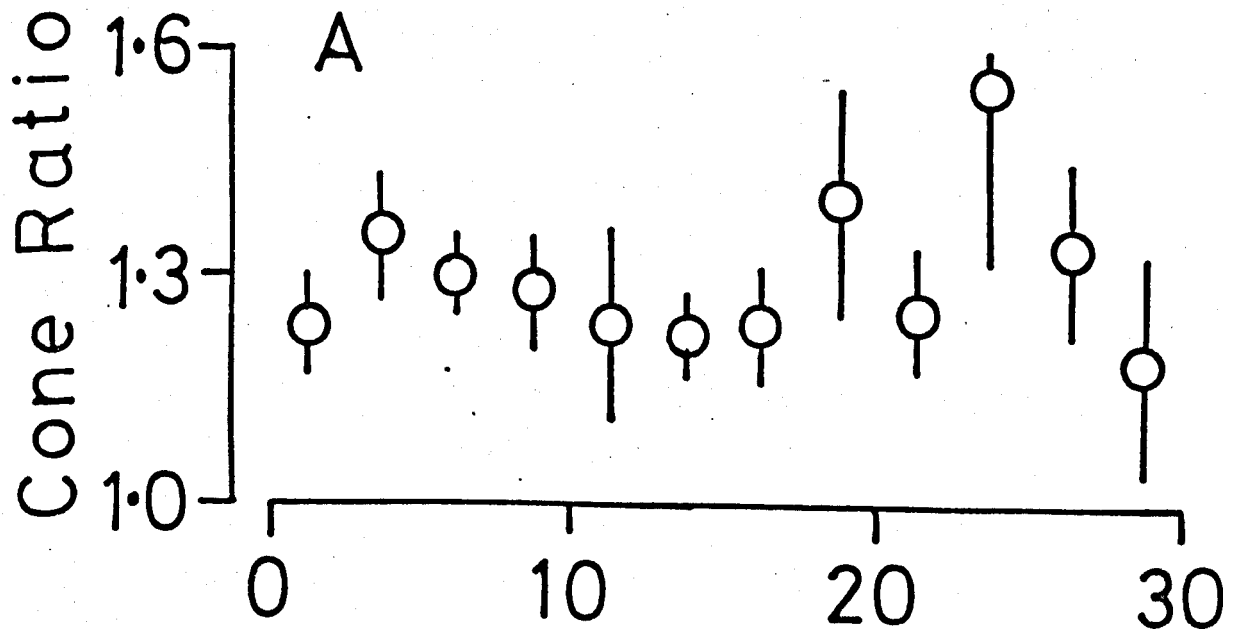
and cone-mediated inputs, any interpretation of the presence of non-concentricity in the rod and cone centres (categories A2 and B2), as well as the existence in some of these units of two regions of maximal sensitivity (see section 4.3.6) must take into account the likely effects of chromatic aberration. Previous single unit electrophysiological studies utilising chromatic stimuli (Daw and Pearlman, 1969, 1970; Andrews and Hammond, 1970a,b; Hammond, 1972; Marrocco, 1972; Ringo, *et al.* 1977; Saunders, 1977; Enroth-Cugell, *et al.* 1977a,b) have not reported any noticeable effects. In fact, in contrast to the present study, a recent report by Enroth-Cugell *et al.* (1977a,b) found rod and cone centres (assessed by the area-threshold technique, using blue and yellow-red lights; see section 4.2.1) always to be concentric. Although, in electrophysiological studies, chromatic aberration effects appear to have been insubstantial, the opposite is the case in human psychophysical experiments (Bahr, 1945; Ivanoff, 1947; Bedford and Wyszecki, 1957; Ditchburn, 1966; Campbell and Gubisch, 1967; Tucker, 1975; D.H. Foster, personal communication).

By treating the cat's optical system as a convergent lens, then from the general refractive properties of light, blue and yellow rays will have different convergence points in the eye (due to their different refractive indices). The following are the expected consequences of longitudinal chromatic aberration:

(i) a point on the retina will be represented in visual space (i.e. on the tangent screen) as two spatially separate points - one for blue and the other for yellow light (Ditchburn, 1966; Campbell and Gubisch, 1967);

(ii) the separation between these points will increase for locations progressively away from the area centralis (D.H. Foster,

personal communication);

(iii) the location of the point for blue light will be shifted

laterally with respect to that for yellow, in a direction

away from the area centralis, but along the projection of

the straight line through the area centralis and the location

for yellow (D.H. Foster, personal communication).

Two regions of maximal sensitivity (regions I and II) within the RFC.
In order to discriminate between the effects of longitudinal chromatic
aberration and functional asymmetry in retinal wiring, the following
parameters were measured:

(i) the separation between regions I and II; and

(ii) the magnitude of non-concentricity of rod and cone centres,

i.e. the lateral displacement and the maximum separation

(Fig. 4.10).

The distribution of the separation between regions I and II versus
eccentricity has already been plotted in Fig. 4.19 (section 4.3.6). A
significant increase in separation with eccentricity favours chromatic
aberration (D.H. Foster, personal communication). Linear regression
analysis of the data, however, shows only a 0.1° increase over the
eccentricity range between 0° and 40° (correlation coefficient = 0.38),
which is comparable to the systematic error in measurement.

The scatter of separation between regions I and II versus the
lateral displacement and the maximum separation is shown in Fig. 4.19A
and B (section 4.3.6). If chromatic aberration were responsible for the
existence of two regions of maximal sensitivity, then it must also
contribute to non-concentricity in the rod and cone centres. Hence, the
magnitude of the separations between these parameters: viz - lateral

displacement or maximum separation versus separation between the maximal sensitivity regions - should be similar. However, in both these cases (Fig. 4.19A and B), the distribution of points are such that they do not show a systematic equality of separation.

A simpler and direct means of deciding between the alternatives - functional versus chromatic - is to measure the positions of maximal sensitivity for a range of narrow-band wavelengths. In the case of chromatic aberration the position of maximal sensitivity will shift systematically with wavelength. If the two regions of maximal sensitivity truly represent rod- and cone-mediated centres, all wavelengths influencing only rods will yield one locus of maximal sensitivity, whereas all wavelengths influencing only cones will yield a distinctly separate locus. From the previous results (section 4.3.6), a mean separation of 0.34° (n=18) was obtained for a wavelength difference of 126nm between blue and yellow; i.e. a separation of 0.27° per 100nm wavelength-difference - which would have been clearly measurable both with ¼° or ½° diameter spots over the visual range from 400nm to 700nm in 100nm steps. Unfortunately, such experiments were not successful and they failed for two reasons.

(i) The RGCs were relatively insensitive to long wavelengths greater than 600nm (Hammond, 1972, 1974). The maximum available intensity of a small diameter, light spot was subthreshold at 650nm and only just suprathreshold at 625nm. Hence, the longest wavelength that could be used effectively was 600nm.

(ii) The intensities of the short wavelengths obtained with interference filters having transmission maxima at 425nm and 400nm were subthreshold for RGCs, using small-spot stimuli. Hence, the shortest effective wavelength was for a filter with

transmission maximum at 452nm.

These limitations resulted in a spectral range of approximately 150nm and made it impossible to decide between the alternative.

An alternative, but difficult, technique involved those units for which two regions of maximal sensitivity could be demonstrated at the mid-mesopic level. Then, by dark adapting to a scotopic level, and consequently increasing the sensitivity of the rod-mechanism at the expense of the cone mechanism, the long wavelength (yellow) light should give a lower threshold value at the region preferentially sensitive to the short wavelengths. Hence, in the case of *functional* asymmetry, the two regions at the mesopic level would resolve to a single region at the scotopic level, specifically by disappearance of the maximal sensitivity region for yellow (P. Hammond, personal communication). The main problem with this technique was that, at the mid-mesopic level, centre-surround interaction leads to steep sensitivity profiles with easily differentiated peak regions. At the scotopic level, the reduced sensitivity of the surround-mechanism relative to the centre-mechanism results in the broadening of the centre-sensitivity profile and of the peak regions. Fig. 4.25 shows the data for a unit which had two clear regions of maximal sensitivity at the mid-mesopic level of +0.53 log cd.m^{-2}. The positions of the regions of maximal sensitivity for short and long wavelengths are denoted on the abscissa by the letters B and Y respectively. The unit was dark adapted for 15 mins to a scotopic level of -0.91 log. cd.m^{-2} and responses to stimulation with blue and with yellow light were obtained in pseudo-random sequence along a diameter of the RFC passing through the two sensitivity regions obtained at the mid-mesopic background. In Fig. 4.25 the percentage responses (averaged from 20 presentations at each position along the diameter) have been plotted against stimulus position

Fig. 4.25

Percentage response of an on-centre brisk sustained unit to stimulation along the diameter of the RFC passing through the two regions of maximal sensitivity at a mid-mesopic level, tested at a scotopic level of -0.91 log. cd.m^{-2}. The two regions of maximal sensitivity for short and long wavelengths (Regions II and I respectively) obtained at the mid-mesopic level, have been denoted on the abscissa by B and Y.

After dark adapting the eye for 15 mins. from +0.53 down to -0.91 log. cd.m^{-2} responses were obtained with a $\frac{1}{2}°$ diameter flashing spot presented every 1.6 s. Each point represents the mean 20 presentations (duration of each presentation, 400ms). Averaged responses for the 452nm-blue (open circles) and 578nm-yellow (closed circles) lights have been normalised to 100%. Error bars represent ±1 S.E.M.
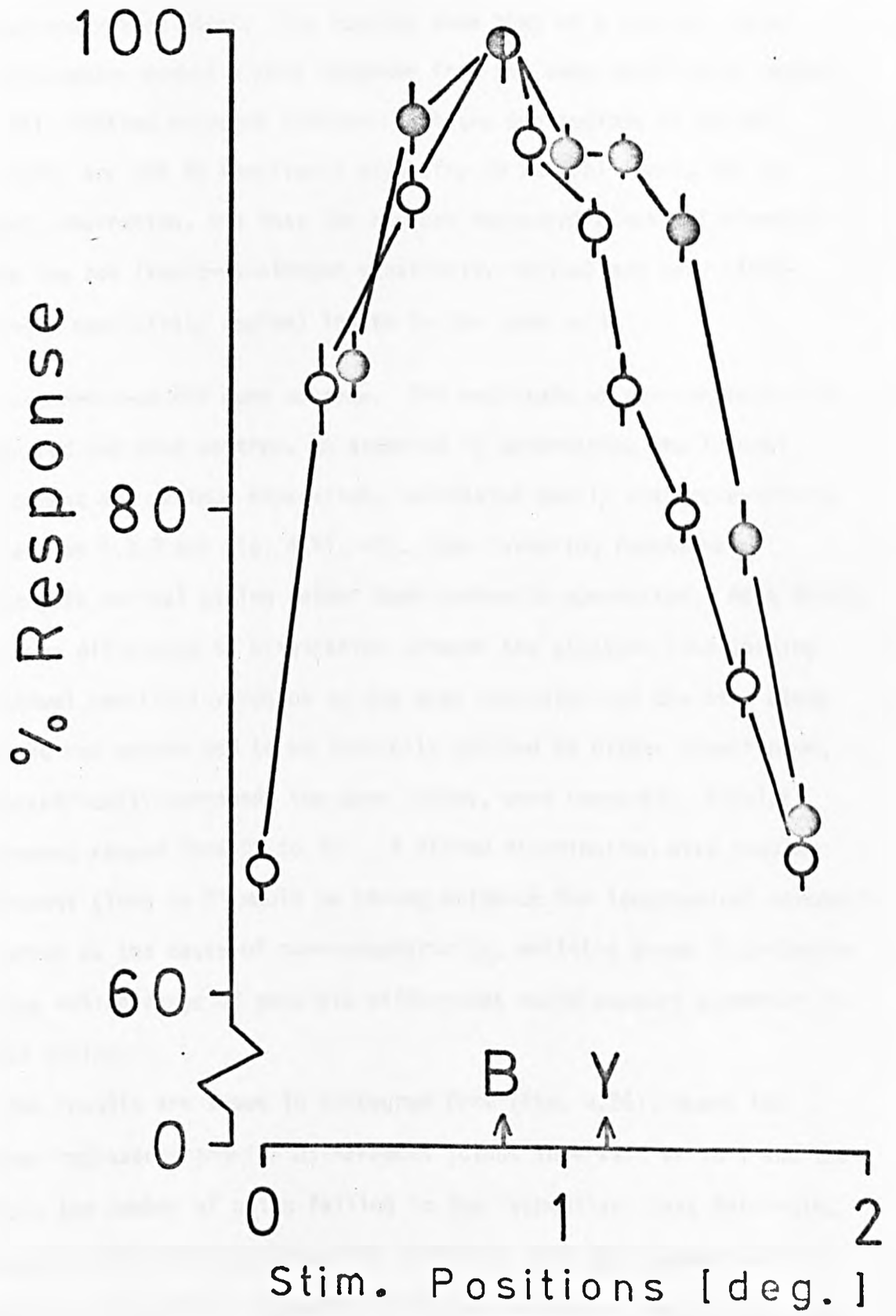
for blue and yellow light. The results show that at a scotopic level both wavelengths evoked a peak response from the same sensitivity region (B). This limited evidence confirms that the two regions of maximal sensitivity are due to functional asymmetry in retinal input, not to chromatic aberration, and that the regions represent a spatial mismatch between the rod (short-wavelength sensitivity region) and cone (long-wavelength sensitivity region) inputs to the same cell.

Non-concentric rod and cone centres. The magnitude of non-concentricity between rod and cone centres, as assessed by determining the lateral displacement and maximum separation, correlated poorly with eccentricity (see section 4.3.3 and Fig. 4.11, 12), thus favouring functional asymmetry in retinal wiring rather than chromatic aberration. As a double check, the difference in orientation between the straight line joining the maximal sensitivity region to the area centralis and the line along which the rod centre had to be laterally shifted to either superimpose, or concentrically surround, the cone centre, were compared. Angular differences ranged from 0° to 90°. A narrow distribution with angular differences close to 0° would be strong evidence for longitudinal chromatic aberration as the cause of non-concentricity, whilst a broad distribution over the entire range of possible differences would support asymmetry in retinal wiring.

The results are shown in histogram form (Fig. 4.26), where the abscissa represents angular differences (class intervals of 10°) and the ordinate the number of units falling in the respective class intervals. The absence of clustering around 0° indicates that non-concentricity is related to a functional asymmetry in retinal wiring of the rod and cone inputs, and not to longitudinal chromatic aberration.

Fig. 4.26

Positional variation between the rod and cone centres, and the visual field location of the unit's receptive field with respect to the area centralis.

The angular differences, between the straight line joining the maximal sensitivity region to the area centralis and the direction along which the rod centre had to be shifted to either superimpose or concentrically surround the cone centre, were obtained for both the retinal and geniculate data. The distribution of these differences is shown in histogram form (angular difference intervals of 10°; n = 67).
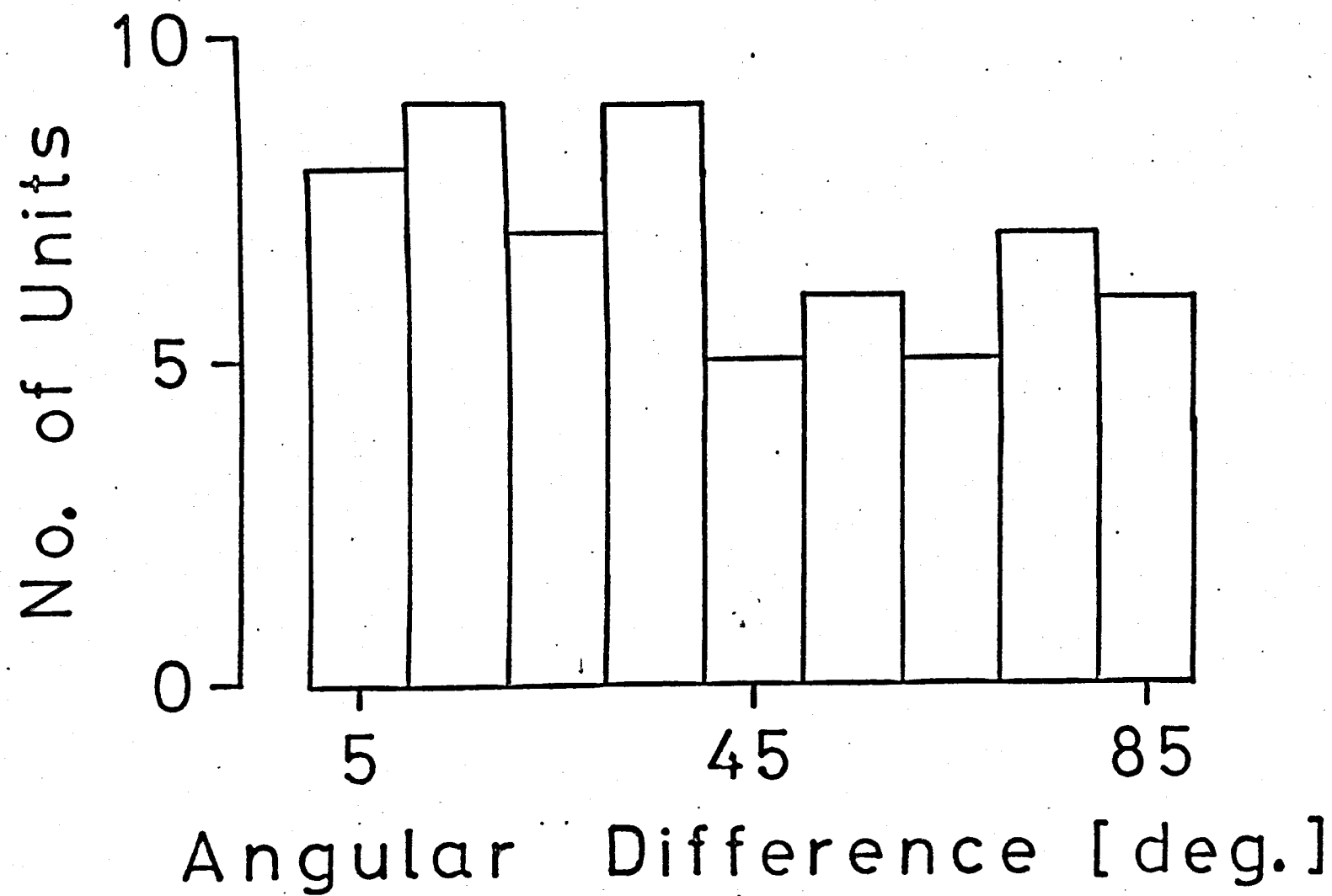
4.5.2 Mixed contribution from the rod- and cone-mechanisms to the rod and cone centres

As pointed out previously (sections 4.1.2 and 4.2.1), the 452nm-blue and 578nm-yellow lights (1 log. unit above centre-threshold) preferentially but not exclusively stimulate the rod- and cone-mechanisms, respectively. Hence, the mapped "rod-" and "cone-" centres have mixed contributions from both mechanisms. The effect on centre size of this dual contribution is therefore considered in this section in terms of:

(i)   models of the sensitivity profiles formulated for the centre- and surround-mechanisms, and

(ii) comparisons between the sizes and shapes of cone centres obtained with a red light (transmission maximum (t_{max}) at 600nm and half-width 8nm) and the yellow light (t_{max} 578nm, half-width 6nm).

4.5.2.1 Models of sensitivity profiles

Models incorporating a change in the sensitivities of the centre- and surround-mechanisms along a diameter of the receptive field have been described by many research workers (Rodieck, 1965; Cleland and Enroth-Cugell, 1968; Hickey, Winters and Pollack, 1973; Hammond, 1975; Hochstein and Shapley, 1976; Robertson, Winters, Christen and Cohen, 1978). In general these models envisage:

(i)   the centre-mechanism having a bell-shaped sensitivity profile with a maximum at the RFC and sharply declining sensitivity away from this region, and

(ii) the surround-mechanism having a similar, but more extensive and less steep sensitivity profile.

Further refinements to these profiles have taken account of the different

response properties of the centre- and surround-mechanisms in the sustained (Group II or X) and transient (Group I or Y) classes (Hammond, 1975; Enroth-Cugell and Pinto, 1972; Hickey *et al*, 1973; Hochstein and Shapley,1976b; Robertson *et al*, 1978).

To assess the significance of the mixed contribution from the rod- and cone-mechanisms to the rod and cone centres, the models of Hammond (1975) for the sustained and transient classes (Fig. 4.27A) were utilised. By assuming that these models invariantly represent the sensitivity profiles of the rod- and cone-inputs to the RGCs, for particular cases the consequences of the mixed contribution are considered below.

(i) The rod centre is larger than the cone centre; then, assuming the centre and surround sensitivity profiles for rod input are less steep than those for the cone input (Fig. 4.27B), the sensitivity profiles for the rod- and cone-mechanisms are shown by the dashed and continuous lines, respectively in Fig. 4.27B. Because of the mixed contribution from both the rod- and cone-mechanisms,beyond the boundary defining the cone centre, blue light evokes a net surround response from the cone mechanism but a net centre response from the rod mechanism. Hence, the mapped rod centre boundary will be defined by a situation where the net cone-surround response cancels the net rod-centre response. This will occur at a position intermediate between the true rod and cone centre boundaries, resulting in a smaller mapped rod centre than the "actual" rod centre defined by centre-surround sensitivity distribution for the rod mechanism.

Yellow light at the true cone centre boundary will evoke a net centre response from the rod mechanism. In order to cancel this net rod-centre response, the yellow stimulus will therefore

have to be positioned so as to evoke a balancing net cone-surround response. Hence, the mapped cone centre will be larger in size than the "actual" cone centre.

In this case, it follows that the mixed contributions from the rod- and cone-mechanisms attenuate the true size differences between the rod and cone centres.

(ii) The true rod- and cone-centres are the same size, so that the sensitivity profiles can be assumed to have the same distribution for both the rod- and cone-mechanisms (Fig. 4.27A). In this case, the mixed contribution will not overtly affect the sizes of the mapped rod and cone centres.

(iii) The cone centre is (exceptionally) larger than the rod centre, so that the cone input has a broader sensitivity distribution compared with the rod input. This is shown in Fig. 4.27C where the cone and rod profiles are represented by the continuous and dashed lines, respectively - the converse of case (i) above.

The considerations (cases i, ii, and iii) are restricted to concentric changes in the sensitivity distributions. Evaluations based upon non-concentric sensitivity distributions between the rod- and cone-mechanisms were also considered.

(iv) In Fig. 4.28 A and B, the dashed profiles represent the rod input and the continuous profiles the cone input, for RFC categories A2 (Fig. 4.28A) and B2 (Fig. 4.28B). By lines of reasoning comparable to cases i and ii above the mapped centre sizes will again show smaller differences in magnitude than the true rod and cone centres.

In general, evaluation of the mixed contribution to the centres based upon the models of the sensitivity profiles for the sustained and transient

Fig. 4.27

Diagrammatic representation of the centre- and surround-
sensitivity distributions (profiles above and below the
horizontal line respectively) for the sustained and transient
classes.

A   -   after Hammond, 1975.

B   -   rod centre larger than cone centre. It is assumed
        that this arises from a broadening of the centre and
        surround sensitivity distributions for rods (dashed
        lines) compared with those for cones (continuous
        profiles).

C   -   cone centre larger than rod centre. In this case, it
        is assumed that the cone sensitivity distribution
        broadens compared to the rod.

Sustained
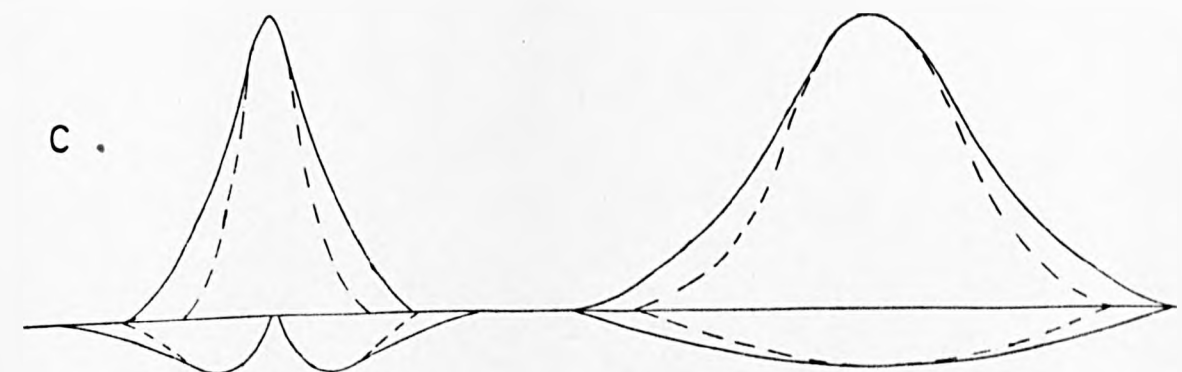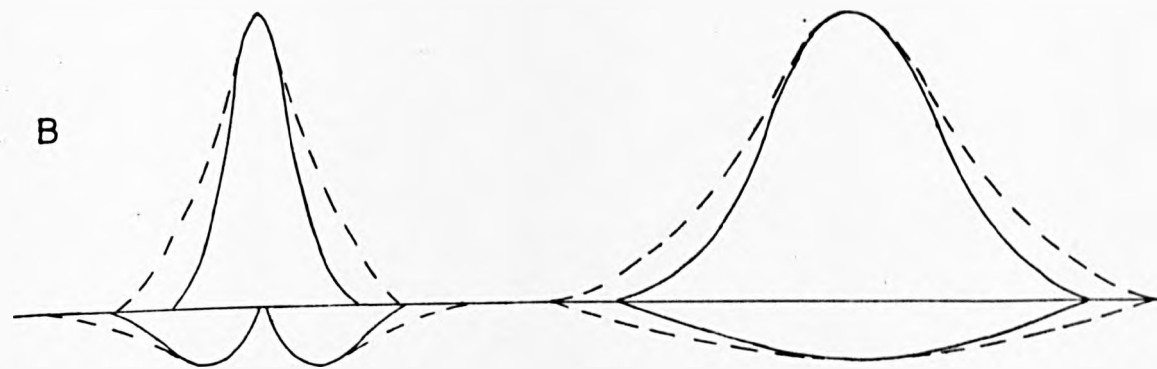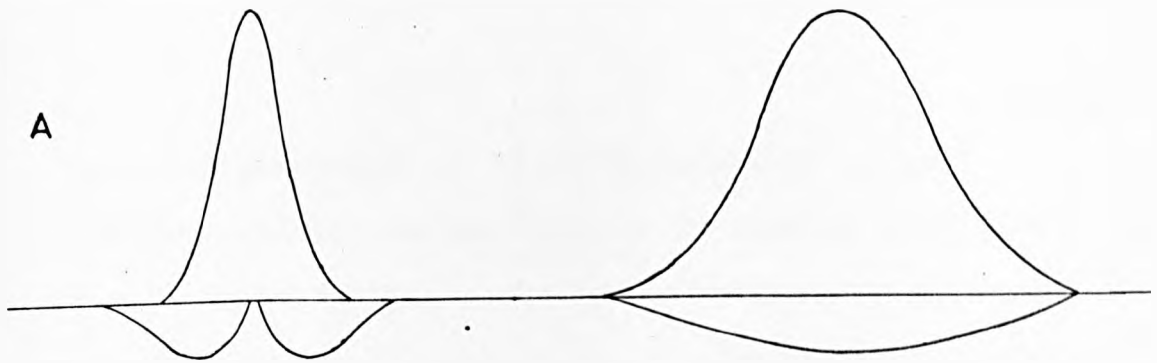
Transient

Fig. 4.28

Diagrammatic representation of the centre- and surround-
sensitivity profiles for the sustained and transient classes
receiving non-concentric rod (dashed profiles) and cone inputs
(continuous profiles).

A - sensitivity distribution for category A2 non-
concentric units.

B - sensitivity distribution for category B2 non-
concentric units.

Sustained

Transient

A
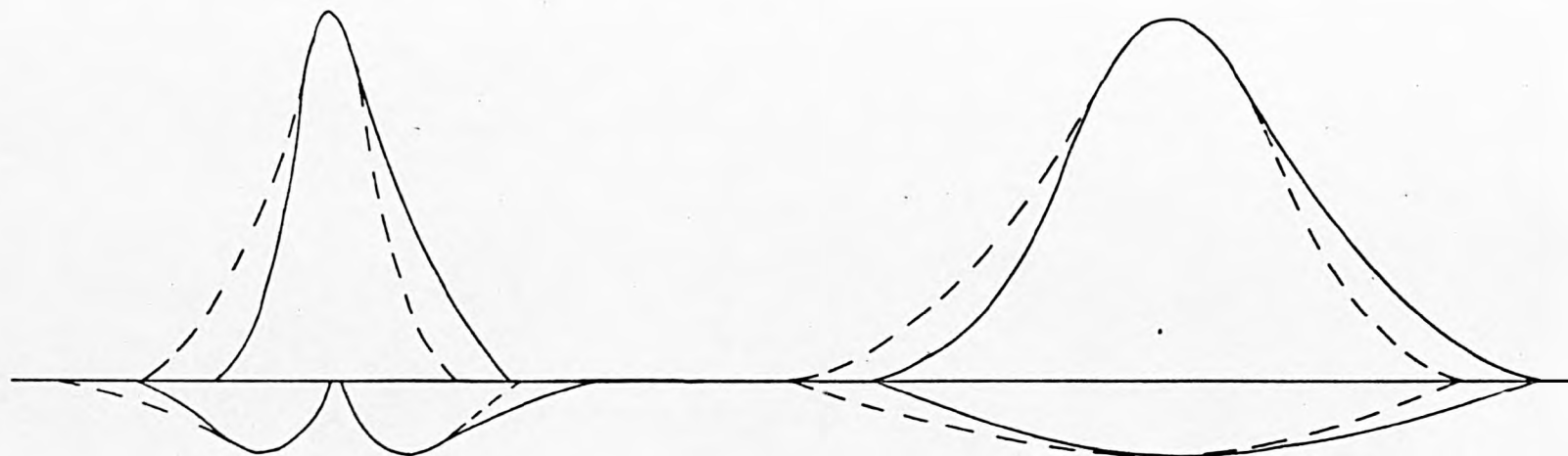
B
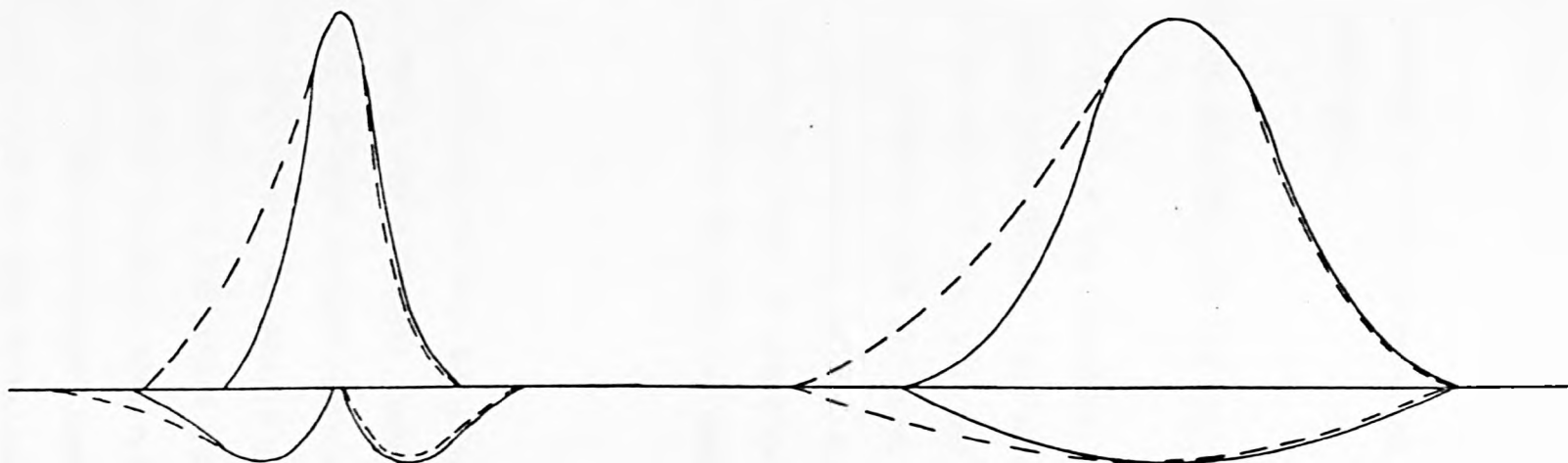
classes suggests that the differences between the *mapped* rod and cone centre sizes will be attenuated, compared with those between *true* rod and cone centre sizes.

In order to obtain a quantitative estimate of this attenuation, cone-centre maps were replotted using 600nm-red light.

4.5.2.2 Comparison between cone centre maps obtained with red and yellow light

A major problem with this comparison related to the insensitivity of cat RGCs to deep red light at wavelengths beyond 600nm. Even at 600nm very few units had centre thresholds even as much as 1 log. unit below the source intensity when a small ($\frac{1}{4}°$ or $\frac{1}{2}°$) diameter spot was used. Cone centres could only be mapped with yellow *and* red light for 5 units. In no case were significant differences obtained. Thus, in practice the rod contribution does not appreciably influence the measured cone-centre size.

4.5.3 Rod and cone centre sizes

Recently, Enroth-Cugell *et al* (1977b) measured the rod- and cone-centre sizes using the area-threshold technique. Their results, taken from a much smaller sample (n=11), suggested that the centres were approximately the same size and concentric (see also section 4.5.4). As pointed out previously (section 4.2.1), this method of determining the centre sizes with circular light spots of progressively greater diameter, does not take into account the ellipticity in RFC shape. An "optimally-sized" circular spot will not, therefore influence the centre- and surround-mechanisms symmetrically. Presumably, this error has been substantial in their data. One other possibility is that, due to the small sample size, their data

were obtained from units belonging exclusively to RFC category A1, and to units in categories B1 and B2 in which the differences in centre-size could not be resolved by the area-threshold technique.

The results of the present study confirm and extend the findings of Andrews and Hammond (1970b), except in the magnitude of the effect. These authors quote a range of rod:cone centre sizes, from equality to a maximum difference in area of 9:1 (mean, 4:1). In contrast, the present more detailed results give a maximum value of 3:1 (mean, 1.6:1). As discussed in section 4.5.2, the mixed rod and cone contribution tends to attenuate the differences between the rod and cone centres, and although this may possibly contribute to the discrepancy, section 4.5.2.2 above suggests that the attenuation effect could not have been substantial.

Hammond (1972) determined the rod- and cone-centre sizes for LGCs. He found the centre sizes to be generally similar and in some instances the rod centre to be slightly the larger of the two. The present data confirm this finding, and the differences between the retinal and geniculate data presumably reflect the pattern of retino-geniculate convergence.

4.5.4 RFC ellipticity

Although non-concentric rod and cone centres were obtained in the majority of units (51/74 for RGCs and 11/31 for LGCs) the centres *themselves* were elliptical in shape. Additionally, ellipticity in centre-shape was still present in units (17 out of 23 RGCs and 19 out of 20 LGCs) with concentric rod- and cone-centres. These findings, therefore, discount the possibility suggested by H.B. Barlow (personal communication) that RFC ellipticity is mediated by circular but non-concentric rod and cone centres. Furthermore, since there is a systematic bias in the orientation of the major axis, the possibility

that ellipticity arises through a local weakness in the surround antagonism (see Fig. 4.1.B) can also be discounted, for the reason that the weakness in surround antagonism should occur randomly which should result in no systematic bias in the orientation of the major axes.

Evidence has been presented in section 4.3.4 showing that brisk sustained units have more circular RFCs at a given visual field location than brisk transient units. This evidence may have been useful in verifying the correlation suggested by Boycott & Wassle (1974), Cleland & Levick (1974a), and Stone & Fukuda (1974a): viz.- the morphologically identified alpha and beta RGCs are equivalent to, respectively, the physiologically categorized brisk transient (Y) and brisk sustained (X) units. Unfortunately, at present no quantitative data are available on the dendritic spreads of the alpha and beta RGCs.

In conclusion, the present study supports Hammond's (1974) suggestion that ellipticity arises from asymmetry in retinal wiring. The spreads of the dendritic arborization for RGCs is known to show an elliptical distribution (Brown, 1965; Brown and Major, 1966; Honrubia and Elliott, 1970; Shkolnik-Yarros, 1971; Boycott and Wassle, 1974). In order to explain the non-concentricity of rod and cone centres, one has to invoke asymmetric connectivity at either earlier levels of interaction (for example in the outer plexiform layer) or a different pattern of synaptic connectivity onto the RGC's dendritic tree, since the dendritic spread of RGCs is fixed.

Chapter 5   ADAPTIVE STUDY

5.1 Introduction

Enroth-Cugell and Shapley (1973b) studied the effect of light adaptation on retinal ganglion cells (RGCs) with various central summing areas. They measured the threshold sensitivities of a 0.18° diameter flashing spot over a range of background adapting levels. They found that the curves obtained by plotting threshold intensity against the background adapting levels, differed for RGCs with different central summing areas. Their example between an on-centre cell (area = 1.6 deg.^{2}) and an off-centre cell (area = 12.5 deg.^{2}) is shown in Fig. 5.1.A. The adapting level at which the threshold intensity of the 0.18° spot began to change is termed the transition level. The scatter of values for the transition level against the central summing areas is shown in Fig. 5.1.B. The relationship between these parameters, giving a slope of -1, led them to conclude that cells with large centres are more light adapted at a particular background luminance than cells with small centres, due to the increased light flux over the larger centres.

Further supporting evidence comes from more recent measurements of threshold sensitivity over a range of background adapting luminances, carried out by Jakiela, Enroth-Cugell and Shapley (1976). They found that for X-cells, with small receptive field centres, the transition from the horizontal to the sloping portion of the increment sensitivity curve (the transition level of Enroth-Cugell and Shapley) took place at higher levels of background illumination than for Y-cells with larger centres.

To test this conclusion, a preliminary study was undertaken, utilising as a measure of the state of adaptation of RGCs the technique described by Hammond and James (1971) and adapted from Barlow and Levick (1968). This

Fig. 5.1

Data showing the relationships between the back-ground adapting levels and the centre summing areas for RGCs.

A - Impulse/Quantum ratio versus background curves for two cells with different centre sizes.

B - Transition level as a function of the centre summing areas for the total data (n = 30).

(From Enroth-Cugell and Shapley, 1973b).
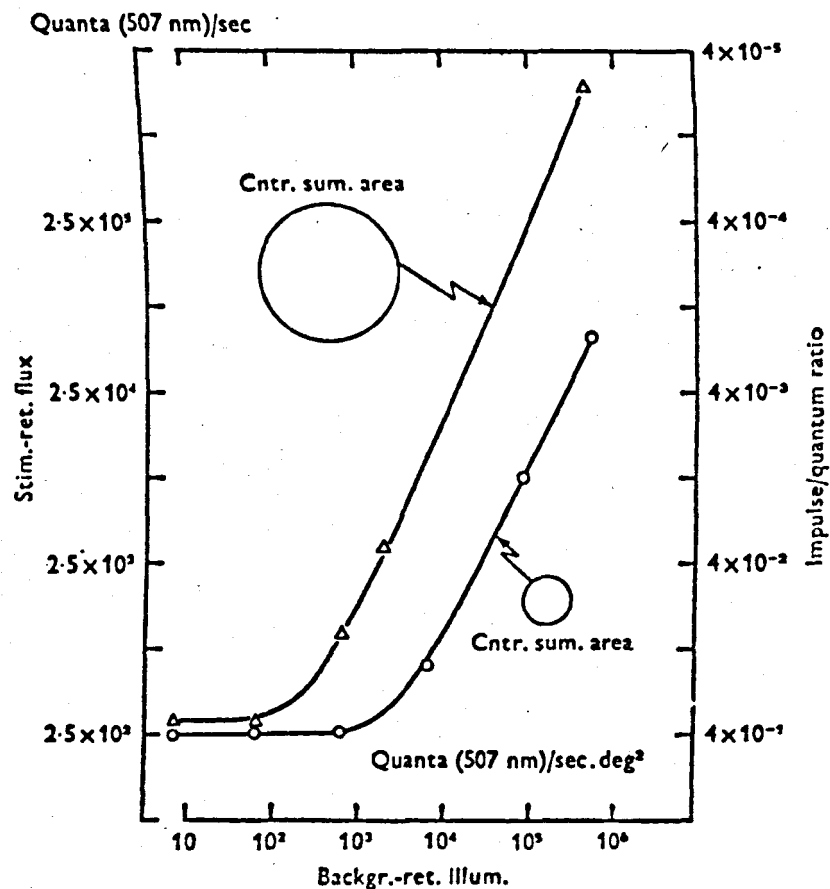
I/Q ratio versus background curves for two cells with different centre sizes. The stimulus was a small, 0·18°, spot centred on the receptive field; the background was a 12° disk concentric with the small spot. The stimulus spot was modulated at 0·4 c/s with a square-wave time course. Log stimulus retinal flux for a constant small response is plotted versus log background retinal illumination. Log I/Q is also plotted on the ordinate. Large cell 40/10 off-centre, $A_t = 12·5$ deg². Small cell 44/1, on-centre, A_t 1·6 deg².
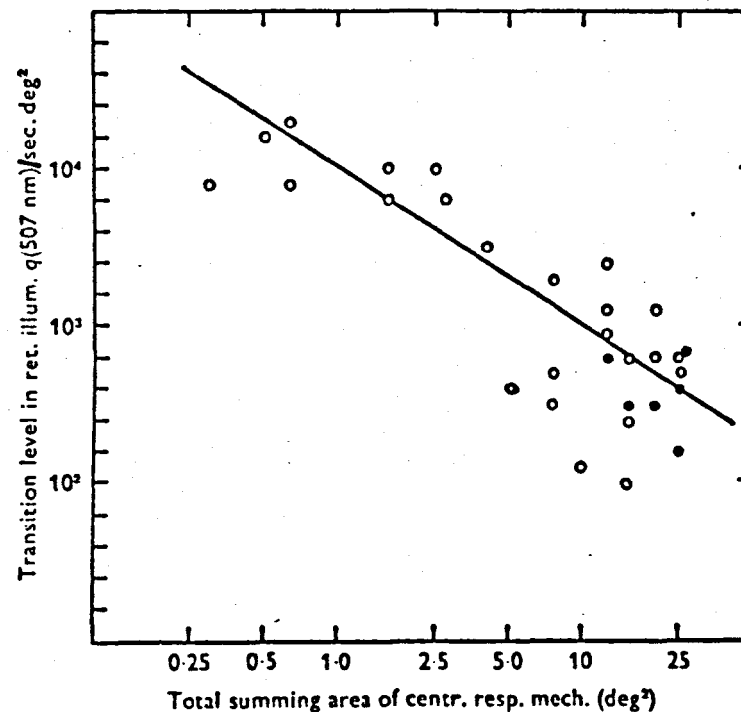
Transition level as a function of centre area A_t. The value of the transition level for I/Q vs. background retinal illumination in units of illumination is plotted vs. A_t in deg². The line is a 45° line representing a constant flux of $1·5 \times 10^4$ quanta/sec incident on retina.

technique involves the measurement of threshold sensitivities of RGCs to two narrow-band interference filters - one having transmission maximum at 578nm (yellow) and the other at 452nm (blue) - at a range of background adaptation levels.

In the scotopic range, where the rod mechanism determines threshold, the RGCs have a higher sensitivity to the 452nm than the 578nm lights. Hence, the ratio between the measured 578nm and the 452nm threshold sensitivities - termed the relative sensitivity (RS) - will have a minimal value. Conversely, in the photopic range, where the cones determine threshold, the RGCs are more sensitive to the 578nm light and the RS will have a maximal value. The limit (minimal and maximal) values of the relative sensitivities to the 578nm and the 452nm wavelengths, predicted from the Dartnall nomogram (Dartnall, 1953) for the 507nm and 556nm cat rods and cat cones, are respectively -0.44 and 0.52 log. units (Hammond and James, 1971). For intermediate levels of adaptation, i.e. the mesopic range, the threshold is determined by the more sensitive receptor mechanism, and the RS values will lie between these limits.

According to Enroth-Cugell and Shapley's result, RS values should systematically differ for RGCs with different centre areas, throughout the mesopic range. Unfortunately, thorough testing would require RGC recording for upwards of three hours; time being required for:

(i) steady-state adaptation to a range of background luminances;

(ii) threshold determinations at each background luminance; and

(iii) RFC size determination at each background luminance.

Since, stable optic tract fibre recordings typically last for only 20-40 mins., exceptionally 110 mins., a different strategy had to be adopted. At a given eccentricity from the area centralis, brisk sustained cells have smaller RFC sizes than brisk transient cells (Cleland *et al.*, 1971,

1974a; Hammond, 1974). Therefore, at each adapting level, the latter should be more light adapted than the former, and a systematic difference in the RS measurements should be found between them.

The results of this study are shown in Fig. 5.2, where the mean RS (log. units) versus adapting luminance (log. cd.m^{-2}) has been plotted for the two classes. Brisk sustained on- and off-centre fibres have been pooled into one group, represented by the filled circles. Similarly, transient on- and off-centre fibres have been grouped and are shown by the open triangles. The distributions of the visual field eccentricities for the two classes were similar. At any given eccentricity, brisk transient units have centre areas 3 to 5 times greater than brisk sustained units (Cleland et al., 1974a; Hammond, 1974). Accordingly, a difference in their adaptation level of the order of 0.5 log units is predicted. From the considerations outlined in section 5.2.2, this should give a mean RS separation of 0.3 log. units. In Fig. 5.2, although the mean values of RS for transient units are very slightly shifted upwards with respect to the mean for sustained units in the mesopic range, these differences are:

(i) not statistically significant at the 5% level, and

(ii) nowhere near the expected value of 0.3 log. units.

This preliminary investigation, therefore, suggested no significant correlation between adaptive state and RFC size. However, two major issues have to be considered. The first concerns the differing summation properties within the receptive fields of these two classes (Enroth-Cugell and Robson, 1966), and the second, the large difference in the sample size of the two classes at each adapting level (Fig. 5.2).

A more detailed comparison was therefore undertaken at one mid-mesopic adapting level.

Fig. 5.2

Mean relative sensitivity (RS) values at different adapting luminances. Data are for cats fitted with 5mm diameter artificial pupils. A log.-log. plot of the data for sustained (s) and transient (T) OTFs (on- and off-centres combined) are shown. The number adjacent to each symbol denotes the number of units for which RS values were determined at that particular adapting luminance.
(From Ahmed *et al.*, 1977).
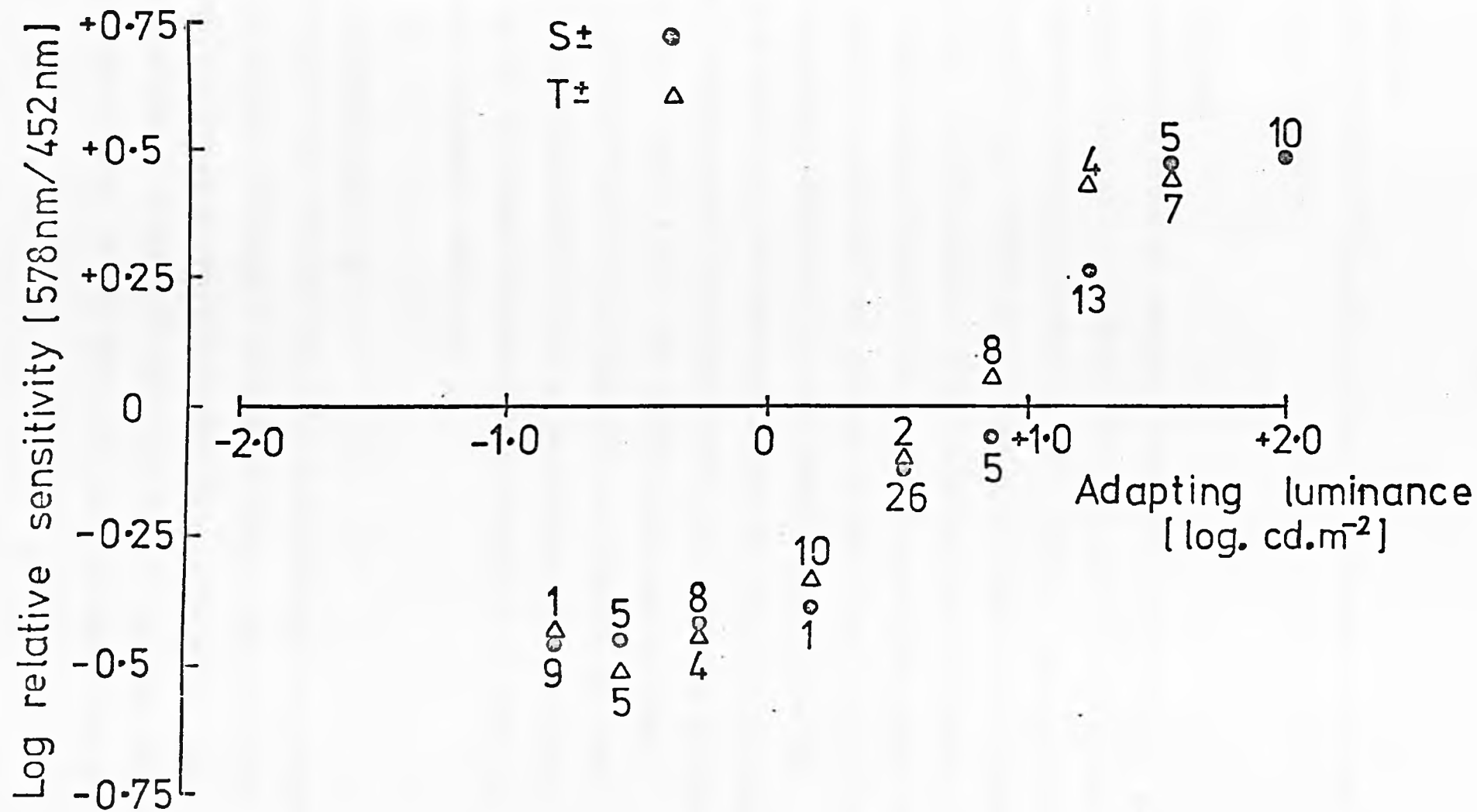
5.2 Procedure

Complete details of preparation, recording, calibration, etc. have been given in Chapter 2.

5.2.1 RFC areas

The following method was adopted. Preliminary classification of each unit into the transient and sustained classes was carried out using some of the tests described by Cleland *et al.* (1971, 1974a). Then the receptive field centre size was obtained by the technique described fully in Chapter 4 section 4.2. Briefly, using $\frac{1}{4}°$, $\frac{1}{2}°$ or 1° flashing spot at an intensity 1 log. unit above centre threshold, iso-sensitivity points lying around the region of maximal sensitivity were obtained for blue (452nm), yellow (578nm) and, in some cases, white light. Joining these points, a contour was obtained delimiting the centre-surround boundary for the particular colour of light. The area within the iso-sensitivity contour was then calculated (see Chapter 4, section 4.3.5). For specific cases where the areas obtained with the blue and yellow lights differed, the mean was taken.

The relative sensitivity in the region of *maximal* sensitivity was defined as the ratio between the threshold sensitivity to the 578nm and 452nm spot presented for 400ms every 1.6s.

5.2.2 Predicted RS variation

As shown in Fig. 5.1A and B and stated in Enroth-Cugell and Shapley's paper, the expected difference in the adaptive state of RGCs is of the same order of magnitude as the ratio between their centre areas. Hence, a ten-fold difference in area will cause a ten-fold (1 log. unit) difference in their adaptive state. On this basis, the adaptive state of RGCs will

vary according to their RFC areas at a fixed background adapting level. The level of light adaptation will correspond to the RS value, and hence a systematic increase in the RS values should occur concomitant with RFC size. From the data of Hammond and James (1971) and Ahmed *et al.,* (1977), the predicted increase should be 0.64 log. units in the RS for 1.0 log. unit change in RFC area (derived from Fig. 5.3).

5.3 Results

The results are based on a total of 131 single optic tract fibre - 92 brisk sustained (on-: off-centre, 61:31) and 39 brisk transient (on-: off-centre, 27:12) - and 37 lateral geniculate cell (LGC) - 15 sustained (on-: off-centre, 13:2) and 22 transient (on-: off-centre, 15:7) - recordings. The RS values were all obtained at a fixed background adapting level of +0.53 log. cd.m^{-2}. This represents a mid-mesopic adapting luminance in conjunction with 5mm diameter artificial pupils.

5.3.1 RS variation with eccentricity

The literature is well documented in showing that RFC size of RGCs increases with eccentricity from the area centralis (Wiesel, 1960; Cleland, 1974a; Ikeda and Wright, 1971, 1972b; Hammond, 1974). Hence, a qualitative verification of the relationship between adaptive state and centre size should be obtained by plotting RS versus receptive field eccentricity (Fig. 5.4).

For both the brisk sustained (Fig. 5.4A) and transient (Fig. 5.4B)

Fig. 5.3

Mean relative sensitivity (RS) values at different adapting
luminances. The left-hand curve (filled triangles) is for
dilated pupils, and the right-hand curve (filled circles) for
5mm diameter artificial pupils. Bars denote 1 S.E.M.

The slope is 0.64 for both curves. Thus, over the mesopic
range, RS values change by 0.64 log. units for one log. unit
change in adapting luminance. Accordingly, one log. unit
increase in centre area should (according to Enroth-Cugell and
Shapley) correlate with one log. unit increase in adaptive state,
equivalent to an increase of 0.64 log. units in the RS value at a
fixed adapting luminance.

The predicted change in RS (ΔRS), for two units with Areas
A_1 and A_2, is given by the relationship:

$$\Delta RS = 0.64 \times \log.(A_1/A_2).$$

(left curve from Hammond & James, 1971; right curve from Ahmed
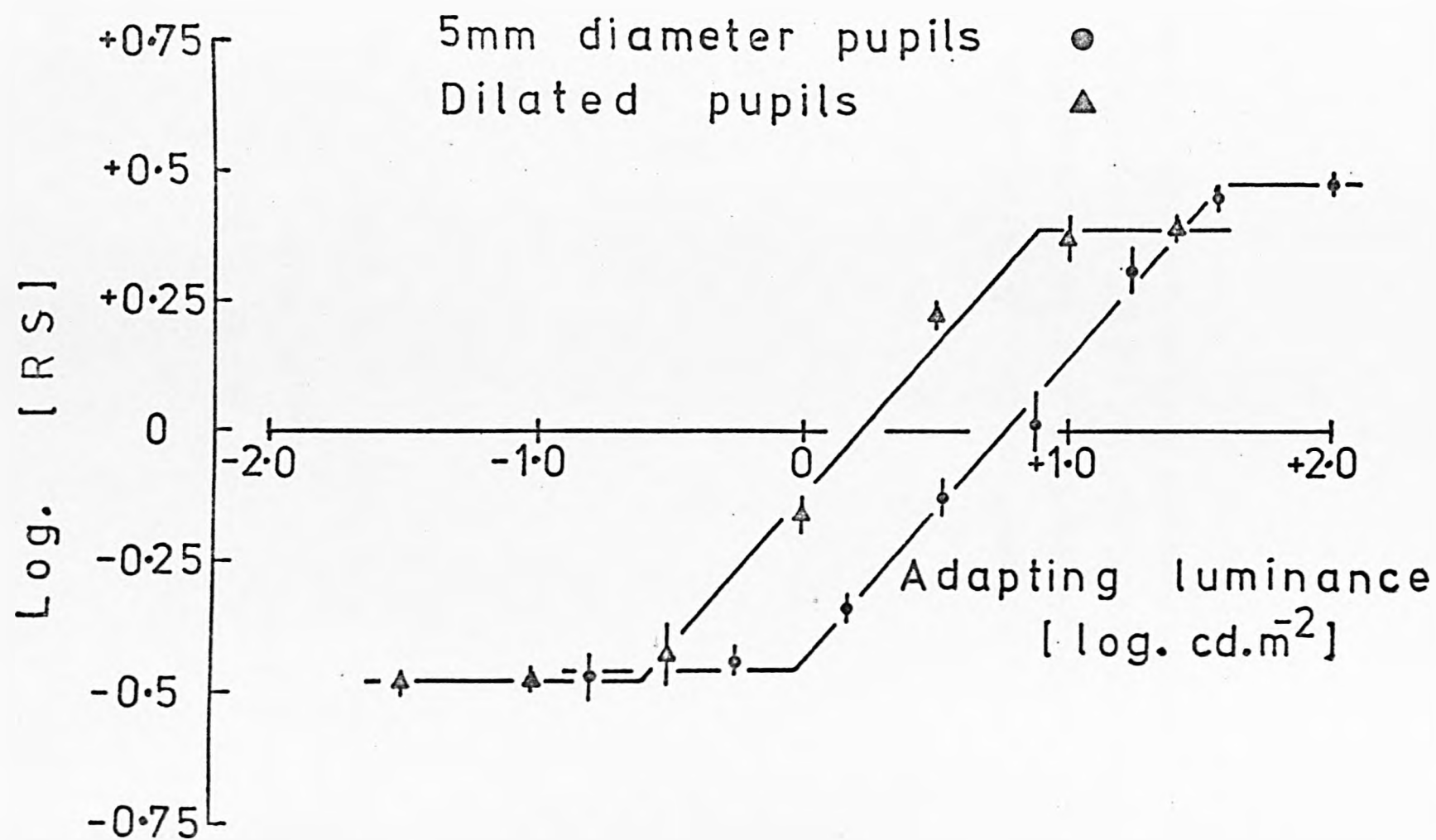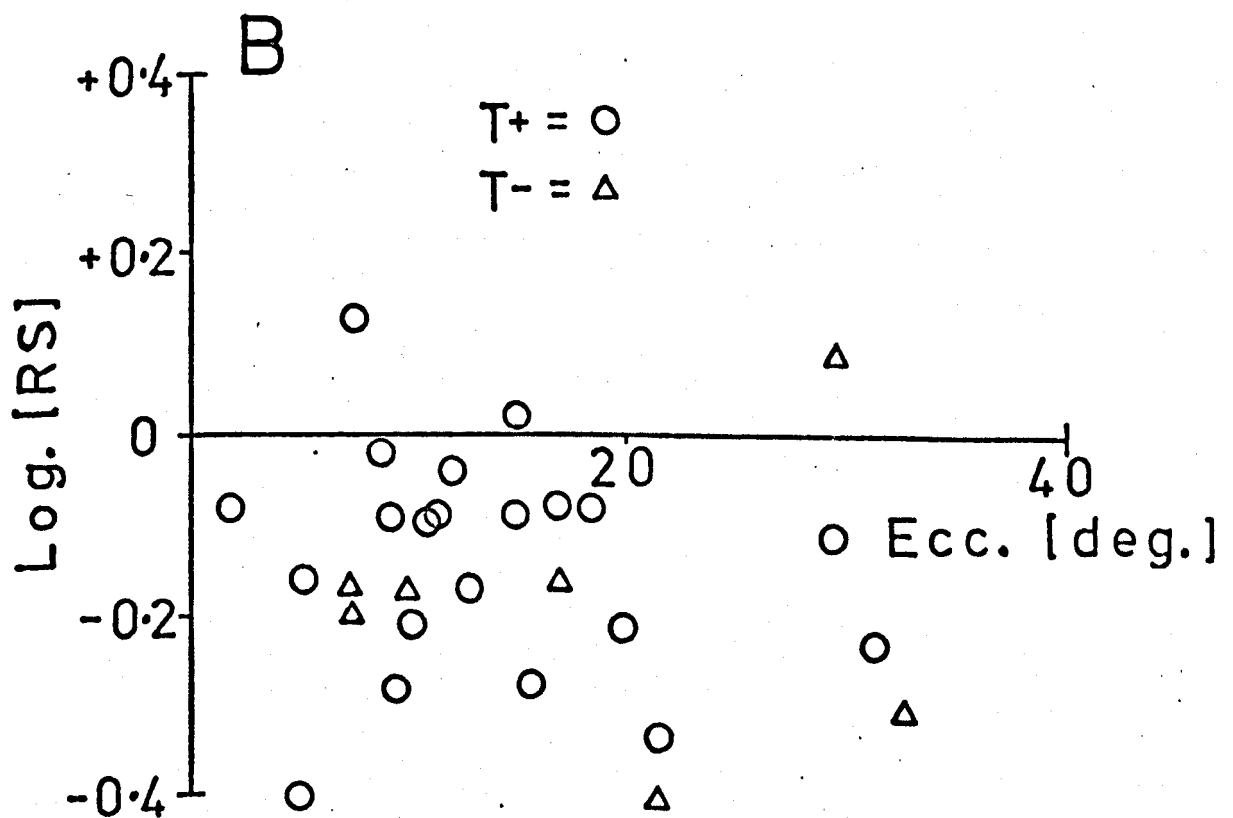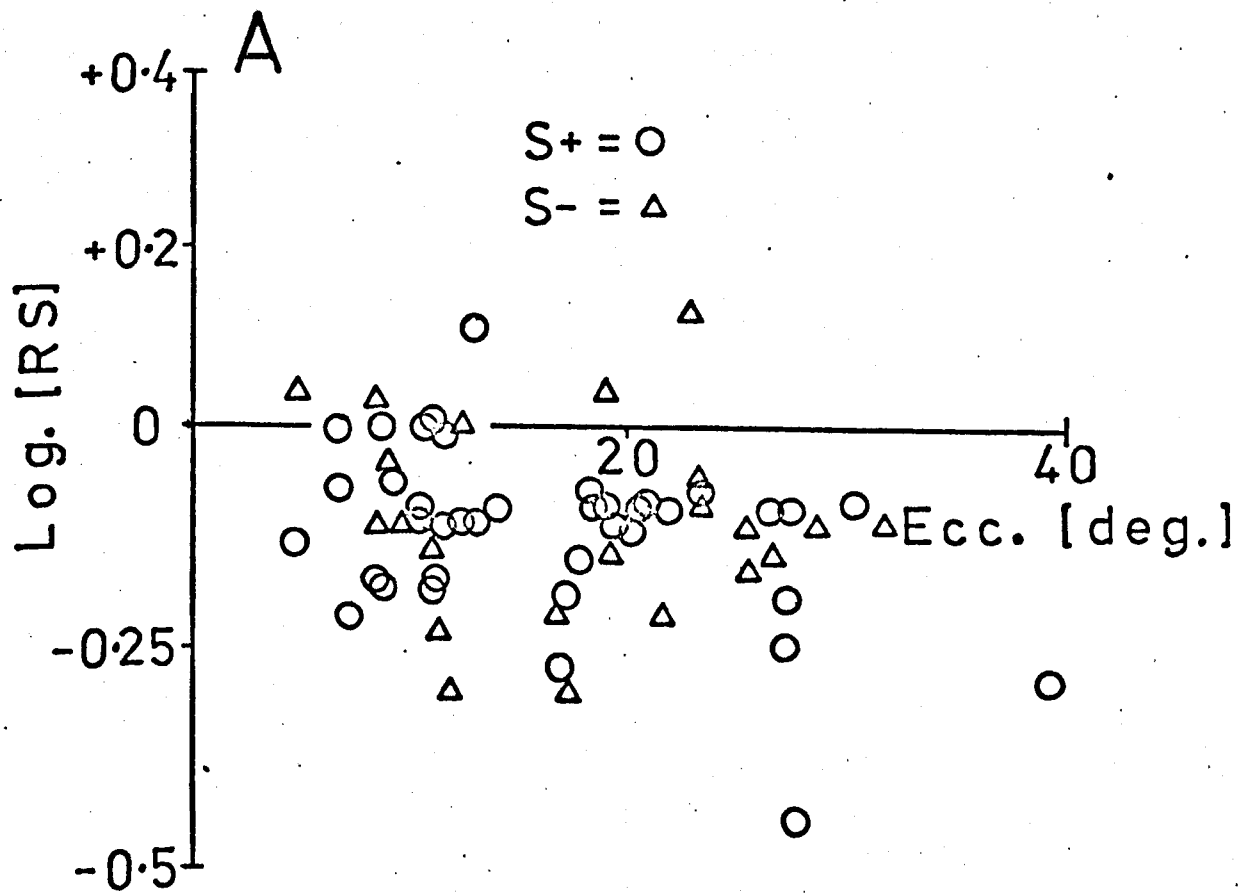*et al* , 1977)

Fig. 5.4

    Relative sensitivity values versus eccentricity of the
units from the area centralis. The scatter for sustained (S)
(n = 92) and transient (T) (n = 39), on- (+) and off- (-)
centre, units is shown, respectively in Fig. 5.4A and B.

data, linear regression analysis gave a value of -0.03 and -0.04 respectively for the correlation coefficient (r). These classes, therefore, show no systematic increase of RS with eccentricity. Furthermore, no significant difference was found between the mean RS for the on- and off-centre sustained data at the 5% significance level[1]. Similarly, the mean RS for the on- and off-centre transient data showed no significant difference[2].

One criticism of the preliminary study (Fig. 5.2) was the variation in the sample size - for example at +0.53 log. cd.m^{-2} two transient compared with 26 sustained units. A more representative comparison is, therefore, made with the present data. For the on-centre sustained recordings, the mean eccentricity was 16.1°, and for the on-centre transient units it was 14.6°. At these eccentricities, the RFC area ratio between the sustained and transient data obtained from Fig. 3.4 of Chapter 3 using the best fit regression lines is 1:2.5. Hence, the transient units should be light adapted by some 0.4 log. units above the sustained. This gives a mean RS separation of 0.25 log. units[3], whereas the actual difference in

---

[1]Sustained units:

    (i) on-centre (n=61): mean log. (RS) = -0.12±0.01
    (ii) off-centre (n=31): mean log. (RS) = -0.15±0.03
Using the t-test, the calculated t value was 1.15, and from tables $t_{0.05, 90}$=1.66. Hence, the means are not significantly different at the 5% probability level.

[2]Transient units:

    (i) on-centre (n=27): mean log. (RS) = -0.10±0.02;
    (ii) off-centre (n=12): mean log. (RS) = -0.15±0.04.
The calculated t value was 1.14, and from tables $t_{0.05, 37}$=1.68.

[3]The sustained:transient centre-area ratio is 1:2.5. This gives a value of 0.4 log units by which the transient units are relatively more light adapted. RS changes by 0.64 log. units for 1 log. unit change in adaptive state. Therefore, 0.4 log. unit change in adaptive state should lead to (0.64 x 0.4) log. unit change in RS, i.e. 0.25 log. units.

the measured mean RS for these was only 0.02 log. units.

In summary, qualitative comparisons indicate that the adaptive state does not change systematically with RFC size.

5.3.2 RS variation with RFC area

Although RS was measured for 131 single optic tract fibre recordings, only 90 were held sufficiently long to complete RFC mapping - 62 were brisk sustained (on-/off-centre, 40/22) and 28 brisk transient (on-/off-centre, 21/7). Fig. 5.5 shows the scatter of RS versus RFC area for these.

The sustained data (Fig. 5.5A) show no systematic increase of RS with RFC area (n = 62, r = -0.06) - the best fit linear regression line having a slope of -0.02.

A substantial difference was found between the mean RFC areas for the on-centre sustained (n = 40, mean RFC area = 1.2 deg.^{2}) and the off-centre sustained (n = 22, mean RFC area = 3.1 deg.^{2}), i.e. a ratio of 1:2.6. Accordingly, the off-centre units might be expected to be relatively more light adapted by 0.4 log. units compared with on-centre units; giving a predicted mean RS difference of 0.25 log. units. In fact, no significant difference was found between the mean RS for the on- and off-centre data at the 5% significance level[1], and the difference (0.01 log. units) was

---

[1]Sustained units:

    (i)   on-centre (n = 40): mean log. (RS) = -0.11±0.02

   (ii) off-centre (n = 22): mean log. (RS) = -0.10±0.03

The calculated t value was 0.35, and from tables $t_{0.05, 60}$ = 1.67. Therefore, the means are not significantly different at the 5% probability level.

negligible compared with that predicted from area considerations.

The off-centre sustained recordings could be separated into two groups according to RFC size - those with small RFCs (n = 8, RFC area < 2.0 deg.^{2}, mean RFC area = 1.1 deg.^{2}) and those with large RFCs (n = 14, RFC area $\geqslant$ 4.0 deg.^{2}, mean RFC area = 6.1 deg.^{2}). The resultant ratio of their mean RFC areas gives a predicted difference in the adaptational level of 0.7 log. units and a predicted mean separation in RS of 0.46 log. units. The experimentally determined RS separation of 0.03 log. units for the off-centre small and large RFC groups compares most unfavourably with this predicted value, again indicating that RFC size is independent of adaptive state.

The data for the transient units, shown in Fig. 5.5B, support the results for sustained units, the best fit linear regression line having a slope of -0.18 (n = 28, r = -0.41). Hence, if anything, the data exhibit a *decrease* in RS as RFC area increases.

Comparisons of mean RS between on- and off-centre transient[1], and between sustained and transient data[2], also reveal no significant differences. The predicted slope of +0.64 was expected between log. (RS)

---

[1]Transient units:
    (i)   on-centre (n = 21): mean log. (RS) = -0.14±0.03
   (ii) off-centre (n = 7): mean log. (RS) = -0.19±0.06
The calculated t value was 0.96, and from tables $t_{0.05, 26} \cong 1.7$.
Hence, the means are not significantly different.

[2]Sustained units (n = 62): mean log. (RS) = -0.10±0.01
Transient units (n = 28): mean log. (RS) = -0.15±0.02
The calculated t value was 1.54, and from tables $t_{0.05, 88} = 1.66$.
Hence, the means for these classes are not significantly different.

Fig. 5.5

Scatter of relative sensitivity (RS) values versus RFC area. The RS values were obtained at +0.53 log.cd.m^{-2} adapting luminance.

A - The data for sustained on- (S+) and off- (S-) centre units (n = 62) are shown on log.-log axes. The best fit linear regression line has a slope of -0.02 (correlation coefficient (r) = -0.06).

B - The data for transient on- (T+) and off- (T-) centre units (n = 28) are shown on log.-log. axes. The best fit linear regression line has a slope of -0.18 (r = -0.41).
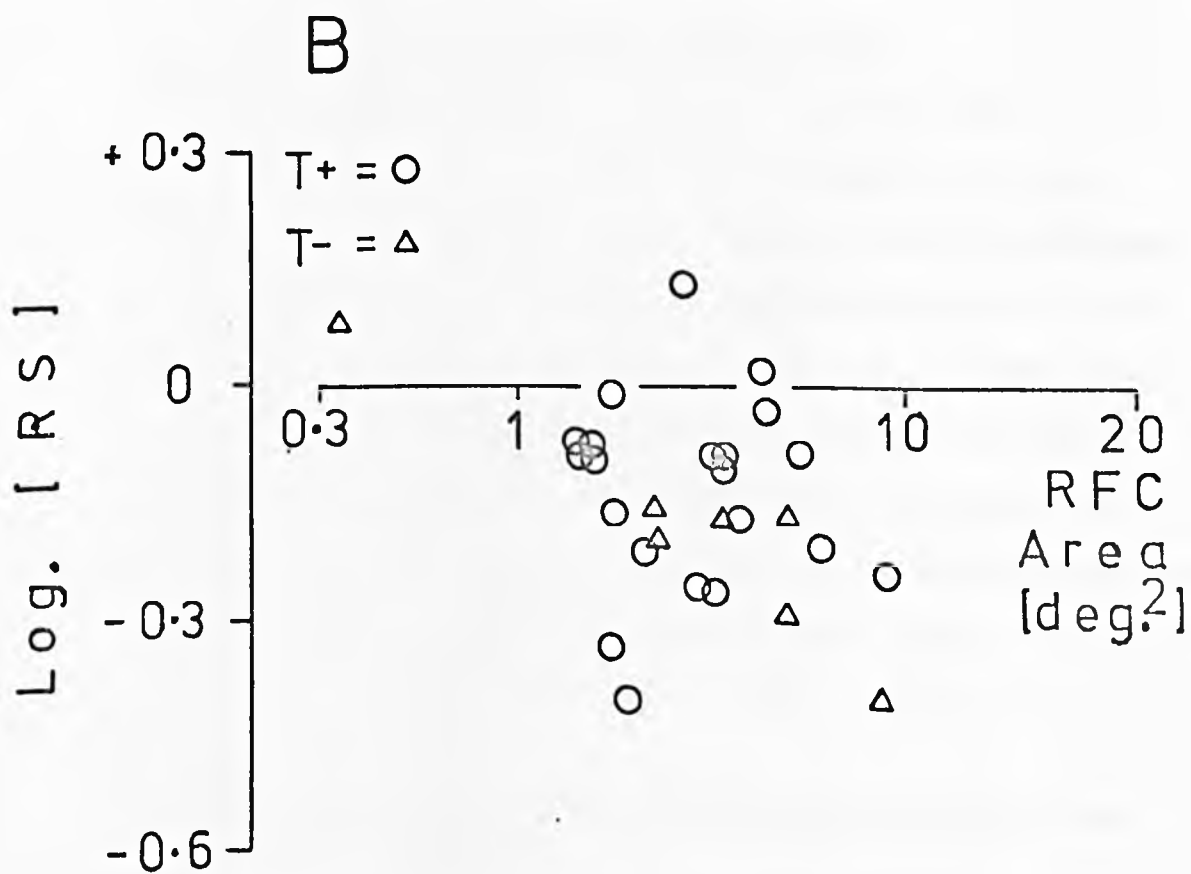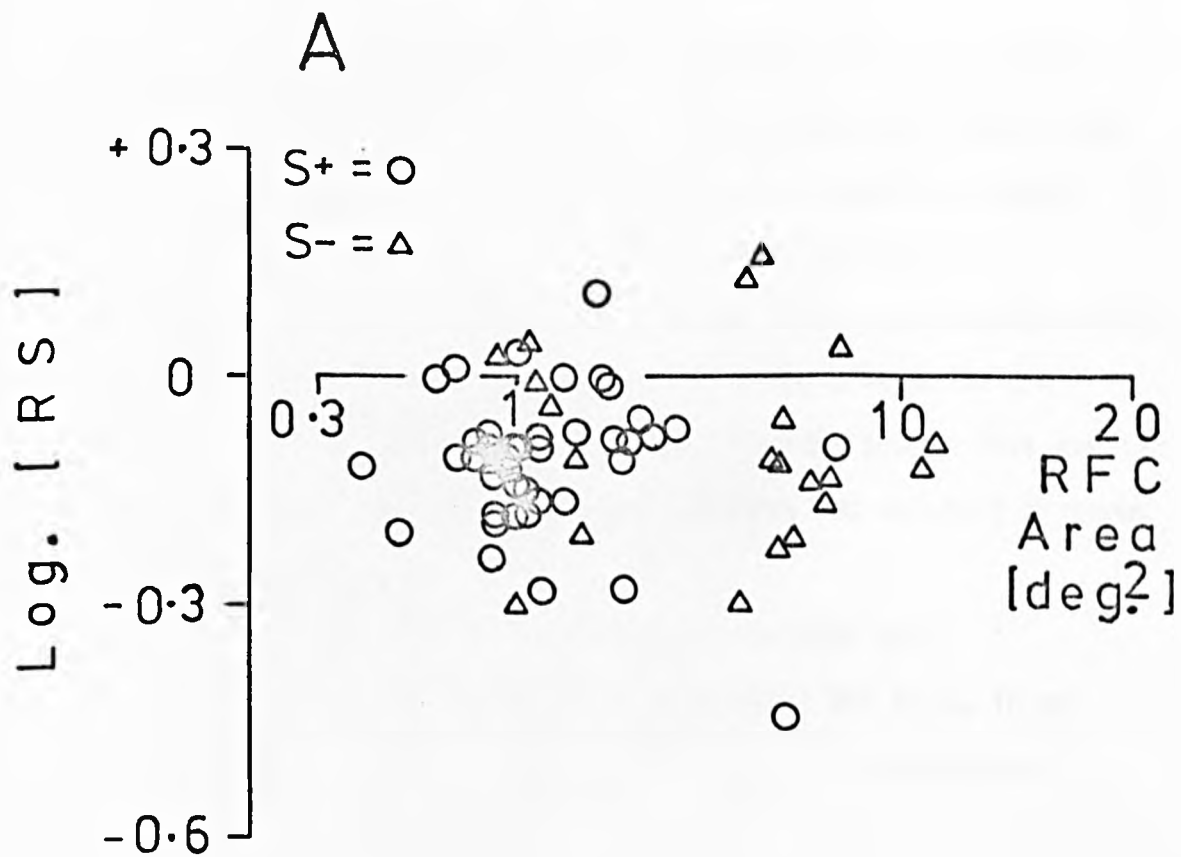
versus log. (RFC area). However, in Fig. 5.5A and B the data give slopes of -0.02 and -0.18 respectively. These slopes are nowhere near the expected value and show either no change, or a tendency towards decrease, in adaptational state with increasing RFC area.

Although these results establish no systematic relationship between RFC size and adaptive state, the data show a large scatter in the experimentally determined values of RS (Fig. 5.4 and 5.5). This scatter in RS is specifically considered in the following two sections in terms of the variation in:

(i)   RFC size for RGCs at similar eccentricities and

(ii) visual field location of RGCs of similar RFC size, in an attempt to unmask any possible evidence of the expected relationship.

5.3.3 RS variation of units at similar eccentricities

In Fig. 5.4A, for the sustained units with receptive field eccentricities between 10°-14° and 16°-20°, a difference of 0.4 log. units is found in each group's RS scatter. Possible correlation between this scatter and RFC size was considered by plotting RS versus RFC area ratios[1] for units in each eccentricity group (Fig. 5.6). In both cases (Fig. 5.6A and B), the best fit linear regression line for the data (continuous line) and the expected line (dashed line) have been drawn for comparison. The slopes of these best fit lines for the eccentricity groups 10°-14° (n = 15; mean eccentricity = 11.6°±0.2) and 16°-20° (n = 11; mean

---

[1]In each eccentricity group, the ratios are expressed in terms of the unit with the smallest RFC area.

Fig. 5.6

      Scatter of relative sensitivity (RS) values versus RFC area ratios for sustained units in two eccentricity groups, plotted on log.-log. axes. The RFC area ratios are expressed in terms of the unit with the smallest RFC area. The sustained on- (S+) and off- (S-) centre units are respectively denoted by the open circles and triangles.

      A - Data for sustained units with receptive fields 10° - 14° from the area centralis. The best linear fit regression line (continuous line) has a slope of -0.01 (n = 15, r = -0.01).

      B - Data for sustained units with receptive fields 16° - 20° from the area centralis. The best fit line (continuous line) has a slope of 0.02 (n = 11, r = 0.06).

      The line for the predicted relationship between adaptive state and RFC area is shown by the dashed line in both Fig. 5.6A and B.

Log. [RS]

-0·3   0   +0·3   +0·6

A   10-14 deg.

S+ = O
S- = Δ

RFC
Ratio

1   5   10

Log. [RS]

-0·3   0   +0·3   +0·6

B   16-20 deg.

S+ = O
S- = Δ

RFC
Ratio

5   10
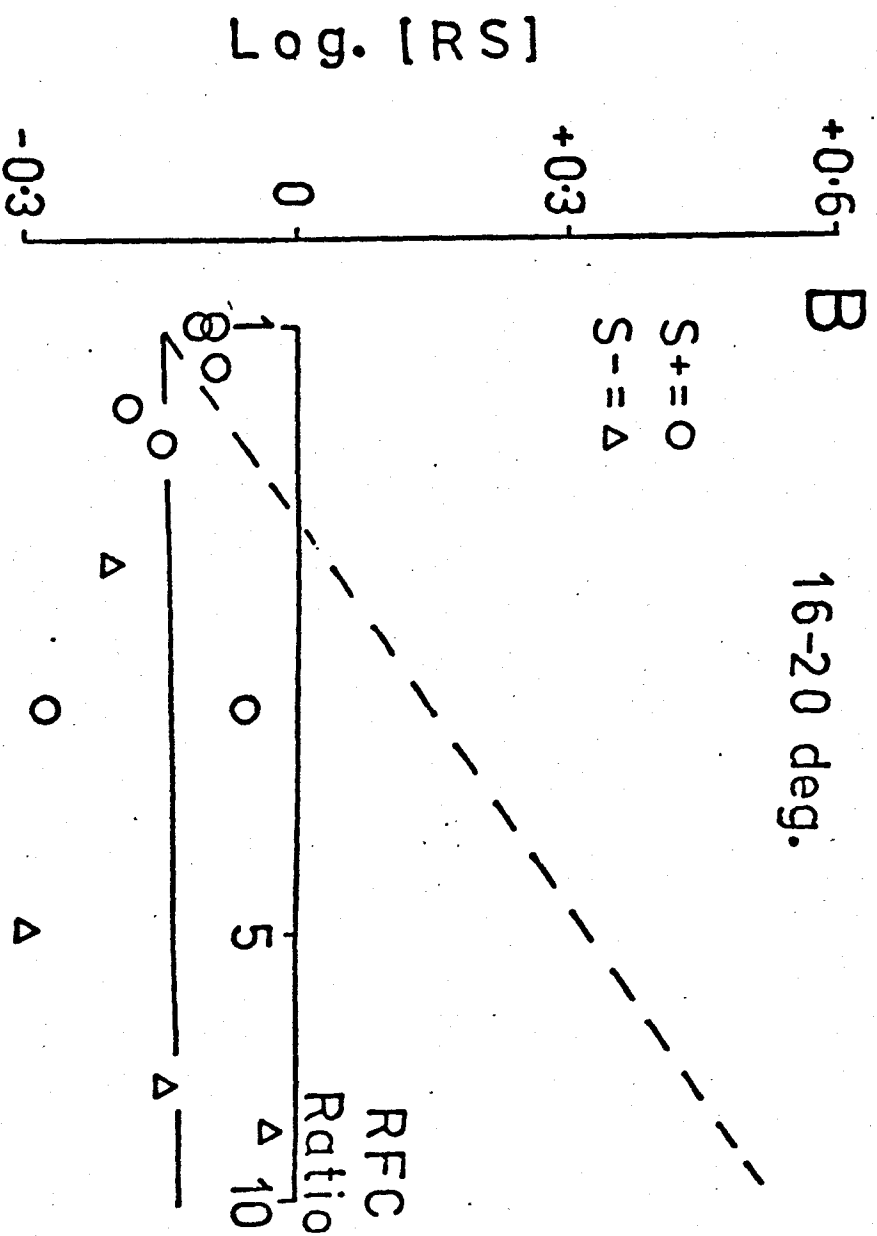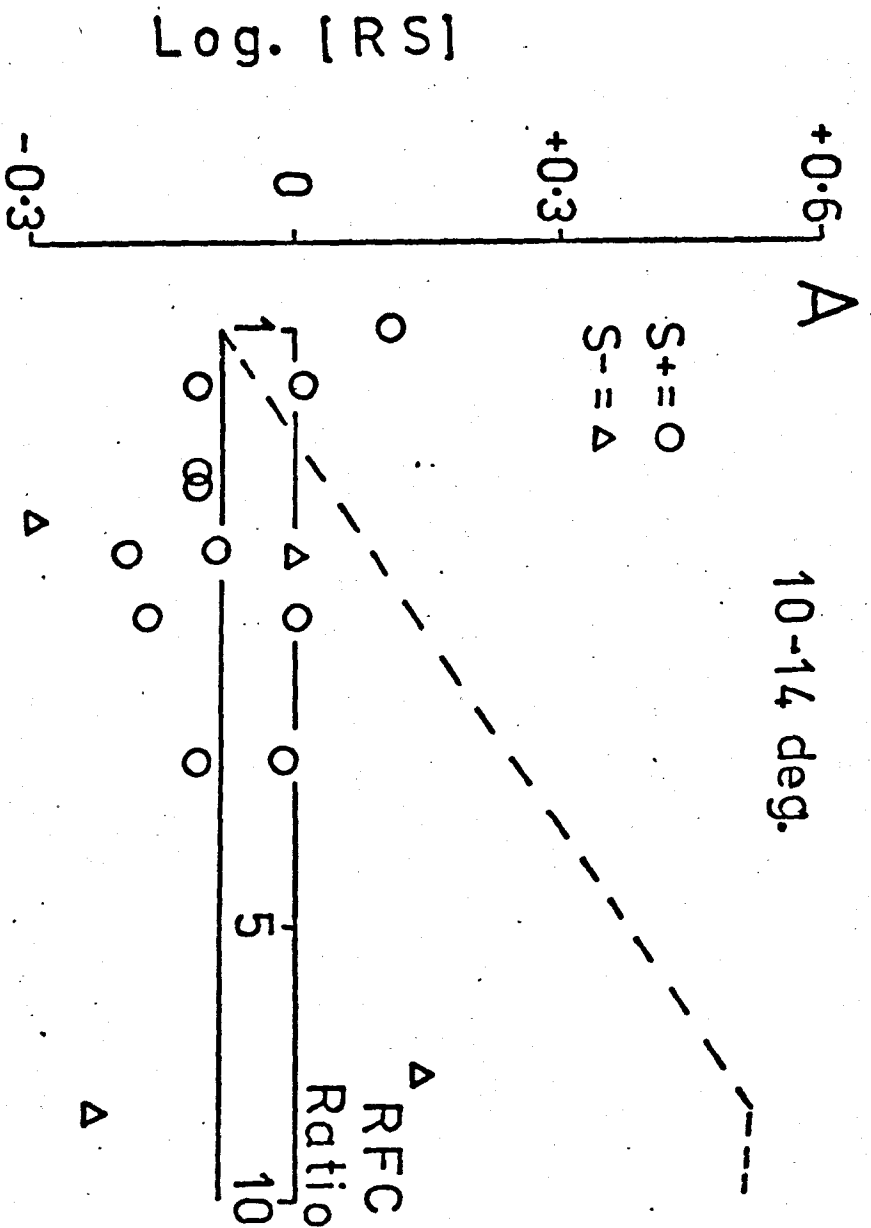
eccentricity = 18.2°±0.3) are, respectively -0.01 and 0.02. Hence, these slopes compare unfavourably with the expected slope of 0.64.

5.3.4 RS variation of units with similar RFC sizes

As the data in Fig. 5.5A show, the units with RFC areas between 0.9 and 1.1 deg.^{2} (n = 20, mean RFC area = 0.98±0.02 deg.^{2}) have a scatter of 0.34 log. units in their RS values. The possibility, therefore, exists that this scatter is due to variation in the "actual", as opposed to the experimentally determined value of, RFC size. This point has been tested by plotting RS versus eccentricity (Fig. 5.7), since RFC size increases with eccentricity from the area centralis. A positive correlation would suggest:

(i) shortcomings in the method of RFC size determination, and/or

(ii) the predicted relationship between adaptive state and RFC area. However, the best fit line drawn through the data (continuous line) has a slope of -0.18 (r = -0.45), clearly indicating that adaptive state is not related to RFC area.

5.3.5 RS variation with central summing area

The previous considerations have been based on the assumptions that:

(i) RFC size increases with eccentricity, and

(ii) the measured RFC sizes, at the mesopic level, are related to the adaptive state of the RGCs.

It may be that both these parameters bear no relationship with the central summing areas calculated by Enroth-Cugell and Shapley (D.M. MacKay, personal communication). These authors obtained their data in the dark adapted retina where the absence of surround antagonism (Barlow *et al.*, 1957b; Kruger and Fischer, 1973) does not, presumably, interfere with the

Fig. 5.7

Scatter of relative sensitivity versus eccentricity of receptive fields from the area centralis, of units with similar RFC areas. The values are plotted on log.-log. axes. The best fit regression line has the slope of -0.18 (n = 20, r = -0.45).
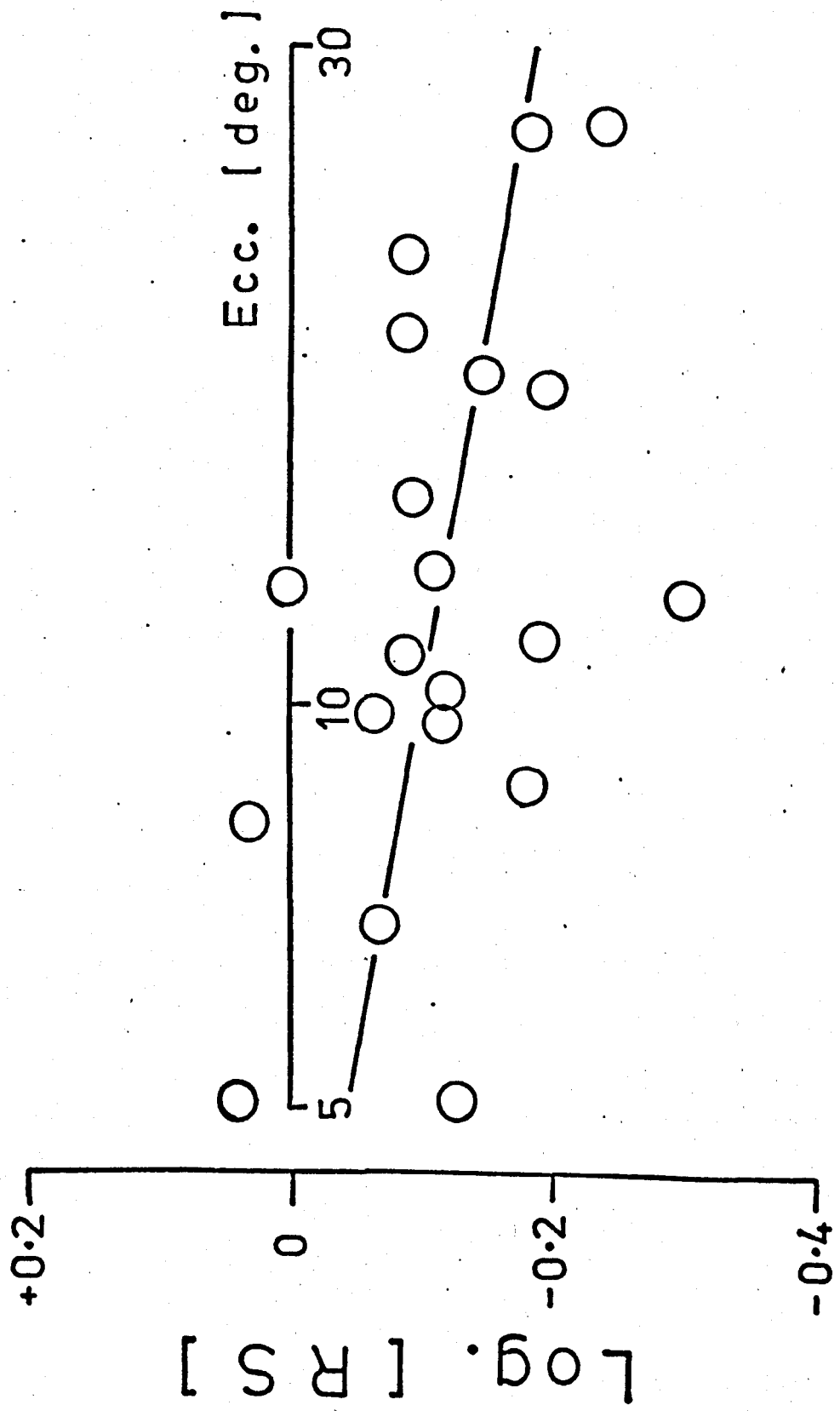
centre size responsible for setting of the adaptive state. To discount this possibility, the following method was adopted:

(i) RS value was obtained, at the mid-mesopic level, for a RGC recording:

(ii) the retina was dark adapted (for at least 15 mins.) to a scotopic level of -0.91 log. cd.m^{-2}; and

(iii) the central summing area for this unit was then determined in the manner described by Enroth-Cugell and Shapley[1].

This procedure was repeated for different RGCs.

The results are plotted in Fig. 5.8. Regression analysis of these data (n = 36) gave the best fit line of slope -0.04 (r = -0.25). Hence, these data also support the previous findings and lead to the conclusion that the adaptive state is not related to the centre size of RGCs, whether the centre sizes are

(i) inferred from the location of the RFC in the visual field or

(ii) determined at mid-mesopic or scotopic levels.

5.4 Discussion

The ratio of the threshold sensitivities - the relative sensitivity - to the blue and yellow lights has been used as a measure of the adaptive

---

[1]Briefly, the threshold sensitivities of the 0.25° and 8° diameter spots, were measured separately at a scotopic luminance of -0.91 log. cd.m^{-2}. The central summing area (A_c) was then calculated from the relationship

$$A_c = A_{0.25} \cdot T_8 / T_{0.25}$$

where T_8 and $T_{0.25}$ represent the measured threshold sensitivities of the 8° and 0.25° diameter spots respectively, and $A_{0.25}$ is the area of the 0.25° diameter spot ($A_{0.25} = 0.05$ deg.^{2}).

Fig. 5.8

Scatter of relative sensitivity versus the central summating area, plotted on log.-log. axes. The data for two cats are shown, respectively by the open and filled circles. The best fit regression line (dashed line) has a slope of -0.04 (n = 36, r = -0.25).
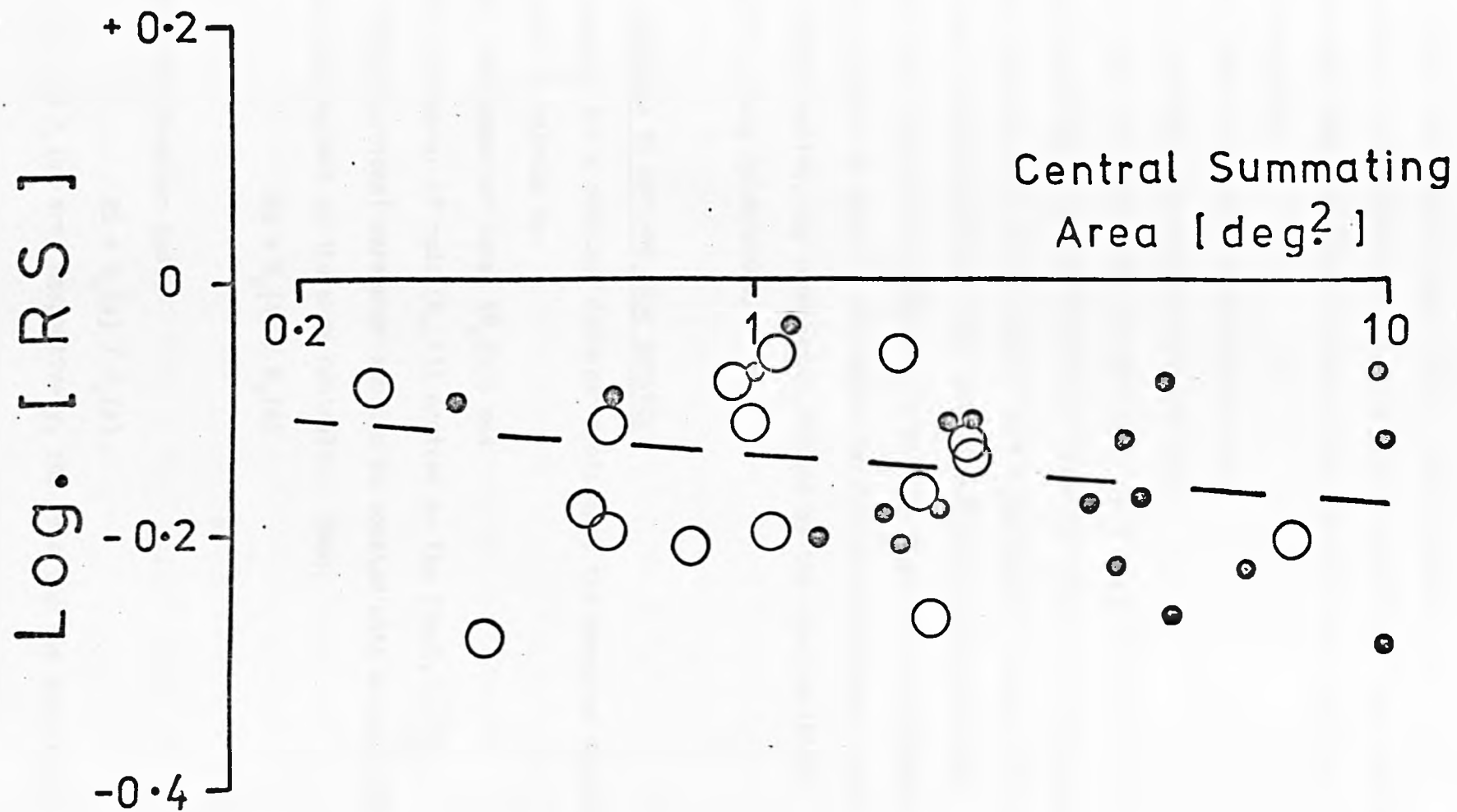
state. Within the mesopic range, these stimuli measure the sensitivities, respectively, of the rod- and cone-mediated inputs to the RGC. Assuming that the sensitivities of the rod and cone inputs are related either to:

(i)   the rod and cone densities, or to

(ii) the number of receptors in the RFC,

then, the negative results may be explained by changes produced in the threshold measurements which effectively mask the predicted relationship - viz. that the values of the RS should show a systematic change with centre area. These two possibilities have been specifically analysed below (sections 5.4.1 and 5.4.2). However, since the nature of convergence from the photoreceptors to RGCs is not known and may differ between central and peripheral retina, *any conclusion* reached by the considerations outlined is *purely speculative*.

5.4.1 Variation in rod and cone density

Assuming, for a constant diameter spot, that the measured threshold sensitivity is related to:

(i)   the number of cones ($N_c(\theta)$) and

(ii) the number of rods ($N_r(\theta)$) excited by the flash,

where θ is a locational parameter and can be equated with eccentricity measured with respect to the area centralis. Then,

$$RS \propto N_c(\theta) \,/\, N_r(\theta)$$

or

for a constant diameter spot,

$$RS \propto P_c(\theta) \,/\, P_r(\theta).$$

where $P_c(\theta)$ and $P_r(\theta)$ are, respectively, the cone and rod densities

at location θ on the retina.

The variation of the rod and cone densities with eccentricity from the area centralis has been plotted in Fig. 5.9. These values have been derived from those given by Steinberg, Reid and Lacy (1973), and converted from densities per mm^2 to densities per $deg.^2$ on the retina (1 deg. on the retina equals 0.22mm; Vakkur, Bishop and Kozak, 1963). The right-hand ordinate in Fig. 5.9A and B shows the change in relative density with respect to the density at the area centralis (0° on the abscissa). Hence, on the assumption that threshold sensitivity depends upon receptor density, the relative density shows how the threshold sensitivity will change with eccentricity for the rod (Fig. 5.9A) and cone (Fig. 5.9 B) inputs. The effect on the measured relative sensitivity of such a change should, therefore, be related to the ratio between the cone and rod relative densities. This predicted change is shown in Fig. 5.10, where the ratio of the cone to rod densities has been plotted in terms of log. relative density versus eccentricity from the area centralis. In terms of density, the ordinate shows the variation of the cone to rod ratio. In terms of sensitivity, it relates how the magnitude of the measured relative sensitivity should change with eccentricity.

The major change in RS predicted by this hypothesis should occur for eccentricities between 0° and 10° from the area centralis. To analyse this prediction, data were plotted for centrally located RGC and LGC recordings (Fig. 5.11). Analysis of the scatter shows no systematic change and, hence, RS is independent of the rod and cone density variation.

Fig. 5.9

Variation of receptor density with eccentricity from the area centralis. Values have been calculated from those given by Steinberg *et al.* (1973) and converted into receptor density per deg.^{2}.

The left-hand ordinates denote the rod (Fig. 5.9A) and cone (Fig. 5.9B) receptor densities. The right-hand ordinates denote the change in rod and cone densities relative to their respective densities at the area centralis (0°).

(Figures have been obtained from data given by Steinberg, Reid and Lacy, 1973).

Fig. 5.10

Change in log. relative density of cones and rods with
eccentricity from the area centralis. This has been derived from
right-hand ordinates of Figs. 5.9A and B.
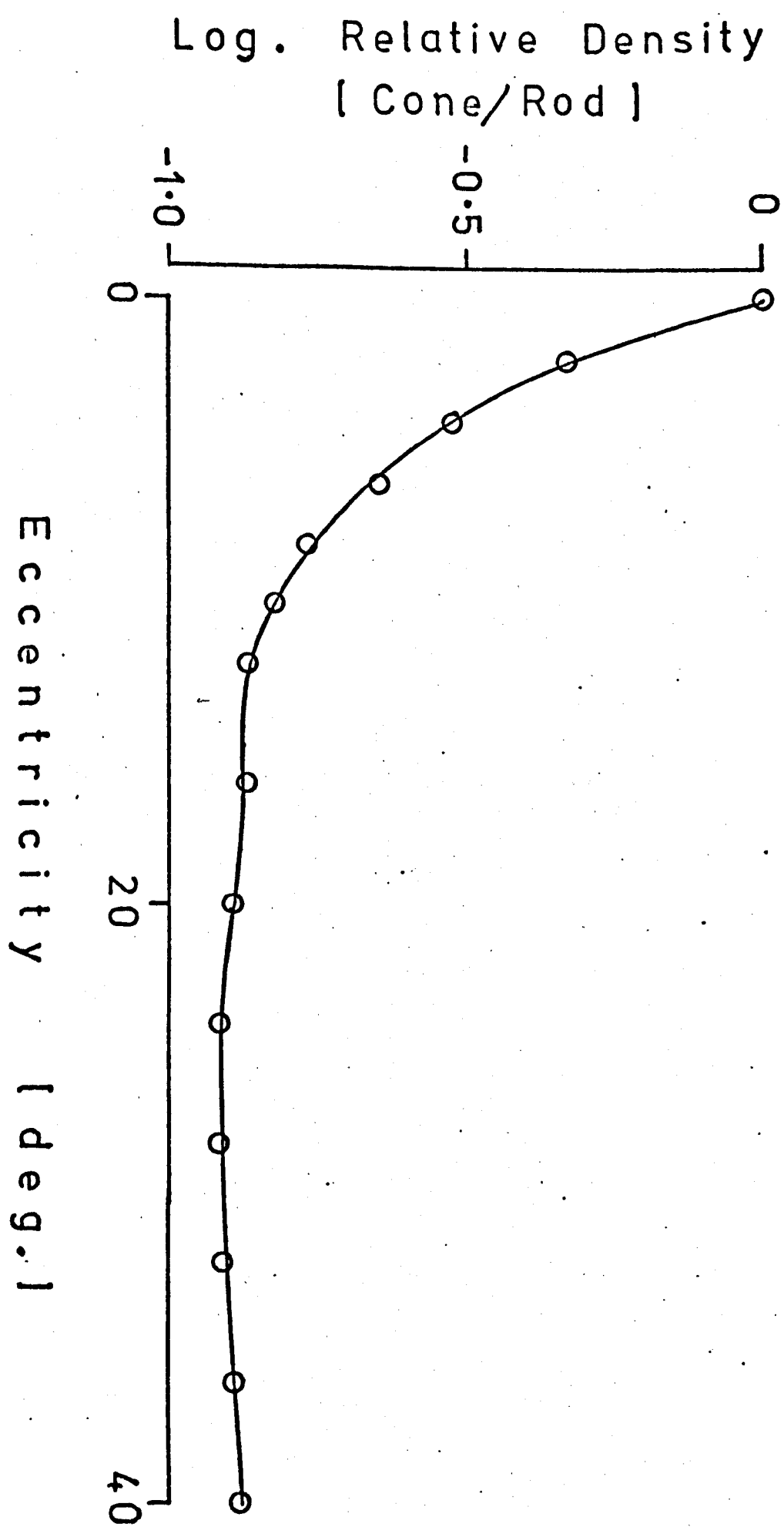
Fig. 5.11

Scatter of relative sensitivity with eccentricity from the area centralis. Data from RGCs (n = 68) and LGCs (n = 37) have been grouped and their scatter between 0° and 20° from the area centralis is shown. Bars denote one S.E.M.
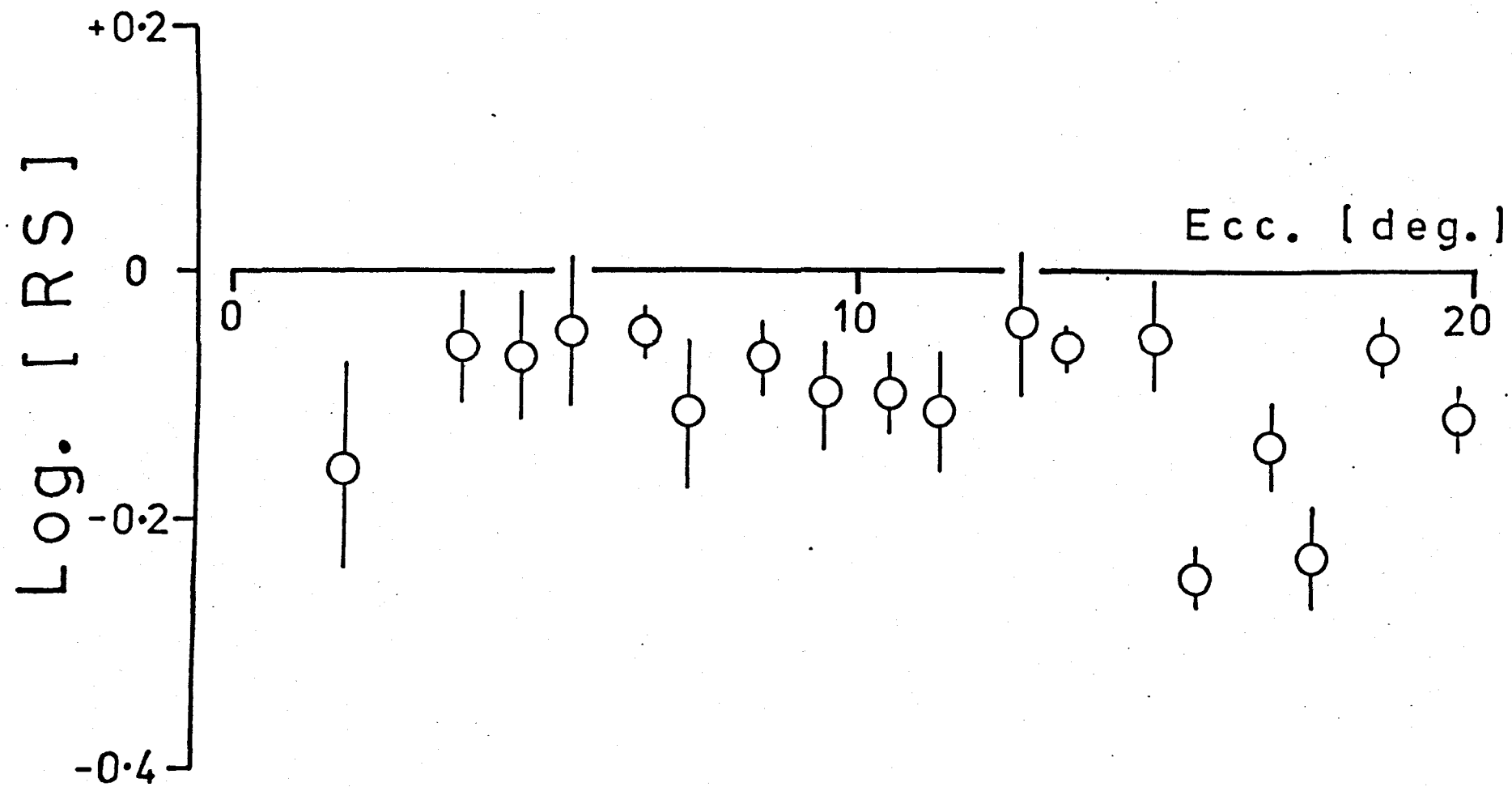
5.4.2 Variation in receptor number

Assuming the adaptive state is set by the interaction of signals from individual receptors (cones and rods) within the RFC, the negative correlation may be explained by the product of receptor density and RFC area being constant for the data with similar RS values. Since there is an inverse relationship between centre size and receptor density - cone and rod densities decrease with eccentricity, from 0° and 10° respectively from the area centralis (Fig. 5.9A and B) - this suggests that RS values may depend on the total number of receptors in the RFC.

The total number of receptors was calculated[1] for each sustained unit and the results are plotted in Fig. 5.12. Regression analysis gives a slope of -0.01 (n = 62, r = -0.03) for the best fit line, and the RS values for units with receptor number less than 5×10^4 show no significant difference[2] from the units with receptor number greater than 5×10^4.

The data giving rise to Fig. 5.12 are for RFC sizes obtained at the mid-mesopic level. In case these sizes do not relate RS with the number

---

[1]For a unit with RFC area A and eccentricity θ°, the rod (P_r) and cone (P_c) densities at this eccentricity were obtained from Fig. 5.9. Then,

$$\text{Total receptor number} = A(P_r + P_c)$$

[2]For units with receptor number less than 5×10^4 (n = 22, mean receptor number = 2.9×10^4), the mean log. (RS) value was -0.10.

For units with receptor number greater than 5×10^4 (n = 40, mean receptor number = 1.1×10^5), the mean log. (RS) value was -0.12.

The calculated t value was 0.72, and from tables $t_{0.05, 60} = 1.67$. Therefore, these means (i.e. log (RS) means) are not significantly different.

Fig. 5.12

Scatter of relative sensitivity versus receptor number,
plotted on log.-log. axes. The total number of receptors,
within the RFC, was calculated from the cone and rod densities
at the eccentricity of the unit's receptive field from the area
centralis. The RFC was determined at +0.53 log. cd.m^{-2} using
the iso-sensitivity mapping technique. The data are for the
sustained on- (S+) and off- (S-) centre units (n = 62).
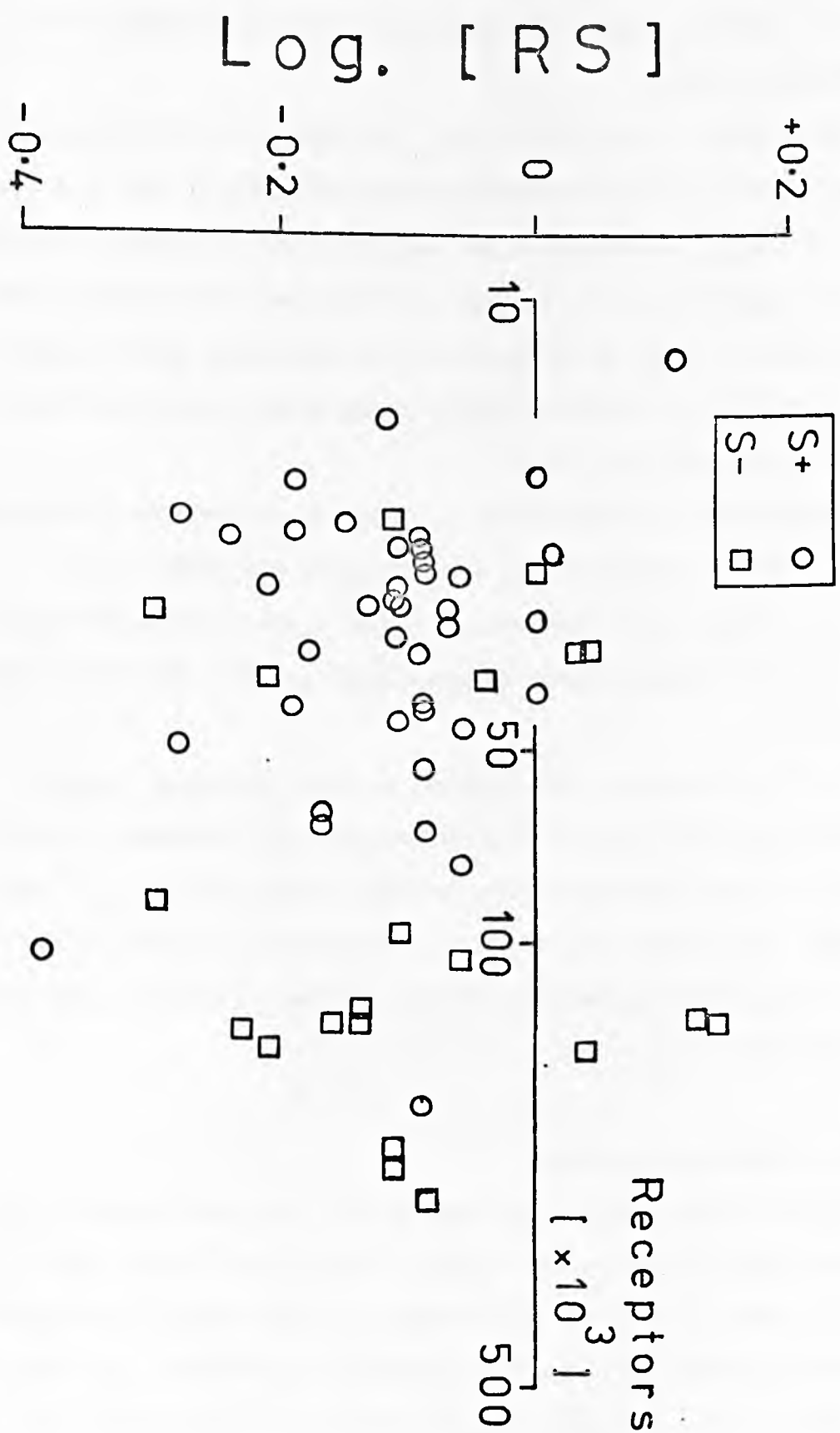
of receptors, but the central summing areas do, the total number of receptors in the central summing area was also calculated. The resultant data are shown in Fig. 5.13. The scatter of values exhibit no systematic increase in RS (n = 36, slope = -0.03, r = -0.19) and, hence, these data support the previous findings in showing that RS is independent of the number of receptors in the RFC.

5.4.3 Conclusions

In confirmation of previous studies (Barlow and Levick, 1968; Hammond and James, 1971; Ahmed et al., 1977), the measured RS values for RGCs varied at a fixed background adapting level (+0.53 log. cd.m^{-2}). Fig. 5.14 shows the distribution, in histogram form, of the number of units versus log. (RS) using a class interval of 0.05 log. units. After allowing for:

(i) the systematic error in determining RS (±0.1 log. units), and

(ii) the fact that units with RS values close to -0.44 log. units may have exclusive rod input (Hammond and James, 1971);

the distribution of the determined RS values still demonstrate that RGCs differ in their adaptive state.

Although, this evidence supports Enroth-Cugell, Hertz and Lennie (1977a) (these authors found variability in the extent of the mesopic range for different RGCs.), it does not corroborate Enroth-Cugell and Shapley's (1973b) proposition - viz adaptive state is directly related to centre area. The evidence establishes unequivocally that at a fixed mid-mesopic level of +0.53 log. cd.m^{-2}, the adaptive state of RGCs is independent of their:

(i) retinal location with respect to the area centralis, and

(ii) RFC areas whether determined at mid-mesopic (from iso-

Fig. 5.13

Scatter of relative sensitivity versus receptor number
plotted on log.-log. axes. The data are for two cats shown,
respectively, by open and filled circles. The total number of
receptors was calculated from rod and cone densities at the
eccentricity of the unit's receptive field from the area
centralis. The RFC size was determined, using the technique
of Enroth-Cugell and Shapley (1973b), at -0.91 log. cd.m^{-2}.

The best fit linear regression line has a slope of -0.03
(n = 36, r = -0.19).
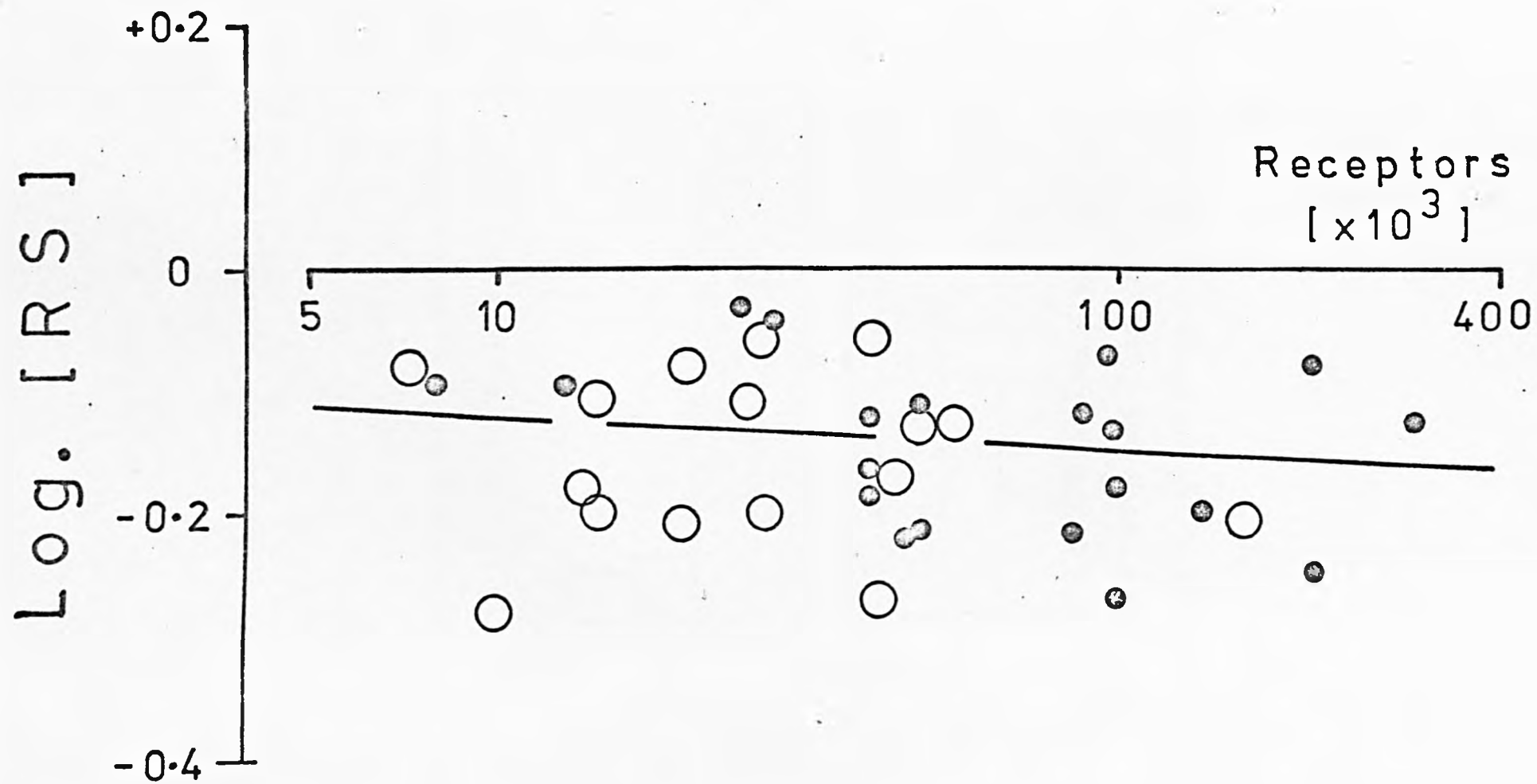
Fig. 5.14

Variation of relative sensitivity using class intervals of 0.05 log units, which shows a total scatter of 0.61 log. units, with a mean RS value of -0.11±0.01 log. units (n = 168).
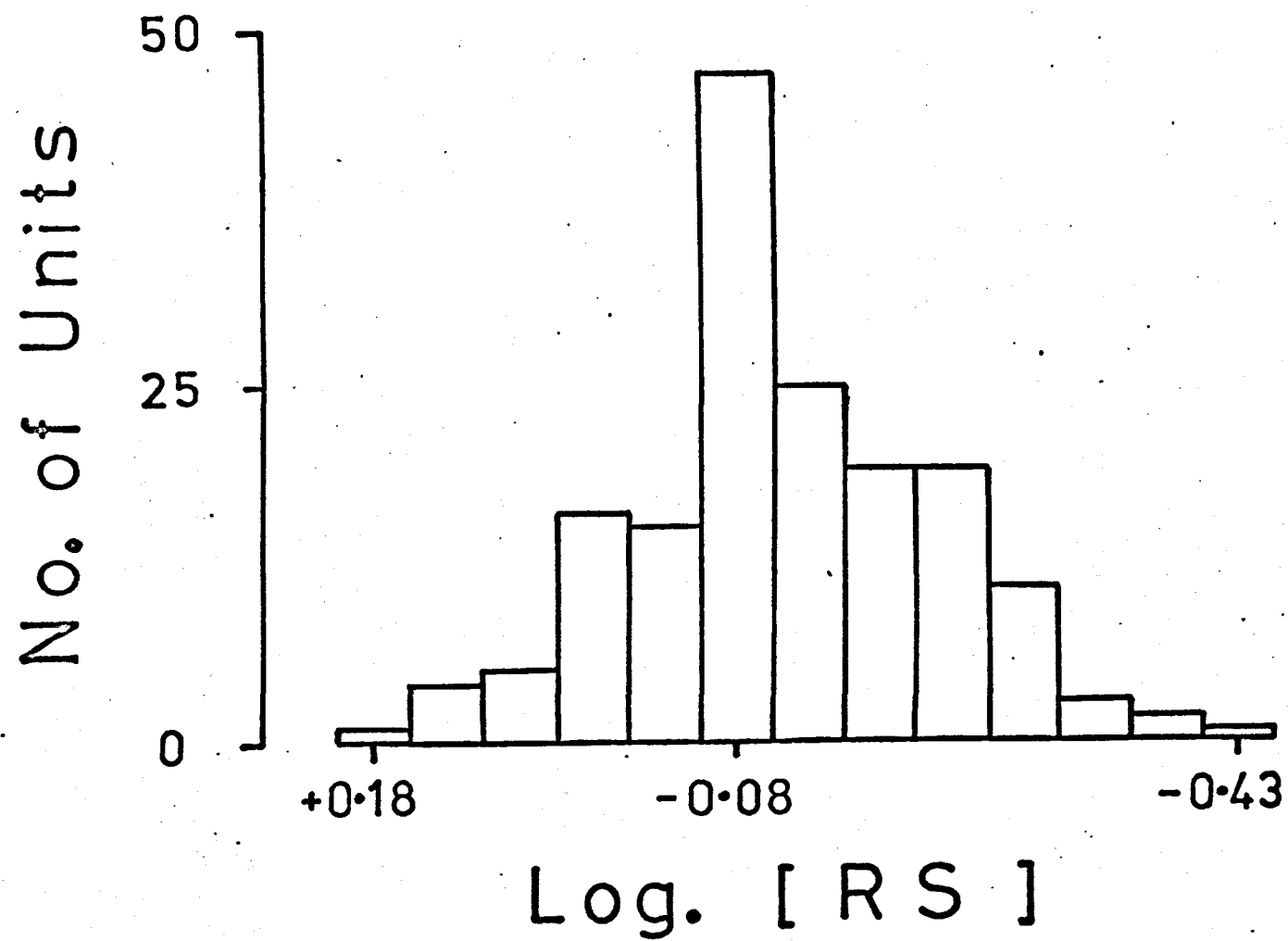
sensitivity contours) or scotopic (from central summing areas)
levels.

Furthermore, in contra-indication to Enroth-Cugell and Shapley, the
present data also establish that it is the general background illumination
which determines (for the majority of RGCs) the extent to which RGCs are
light adapted in the mesopic range. The data of Enroth-Cugell and Shapley
were obtained exclusively in the scotopic range of adapting luminances
and, hence, their hypothesis is probably valid only over these particular
luminance values.

Rushton (1963, 1965a,b) has suggested that the signals from
individual receptors are pooled into a *summation pool* which sets the
adaptational state. Enroth-Cugell and Shapley point out that their data
further confirm the concept of a "summation pool" in the cat retina, the
spatial extent of this pool being equal to the central summing area of
RGCs.

The results presented in this chapter also confirm the concept
of a "summation pool", but indicate that the pool is independent of:

    (i)   RFC area of RGCs,

    (ii)   regional variation in rod and cone densities, and

    (iii) the total number of receptors within the RFC.

Furthermore, since the adaptive state of RGCs is approximately constant
over the retina, the evidence suggests that centrally and peripherally
located "summation pools" smooth out differences related to retinal
asymmetries, i.e. variation in receptor and synaptic densities.

Chapter 6   <u>SUMMARY</u>

This study was undertaken to examine the chromatic, adaptive, and general properties of cat retinal ganglion and lateral geniculate cells at a mid-mesopic adapting luminance. The findings are summarised below, in sections appropriately related to the preceding experimental chapters.

6.1 <u>General properties</u>

By using some of the tests described by Cleland *et al*. (1971, 1974a), the properties of 610 retinal ganglion and 105 lateral geniculate cells were analysed. However, only a proportion of this sample gave sufficient data for detailed analysis. The main reason for this was related to the difficulty in holding units for durations in excess of 30 mins. - especially where optic tract fibre recordings were concerned.

Contrast test. By presenting a small diameter light spot, appropriately positioned in the receptive field centre at 1 log. unit above centre threshold, the spike rate before, during, and after presentation (response profile) was recorded. Analyses of these response profiles confirmed the findings of Cleland *et al*. (1971, 1972, 1973, 1974a) since the majority of units could be classified as sustained (brisk/sluggish, on- or off-centre) and transient (brisk, on- or off-centre). However, for a number of RGCs the well-defined difference in the maintained components of the response profile (i.e. difference in the spike activity before and during presentation of the contrast stimulus) fluctuated from one displaying a sustained characteristic to one displaying a transient. This occurred for units at comparable eccentricities. It was, therefore, suggested that their may be a continuum from units with sustained type response

profiles to units with transient type profiles.

Unmodulated response from transient units. As the spatial frequency of a sinusoidal or a square-wave grating is successively increased, according to Enroth-Cugell and Robson (1966) and Cleland *et al.* (1971, 1974a) the modulated response (spike discharge related to the spacing of the light and dark regions of the grating), during the passage of the grating across the receptive field, gives way to an unmodulated increase in spike activity above the maintained prestimulus discharge rate for transient (or Y-cells) units. This finding was not confirmed for square-wave gratings. In contra-indication, the results show that at slow velocities of passage (<2°/sec), the firing rate was attenuated for brisk transient on-centre units and increased for off-centre units. Unfortunately, a detailed analysis was not attempted, the data being obtained only for:

(i) the first spatial frequency that gave an unmodulated response, and

(ii) a single velocity of grating passage.

Hence, these findings are tentative and require a more thorough investigation, utilising variations in spatial and temporal parameters of the grating, to unequivocally refute the results of the above investigators.

Maintained discharge rate. The maintained activity of RGCs was analysed under two anaesthetic regimes - pentobarbitone and nitrous oxide: oxygen (supplemented with pentobarbitone). The results show that:

(i) under pentobarbitone, the activity is depressed compared with the activity under nitrous oxide: oxygen; and

(ii) this effect occurs equally in all classes of cells such that the overall trend in mean firing rates (S+ > S- ≈ T+ > T-) is maintained.

Apart from the magnitude of spike activity, these findings are in agreement with Stone and Fukuda (1974a), Cleland, Levick and Sanderson (1973), and Pollack and Winters (1978). Additionally, a similar trend in activity was found at the geniculate level using the nitrous oxide: oxygen anaesthetic regime.

Additional findings. Further conclusions from this investigation are summarised below.

(i) The RFC size of RGCs increases with eccentricity from the area centralis (Wiesel, 1960; Ikeda and Wright, 1972b; Cleland *et al.* 1973, 1974a; Hammond, 1974; Stone and Fukuda, 1974a).

(ii) At a given eccentricity, on-centre brisk sustained units have smaller RFCs than brisk transient units (Enroth-Cugell and Robson, 1966; Cleland *et al.*, 1971, 1974a; Hammond, 1974).

(iii) The periphery effect was found to be strongest in brisk transient units and weak or absent in brisk sustained units (Cleland *et al.* 1971, 1974a; Ikeda and Wright, 1972a; Barlow, Derrington, Harris and Lennie, 1977).

The data obtained for lateral geniculate cells were inadequate in deciding whether RFC size (a) increased with eccentricity or (b) differed between the sustained and transient classes.

6.2 Chromatic study

This investigation was designed basically to map the rod- and cone-mediated inputs of retinal ganglion and lateral geniculate cells; the study being an attempt to:-

(i) resolve discrepancies between the findings of Andrews and Hammond (1970b) and Enroth-Cugell, Hertz and Lennie (1977b), and

(ii)   test the suggestion of H.B. Barlow that ellipticity in RFC

shape may arise through circular, but non-concentric, rod and

cone centres.

The results confirm the findings of Andrews and Hammond (1970b) except

in the magnitude of the difference between rod- and cone-centre sizes.

The data from this study gave area ratios of rod to cone centres ranging

from 0.6:1 to 2.9:1 (mean, 1.6:1), whereas Andrews and Hammond quote a

range from equality to 9:1 (mean, 4:1). The discrepancy may be related

to the use by Andrews and Hammond of the P1 and P2 components (see section

4.1.1) as the measuring parameters for cone- and rod-mediated inputs,

respectively. The findings of Enroth-Cugell, Hertz and Lennie - viz.:

rod and cone centres are the same size - may be due to the following

possibilities:

(i)   use of the area-threshold technique (see section 4.2.1);

(ii)   small sample size (n=11); and

(iii) data may have been obtained exclusively from RFC category

Al units and/or from units in categories B1 and B2 in which

the differences in centre-size could not be resolved by

their technique.

The rod- to cone-centre area ratios determined for LGCs ranged from

equality to 1.4:1, values in close agreement with those given by

Hammond (1972).

The possibility suggested by H.B. Barlow was discounted because,

although the rod and cone centres were non-concentric for the majority

of units (51 out of 74 for RGCs, and 11 out of 31 for LGCs), the centres

were *themselves* elliptical in shape. Hammond's suggestion (Hammond,

1974) - viz.: that RFC ellipticity may arise from asymmetry in the

dendritic arborization of retinal ganglion cells - was supported.

However, in order to explain the non-concentricity of rod and cone centres, additionally it was proposed that:

(i) asymmetric connectivity occurred at earlier levels of interaction (for example in the outer plexiform layer), or

(ii) a different pattern of connectivity occurred onto the RGC's dendritic tree,

since the dendritic spread of RGCs is fixed. These propositions, relating to the possible ways that *non-concentricity in rod and cone centres may arise,* are tentative since evidence from this study does not unequivocally discriminate between *functional asymmetry* in retinal wiring and effects of *longitudinal chromatic aberration.* However, the presence of:

(i) two regions of maximal sensitivity within the RFC shown possibly to be due to a mismatch between rod and cone inputs (section 4.5.1.2), and

(ii) concentric rod and cone centres (RFC categories A1 and B1), does favour functional asymmetry in retinal connectivity.

In addition to the above findings, the data for retinal ganglion and lateral geniculate cells show that:

(i) the orientation of the major axis of rod and cone centres has a systematic bias in favour of the horizontal; and

(ii) the mean rod and cone ratios do not differ significantly for the sustained or transient classes.

6.3 Adaptive state and receptive field centre area

Enroth-Cugell and Shapley (1973b) have proposed that the adaptive state of RGCs is set by the light flux over the RFC. They suggested, accordingly, that RGCs with large RFCs will be relatively more light

adapted, at a fixed background adapting luminance, than cells with small centres due to the increased light flux over the larger centre. This proposition, although indirectly supported by evidence from Barlow and Levick (1968), Hammond and James (1971), and Enroth-Cugell, Hertz and Lennie (1977a) - viz.: that at a fixed adapting luminance, there is variability in the extent of the mesopic range for different RGCs - was not confirmed in a recent investigation undertaken by Ahmed *et al.* (1977). The study by Ahmed *et al.*, however, was subject to the following criticisms:

(i) it exclusively relied on differences between the RFC sizes of brisk transient and brisk sustained units - i.e. at a given eccentricity, brisk transient units have RFC areas larger than brisk sustained units (Enroth-Cugell and Robson, 1966; Cleland *et al.*, 1974a; Hammond, 1974) - no attempt was made to map the RFCs;

(ii) the summation properties within the receptive field differed for the two classes; and

(iii) an inadequate sample size was compared.

In order to overcome these criticisms a more detailed study was undertaken at a fixed, mid-mesopic background adapting luminance of +0.53 log. cd.m^{-2}.

The RFC of each unit was mapped using either the iso-sensitivity (section 4.2.3) or the central summing area (section 5.3.5) techniques; and the threshold sensitivity was then measured separately for blue (452 nm) and yellow (578 nm) narrow-band lights with a small diameter spot. The results, unequivocally, show that the adaptive state of RGCs is independent of their retinal location, with respect to the area centralis, and their RFC areas, whether determined at a mid-mesopic or a scotopic adapting level. Furthermore, although there is a 0.6 log.unit change in

relative sensitivity, the mean value of the adaptive state does not significantly differ between:

    (i)   retinal and geniculate data,

    (ii) brisk sustained and transient classes, and

    (iii) on- and off-centre units.

APPENDIX A

To correct for the distortion produced by the use of a tangent screen (situated 57 in. in front of the cat), the following procedure was adopted.

The co-ordinates of a point (say A) were measured (Fig. A.1) with respect to the normal-point (O), i.e. the point located on the tangent screen normal to the cat's eyes (denoted by E) with co-ordinates (zero meridian, zero fixation planes). The distance EO being 57 in.

Let the co-ordinates of A be (x_i, y_i), and the visual angle subtended at the eye (E) between O and A be denoted by θ.

Since, θ in deg. = θ in inches

and   length of AO = $L = (x_i^2 + y_i^2)^{\frac{1}{2}}$

Then, the corrected co-ordinates of point A are given by

$$\left(\frac{x_i \cdot \theta}{L} , \frac{y_i \cdot \theta}{L} \right)$$

where $\theta = \tan^{-1} \left(\frac{L}{57} \right)$.

Since this correction process is iterative for all points, a computer program was devised which calculated the correct co-ordinates when the measured co-ordinates (from the tangent screen) were inputed. Furthermore, for a series of points defining a receptive field centre, the corrected co-ordinates were then used to calculate the vector area (equation is given as footnote on page 97 of Chapter 4).
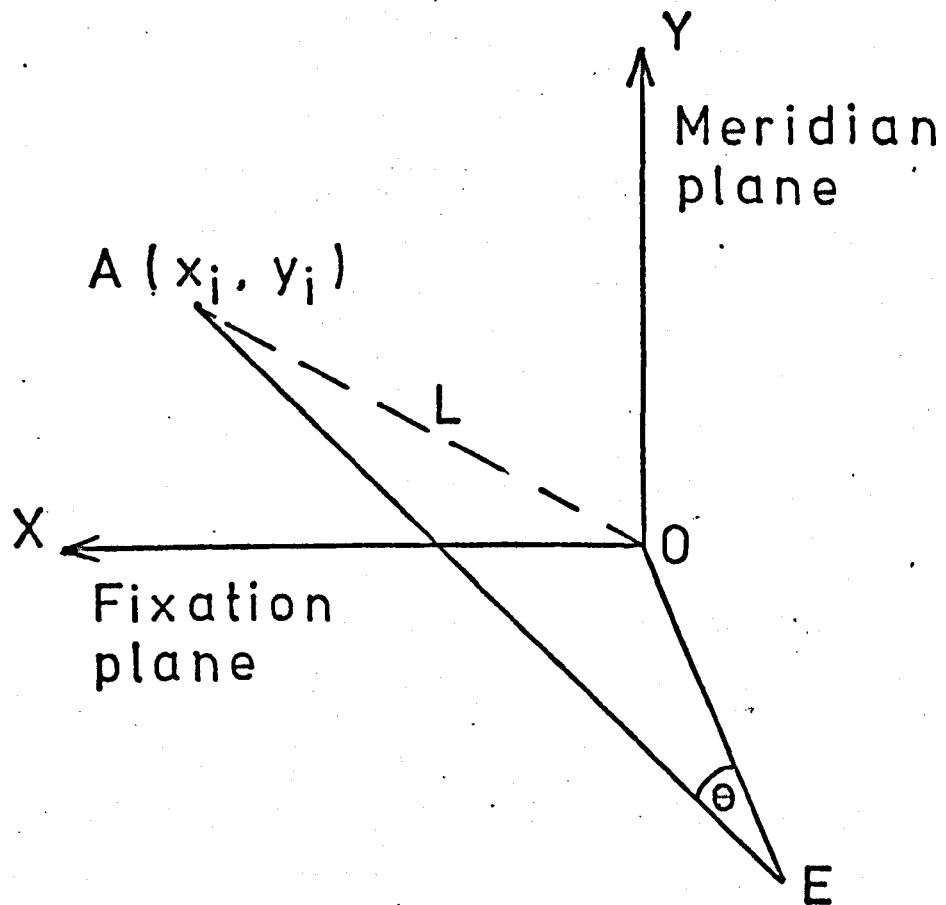
Fig. A.1

[refer to Appendix A]

REFERENCES

Ahmed, B., Hammond, P. and Nothdurft, H. Chr. (1977). A reappraisal of the feline mesopic range. J. Physiol. (Lond.). 266, 94P.

Andrews, D.P. and Hammond, P. (1970a). Mesopic increment threshold spectral sensitivity of single optic tract fibres in the cat: cone-rod interaction. J. Physiol. (Lond.). 209, 65-81.

Andrews, D.P. and Hammond, P. (1970b). Suprathreshold spectral properties of single optic tract fibres in cat, under mesopic adaptation: cone-rod interaction. J. Physiol. (Lond.). 209, 83-103.

Bahr, G.V. (1945). Investigations into the spherical and chromatic aberrations of the eye and their influence on its refraction. Acta Ophthal. 23, 1-47.

Barlow, H.B., Fitzhugh, R. and Kuffler, S.W. (1957a). Dark adaptation, absolute threshold and Purkinje shift in single units of the cat's retina. J. Physiol. (Lond.). 137, 327-337.

Barlow, H.B., Fitzhugh, R. and Kuffler, S.W. (1957b). Change of organisation in the receptive fields of the cat's retina during dark adaptation. J. Physiol. (Lond.). 137, 338-354.

Barlow, H.B. and Levick, W.R. (1968). The Purkinje shift in the cat retina. J. Physiol. (Lond.). 196, 2-3P.

Barlow, H.B., Derrington, A.M., Harris, L.R. and Lennie, P. (1977). The effect of remote retinal stimulation on the responses of cat retinal ganglion cells. J. Physiol. (Lond.). 269, 177-194.

Bedford, R.E. and Wyszecki, G. (1957). Axial chromatic aberration of the human eye. J. Opt. Soc. Am. 47, 564-565.

Bishop, P.O., Burke, W. and Davis, R. (1962a). The identification of single units in central visual pathways. J. Physiol. (Lond.). 162, 409-431.

Bishop, P.O., Burke, W. and Davis, R. (1962b). Single-unit recording from antidromically activated optic radiation neurones. J. Physiol. (Lond.). 162, 432-450.

Bishop, P.O., Burke, W. and Davis, R. (1962c). The interpretation of the extracellular response of single lateral geniculate cells. J. Physiol. (Lond.). 162, 451-472.

Bishop, P.O. and Henry, G.H. (1972). Striate neurons: receptive field concepts. Invest. Ophthalmol. 11, 346-354.

Bishop, P.O., Coombs, J.S. and Henry, G.H. (1973). Receptive fields of simple cells in the cat striate cortex. J. Physiol. (Lond.). 231, 31-60.

Bonaventure, N. (1964). La vision chromatique du chat. C.r. Hebd. Séanc Acad. Sci., Paris, 259, 2012-2015.

Bonds, A.B., Enroth-Cugell, C. and Pinto, L.H. (1972). Image quality of the cat eye measured during retinal ganglion cell experiments. J. Physiol. (Lond.). 220, 383-401.

Bonds, A.B. (1974). Optical quality of the living cat eye. J. Physiol. (Lond.). 243, 777-795.

Boycott, B.B. and Wässle, H. (1974). The morphological types of ganglion cells of the domestic cat's retina. J. Physiol. (Lond.). 240, 397-419.

Brown, J.E. (1965). Dendritic fields of retinal ganglion cells of the rat. J. Neurophysiol. 28, 1091-1100.

Brown, J.E. and Major, D. (1966). Cat retinal ganglion cell dendritic fields. Expl. Neurol. 15, 70-78.

Brown, J.L., Shively, F.D., La Motte, R.H. and Sechzer, J.A. (1973). Colour discrimination in the cat. J. comp. Physiol. Psychol. 84, 534-544.

Burke, W. and Sefton, A.J. (1966a). Discharge patterns of principal cells and interneurones in the lateral geniculate nucleus of the rat. J. Physiol. (Lond.). 187, 201-212.

Burke, W. and Sefton, A.J. (1966b). Recovery of responsiveness of cells of lateral geniculate nucleus of rat. J. Physiol. (Lond.), 187, 213-229.

Burke, W. and Sefton, A.J. (1966c). Inhibitory mechanisms in lateral geniculate nucleus of rat. J. Physiol. (Lond.) 187, 231-246.

Campbell, F.W. and Gubisch, R.W. (1967). The effect of chromatic aberration on visual acuity. J. Physiol. (Lond.). 192, 345-358.

Clayton, K.N. (1961). Colour vision in the cat. Amer. Psychol. 16, 415.

Clayton, K.N. and Kamback, M. (1966). Successful performance by cats on several colour discrimination problems. Can. J. Psychol. 20, 173-182.

Cleland, B.G. and Enroth-Cugell, C. (1968). Quantitative aspects of sensitivity and summation in the cat retina. J. Physiol. (Lond.). 198, 17-38.

Cleland, B.G., Dubin, M.W. and Levick, W.R. (1971). Sustained and transient neurones in the cat's retina and lateral geniculate nucleus. J. Physiol. (Lond.). 217, 473-496.

Cleland, B.G. and Levick, W.R. (1972). Physiology of cat retinal ganglion cells. Invest. Ophthalmol. 11, 285-291.

Cleland, B.G., Levick, W.R. and Sanderson, K.J. (1973). Properties of sustained and transient ganglion cells in the cat retina. J. Physiol. (Lond.), 228, 649-680.

Cleland, B.G. and Levick, W.R. (1974a). Brisk and sluggish concentrically organised ganglion cells in the cat's retina. J. Physiol. (Lond.). 240, 421-456.

Cleland, B.G. and Levick, W.R. (1974b). Properties of rarely encountered types of ganglion cells in the cat's retina and an overall classification. J. Physiol. (Lond.). 240, 457-492.

Cleland, B.G., Levick, W.R. and Wässle, H. (1975). Physiological identification of a morphological class of cat retinal ganglion cells. J. Physiol. (Lond.). 248, 151-171.

Cleland, B.G., Morstyn, R., Wagner, H.G. and Levick, W.R. (1975). Long latency retinal input to lateral geniculate neurones of the cat. Brain Res. 91, 306-310.

Cleland, B.G., Levick, W.R., Morstyn, R. and Wagner, H.G. (1976). Lateral geniculate relay of slowly conducting retinal afferents to cat visual cortex. J. Physiol. (Lond.). 255, 299-320.

Dartnall, H.J.A. (1953). The interpretation of spectral sensitivity curves. Br. med. Bull., 9, 24-30.

Daw, N.W. and Pearlman, A.L. (1969). Cat colour vision: one cone process or several. J. Physiol. (Lond.). 201, 745-764.

Daw, N.W. and Pearlman, A.L. (1970). Cat colour vision: Evidence for more than one cone process. J. Physiol. (Lond.). 211, 125-137.

Daw, N.W. (1973). Neurophysiology of colour vision. Physiol. Rev. 53 571-611.

Devoss, J.C. and Ganson, R. (1915). Color blindness in cats. J. Animal Behaviour, 5, 115-139.

Ditchburn, R.W. (1966). Light. 2nd Edition, London: Blackie & Son.

Dodt, E. and Elenius, U. (1960). Change of threshold during dark adaptation measured with orange and blue light in cats and rabbits. Experientia, 16, 313-316.

Dubin, M.W. and Cleland, B.G. (1977). Organisation of visual inputs to interneurons of lateral geniculate nucleus of the cat. J. Neurophysiol. 40, 410-427.

Dücker, G. (1957). Farb- und Helligkeitssehen und Instinkte bei Viverriden und Feliden. Zoologische Beiträge Neue Folge, 3, 25-99.

Enroth-Cugell, C. and Robson, J.G. (1966). The contrast sensitivity of retinal ganglion cells of the cat. J. Physiol. (Lond.). 187 517-552.

Enroth-Cugell, C. and Pinto, L.H. (1972). Properties of the surround response mechanism of cat retinal ganglion cells and centre-surround interaction. J. Physiol. (Lond.). 220, 403-439.

Enroth-Cugell, C. and Shapley, R.M. (1973a). Adaptation and dynamics of cat retinal ganglion cells. J. Physiol. (Lond.). 233, 271-309.

Enroth-Cugell, C. and Shapley, R.M. (1973b). Flux, not retinal illumination, is what cat retinal ganglion cells really care about. J. Physiol. (Lond.). 233, 311-326.

Enroth-Cugell, C., Hertz, B.G. and Lennie, P. (1977a). Cone signals in the cat's retina. J. Physiol. (Lond.) 269, 273-296.

Enroth-Cugell, C., Hertz, B.G. and Lennie, P. (1977b). Convergence of rod and cone signals in the cat's retina. J. Physiol. (Lond.). 269, 297-318.

Famighetti, E.V., Jr., Køneko, A. andTachibana, M. (1977). Neuronal architecture of on and off pathways to ganglion cells in carp retina. Science, 198, 1267-1268.

Fernald, R. and Chase, R. (1971). An improved method for plotting retinal landmarks and focusing the eyes. Vision Res. 11, 95-96.

Fukada, Y. (1971). Receptive field organisation of cat optic nerve fibers with special reference to conduction velocity. Vision Res., 11, 209-226.

Fukada, Y. and Saito, H. (1971). The relationship between response characteristics to flicker stimulation and receptive field organisation in the cat's optic nerve fibers. Vision Res. 11, 227-240.

Fukuda, Y. and Stone, J. (1974). Retinal distribution and central projections of Y-, X-, and W-cells of the cat's retina. J. Neurophysiol. 37, 749-772.

Fukuda, Y. and Stone, J. (1975). Direct identification of the cell bodies of Y-, X- and W-cells in the cat's retina. Vision Res. 15, 1034-1036.

Granit, R. (1943). The spectral properties of the visual receptors of the cat. Acta Physiol. Scand. 5, 219-229.

Granit, R. (1945). The colour receptors of the mammalian retina. J. Neurophysiol. 8, 195-210.

Gregg, F.M., Jamison, E., Wilkie, R. and Radinsky, T. (1929). Are dogs, cats, and raccoons color blind? J. Comp. Psychol. 9, 379-395.

Guillery, R.W. (1970). The laminar distribution of retinal fibres in the dorsal lateral geniculate nucleus of the cat: a new interpretation. J. Comp. Neurol. 138, 339-368.

Gunter, R. (1952). The spectral sensitivity of dark-adapted cats. J. Physiol. (Lond.). 118, 395-404.

Gunter, R. (1954a). The spectral sensitivity of light adapted cats. J. Physiol. (Lond.). 123, 409-416.

Gunter, R. (1954b). The discrimination between lights of different wavelengths in the cat. J. Comp. Physiol. Psychol. 47, 169-172.

Hamasaki, D.I., Campbell, R. and Zengel, J. (1972). Response of cat optic tract fibres to moving stimulus. Presented at the annual meeting of the Association for Research in Vision and Ophthalmology, Sarasota.

Hamasaki, D.I., Zengel, J. and Campbell, R. (1973). Two types of response patterns from cat retinal ganglion cells to moving stimuli. Experientia, 29, 808-809.

Hamasaki, D.I., Campbell, R., Zengel, J. and Hazelton, L.R. Jr. (1973). Response of cat retinal ganglion cell to moving stimuli. Vision Res. 13, 1421-1432.

Hammond, P. and James, C.R. (1971). The Purkinje shift in cat: extent of the mesopic range. J. Physiol. (Lond.). 216, 99-109.

Hammond, P. (1972). Chromatic sensitivity and spatial organisation of LGN neurone receptive fields in cat: cone-rod interaction. J. Physiol. (Lond.). 225, 391-443.

Hammond, P. (1973). Contrasts in spatial organisation of receptive fields at geniculate and retinal levels: centre, surround and outer surround. J. Physiol. (Lond.). 228, 115-137.

Hammond, P. (1974). Cat retinal ganglion cells: size and shape of receptive field centres. J. Physiol. (Lond.). 242, 99-118.

Hammond, P. (1975). Receptive field mechanisms of sustained and transient retinal ganglion cells in the cat. Exp. Brain Res., 23, 113-128.

Hammond, P. (1978a). The neural basis for colour discrimination in the domestic cat. Vision Res. 18, 233-235. ·

Hammond, P. (1978b). On the use of nitrous oxide oxygen mixtures for anaesthesia in cats. J. Physiol. (Lond.). 275, 64P.

Hammond, P. (1978c). Inadequacy of nitrous oxide/oxygen mixture for maintaining anaesthesia in cats: satisfactory alternatives. Pain, 5, 143-152.

Henry, G.H. and Bishop, P.O. (1972). Striate neurons: Receptive field organisation. Invest. Ophthalmol. 11, 357-368.

Hickey, T.L., Winters, R.W. and Pollack, J.G. (1973). Center-surround interactions in two types of on-center retinal ganglion cells in the cat. Vision Res. 13, 1511-1526.

Hochstein, S. and Shapley, R.M. (1976a). Quantitative analysis of retinal ganglion cell classification. J. Physiol. (Lond.). 262, 237-264.

Hochstein, S. and Shapley, R.M. (1976b). Linear and non-linear spatial subunits in Y cat retinal ganglion cells. J. Physiol. (Lond.). 262, 265-284.

Hoffmann, K.P. (1973). Conduction velocity in pathways from retina to superior colliculus in the cat. A correlation with receptive field properties. J. Neurophysiol. 36, 409-424.

Honrubia, F.M. and Elliott, J.H. (1970). Dendritic fields of the retinal ganglion cells in the cat. Arch. Ophthal. 84, 221-226.

Hubel, D.H. and Wiesel, T.N. (1962). Receptive fields, binocular interaction and functional architecture in the cat's visual cortex. J. Physiol. (Lond.). 160, 106-154.

Ikeda, H. and Pringle, J. (1971). A microelectrode advancer for intraretinal recording from the cat. Vision Res. 11, 1169-1173.

Ikeda, H. and Wright, M.J. (1971). How large is the receptive field of a single retinal ganglion cell? J. Physiol. (Lond.). 217, 52-53P.

Ikeda, H. and Hill, R.M. (1971). Can a peripheral retinal ganglion cell respond differentially to images in or out of focus? Nature (Lond.). 229, 557-558.

Ikeda, H. and Wright, M.J. (1972a). Receptive field organisation of 'sustained' and 'transient' retinal ganglion cells which subserve different functional roles. J. Physiol. (Lond.). 227, 769-800.

Ikeda, H. and Wright, M.J. (1972b). Differential effects of refractive errors and receptive field organisation of central and peripheral ganglion cells. Vision Res. 12, 1465- 1476.

Ikeda, H., Wright, M.J., Young, S. and Nuza, J. (1973). Relation between refractive error and the spread of the image on the cat's retina. Vision Res., 13, 867-871.

Ivanoff, A. (1947). The chromatic and spherical aberrations of the eye - their role in night vision. Revue d'Optique, 26, 145-171.

Jakiela, H.G., Enroth-Cugell, C., and Shapley, R.M. (1976). Adaptation and dynamics in X- and Y-cells of the cat retina. Exp. Brain Res. 24, 335-342.

Kirk, D.L., Levick, W.R., Cleland, B.G. and Wässle, H. (1976). Crossed and uncrossed representation of the visual field by brisk-sustained and brisk-transient cat retinal ganglion cells. Vision Res. 16, 225-231.

Kirk, D.L., Levick, W.R. and Cleland, B.G. (1976). The crossed or uncrossed destination of axons of sluggish-concentric and non-concentric cat retinal ganglion cells, with an overall synthesis of the visual field representation. Vision Res., 16, 233-236.

Kruger, J. and Fischer, B. (1973). Dependence of surround effects on receptive field centre illumination in cat retinal ganglion cells. Exp. Brain Res., 18, 287-303.

Kuffler, S.W. (1953). Discharge patterns and functional organisation of mammalian retina. J. Neurophysiol. 16, 37-68.

La Motte, R.H. and Brown, J.L. (1970). Dark adaptation and spectral sensitivity in the cat. Vision Res. 10, 703-716.

Leicester, J. and Stone, J. (1967). Ganglion, amacrine and horizontal cells of the cat's retina. Vision Res. 7, 695-705.

Levick, W.R., Oyster, C.W. and Davis, D.L. (1965). Evidence that McIlwain's periphery effect is not a stray light artifact. J. Neurophysiol. 28, 555-559.

Levick, W.R. (1967). Receptive fields and trigger features of ganglion cells in the visual streak of the rabbit's retina. J. Physiol. (Lond.). 188, 285-307.

Loop, M.S. and Bruce, L.L. (1978). Cat color vision: The effect of stimulus size. Science, 199, 1221-1222.

Marracco, R.T. (1972). Responses of monkey optic tract fibers to monochromatic lights. Vision Res. 12, 1167-1174.

Mason, R. (1976). Neuronal organization within the mammalian dorsal lateral geniculate complex and adjacent pulvinar nuclei: A comparative approach. Ph.D. Thesis (Keele).

McCann, J.J. and Benton, J.L. (1969). Interaction of the long wave cones and the rods to produce colour sensations. J. Opt. Soc. Am. 59, 103-107.

McCann, J.J. (1972). Rod-cone interactions: different colour sensations from identical stimuli. Science, 176, 1255-1257.

McIlwain, J.T. (1964). Receptive fields of optic tract axons and lateral geniculate cells: Peripheral extent and barbiturate sensitivity. J. Neurophysiol. 27, 1154-1173.

McIlwain, J.T. (1966). Some evidence concerning the physiological basis of the periphery effect in the cat's retina. Exp. Brain Res. 1, 265-271.

Mello, N.K. and Peterson, N.J. (1964). Behavioral evidence for color discrimination in cat. J. Neurophysiol. 27, 323-333.

Merrill, E.G. and Ainsworth, A. (1972). Glass-coated platinum-plated tungsten microelectrodes. Med. and Biol. Eng., 10, 662-672.

Meyer, D.R, Miles, R.C. and Ratoosh, P. (1954). Absence of colour vision in cat. J. Neurophysiol. 17, 289-294.

Meyer, D.R. and Anderson, R.A. (1965). Colour discrimination in cats. Colour Vision (ed. De Reuck, A.V.S. & Knight, J.), pp.325-339, Boston:Little-Brown.

Nelson, R., Famiglietti, E.V. Jr. and Kolb, H. (1978). Intracellular staining reveals different levels of stratification for on- and off-centre ganglion cells in cat retina. J. Neurophysiol. 41, 472-483.

Pearlman, A.L. and Daw, N.W. (1970). Opponent color cells in the cat lateral geniculate nucleus. Science, N.Y., 167, 84-86.

Pollack, J.G. and Winters, R.W. (1978). Effect of adaptation level on maintained firing and sensitivity in receptive field centre of X and Y cells. Experientia, 34, 80-81.

Rabin, A.R., Mehaffey, L. III, and Berson, E.L. (1976). Blue cone function in the retina of the cat. Vision Res. 16, 799-801.

Richards, C.D. and Webb, A.C. (1975). The effect of nitrous oxide on cat anaesthetized with brietal. J. Physiol. (Lond.) 245, 72-73P.

Ringo, J., Wolbarsht, M.L., Wagner, H.G., Crocker, R. and Amthor, F. (1977). Trichromatic vision in the cat. Science, 198, 753-755.

Robertson, T.W., Winters, R.W., Christen, W.G. and Cohen, H.I. (1978). The effect of adapting target location on the gain of the surround mechanism in cat retinal ganglion cells. Brain Res. 156, 360-363.

Robson, J.G. and Enroth-Cugell, C. (1978). Light distribution in the cat's retinal image. Vision Res., 18, 159-174.

Rodieck, R.W. (1965). Quantitative analysis of cat retinal ganglion cell response to visual stimuli. Vision Res., 5, 583-601.

Rodieck, R.W. and Stone, J. (1965a). Response of cat retinal ganglion cells to moving visual patterns. J. Neurophysiol. 28, 819-832.

Rodieck, R.W. and Stone, J. (1965b). Analysis of receptive fields of cat retinal ganglion cells. J. Neurophysiol. 28, 833-849.

Rodieck, R.W. (1967). Receptive fields in the cat retina: A new type. Science, 157, 90-92.

Rodieck, R.W., Pettigrew, J.D., Bishop, P.O. and Nikara, T. (1967). Residual eye movements in receptive field studies of paralyzed cats. Vision Res., 7, 107-110.

Rowe, M.H. and Stone, J. (1976). Properties of ganglion cells in the visual streak of the cat's retina. J. Comp. Neurol. 169, 99-126.

Rowe, M.H. and Stone, J. (1977). Naming of neurones: Classification and naming of cat retinal ganglion cells. Brain, Behav. & Evol. 14, 185-216.

Rushton, W.A.H. (1963). Increment threshold and dark adaptation. J. Opt. Soc. Am. 53, 104-109.

Rushton, W.A.H. (1965a). The Ferrier lecture: Visual adaptation. Proc. R. Soc. B., 162, 20-46.

Rushton, W.A.H. (1965b). The sensitivity of rods under illumination. J. Physiol. (Lond.); 178, 141-160.

Russell, W.J. (1973). Nitrous oxide - is it an adequate anaesthetic in cats? J. Physiol. (Lond.), 231, 20P.

Saito, H., Shimahara, T. and Fukada, Y. (1970). Four types of responses to light and dark spot stimuli in the cat optic nerve. Tohoku J. Exp. Med., 102, 127-133.

Saunders, R. McD. (1977). The spectral responsiveness and the temporal frequency response (TFR) of cat optic tract and lateral geniculate neurons: Sinusoidal stimulation studies. Vision Res. 17, 285-292.

Sechzer, J.A. and Brown, J.L. (1964). Colour discrimination in the cat. Science, 144, 427-429.

Sefton, A.J. and Bruce, I.S.C. (1971). Properties of cells in the lateral geniculate nucleus. Vision Res. Supp. 3, 239-252.

Shkolnik-Yarros, E.G. (1971). Neurons of the cat's retina. Vision Res. 11, 7-26.

Snider, R.S. and Niemer, W.T. (1961). A stereotaxic atlas of the cat brain. University of Chicago Press, Chicago.

Spinelli, D.N. (1966). Visual receptive fields of the cat's retina: Complications. Science, 152, 1768-1770.

Spinelli, D.N. (1967). Receptive field organisation of ganglion cells in the cat's retina. Expl. Neurol. 19, 291-315.

Steinberg, R.H., Reid, M. and Lacy, P.L. (1973). The distribution of rods and cones in the retina of the cat (Felis domesticus). J. Comp. Neurol. 148, 229-248.

Stone, J. and Fabian, M. (1966). Specialised receptive fields in the cat's retina. Science, 152, 1277-1279.

Stone, J. and Hoffmann, K.-P. (1972). Very slow-conduction ganglion cells in the cat's retina: A major new functional type? Brain Res. 43, 610-616.

Stone, J. and Fukuda, Y. (1974a). Properties of cat retinal ganglion cells: a comparison of W-cells with X- and Y-cells. J. Neurophysiol. 37, 722-748.

Stone, J. and Fukuda, Y. (1974b). The naso-temporal division of the cat's retina re-examined in terms of W-, X-, and Y-cells. J. Comp. Neurol. 155, 377-394.

Suzuki, H., Taira, N. and Motokawa, K. (1960). Spectral response curves and receptive fields of pre- and post geniculate fibers of the cat. Tohoku J. Exp. Med., 71, 401-415.

Tucker, J. (1975). The chromatic aberration of the eye between wavelengths 200nm and 2,00nm: some theoretical considerations. Brit. J. Physiol. Opt., 29, 118-125.

Vakkur, G.J., Bishop, P.O. and Kozak, W. (1963). Visual optics in the cat, including posterior nodal distance and retinal landmarks. Vision Res. 3, 289-314.

Vakkur, G.J. and Bishop, P.O. (1963). The schematic eye in the cat. Vision Res. 3, 357-381.

Wässle, H. (1971). Optical quality of the cat eye. Vision Res. 11, 995-1006.

Wässle, H., Levick, W.R. and Cleland, B.G. (1975). The distribution of the alpha type of ganglion cells in the cat's retina. J. Comp. Neurol. 159, 419-438.

Weale, R.A. (1953). Photochemical reactions in the living cat's retina. J. Physiol. (Lond.). 122, 322-331.

Wiesel, T.N. (1960). Receptive fields of ganglion cells in the cat's retina. J. Physiol. (Lond.), 153, 583-594.

Wilson, P.D. and Stone, J. (1975). Evidence of W-cell input to the cat's visual cortex via the C laminae of the lateral geniculate nucleus. Brain Res. 92, 472-478.

Winters, R.W., Pollack, J.G. and Hickey, T.L. (1972). Two types of on-centre cells in cat optic tract. Brain Res. 47, 501-505.

Winters, R.W., Hickey, T.L. and Pollack, J.G. (1973). Effect of variations of target location upon the peripheral responses of on-centre retinal ganglion cells in the cat. Vision Res. 13, 1487-1498.

Winters, R.W., Hickey, T.L. and Skaer, D.H. (1973). Spatial summation in the receptive field periphery of two types of on-centre neurons in cat retina. Vision Res., 13, 1499-1509.